THE ROLE OF CLIMATE AND AIR POLLUTION IN HUMAN HEALTH AND URBAN CHEMISTRY IN ASIAN CITIES

EDITED BY: Prashant Rajput, Atinderpal Singh, Jai Prakash and Manish Kumar
PUBLISHED IN: Frontiers in Sustainable Cities

frontiers Research Topics

About Frontiers

Frontiers is more than just an open-access publisher of scholarly articles: it is a pioneering approach to the world of academia, radically improving the way scholarly research is managed. The grand vision of Frontiers is a world where all people have an equal opportunity to seek, share and generate knowledge. Frontiers provides immediate and permanent online open access to all its publications, but this alone is not enough to realize our grand goals.

Frontiers Journal Series

The Frontiers Journal Series is a multi-tier and interdisciplinary set of open-access, online journals, promising a paradigm shift from the current review, selection and dissemination processes in academic publishing. All Frontiers journals are driven by researchers for researchers; therefore, they constitute a service to the scholarly community. At the same time, the Frontiers Journal Series operates on a revolutionary invention, the tiered publishing system, initially addressing specific communities of scholars, and gradually climbing up to broader public understanding, thus serving the interests of the lay society, too.

Dedication to Quality

Each Frontiers article is a landmark of the highest quality, thanks to genuinely collaborative interactions between authors and review editors, who include some of the world's best academicians. Research must be certified by peers before entering a stream of knowledge that may eventually reach the public - and shape society; therefore, Frontiers only applies the most rigorous and unbiased reviews.
Frontiers revolutionizes research publishing by freely delivering the most outstanding research, evaluated with no bias from both the academic and social point of view.
By applying the most advanced information technologies, Frontiers is catapulting scholarly publishing into a new generation.

What are Frontiers Research Topics?

Frontiers Research Topics are very popular trademarks of the Frontiers Journals Series: they are collections of at least ten articles, all centered on a particular subject. With their unique mix of varied contributions from Original Research to Review Articles, Frontiers Research Topics unify the most influential researchers, the latest key findings and historical advances in a hot research area! Find out more on how to host your own Frontiers Research Topic or contribute to one as an author by contacting the Frontiers Editorial Office: frontiersin.org/about/contact

ISSN 1664-8714
ISBN 978-2-88974-673-6
DOI 10.3389/978-2-88974-673-6

THE ROLE OF CLIMATE AND AIR POLLUTION IN HUMAN HEALTH AND URBAN CHEMISTRY IN ASIAN CITIES

Topic Editors:
Prashant Rajput, Banaras Hindu University, India
Atinderpal Singh, University of Delhi, India
Jai Prakash, Washington University in St. Louis, United States
Manish Kumar, Stockholm University, Sweden

Citation: Rajput, P., Singh, A., Prakash, J., Kumar, M., eds. (2022). The Role of Climate and Air Pollution in Human Health and Urban Chemistry in Asian Cities. Lausanne: Frontiers Media SA. doi: 10.3389/978-2-88974-673-6

Table of Contents

frontiers in Sustainable Cities

EDITORIAL
published: 18 February 2022
doi: 10.3389/frsc.2022.858060

Editorial: The Role of Climate and Air Pollution in Human Health and Urban Chemistry in Asian Cities

Prashant Rajput[1]*, *Atinderpal Singh*[2], *Jai Prakash*[3] *and Manish Kumar*[4]

[1] DST-Mahamana Centre of Excellence in Climate Change Research, IESD, Banaras Hindu University, Varanasi, India, [2] Department of Environmental Studies, University of Delhi, New Delhi, India, [3] Energy, Environmental and Chemical Engineering, Washington University in St. Louis, St. Louis, MO, United States, [4] Department of Environmental Science and Analytical Chemistry (ACES), Stockholm University, Stockholm, Sweden

Keywords: climate change in Asian cities, air pollution in Asian cities, human health, urban chemistry, aerosols, trace gases, urban hotspots, atmospheric chemistry

Editorial on the Research Topic

The Role of Climate and Air Pollution in Human Health and Urban Chemistry in Asian Cities

The Asian cities are experiencing unprecedented climate, poor air quality, and human health due to existing rapid urbanization, air pollution, unsustainable land-use planning, and industrialization. Therefore, air pollution is now one of the biggest threats to human health in urban cities of Asia. The association between air pollution and human health is very complex due to atmospheric processes and the transformation of pollutants which are considered as exposure variables. Furthermore, biomass burning and climate change effects for example rise in temperature and the perturbed hydrological cycle can significantly impact the atmospheric chemistry, and human health in urban air-sheds in Asia.

A total of 10 articles are provided in this special issue, which is aimed at recent developments in the area of air pollution, urban atmospheric chemistry, and its impact on public health and climate change in Asian cities. This issue is centered on the novelty of work reported from experimental as well as modeling analysis in the field of air pollution, climate change, and human health. The manuscripts went through a rigorous, transparent, single-blinded, and interactive peer-review process involving the authors, the Reviewers, and the Guest Editors prior to acceptance for publication in this special issue. The gist of these publications is given below:

Many researchers have reported the bursting of firecrackers (FC) during the Diwali festival (celebrated on a particular date either in the month of October or November) in India which leads to further increase the air pollution above the background levels and plausibly affects the human health. During post-monsoon (October-November), the long-range transport of biomass burning emissions (LRT-BB) also affects the air quality in downwind locations in Northern India. Rajput et al. revealed that FC burst in Diwali and LRT-BB increased the daily $PM_{2.5}$ concentration by 11 and 36%, respectively over its urban background level (286 $\mu g\ m^{-3}$) at Kanpur using the Lenschow-type approach on a temporal domain for the first time. Bangar et al. reported the source apportionment of $PM_{2.5}$ from Northern India (Delhi) during the post-monsoon season and they also found that LRT-BB has the highest contribution to $PM_{2.5}$ during this season as reported by Rajput et al. Along with LRT-BB, they identified the other major sources of $PM_{2.5}$ such as uplifted mineral dust, vehicular emissions, road dust resuspension, secondary aerosols formation, industrial emission, coal combustion, and solid-waste burning.

The urban population is subjected to multiple exposures to air pollution and heat stress that have several negative health impacts. Indian cities are highly vulnerable to extreme weather events for example heatwaves and cold waves. A review article by Menon and Sharma highlights the use Nature-Based Solutions (NBS) to tackle the environmental issue due to their multi-functional

OPEN ACCESS

Edited and reviewed by:
Prashant Kumar,
University of Surrey, United Kingdom

****Correspondence:***
Prashant Rajput
prajput.prl@gmail.com

Specialty section:
This article was submitted to
Climate Change and Cities,
a section of the journal
Frontiers in Sustainable Cities

Received: *19 January 2022*
Accepted: *27 January 2022*
Published: *18 February 2022*

Citation:
Rajput P, Singh A, Prakash J and Kumar M (2022) Editorial: The Role of Climate and Air Pollution in Human Health and Urban Chemistry in Asian Cities. Front. Sustain. Cities 4:858060.
doi: 10.3389/frsc.2022.858060

nature and cost-effectiveness. In their review article, they highlighted co-benefits of using NBS such as reduction in energy cost as well as conservation of biodiversity in addition to improving public health (through a reduction in air pollution and urban heat). Dutta et al. examined the impact of heat stress on the stone quarry workers. The result findings suggest that around 14% of workers were vulnerable to heat stress.

Tuladhar et al. estimated the health impacts of $PM_{2.5}$ exposure using the WRF-Chem Model in Kathmandu Valley, Nepal. The exposure analysis indicates that 19 people could die due to lung cancer and 175 people could die due to all-cause (non-accidental) diseases due to $PM_{2.5}$ exposure in December. Furthermore, their simulation estimated that reducing the 50% $PM_{2.5}$ level in the valley could lead to a reduction in the monthly mortality by 51.4%. Pavel et al. estimated the human health risk due to the criteria pollutants in Dhaka, Bangladesh. They found that hazard quotient (HQ) values were not antagonistic (HQ < 1) while assessing acute exposure in the three age groups (infants, children, and adults). However, their study showed a significant health risk (HQ > 1) in chronic exposure for infants and children. They identified children are the worst sufferers among the age groups. Air pollution due to nanoparticles (NPs) is receiving increasing attention in scientific communities due to their strong influence on human health. Sonwani et al. provided a comprehensive review on the atmospheric NPs and their association with human health. Exposure to NPs causes the generation of ROS, resulting in cytotoxicity that leads to genotoxicity and tumorigenesis. The overproduction of ROS and the weakening of the antioxidant defense system cause oxidative stress which can trigger the release of more pro-inflammatory hormones that lead to inflammation as well as acute and chronic lung diseases.

Climate change is one of the biggest challenges of sustainability in today's world. Kaur and Pandey reviewed the present status of climate change, air pollution, and human health in Indian cities. In this review, they stated that the Indian population is experiencing adverse human health impacts due to air pollution and climate change. Further, they emphasized the role of climate change in arising extreme weather events in India. They also highlighted the use of satellite data with geospatial techniques in monitoring and mapping spatial-temporal distribution patterns of air pollution and climate change and associated health impacts. Therefore, to make sustainable cities in developing countries like India, there is a need for stringent urban planning, electric mobility, and action plans to curtail urban air pollution and improve the public health system.

The COVID-19 pandemic has affected our economic growth and health care system. Mishra et al. assessed the impact of lockdown and unlock phases on ambient atmospheric air quality parameters across 16 major cities of India covering the north-to-south stretch of the country. They reported a reduction in $PM_{2.5}$ by 49% over north India during the lockdown period. Their results indicate that by adopting cleaner fuel technology and avoiding poor combustion activities across the urban cities of India a reduction in $PM_{2.5}$ up to 30% can be achieved. Another study (Yadav et al.) focused on the substantial improvement in air quality over 6 cities of the states of Rajasthan (India) during the nationwide lockdown amid COVID-19.

AUTHOR CONTRIBUTIONS

All authors listed have made a substantial, direct, and intellectual contribution to the work and approved it for publication.

Conflict of Interest: The authors declare that the research was conducted in the absence of any commercial or financial relationships that could be construed as a potential conflict of interest.

Publisher's Note: All claims expressed in this article are solely those of the authors and do not necessarily represent those of their affiliated organizations, or those of the publisher, the editors and the reviewers. Any product that may be evaluated in this article, or claim that may be made by its manufacturer, is not guaranteed or endorsed by the publisher.

frontiers in Sustainable Cities

ORIGINAL RESEARCH
published: 21 January 2021
doi: 10.3389/frsc.2020.622050

Source Contribution of Firecrackers Burst vs. Long-Range Transport of Biomass Burning Emissions Over an Urban Background

Prashant Rajput[1*†], *Amit Kumar Singh*[1], *Kaniska Biswas*[2], *Adnan Mateen Qadri*[1] and *Tarun Gupta*[1,3*]

[1] *Department of Civil Engineering, Indian Institute of Technology Kanpur, Kanpur, India,* [2] *Design Programme, Indian Institute of Technology Kanpur, Kanpur, India,* [3] *Atmospheric Particle Technology Laboratory at Centre for Environmental Science and Engineering (CESE), Indian Institute of Technology Kanpur, Kanpur, India*

OPEN ACCESS

Edited by:
Konstantinos E. Kakosimos, Texas A&M University at Qatar, Qatar

Reviewed by:
Leila Droprinchinski Martins, Federal Technological University of Paraná, Brazil
Sreekanth Vakacherla, Center for Study of Science, Technology and Policy—CSTEP, India

***Correspondence:**
Prashant Rajput
prashant.rajput@phfi.org
Tarun Gupta
tarun@iitk.ac.in

†Present address:
Prashant Rajput, Centre for Environmental Health (CEH), Public Health Foundation of Indian, Gurugram, India

Specialty section:
This article was submitted to Climate Change and Cities, a section of the journal Frontiers in Sustainable Cities

Received: *27 October 2020*
Accepted: *16 December 2020*
Published: *21 January 2021*

Citation:
Rajput P, Singh AK, Biswas K, Qadri AM and Gupta T (2021) Source Contribution of Firecrackers Burst vs. Long-Range Transport of Biomass Burning Emissions Over an Urban Background. Front. Sustain. Cities 2:622050. doi: 10.3389/frsc.2020.622050

This study reports on the high-resolution data set of ground-level O_3, surface-bound polycyclic aromatic hydrocarbons (SB-PAHs), and particle's number concentrations (range: 10 to 1,000 nm, referred to as condensation nucleus concentration: CNC) during a Diwali festival campaign (conducted from 08th to 16th Nov.2015) at Kanpur location. In this study, we have made an attempt to assess the change in atmospheric composition and chemistry (based on SB-PAHs, O_3, and CNC) during Diwali festival (11th Nov.) and compared the results with pre-Diwali (08th—10th Nov.) and post-Diwali (12th—16th Nov.) scenarios. The wind pattern and cluster analysis have revealed a quite similar feature that from 10th to 16th of November the prevailed winds were north-westerly (NW). It is noteworthy that NW-winds during post-monsoon season (Oct–Nov) favors the long-range transport of biomass burning emissions (LRT-BB) from its source region in upwind Indo-Gangetic Plain (IGP). The influence of LRT-BB emissions at the receptor site during Diwali and post-Diwali period was reflected by the substantial increase in average concentrations of $PM_{2.5}$, O_3 and CNC (difference has been ascertained from a two-tailed *t*-test). The Lenshchow-type analysis revealed that the firecrackers (FC) burst and LRT-BB emissions have lead to increase the concentrations of CNC by 54% and 86%, respectively over the urban background level. On the other hand, the FC burst and LRT-BB increased the concentrations of O_3 by 12% and 31% (over the urban background), respectively. Lenschow-type analysis revealed that FC burst and LRT-BB increased the daily $PM_{2.5}$ concentration by 11% and 36%, respectively over its urban background level (286 $\mu g\ m^{-3}$). However, the SB-PAHs concentrations were found to be decreased by 6% and 2%, respectively, during the FC burst activity and LRT-BB emissions. Based on the observations pertaining to the decrease in SB-PAHs concentrations from the Lenschow-type analysis and anti-correlation between SB-PAHs and O_3 the heterogeneous-phase chemical reactivity and loss of SB-PAHs has been inferred in this study.

Keywords: PAHs, O_3, Diwali, Indo-Gangetic Plain, Air pollution, Heterogeneous-phase chemical reactivity

INTRODUCTION

Diwali festival is one the major festivals celebrated across India. It is also known as the Festival of Lights and people celebrate it with lots of enthusiasm and through cultural activities. This festival is celebrated on a particular date either in the month of October or November based on the Indian Vedic Calendar. However, worsening of air quality on Diwali festival due to bursting of firecrackers (FC) is one of the major concerns raised by many researchers (Singh et al., 2010; Joshi et al., 2016; Ambade, 2018; Izhar et al., 2018; Rastogi et al., 2019). It is worthwhile mentioning that unlike in the western and southern parts of India, the air quality in northern part of India worsens during October–November due to additional input of pollutants from the long-range transport of biomass burning emissions (LRT-BB) (Rajput et al., 2011, 2016; Kaskaoutis et al., 2014; Jethva et al., 2019; Sharma et al., 2019). Thus, LRT-BB poses a challenge in estimating the emissions due to FC burst over the urban background emission (manifested primarily by vehicular exhaust, industrial emission, and soil dust resuspension) in northern India. The overall pollution load at any given time over a city site is due to, the emissions occuring within the urban agglomeration (hereafter referred to as urban background emissions) and those getting transported from long distances (e.g., LRT-BB), atmospheric chemistry resulting into the formation of new compounds, and episodic emissions (e.g., FC burst on Diwali). To the best of our knowledge, the quantitative estimate of pollutant's concentration only due to FC, after correcting for the contribution of LRT-BB, has not been examined previously for the northern India.

Besides the characterization and impact of primary species (Menon et al., 2002; Ramana et al., 2010; Andreae and Ramanathan, 2013; Sahu et al., 2017; Satish and Rastogi, 2019), there has been a deep interest globally in looking at the features pertaining to chemical transformations occuring under ambient atmospheric conditions (Perraudin et al., 2007; Rudich et al., 2007; Kaiser et al., 2011; George et al., 2015; Nguyen et al., 2016; Pöhlker et al., 2018; Rajput et al., 2018; Rajput and Gupta, 2020). For example, a recent study assesses the secondary organic aerosols (SOA) formation due to ozone utlizing the instrumental variable analysis (IVA) (Rajput and Gupta, 2020). In fact, many studies have focussed on the atmospheric reactivity and health impacts of several types of organic compounds including the polycyclic aromatic hydrocarbons (PAHs) (Ackerman et al., 1994; Maria et al., 2004; Che et al., 2016; Ruehl et al., 2016; Singh and Gupta, 2016; Agarwal et al., 2018). The surface layer reactivity of PAHs with the atmospheric oxidants (e.g., O_3 or OH radical) has been found to be asociated with an enhanced cloud condensation nuclei (CCN) activation efficiency and toxicity (of a particle) (Perraudin et al., 2007; Kaiser et al., 2011). The surface-layer oxidation reaction of PAHs plausibly leading to an enhanced CCN activation efficiency is shown through a schematic diagram (**Figure 1**). This study was conducted with two major objectives: (i) to quantify the contribution of FC burst vis-à-vis LRT-BB emissions to the total burden of pollutants (SB-PAHs, $PM_{2.5}$, O_3 and CNC) above the urban background level at central IGP (Kanpur location) and, (ii) to investigate the association between the SB-PAHs and O_3 concentrations during day and nighttime of pre-Diwali, Diwali, and post-Diwali periods.

METHODOLOGY

Field Campaign

A 9 day campaign from 08th Nov 2015 (local time: 10:00 h) to 16th Nov 2015 (local time: 06: 00 h) was conducted at Kanpur site (26.30 °N, 80.14 °E, 142 m amsl.) in central part of the Indo-Gangetic Plain (IGP). In order to assess the atmospheric chemistry and episodic emission strength from FC burst on Diwali festival day, the entire campaign has been sub-divided into three periods: pre-Diwali (08th−10th Nov.), Diwali (11th Nov.) and post-Diwali (12th−16th Nov.). In this campaign, we have measured high-resolution (Δt = 1-min, $n \approx 10$ k data points) near ground-level O_3, surface-bound polycyclic aromatic hydrocarbons (SB-PAHs), and particle's number concentrations from 10 to 1,000 nm by condensation particle counter (referred to as CNC, condensation nucleus concentration). For these measurements, three online analyzers have been utilized which were housed in the Atmospheric Particle Technology Laboratory (APTL, first floor, ∼25 ft. from the ground) at the Center for Environmental Science & Engineering (CESE) building in the premises of Indian Institute of Technology Kanpur (IITK). The APTL lab remains usually maintained at temperature ∼22°C. These instruments were kept nearby on a platform in the lab, and their inlets (separated by < 1 m) were allowed to sample air from one of the windows. The window from which the air was sampled for the real-time analysis is situated on the rear side of the CESE building and it does not faces any direct road emission. Relevant details on each instrumentation are explained below:

Real-Time Measurements of Particle's Surface-Bound PAHs

The desktop model of the photoelectric aerosol sensor (PAS 2000, **Table 1**, Δt = 1-min, $n \approx 10$ k data points) uses a Krypton Chlorine excimer lamp that produces photons of energy 5.6 eV peaking at 222 nm wavelength (Niessner and Walendzik, 1989). These photons of 5.6 eV are utilized to photo-ionize PAHs molecules that are adsorbed onto the surface of a sampled particle (Marr et al., 2006). SB-PAHs (unsubstituted) have lower ionization energies and so get ionized upon exposure to photons from KrCl lamp whereas the gas-phase PAHs have higher ionization energies and so neither they get ionized nor be measured by PAS (photoelectric aerosol sensor) (Seki, 1989). Followed by ionization, an electric field removes the ejected electrons whereas the positively charged particles are collected on a filter element and the electric current thus generated is measured by an inbuilt electrometer. The output signal measured by the electrometer is theoretically proportional to the PAHs mass collected by the filter element. It is worthwhile mentioning here that the PAS instrument can measure only "PM surface-bound total PAHs (SB-PAHs)" and cannot provide PAH speciation which will require techniques such as gas

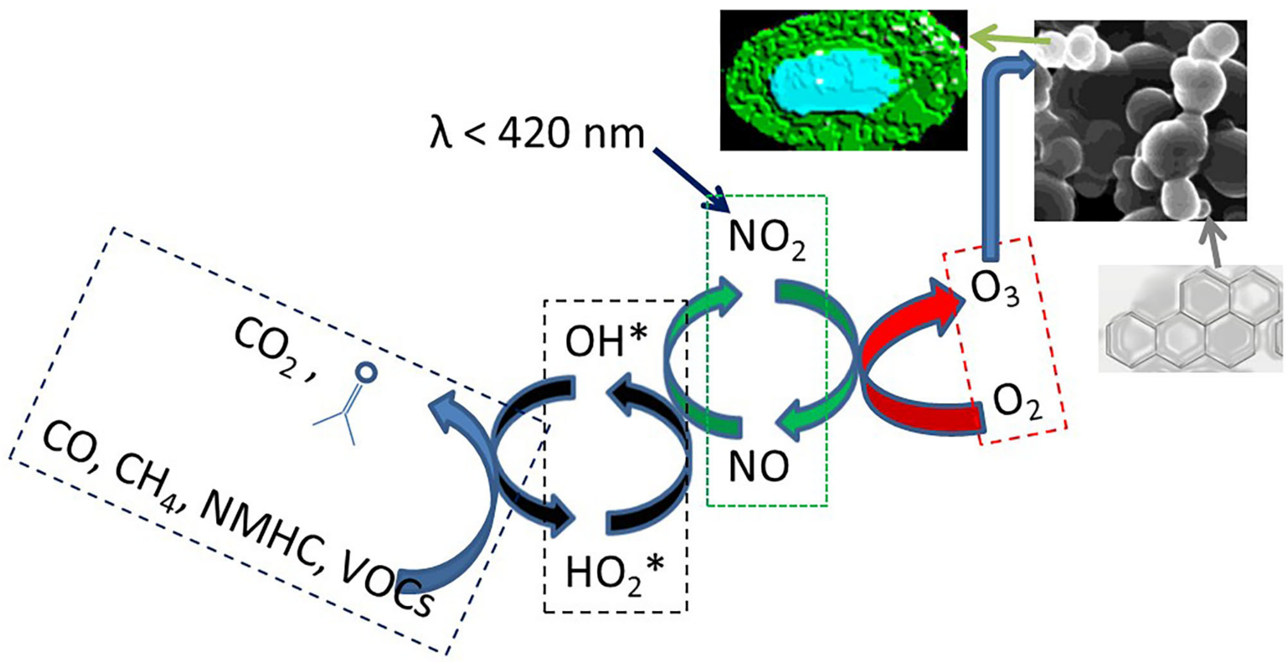

FIGURE 1 | A cartoon mimicking tropospheric coupled system of HO_x and NO_x cycle involving the oxidation of CO/NMHCs/VOCs/CH_4 and forming O_3 that further oxidizes SB-PAHs (and other organics) plausibly leading to the formation of CCN (cloud condensation nuclei).

TABLE 1 | Specific details of the instruments deployed in this campaign.

Parameters	Instrument (Model)	Manufacturer	Flow rate (LPM)	Data monitoring/ acquisition adds-on
SB-PAHs	Real-time Desktop PAS (Photoelectric Aerosol Sensor; Model # 2000)	EcoChem Analytics	1.98	PAH DAS (Data Acquisition System, v 6.0.0)
O_3	Ozone Analyzer (Model # 49i)	Thermo Scientific	0.65	Visual monitor and equipped with Ethernet port
CNC	CPC (Condensation particle counter; Model # 3007)	TSI Inc.	0.7	AIM (Aerosol Instrument Manager)

SB-PAHs, Surface-bound PAHs; CNC, Condensation nucleus concentration.

chromatography coupled with mass spectrometery (GC-MS) or liquid chromatography coupled with mass spectrometery (LC-MS), among others. The sample preparation followed by chemical analysis of PAHs by GC-MS or LC-MS is time-consuming and results into low-resolution data. Therefore, a sensor technique viz. PAS has been utilized for continuous monitoring of SB-PAHs in this study. The main advantages of PAS (works on aerosol photoionization technique) are its high sensitivity and ability to perform continuous (real-time) measurements with a response time of < 10 s. The PAS sensor for the detection of SB-PAHs has been developed by EcoChem Analytics, USA. The instrument was factory-calibrated for measuring PAHs concentrations up to 1,000 ng m^{-3} (limit of detection: 10 ng m^{-3}) with an uncertainty of < 20%. The instrument performance and background signal check were routinely assessed as per technical specifications provided by the manufacturer.

Real-Time Monitoring of O_3

Ozone Analyzer (Thermo Scientific; Model # 49i, **Table 1**, $\Delta t =$ 1-min, $n \approx 10$ k data points), designated by the United States Environmental Protection Agency (USEPA # EQOA-0880-047), is equipped with dual cell (sample and reference) and measures the concentration of O_3 in ambient air by UV-photometric technique. The O_3 measurement technique is a well-established technique, the details of which can be found in several papers, e.g., Lal et al. (2000). Briefly, O_3 molecule absorbs UV photon at a wavelength of 254 nm and the quantum of absorbed UV photons is directly proportional to the O_3 concentration. The instrument has a response time of 20 s with a detection limit of 5 ppb and can

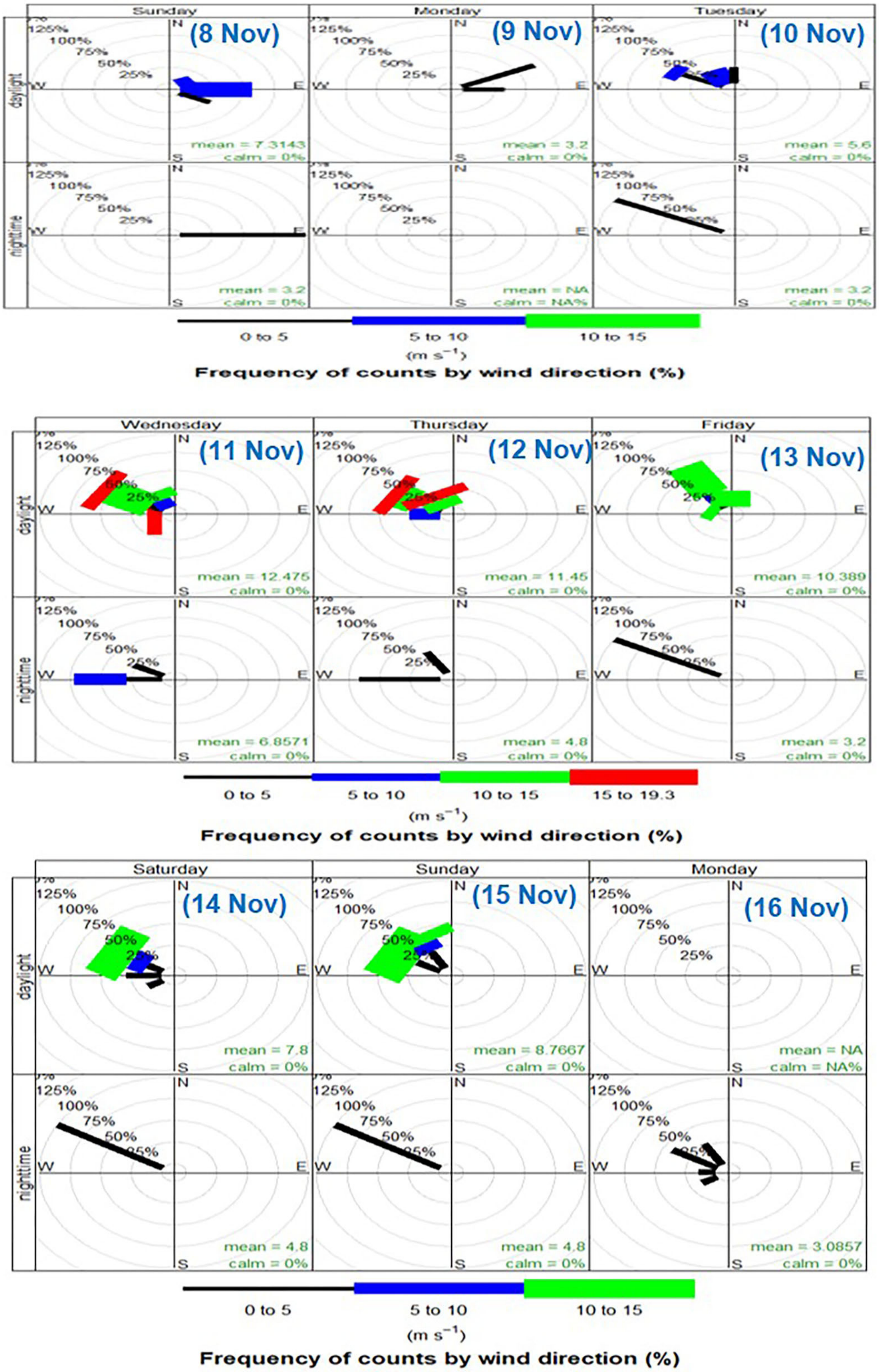

FIGURE 2 | Wind-rose diagram showing day-night variability pattern of wind speed (shown by different colors) and direction frequencies during the entire campaign.

TABLE 2 | Summary of meteorological conditions (Avg. ± SD) during the period of measurements.

Variable	Pre-Diwali		Diwali		Post-Diwali	
	Day-Value	Night-Value	Day-Value	Night-Value	Day-Value	Night-Value
[1]RH (%)	57 ± 15	82 ± 4	56 ± 15	78 ± 4	66 ± 11	79 ± 5
[1]T (°C)	26 ± 4	19 ± 0.5	26 ± 3.8	19 ± 0.5	22 ± 3.6	17 ± 2
[1]Wind (m/s)	5.0 ± 3.0	0.5 ± 0.4	11.0 ± 6.3	3.2 ± 1.6	3.9 ± 3.8	0.4 ± 0.3
[2]BLH (m)	1,819 ± 671	1,023 ± 458	1,811 ± 683	965 ± 589	1,373 ± 221	834 ± 364
[2]Sol flux (W/m^2)	536 ± 56	N/A	545 + 61	N/A	560 ± 41	N/A

[1]Data retrieved from on-campus (@IIT Kanpur) weather station; [2]Data retrieved from National Oceanic and Atmospheric Administration (NOAA). BLH represents boundary layer height and Sol flux is solar flux.

measure up to 200 ppm. The averaging time for data retrieval was set to 1 min (= 60 s). At the inlet, a Teflon particulate filter was mounted to not allow the entry of any particle in the gas analyzer. The measuring principle of O_3 analyzer is based on the Beer-Lambert law. The calibration and zero checks were performed as per the manufacturer's specifications for data quality control and assurance. The uncertainty on O_3 measurement is < 5%.

Real-Time Monitoring of CNC

Condensation particle counter (CPC model 3007, TSI Inc., **Table 1**, Δt = 1-min, $n \approx 10$ k data points) is a portable condensation nucleus counter (CNC) which measures the condensation nucleus concentration (CNC) in the size range of 0.01–1 µm. The field performance and single particle detection efficiency of this instrument are provided elsewhere (Hämeri et al., 2002; Devi et al., 2013). This instrument was factory calibrated and is capable of measuring particles concentrations as high as 10^5 cm^{-3}. The zero counts were routinely checked by connecting the CPC monitoring unit inlet with a High-Efficiency Particulate Air (HEPA) filter and we were always satisfied to conduct the measurements. The TSI CPC-3007 is operated with isopropyl alcohol as a condensing fluid. The uncertainty of cumulative CNC measurements by CPC was < 1%.

Lenschow-Type Analysis

The Lenschow-type analysis was carried out for each parameter viz. O_3, CNC, $PM_{2.5}$, and SB-PAHs. The details of $PM_{2.5}$ data set can be found elsewhere (Rajput and Gupta, 2020). Briefly, the hourly averaged data set was segregated into 3-different bins corresponding to UB (urban background), UB+FC+BB (urban background+firecrackers burst+biomass burning contribution), and UB+BB (urban background+biomass burning contribution) depending on their association with wind profile and information on FC burst (on Diwali). The north-westerly wind system favoring LRT-BB emissions was marked for the BB contribution. The UB was represented by the data set which has neither any contributions from FC burst nor from the LRT-BB. For details on finger-printing of sources, based on the analysis of air pollutants data coupled to prevailing winds, the reference is made to the original work by Lenschow et al. (2001).

RESULTS AND DISCUSSION

Wind Pattern Analyses

Real-time diurnal measurements have encouraged us to look into more detailed features of atmospheric composition variability during the campaign. The wind direction and wind-speed (refer to scale at the bottom, **Figure 2**) along with the statistics (given on each panel) were studied through the wind-rose plot. Statistical and data analysis have been carried out utilizing openair package in R software (Carslaw and Ropkins, 2012). The frequency pattern of wind along with its direction and speed are shown here for entire sampling dates during daylights (aka daytime: from 07:00 h to 17:00 h local time, top panel) and nighttime (from 00:00 h to 06:59 h and from 17:01 h to 23:59 h; bottom panel). The winds for each one of the sampling dates (i.e., from 08th to 16th Nov) are shown under the dedicated panel both for the daylight and nighttime periods (**Figure 2**).

During the entire campaign, the winds were calm for most of the nighttime hours (80–93%) with an average speed < 1 m s^{-1}, exception being on Diwali festival night (average speed = 3.2 m s^{-1}). The wind patterns during daylight hours suggested that on 08th and 09th Nov (pre-Diwali) winds were easterly to north-easterly whereas on the 10th Nov (also a pre-Diwali period) the wind-direction changed to north–to–north-westerly. During the entire pre-Diwali period (08th—10th Nov) the daytime wind speed was < 10 m s^{-1}. More interestingly, the winds on Diwali festival day (11th Nov) continued blowing from the north-west direction with some contributions from south direction too. As far as the wind speed is concerned, it was > 15 m s^{-1} with an average value of 11 m s^{-1} on the 11th Nov (Diwali festival daylight hours). During rest of the dates (post-Diwali from 12th to 16th Nov) the prevailed winds were mainly north-westerly both during daylight and nighttime hours (**Figure 2**). It is worthwhile mentioning that during October–November period the north-westerly winds favor transport of emissions from source-region of open biomass (paddy-residue) burning, active in upwind IGP, to the downind locations and marine atmospheric boundary layer over the Bay of Bengal (Kaskaoutis et al., 2014; Rajput et al., 2014). Furthermore, for the entire campaign, during daylight hours the winds were calm for < 22% of the time, exception being on 10th Nov (calm wind: 33%). A day-night summary of meteorological conditions

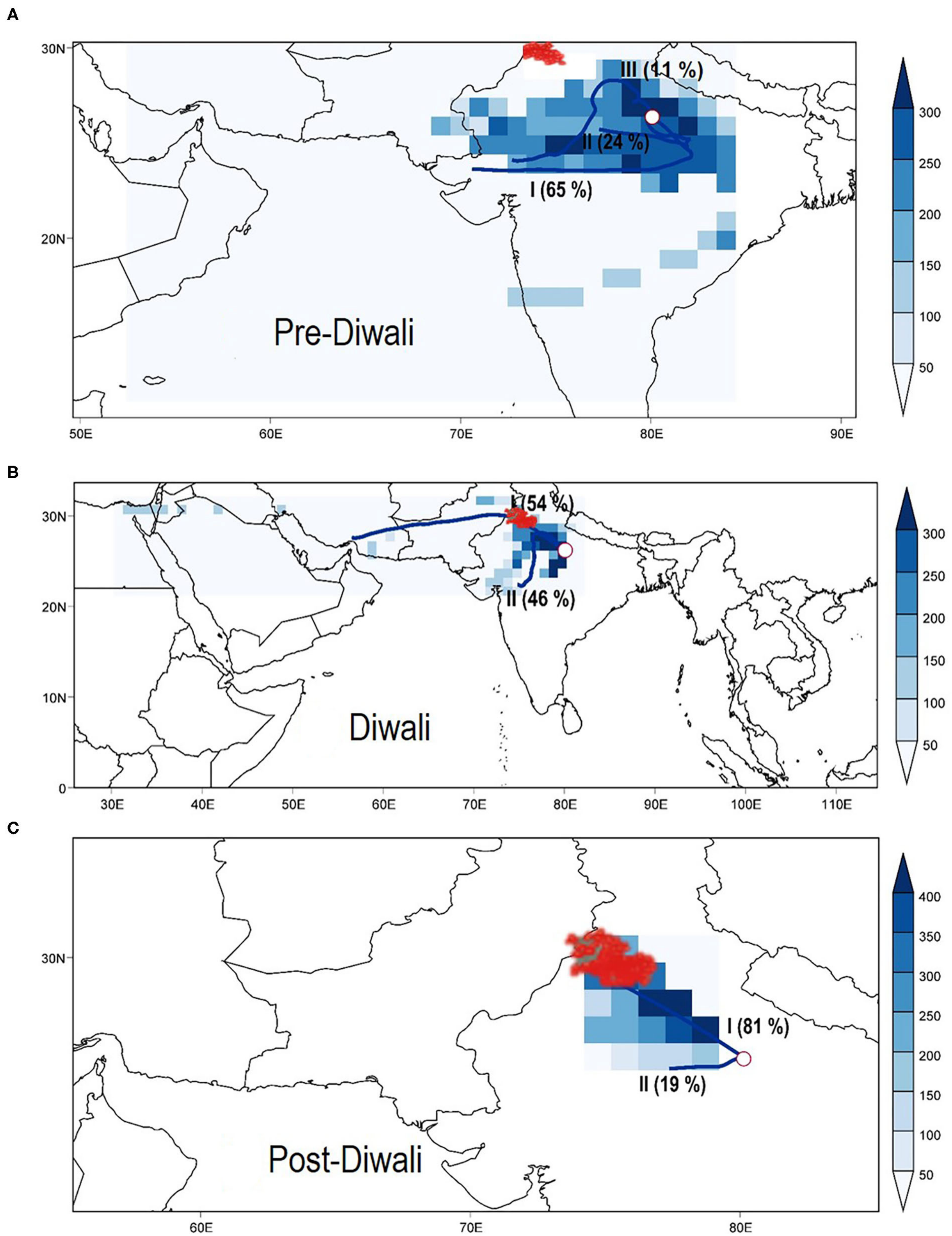

FIGURE 3 | Air-mass cluster analysis and fire-count imageries (shown by red-circles, over source region of biomass burning) during **(A)** pre-Diwali, **(B)** Diwali, and **(C)** post-Diwali periods.

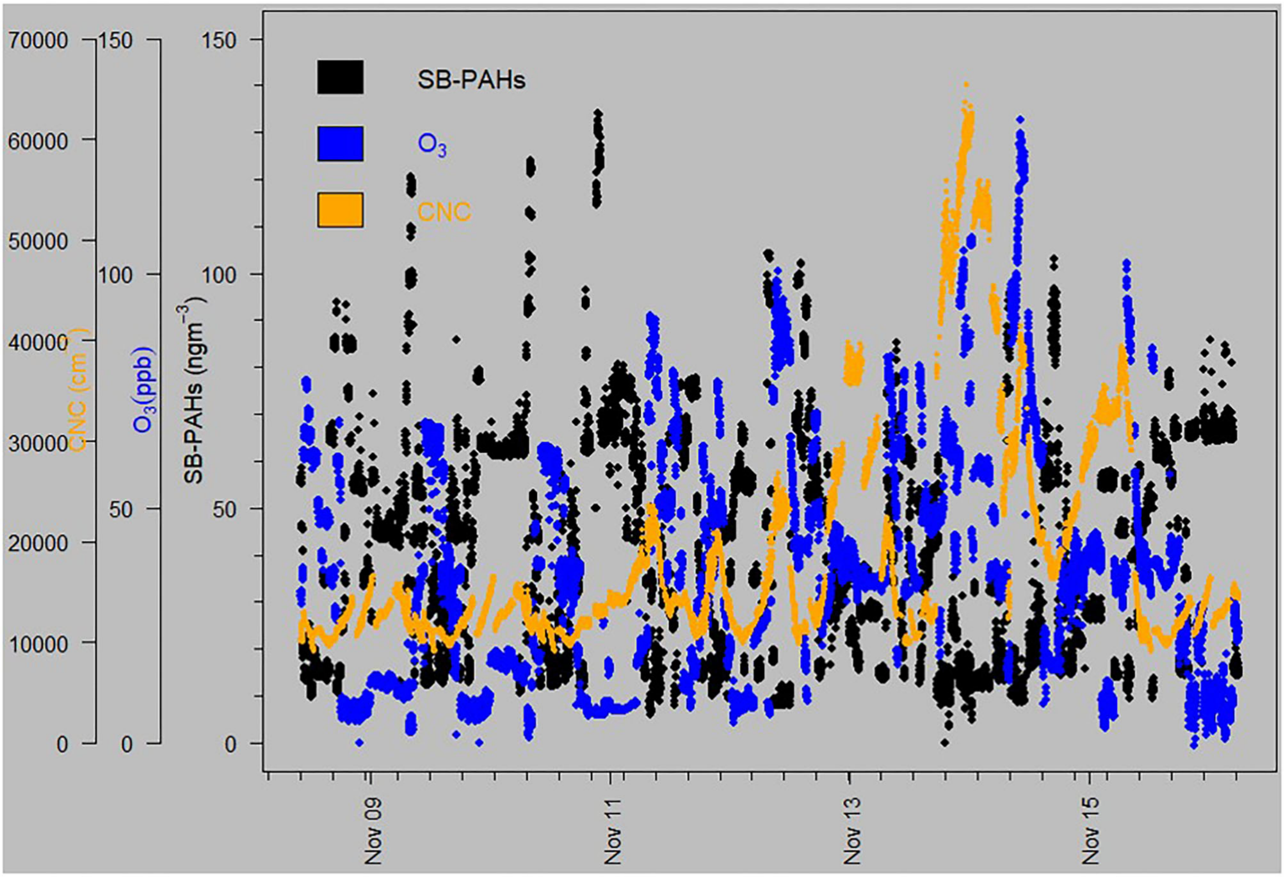

FIGURE 4 | Diurnal profile of simultaneously measured surface-bound PAHs, ozone, and CPC-based particle's number concentration (CNC) during entire campaign.

during pre-Diwali, Diwali, and post-Diwali periods are given in **Table 2**.

Fire-Count Imageries (Over the Source-Region of Biomass Burning Emissions in IGP) and Air-Mass Cluster Analysis

MODIS (Moderate Resolution Imaging Spectroradiometer sensor, onboard NASA Terra and Aqua satellite) fire-count imageries (spatial resolution: 10 km) showing an intense open biomass (agricultural-waste paddy-residue) burning activity in north-western part of during the study period are shown in **Figure 3**. This observation is quite consistent with earlier observations reporting massive emissions of air pollutants from agricultural-waste burning in upwind IGP (Rajput et al., 2014, 2018). The details on land-use activity pattern and mapping of source-region of biomass burning emissions in upwind IGP are adopted from previous studies and shown in the **Supplementary Material**. Furthermore, a GIS-based open-source software viz. TrajStat was utilized for the air-mass cluster analysis (**Figure 3**). The cluster analysis is a widely used tool to understand the influence of cluster of trajectories on ambient level of air pollutants at the receptor site (Bansal et al., 2019; Rajput and Gupta, 2020). Briefly, in the cluster analysis method, the measured air pollutant concentrations are assigned to the corresponding trajectories and the nearest trajectories are clustered according to an angle distance function (Sirois and Bottenheim, 1995). Relevant details on cluster analysis are given elsewhere (Wang et al., 2009). To carry out the cluster analysis, a 5-day air-mass back trajectories (AMBTs, GDAS 0.5°m, @ 1,000 m above ground level) data have been utilized. These AMBTs were retrieved from NOAA HYSPLIT (Hybrid Single-Particle Lagrangian Integrated Trajectory) model (Draxler and Rolph, 2003; Stein et al., 2015).

One of the observations from **Figure 3** relates that if a trajectory cluster is passing more frequently through NW-direction to the receptor site then it is expected to have elevated levels of air pollutants from LRT-BB as compared to the case when trajectories were arriving from other directions. Let us now analyze the clusters shown in **Figure 3**. During Pre-Diwali period (**Figure 3A**), there was very little influence of NW-air masses (11%) but more importantly not passing through the source-region of biomass burning emission. It is important to mention here that these 11% NW-air masses were prevailed on 10th Nov. Furthermore, during the Post-Diwali period (**Figure 3C**), majority of air masses (81%) were originating from source-region of biomass burning emission and arriving from NW-direction

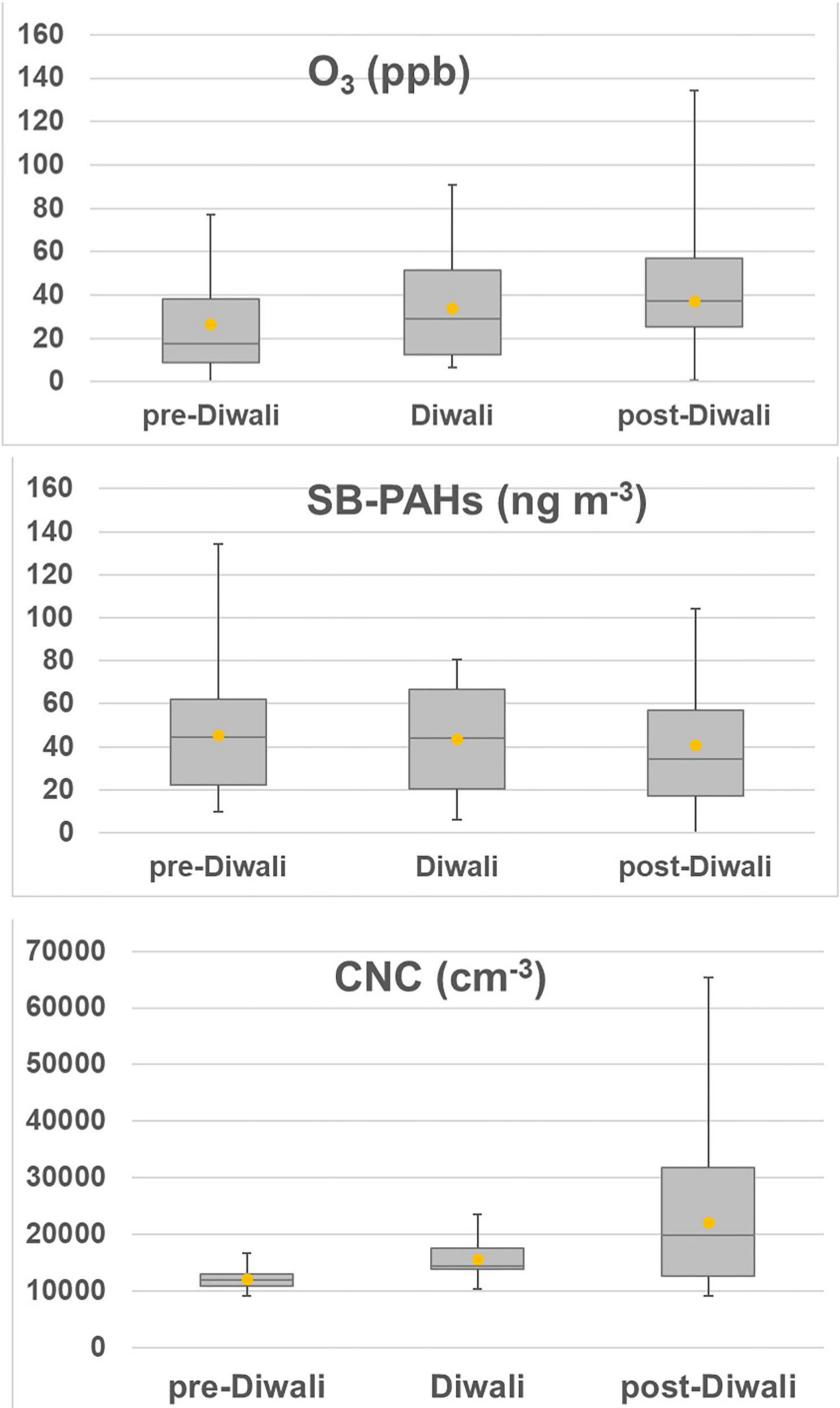

FIGURE 5 | Boxplot showing a summary of overall variability [minimum, maximum, median (horizontal line), and mean (filled circle)] of O_3, SB-PAHs, and CNC during pre-Diwali, Diwali, and post-Diwali periods.

TABLE 3 | Concentration [Avg.±SD; median; range (no. of samples)] of O_3, SB-PAHs and CNC during the three events (pre-Diwali, Diwali, and post-Diwali).

Events	O_3 (ppb)	SB-PAHs (ng m^{-3})	CNC (cm^{-3})
pre-Diwali	26.5 ± 20.5; 17.5; 0.0–77.3 (n = 3,652)	45.5 ± 25.1; 44.7; 9.6–134.1 (n = 3,666)	12,069 ± 1,499; 11,880; 9,088–16,652 (n = 3,126)
Diwali	33.9 ± 22.3; 29.0; 6.7–91.0 (n = 1,380)	43.7 ± 21.3; 44.1; 5.9–80.7 (n = 1,396)	15,689 ± 2,899; 14,454; 10,406–23,628 (n = 1,240)
post-Diwali	37.3 ± 16.0; 37.1; 0.7–134.1 (n = 5,919)	41.0 ± 12.0; 34.1; 0.0–104.3 (n = 5,767)	22,189 ± 7,831; 19,844; 9,088–65,410 (n = 5,078)

to the receptor site. Summing up, clubbing the data set from our campaign, satellite observations on fire-counts along with the cluster analysis, it can be summarized that the receptor site (at Kanpur) was influenced with the LRT-BB emissions through NW-direction (from upwind IGP) mainly during post-Diwali and Diwali periods.

Co-variability Analysis of SB-PAHs, O_3, and CNC

The co-variability features of SB-PAHs (n = 10,829), O_3 (n = 10,951), and the sub-micron particles number concentrations (CNC, n = 9,444) are shown in **Figure 4**. It is evident from this figure that the high abundance of CNC (i.e., submicron particles, orange dots) was associated with higher concentration of O_3 (blue dots) and with the lower concentration of SB-PAHs (black dots, **Figure 4**). Thus, field based observations revealed that peaks in O_3 concentration were associated with dips in SB-PAHs concentration. This observation is much more pronounced during Diwali and post-Diwali period (i.e., from 11th to 16th Nov). Further features in this regard have been discussed in the following section. The summary of the data set is shown in **Figure 5** and also given in **Table 3**. We have carried out statistical two-tailed t-test analysis to infer about difference in measured species concentrations during Diwali as compared to those in Pre-Diwali and Post-Diwali periods. Accordingly, comparing the concentrations during Diwali vs. Pre-Diwali it revealed that O_3 (t = 11.1; $p < 0.0001$), SB-PAHs (t = 2.4; $p < 0.05$), and CNC (t = 53.9; $p < 0.0001$) were significantly different during these periods. Furthermore, comparing the concentrations during Diwali vs. Post-Diwali periods it revealed that O_3 (t = 4.5; $p < 0.0001$), SB-PAHs (t = 6.3; $p < 0.05$), and CNC (t = 28.7; $p < 0.0001$) were also significantly different during these periods.

Correlation Analyses of O_3 vs. SB-PAHs as a Function of CNC

A 3-D linear correlation plot is shown in **Figure 6** for three events (pre-Diwali, Diwali, and post-Diwali) and two periods (daylight and nighttime). The first assessment on maximum concentrations revealed that O_3 was < 150 ppb, SB-PAHs is < 150 ng m^{-3} and CNC is < 66 k cm^{-3} during the entire campaign (**Figure 6**). The CNC was < 20 k cm^{-3} during pre-Diwali, < 30 k cm^{-3} during Diwali and < 66 k cm^{-3} during post-Diwali (CNC concentration pattern: post-Diwali >Diwali >pre-Diwali). Furthermore, the maximum concentrations of CNC were observed in nighttime hours during the post-Diwali period (12th−16th Nov). The correlation analyses revealed that during daylight hours, O_3 and SB-PAHs were significantly anti-correlated on pre-Diwali ($R^2 = 0.57$, $p < 0.05$), Diwali ($R^2 = 0.71$, $p < 0.05$) and post-Diwali period ($R^2 = 0.71$, $p < 0.05$). During nighttime hours, the anti-correlation was found to be weak during pre-Diwali ($R^2 = 0.09$, $p > 0.05$) and post-Diwali period ($R^2 = 0.37$, $p > 0.05$). However, the anti-correlation was found to be strong during Diwali ($R^2 = 0.71$, $p < 0.05$). It is worthwhile mentioning here that a previous study has suggested the production of ozone from firecrackers burst (Attri et al., 2001). Summing up, the linear correlation analysis revealed that SB-PAHs and O_3 have moderate-to-high association ($p < 0.05$) during all the period exception being that on pre-Diwali and post-Diwali nighttime while the anti-correlation was weak ($p > 0.05$). Furthermore, the CNC concentrations showed a large gradient in the correlation plot during Diwali and post-Diwali (varying from ∼10 k to 65 k particles cm^{-3}) as O_3 increases and SB-PAHs decreases. However, the overall variability in CNC during the pre-Diwali period, varying from ∼10 k to 16 k cm^{-3}, is quite less as compared to those in Diwali and post-Diwali periods (also refer to **Figure 5**). It is important to note here that maximum CNC concentrations were observed during post-Diwali followed by Diwali and then pre-Diwali. Toward this, the explanation for higher abundance of CNC during Diwali period is attributable to additional input (i.e., besides urban background emissions) from FC burst and LRT-BB emissions. However, the higher CNC during post-Diwali period was by-and-large due to additional input from LRT-BB. It is worthwhile mentioning that the poor ventilation and shallower boundary layer height could also be responsible for a small fractional rise in the air pollutant's levels during the post-Diwali period (**Table 2**). The anti-correlation between SB-PAHs and O_3 could be attributable to chemical oxidation of SB-PAHs by O_3. It has been suggested previously that such chemical reactions have implications to enhanced CCN activity and toxicity of ambient aerosols (Perraudin et al., 2007; Kaiser et al., 2011).

Lenschow-Type Analysis: Assessment of Predominant Source Impact Over an Urban Background

Before we discuss on the Lenschow-type analysis and its application for quantifying emissions impact above the urban background level, let us first understand the need for applying this analysis. One of the simple ways to do that is to look into similar type of studies (e.g., from previous Diwali campaigns) and their conclusions drawn. There are two things which we need to reiterate here that (i) Diwali is celebrated during a day in October–November period and, (ii) almost the entire IGP experiences massive emisssions throughout these 2 months period from LRT-BB. Now, let us discuss briefly how the previous studies around Diwali period have assessed the change in pollutants concentration due to the FC burst. Previous researchers have documented very systematically the ambient concentrations of air pollutants [both particulate matter (PM) as well as trace gases] around Diwali period (Singh et al., 2010; Chatterjee et al., 2013; Ambade, 2018). For example, a study from an upwind IGP location at Delhi has documented pollutants concentrations for 6 years from 2002 to 2007 (Singh et al., 2010). Another study from a downwind location at Jamshedpur has documented PM and trace gases concentrations around Diwali period in 2014 (Ambade, 2018). From a further downwind location at Kolkata in IGP, a study has reported lots of species including metals, ionic composition in PM_{10} and SO_2 around Diwali period

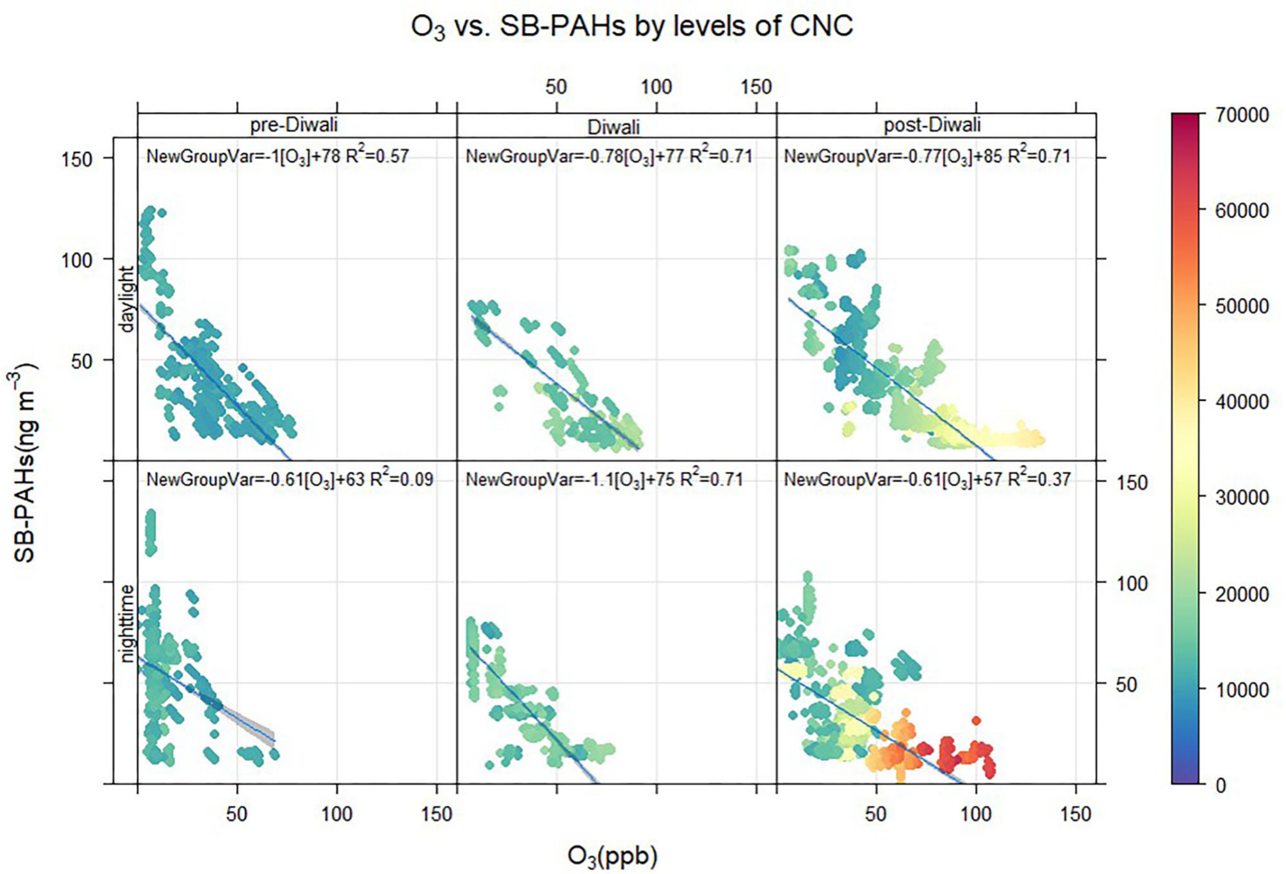

FIGURE 6 | Linear regression analyses ($p < 0.05$, exception being on pre-Diwali and post-Diwali nighttime when $p > 0.05$) of O_3 (X-axis, in ppb) vs. SB-PAHs (Y-axis, in ng m^{-3}) by levels of CPC-based particle's number concentration (CNC, Z-axis in cm^{-3} shown on a scale at the right side of the plot) during pre-Diwali, Diwali, and post-Diwali periods for both daylight and nighttime hours.

TABLE 4 | Lenschow-type analysis to estimate episodic source impact over the local background emission in central IGP at Kanpur.

Sr. No	Event/Analysis	Emission	CNC (cm^{-3})	O_3 (ppb)	SB-PAHs (ng m^{-3})	$^{\$}PM_{2.5}$ (μg m^{-3})
1	Pr-D*	UB (no FC + no BB)	11,915 ± 396	28.4 ± 7.2	41.9 ± 4.8	286 ± 74
2	D	UB + FC + BB	15,689 ± 2,899	33.9 ± 22.3	43.7 ± 21.3	359 ± 71
3	Po-D	UB + BB	22,189 ± 7,831	37.3 ± 16.0	41.0 ± 12.0	390 ± 172
4	(Po-D–Pr-D)/Pr-D	BB/UB	0.86	0.31	−0.02	0.36
5	(Po-D–D)/Pr-D	FC/UB	0.54	0.12	−0.06	0.11

*In view of NW winds on 10th Nov, for Lenschow-type analysis the data set measured only on 08th and 09th Nov are included to represent the impact of urban background (UB) emissions. FC, firecrackers burst; BB, biomass (paddy-residue) burning emission through long-range transport (LRT-BB); D, Diwali; Pr-D, pre-Diwali; Po-D, post-Diwali.

$^{\$}$For details on $PM_{2.5}$ data set, the reference is made to our recent publication (Rajput and Gupta, 2020).

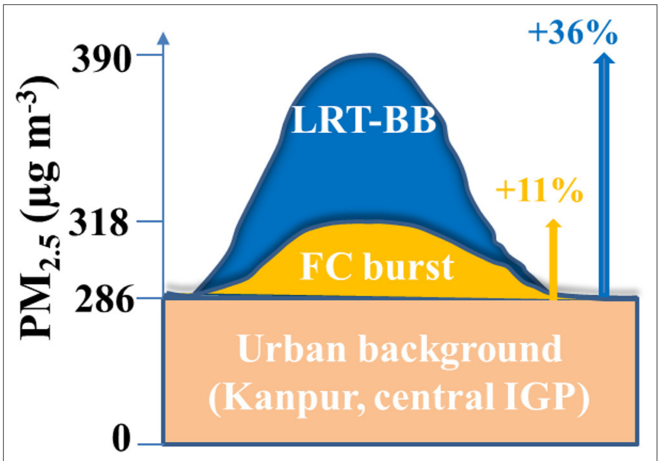

FIGURE 7 | Sources contributions schematic (deduced from Lenschow-type analysis) over an urban agglomeration (Kanpur) in central Indo-Gangetic Plain.

in 2010 (Chatterjee et al., 2013). It is important to mention here that all these aforementioned studies have compared on a 1-to-1 basis the pre-/post-Diwali emissions with Diwali emissions and attributed the change in a particular polutant's concentration on Diwali due to the FC burst. These studies from various locations in IGP concluded that due to FC burst the pollutants concentrations do rise by a factor of 1.5–3 or 50–300%. However, if these previous studies (from the IGP) would have accounted for massive emissions from LRT-BB then the actual rise in pollutants concentrations due to the FC burst could have been quantified. With this regional background information, here we present an approach called the Lenschow-type analysis which would serve the purpose of quantifying emissions due to FC burst and LRT-BB over the regional background.

Lenschow et al. (2001) proposed an approach in 2001 to quantitatively estimate the contribution of PM sources spiking pollutants concentration above the regional background level. Their idea was basically to conduct a set of ambient PM measurements (spatially resolved) representative of regional background and those capturing records for episodic or long-range transported source components. Subsequently, grouping the data set into bins of sources corresponding to regional background emission and then estimating the contribution of episodic source and long-range transport was suggested in their study. The Lenschow-type analysis (**Table 4**) has been carried out to estimate quantitatively the impact of additional sources leading to increase (above the UB) the levels of air pollutants (Lenschow et al., 2001). It is worthwhile mentioning here that in this study we have applied the similar approach but on a temporally resolved ambient data set. Based on the Lenshchow-type analysis, we have estimated that only due to FC burst the CNC concentrations were increased by 54% whereas due to the impact from LRT-BB the CNC concentrations were increased by 86% over the urban background concentration level (at the receptor site). Thus, LRT-BB emissions appeared to be the major source (as evident from the increase in CNC concentrations by 86% than the urban background) of air pollution during the study period and results in enhancing the CNC burden by a facor of 1.6 when compared to that with the FC burst. Likewise, Lenschow-type analysis further revealed that O_3 concentrations increased by 31% and 12% due to the LRT-BB and FC burst, respectively, over the urban background emission. However, in sharp contrast the SB-PAHs concentrations were found to be decreased by 2 and 6% (over the urban backgound emission), respectively, during the LRT-BB emission and FC burst (**Table 4**). Lenschow-type analysis also revealed that the urban background concentration of daily $PM_{2.5}$ was 286 µg m^{-3} (**Table 4**). The FC burst and LRT-BB increased the daily $PM_{2.5}$ concentration by 11% and 36%, respectively over its urban background level (286 µg m^{-3}) (**Figure 7**). The application of Lenschow-type analysis in this study from IGP has led to the new insights of estimating the impact of additional sources spiking the pollutants concentrations over typical emissions within an urban agglomeration.

CONCLUSIONS

In this study, we have conducted a 9 day (from 8th to 16th Nov 2015) long real-time (high-resolution: 1 min, $n \approx$ 10 k data points) measurement campaign assessing the diurnal profiles of SB-PAHs, O_3 and CNC during pre-Diwali (8th–10th Nov), Diwali (11th Nov) and post-Diwali periods (12th–16th Nov). Wind analysis indicated that initially on 08th and 09th Nov the winds were easterly–to–north-easterly with intensity (mostly $<$ 5 m s^{-1}) whereas from 10th onwards the winds were predominantly north-westerly (varying from 10 m s^{-1} to $>$ 15 m s^{-1}). A quite similar inference has been made based on the air-mass cluster analysis. The source-region of large-scale post-harvest agricultural-waste burning emissions lies in the north-west direction of the study region. Under prevailing NW winds, the LRT-BB emissions appeared to change the atmospheric composition and chemistry over the central IGP. Higher concentrations of CNC, $PM_{2.5}$, and O_3 during Diwali are attributable to the additional input from FC burst, and substantial contribution from LRT-BB emissions. However, higher concentrations of CNC, $PM_{2.5}$, and O_3 on post-Diwali period are mainly due to the LRT-BB emissions.

The daily average concentrations of O_3 and CNC exhibited a quite similar pattern: post-Diwali >Diwali >pre-Diwali, whereas the SB-PAHs showed a different pattern with the highest concentration during pre-Diwali >Diwali >post-Diwali (trends are confirmed based on the two tailed *t*-test). Their diurnal profile also relates to the similar findings that when CNC and O_3 concentrations peaked up then the SB-PAHs showed a dip and vice-versa. The daylight and nighttime linear correlation analyses of SB-PAHs and O_3 as a function of CNC were carried out, and the results showed a moderate to strong anti-correlation during the entire study period, with exceptions being observed for pre-Diwali and post-Diwali nighttime hours when the correlation was weak. Based on the Lenshchow-type analysis, it has been estimated from this study that the CNC and O_3 concentrations were increased (over UB) by 86 and 31%, respectively due to the LRT-BB emissions. Furthermore, only due to the FC burst the CNC and O_3 concentrations were increased by 54 and 12%, respectively. Lenschow-type analysis further revealed that FC burst and LRT-BB increased the daily $PM_{2.5}$ concentration over the urban agglomeration by 11% and 36%, respectively. However, the SB-PAHs concentrations were found to be decreased by 2 and 6% during LRT-BB emissions and FC burst, respectively. This study, highlighting the plausibility of surface-layer (heterogeneous-phase) reactivity of SB-PAHs with O_3 has potential implications to enhanced particle's toxicity and CCN activity of aerosols over the IGP. Future studies would be required to examine the causal inference of the chemical reactivity of individual PAH.

DATA AVAILABILITY STATEMENT

The raw data supporting the conclusions of this article will be made available by the authors, without undue reservation.

AUTHOR CONTRIBUTIONS

PR and TG conceptualized this study. The data analysis presented in this paper was performed by PR. The manuscript has been written by PR. All authors were involved in collection of data during entire campaign used in this analysis. All authors discussed the results and commented on the manuscript.

FUNDING

TG was thankful to the Indian National Science Academy for partial funding support [INSA Grant # SP/YSP/113/2015(1091)] to conduct this study.

ACKNOWLEDGMENTS

Authors thank Prof. Shivam Tripathi for providing access to meteorological data from met-station situated nearby the sampling site inside the IITK campus. We are also thankful to Mr. Sanjay Gupta and Rajendra Maurya for technical support during successful conduct of this campaign. PR thanks to Onam Bansal (PhD, Punjabi University, Patiala) for sharing her expertise in cluster analysis. We express our sincere thanks to the reviewers for providing constructive comments and suggestions.

SUPPLEMENTARY MATERIAL

The Supplementary Material for this article can be found online at: https://www.frontiersin.org/articles/10.3389/frsc.2020.622050/full#supplementary-material

REFERENCES

Ackerman, A. S., Toon, O. B., and Hobbs, P. V. (1994). Reassessing the dependence of cloud condensation nucleus concentration on formation rate. *Nature* 367, 445–447. doi: 10.1038/367445a0

Agarwal, A. K., Singh, A. P., Gupta, T., Agarwal, R. A., Sharma, N., Rajput, P., et al. (2018). Mutagenicity and cytotoxicity of particulate matter emitted from biodiesel-fueled engines. *Environ. Sci. Technol.* 52, 14496–14507. doi: 10.1021/acs.est.8b03345

Ambade, B. (2018). The air pollution during Diwali festival by the burning of fireworks in Jamshedpur city, India. *Urban Clim.* 26, 149–160. doi: 10.1016/j.uclim.2018.08.009

Andreae, M. O., and Ramanathan, V. (2013). Climate's dark forcings. *Science* 340, 280–281. doi: 10.1126/science.1235731

Attri, A. K., Kumar, U., and Jain, V. K. (2001). Formation of ozone by fireworks. *Nature* 411:1015. doi: 10.1038/35082634

Bansal, O., Singh, A., and Singh, D. (2019). Characteristics of Black Carbon aerosols over Patiala Northwestern part of the IGP: source apportionment using cluster and CWT analysis. *Atmos. Poll. Res.* 10, 244–256. doi: 10.1016/j.apr.2018.08.001

Carslaw, D. C., and Ropkins, K. (2012). Openair — an R package for air quality data analysis. *Environ. Modell. Softw.* 27–28, 52–61. doi: 10.1016/j.envsoft.2011.09.008

Chatterjee, A., Sarkar, C., Adak, A., Mukherjee, U., Ghosh, S. K., and Raha, S. (2013). Ambient air quality during Diwali festival over Kolkata – a mega-city in India. *Aerosol Air Qual. Res.* 13, 1133–1144. doi: 10.4209/aaqr.2012.03.0062

Che, H. C., Zhang, X. Y., Wang, Y. Q., Zhang, L., Shen, X. J., Zhang, Y. M., et al. (2016). Characterization and parameterization of aerosol cloud condensation nuclei activation under different pollution conditions. *Sci. Rep.* 6:24497. doi: 10.1038/srep24497

Devi, J. J., Gupta, T., Jat, R., and Tripathi, S. N. (2013). Measurement of personal and integrated exposure to particulate matter and co-pollutant gases: a panel study. *Environ. Sci. Poll. Res. Int.* 20, 1632–1648. doi: 10.1007/s11356-012-1179-3

Draxler, R. R., and Rolph, G. D. (2003). *HYSPLIT (Hybrid Single-Particle Lagrangian Integrated Trajectory) Model Access via NOAA ARL READY Website. NOAA Air Resources Laboratory*. Silver Spring, MD. Available online at: http://www.arl.noaa.gov/ready/hysplit4.html (accessed February 3, 2019).

George, C., Ammann, M., D'Anna, B., Donaldson, D. J., and Nizkorodov, S. A. (2015). Heterogeneous photochemistry in the atmosphere. *Chem. Rev.* 115, 4218–4258. doi: 10.1021/cr500648z

Hämeri, K., Koponen, I. K., Aalto, P. P., and Kulmala, M. (2002). The particle detection efficiency of the TSI-3007 condensation particle counter. *J. Aerosol Sci.* 33, 1463–1469. doi: 10.1016/S0021-8502(02)00090-3

Izhar, S., Rajput, P., and Gupta, T. (2018). Variation of particle number and mass concentration and associated mass deposition during Diwali festival. *Urban Clim.* 24, 1027–1036. doi: 10.1016/j.uclim.2017.12.005

Jethva, H., Torres, O., Field, R. D., Lyapustin, A., Gautam, R., and Kayetha, V. (2019). Connecting crop productivity, residue fires, and air quality over Northern India. *Sci. Rep.* 9, 16594. doi: 10.1038/s41598-019-52799-x

Joshi, M., Khan, A., Anand, S., and Sapra, B. K. (2016). Size evolution of ultrafine particles: differential signatures of normal and episodic events. *Environ. Poll.* 208, 354–360. doi: 10.1016/j.envpol.2015.10.001

Kaiser, J. C., Riemer, N., and Knopf, D. A. (2011). Detailed heterogeneous oxidation of soot surfaces in a particle-resolved aerosol model. *Atmos. Chem. Phys.* 11, 4505–4520. doi: 10.5194/acp-11-4505-2011

Kaskaoutis, D. G., Kumar, S., Sharma, D., Singh, R. P., Kharol, S. K., Sharma, M., et al. (2014). Effects of crop residue burning on aerosol properties, plume characteristics, and long-range transport over northern India. *J. Geophys. Res. Atmos.* 119, 5424–5444. doi: 10.1002/2013JD021357

Lal, S., Naja, M., and Subbaraya, B. H. (2000). Seasonal variations in surface ozone and its precursors over an urban site in India, *Atmos. Environ.* 34, 2713–2724. doi: 10.1016/S1352-2310(99)00510-5

Lenschow, P., Abraham, H. J., Kutzner, K., Lutz, M., Preuß, J. D., and Reichenbächer, W. (2001). Some ideas about the sources of PM10. *Atmos. Environ.* 35, S23–S33. doi: 10.1016/S1352-2310(01)00122-4

Maria, S. F., Russell, L. M., Gilles, M. K., and Myneni, S. C. (2004). Organic aerosol growth mechanisms and their climate-forcing implications. *Science* 306:1921. doi: 10.1126/science.1103491

Marr, L. C., Dzepina, K., Jimenez, J. L., Reisen, F., Bethel, H. L., Arey, J., et al. (2006). Sources and transformations of particle-bound polycyclic aromatic hydrocarbons in Mexico City. *Atmos. Chem. Phys.* 6, 1733–1745. doi: 10.5194/acp-6-1733-2006

Menon, S., Hansen, J., Nazarenko, L., and Luo, Y. (2002). Climate effects of black carbon aerosols in China and India. *Science* 297, 2250–2253. doi: 10.1126/science.1075159

Nguyen, T. K. V., Zhang, Q., Jimenez, J. L., Pike, M., and Carlton, A. G. (2016). Liquid water: ubiquitous contributor to aerosol mass. *Environ. Sci. Technol. Lett.* 3, 257–263. doi: 10.1021/acs.estlett.6b00167

Niessner, R., and Walendzik, G. (1989). The photoelectric aerosol sensor as a fast-responding and sensitive detection system for cigarette smoke analysis. *Z. Anal. Chem.* 333, 129–133. doi: 10.1007/BF00474022

Perraudin, E., Budzinski, H., and Villenave, E. (2007). Kinetic study of the reactions of ozone with polycyclic aromatic hydrocarbons adsorbed on atmospheric model particles. *J. Atmos. Chem.* 56, 57–82. doi: 10.1007/s10874-006-9042-x

Pöhlker, M. L., Ditas, F., Saturno, J., Klimach, T., de Angelis, I. H., Araùjo, A. C., et al. (2018). Long-term observations of cloud condensation nuclei over the Amazon rain forest – Part 2: variability and characteristics of biomass burning, long-range transport, and pristine rain forest aerosols. *Atmos. Chem. Phys.* 18, 10289–10331. doi: 10.5194/acp-18-10289-2018

Rajput, P., and Gupta, T. (2020). Instrumental variable analysis and atmospheric and aerosol chemistry. *Front. Environ. Sci.* 8, 1–13. doi: 10.3389/fenvs.2020.609846

Rajput, P., Mandaria, A., Kachawa, L., Singh, D. K., Singh, A. K., and Gupta, T. (2016). Chemical characterisation and source apportionment of PM_1 during massive loading at an urban location in Indo-gangetic plain: impact of local sources and long-range transport. *Tellus B: Chem. Phys. Meteorol.* 68:30659. doi: 10.3402/tellusb.v68.30659

Rajput, P., Sarin, M., Sharma, D., and Singh, D. (2014). Characteristics and emission budget of carbonaceous species from post-harvest agricultural-waste burning in source region of the Indo-Gangetic Plain. *Tellus B Chem. Phys. Meteorol.* 66:21026. doi: 10.3402/tellusb.v66.21026

Rajput, P., Sarin, M. M., Rengarajan, R., and Singh, D. (2011). Atmospheric polycyclic aromatic hydrocarbons (PAHs) from post-harvest biomass burning emissions in the Indo-Gangetic Plain: isomer ratios and temporal trends. *Atmos. Environ.* 45, 6732–6740. doi: 10.1016/j.atmosenv.2011.08.018

Rajput, P., Singh, D. K., Singh, A. K., and Gupta, T. (2018). Chemical composition and source-apportionment of sub-micron particles during wintertime over Northern India: New insights on influence of fog-processing. *Environ. Poll.* 233, 81–91. doi: 10.1016/j.envpol.2017.10.036

Ramana, M. V., Ramanathan, V., Feng, Y., Yoon, S. C., Kim, S. W., Carmichael, G. R., et al. (2010). Warming influenced by the ratio of black carbon to sulphate and the black-carbon source. *Nat. Geosci.* 3, 542–545. doi: 10.1038/ngeo918

Rastogi, N., Singh, A., and Satish, R. (2019). Characteristics of submicron particles coming from a big firecrackers burning event: implications to atmospheric pollution. *Atmos. Poll. Res.* 10, 629–634. doi: 10.1016/j.apr.2018.11.002

Rudich, Y., Donahue, N. M., and Mentel, T. F. (2007). Aging of organic aerosol: bridging the gap between laboratory and field studies. *Ann. Rev. Phys. Chem.* 58, 321–352. doi: 10.1146/annurev.physchem.58.032806.104432

Ruehl, C. R., Davies, J. F., and Wilson, K. R. (2016). An interfacial mechanism for cloud droplet formation on organic aerosols. *Science* 351:1447–1450. doi: 10.1126/science.aad4889

Sahu, L. K., Tripathi, N., and Yadav, R. (2017). Contribution of biogenic and photochemical sources to ambient VOCs during winter to summer transition at a semi-arid urban site in India. *Environ. Poll.* 229, 595–606. doi: 10.1016/j.envpol.2017.06.091

Satish, R., and Rastogi, N. (2019). On the use of brown carbon spectra as a tool to understand their broader composition and characteristics: a case study from crop-residue burning samples. *ACS Omega* 4, 1847–1853. doi: 10.1021/acsomega.8b02637

Seki, K. (1989). Ionization energies of free molecules and molecular solids. *Mol. Cryst. Liq. Cryst. Inc. Nonlinear Opt.* 171, 255–270. doi: 10.1080/00268948908065800

Sharma, G., Sinha, B., Pallavi, N., Hakkim, H., Chandra, B. P., Kumar, A., et al. (2019). Gridded emissions of CO, NO_x, SO_2, CO_2, NH_3, HCl, CH_4, $PM_{2.5}$, PM_{10}, BC and NMVOC from open municipal waste burning in India. *Environ. Sci. Technol.* 53, 4765–4774. doi: 10.1021/acs.est.8b07076

Singh, D. K., and Gupta, T. (2016). Effect through inhalation on human health of PM_1 bound polycyclic aromatic hydrocarbons collected from foggy days in northern part of India. *J. Hazard. Mater.* 306, 257–268. doi: 10.1016/j.jhazmat.2015.11.049

Singh, D. P., Gadi, R., Mandal, T. K., Dixit, C. K., Singh, K., Saud, T., et al. (2010). Study of temporal variation in ambient air quality during Diwali festival in India. *Environ. Monit. Assess.* 169, 1–13. doi: 10.1007/s10661-009-1145-9

Sirois, A., and Bottenheim, J. W. (1995). Use of backward trajectories to interpret the 5-year record of PAN and O_3 ambient air concentrations at Kejimkujik National Park, Nova Scotia. *J. Geophys. Res.* 100, 2867–2881. doi: 10.1029/94JD02951

Stein, A. F., Draxler, R. R., Rolph, G. D., Stunder, B. J. B., Cohen, M. D., and Ngan, F. (2015). NOAA's HYSPLIT atmospheric transport and dispersion modeling system. *Bull. Am. Meteorol. Soc.* 96, 2059–2077. doi: 10.1175/BAMS-D-14-00110.1

Wang, Y. Q., Zhang, X. Y., and Draxler, R. R. (2009). TrajStat: GIS-based software that uses various trajectory statistical analysis methods to identify potential sources from long-term air pollution measurement data. *Environ. Modell. Softw.* 24, 938–939. doi: 10.1016/j.envsoft.2009.01.004

Conflict of Interest: The authors declare that the research was conducted in the absence of any commercial or financial relationships that could be construed as a potential conflict of interest.

frontiers in Sustainable Cities

ORIGINAL RESEARCH
published: 16 February 2021
doi: 10.3389/frsc.2021.640426

Perceived Thermal Response of Stone Quarry Workers in Hot Environment

Priya Dutta [1†], Varsha Chorsiya [2*†] and Pranab Kumar Nag [3†]

[1] Indian Institute of Public Health, Gandhinagar, India, [2] School of Physiotherapy, Delhi Pharmaceutical Sciences and Research University, New Delhi, India, [3] National Institute of Occupational Health, Ahmedabad, India

OPEN ACCESS

Edited by:
Prashant Rajput,
Public Health Foundation of India, India

Reviewed by:
Yuan Shi,
The Chinese University of Hong Kong, China
Xiangfei Kong,
Hebei University of Technology, China

***Correspondence:**
Varsha Chorsiya
vkc.chorsiya@gmail.com
orcid.org/0000-0002-6393-1422

† These authors have contributed equally to this work and share first authorship

Specialty section:
This article was submitted to Climate Change and Cities, a section of the journal Frontiers in Sustainable Cities

Received: 11 December 2020
Accepted: 28 January 2021
Published: 16 February 2021

Citation:
Dutta P, Chorsiya V and Nag PK (2021) Perceived Thermal Response of Stone Quarry Workers in Hot Environment. Front. Sustain. Cities 3:640426. doi: 10.3389/frsc.2021.640426

Introduction: Impact of heat on health of workers goes unrecognized by the virtue of the indispensable fact that every individual has varied perception and tolerance capacity. The present study determine the physiological signs with perceived subjective responses under the thermal stress.

Materials and Methods: The study was spread on open field stone quarry workers ($N = 934$) during the summer (May to June), post monsoon (September to October), and winter (December to January).

Results: In the summer months, dry bulb temperature range from 36.1 to 43.2°C and the distribution of Wet Bulb Globe temperature (WBGT) outdoor values were outlier-prone than normal distribution indicated heat vulnerability. The environmental effect on weighted average skin temperature (T_{sk}) local segmental T_{sk} and deep body temperature (T_{cr}) were greater than the effects that might be attributed to work severity. The tolerance time level in summer months (65 ± 13 min at WBGT 35 ± 2.3°C) was less than in other two season. About 85% of workers in summer, 68% in post monsoon and 79% in winter recorded working heart rate greater than 90 beats/min. Physiological and subjective responses to heat stress indicated that during summer month the workers complained of excessive sweating (93.5%), feeling of thirst/dry mouth (88.7%), elevated Core temperature (T_{cr}) (58.7%) and decreased working capacity (75.6%). The observation found that around 14% workers were vulnerable to heat stress and the workers had no knowledge to mitigate the heat related illnesses.

Discussion and Conclusions: The stone quarry work as compared to other outdoor workers have environmental adversaries which becomes confounding variables in the study of such occupations. There was significant difference ($p < 0.001$) as far as the physiological and thermoregulatory responses were concerned in three different months of investigation.

Keywords: stone quarry, heat wave, WBGT, tolerance time, perceived response

INTRODUCTION

Heat waves are becoming increasingly severe and frequent, exacerbated by climate change threatening health and livelihood directly or indirectly (Dutta and Chorsiya, 2013; Azhar et al., 2014; Nag et al., 2014). Over a million workers are employed in quarrying and related activities in India (Saiyed and Tiwari, 2004). Types of rock extracted from quarries include cinder, chalk, china clay, clay, coal, coquina, construction aggregate (sand and gravel), globigerina limestone (Malta), granite, grit stone, gypsum, limestone, marble, phosphate rock, and sandstone. A number of sand stone quarries are located in different states of India, e.g., Rajasthan, Madhya Pradesh, Gujarat, Orissa, Karnataka, Tamil Nadu, and Andaman and Nicobar islands. Sand stone quarry is an open excavation from which the stone is obtained, by labor-intensive and strenuous methods. The workers use heavy hand tools for extracting process (layers of hard rocks) and perform many manual material handling tasks like breaking, drilling the hard rocks and lifting/carrying those for loading and unloading to transport to desired destination. The workers are exposed directly under the sun throughout their working day. Huge hammers or mechanical drilling are used to separate the stone blocks. Grecchi et al. (2009) have found that the traditional working methods cause musculoskeletal pain and discomfort among the stone quarry workers due to awkward postures and lifting of heavy weights. Epidemiological surveys on stone cutters and carvers found that the hand arm vibration induced white finger, sensor-neural, and musculoskeletal symptoms among the workers (Griffin et al., 2003; Makoto et al., 2005; TaMrin et al., 2012). Mathur (2005) reported that the average life span of stone quarry workers is ~10 years less than their fellow villagers who never worked in quarries. In the western part of India summer temperatures in stone quarries often exceed 45°C, indicating the risks of heat-induced illnesses and disorders among workers, with the relative vulnerability of young and elderly workers.

Literature reviewed suggested enough evidence to demonstrate the increasing certainty that climate change significantly aggregates the probability of extreme weather conditions, most often in directions that lead to dangerous health consequences especially to people who carry out heavy physical labor as a part of their daily jobs like steel plant, power plant, forge plant, etc. (Krishnamurthy et al., 2017; Varghese et al., 2018). In developing countries like India these workers are generally migratory and work on daily wages. When the ambient temperature exceed that of body temperature (37°C), the body loose heat by evaporation or sweating by the mechanism of thermoregulation controlled by the hypothalamus section of the human brain But, humidity affects this thermodynamic stability by limiting sweat evaporation and heat loss, which creates health impacts and loss of work capacity among the exposed workers (Saghiv and Sagiv, 2020). A thermodynamic model of heat balance is applied, with due account of heat exchanges through the segmental and compartmental interfaces of the human body, microclimatic and outer environment (Nag et al., 2007).

During the hot season, because of the strenuous physical activity and climatic condition the workers in stone quarry accumulate heat load and heat stress which effects their occupational health and work capacity. The health hazards get severe if the person is exposed higher temperature for a longer time. With increasing temperature in future it is likely that the health of vulnerable occupational groups like stone quarry workers are big challenge. Studies have found that the work environment higher than temperature 40°C causes human discomfort and high mortality (Steeneveld et al., 2011; Petitti et al., 2015; Bunker et al., 2016). Literature related to response of extreme climate exposure of workers in stone quarry is lacking. Since the combined load of strenuous physical work and exposure to extremely hot environment have negative impacts on human health and safety, the present study focused on generating epidemiological data on the heat-exposed stone quarry working population, with reference of biophysical perspective. Furthermore, these findings are needed to be substantiated by the subjective symptoms reported as perceived response under the thermal stress which underlies the utility of the present research work.

MATERIALS AND METHODS

Ethics

The written informed consent to participate in the study was taken as per the Indian Council of Medical Research (2000) ethical guidelines from the individuals (as all were above 18 years) for the publication of any potentially identifiable images or data included in this article.

A total of 934 men in the age range between 18 and 60 years were selected in the present crosssectional study of stone quarry workers from western part of India (**Figure 1**). Environmental and health risk surveillance were undertaken in stone quarry works, during the months of summer (May to June, $N = 521$), post monsoon (September to October, $N = 214$), and winter (December to January, $N = 199$) months. Workers underwent seasonal extremes of climate scenarios and experience hardships which may sometimes fall beyond their coping levels, resulting in heat injuries. Direct measurements of the thermometric parameter include ambient dry bulb temperature (T_a), wet bulb temperature (T_{wb}), dew point, wind velocity and globe temperature (T_g) were measured by Wet-Bulb Globe Temperature (WBGT) Monitor, Delta OHM (HD 32.1, Thermal Microclimate, Italy) and Relative Humidity/Temperature data by Lascar EL-USB-2-LCD, Sweden for several hours of observation period and continued for a number of days at each workplace. The environmental warmth was expressed in terms of WBGT index (Liljegren et al., 2008). The locations of stone quarry were same in the summer, post monsoon, and winter seasons during the investigations. However, same workers could not be followed up in different seasons since the workers were migratory and casual laborers worked on daily wages.

In order to ascertain susceptibility of workers to heat stress, a checklist enquiry was introduced for health risk surveillance, heat exposure- related morbidity of the work groups, including environmental warmth assessment, physical fatigue and perceived effort. The workers' subjective responses

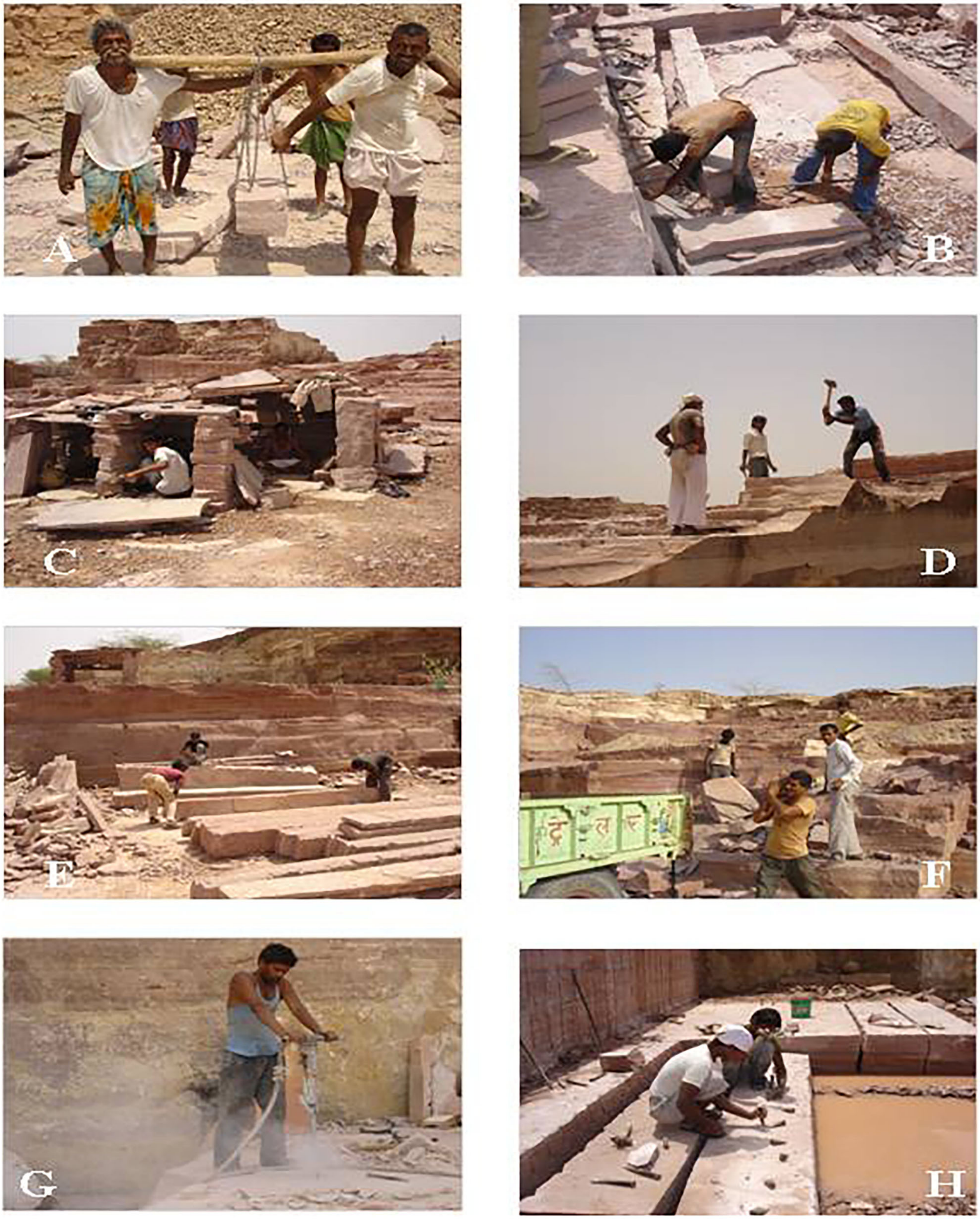

FIGURE 1 | Stone quarrying activities in the open cast mine: **(A)** carrying stone slab; **(B)** Removing slab for breaking; **(C)** self–made stone shelter in the mine; **(D)** Breaking stone with hammer; **(E)** Manually lifting slab for breaking; **(F)** Loading stone slab; **(G)** Drilling stone; **(H)** Separating stone slabs.

were recorded on a five-point Likert scale, and a score of 4 and 5 were taken as an indication of high strain response. Every worker was subjected to physiological variables measurement that included heart rate responses, blood pressure measurements, thermographic profile of the skin areas (T_{sk}) and deep body temperature (T_{cr}). The thermographic profile of the skin (T_{sk}) areas were recorded, using ThermoCAM, FLIR system (Sweden) from four exposed sites, i.e., head, hand, trunk, leg, and back trunk. The measurements were repeated thrice, i.e., pre-exposure and at an interval of about 2–3 h during work. Heart rate was measured by polar heart rate meter (S810^{TM} Polar Electro Oy, Finland); deep body temperature (T_{cr}) as oral temperature by thermometer and OMRON digital BP instrument was used to record the blood pressure during the work. The polar heart rate monitor and cuff of BP apparatus was tied to the chest and the arm of the worker respectively before the commencement of the work. The polar heart rate automatically record the heart rate and when BP need to monitor the OMRON BP apparatus was connected to the lead of the cuff and BP was measured in less than a minute for a single worker without interrupting their main work process. The data of Polar heart rate meter was later transferred to the computer. During the occupational exposures, the workers wore light clothing—wearing shorts, trouser or a lungi/dhuti (a loose fabric wrapped around join at ankle length) and a half-sleeve banian or t-shirt, with clothing insulation value approx. 0.6 clo (Summer clothing insulation unit).

The algorithm allowed computation of heat exchange parameters, including heat conductance, metabolic load, effective heat load, body heat storage, and the overall rate of change of body core temperatures. These dimensions led to the prediction of the limits of tolerance to work in hot environments. This algorithm is based on premise of biophysical approach propagated by Nag et al. (2007), utilizing the heat exchanges through different avenues across the segment (i.e., head, trunk, arm, hand, leg and feet) and body layers- blood, core (viscera plus skeleton), muscle, fat and skin (i.e., 6 segment × 5 layers = 30 compartments) (Nag et al., 2007). These are the following equations with thermodynamic model of heat balance of each segment (where storage δ H = 0) adopted from Nag et al. (2007).

$$
\begin{aligned}
Y\Delta T/\Delta t = {} & (V\rho\times S)_{Blood}\times(T_{Blood}) + \Delta M \\
& -[\{K_{Blood-core}(T_{Blood} - T_{core}) + K_{Core-Muscle} \\
& (T_{Core} - T_{Muscle}) + K_{Muscle-Fat}(T_{Muscle-}T_{Fat}) \\
& +K_{Fat-Skin}(T_{Fat} - T_{Skin}) + H(i)(T_{Skin-}T_{Environment})\} \\
& \times SA + (C_{Res} + E_{Res} + E_{Skin})]
\end{aligned}
$$

Where Y, product of compartmental mass and specific heat, $\Delta T/\Delta t$, change in temperature with time, V, volume (liter), ρ, density (kg/L), S, Specific heat of blood (W h/kg °C), ΔM, (total-basal metabolic energy, W.h), K, conductance of body compartments (W/m^2.°C), T, resultant body temperature (°C), H(i), combined heat transfer coefficients of segments (W/m^2.°C), SA, surface area (m^2), C_{Res} and $E_{Res,}$ resoiratory heat loss through convention and evaporation (W.h), E_{skin}, evaporation heat loss for skin (W.h).

STATISTICAL ANALYSIS

Data analysis was performed using SPSS statistical software, version 16.0. Descriptive statistics was applied to understand the charactersitics of temperature profile and physiological variables of the workers. One way ANOVA was used to study the differences of these variables among three different seasons. Percent prevalence was calculated for perceived sign and symptoms responses of the workers. The level of significance was set at $p < 0.05$.

RESULT

The open-field day-time ambient conditions are presented in **Table 1**. The percentile distribution, skewness, and kurtosis values of WBGT estimated during the three seasons of investigation reflected the variations in environmental warmth. During summer (May to June), the distribution of WBGT outdoor values was more outlier-prone than the normal distribution. The positive kurtosis indicated a relatively peaked distribution. The WBGT values spread out more to the right from the proximity of the mean (35 ± 2.3°C) and thereby indicating a component of heat vulnerability of the sample population concerned. The environmental data were found to be statistically different in three seasons (summer, post monsoon, and winter) of the investigation. The workers had mean body weight 53.8 ± 9 kg and body surface area 1.6 ± 0.1 sqm.

Beside variation in the environmental conditions, the magnitude of physiological responses of the stone workers attributed to the combined stress of environmental exposure and the intensity of the work performed, with the potential to health consequences. A comparison of local T_{sk} and weighted average T_{sk} of workers in summer, post monsoon and winter are in **Table 2**, indicating their T_{sk} responses differed significantly. During the summer and post-monsoon months, the 5th−95th percentile values of T_{sk} of varied from 30.1 to 40°C and 32.7 to 37.3°C, respectively. Whereas, in the winter months, the 5th−95th percentile values of T_{sk} of local areas ranged from 24.6 to 34.7°C. The profile of segmental T_{sk} indicated the relative space for adjustment against the extent of the core temperature buildup of the workers. **Table 2** also includes the weighted average T_{sk} of the whole body, which was obtained from the surface area and sensitivity weighting of local area T_{sk}. The weighted T_{sk} during summer and post monsoon remained at 35.3 ± 1.3°C and 35.0 ± 1.0°C, respectively, whereas the value during winter was 31.6 ± 1.4°C. One-way ANOVA shows that the T_{sk} of the local areas significantly differed during the three investigating seasons. The trunk, upper arm, hand, thigh, and foot temperatures in summer and post monsoon were relatively more than a winter month.

Different physiological responses, given in **Table 3**, indicates significant differences ($p < 0.001$) in bodily strains of the stone quarry workers in three seasons of investigation. The average heart rate response of the workers during work in summer and winter seasons were 108 ± 14.6 and 109 ± 21.2 beats/min, respectively, whereas the heart rates were relatively less (99 ± 14.6 beats/min) in the month of post monsoon. The increase in heart

TABLE 1 | Environmental conditions at workplaces.

Variable	Statistics	Summer (*N* = 521)	Post monsoon (*N* = 214)	Winter (*N* = 199)
Dry bulb temperature (^{0}C)	Mean ± SD	40.0 ± 2.4	35.2 ± 2.2	26.6 ± 5.3
	5th Percentile	36.1	33.1	20.0
	95th Percentile	43.2	38.9	34.5
	Skewness	0.3	0.6	0.2
	Kurtosis	0.5	−0.9	−1.6
	F Value		1,265.8 ($p < 0.001$)	
Outdoor WBGT (^{0}C)	Mean ± SD	35.5 ± 2.3	32.2 ± 1.8	23.1 ± 2.0
	5th Percentile	31.8	28.1	20.0
	95th Percentile	39.4	35.4	26.8
	Skewness	0.7	−0.4	0.1
	Kurtosis	0.6	0.2	−0.7
	F Value		2,382.0 ($p < 0.001$)	

TABLE 2 | Local skin temperature profile of workers at workplaces.

Segmental T_{sk}	Statistics	Summer (*N* = 521)	Post monsoon (*N* = 214)	Winter (*N* = 199)
Head (^{0}C)	Mean ± SD	35.8 ± 1.2	34.8 ± 1.0	30.7 ± 2.4
	5th Percentile	33.0	33.2	26.8
	95th Percentile	37.4	36.7	34.6
	Skewness	−0.1	1.1	−0.1
	Kurtosis	−0.4	0.1	−0.8
	F Value		264.4 ($p < 0.001$)	
Trunk (^{0}C)	Mean ± SD	35.1 ± 1.6	34.9 ± 1.2	32.1 ± 1.8
	5th Percentile	32.6	33.0	28.8
	95th Percentile	37.5	36.8	34.7
	Skewness	−0.2	1.2	−0.4
	Kurtosis	0.2	0.1	−0.1
	F Value		282.8 ($p < 0.001$)	
Upper arm (^{0}C)	Mean ± SD	35.1 ± 2.1	35.2 ± 1.2	29.3 ± 2.1
	5th Percentile	31.2	33.1	25.3
	95th Percentile	38.2	37.0	32.6
	Skewness	−0.5	1.2	−0.4
	Kurtosis	−0.1	0.1	0.2
	F Value		672.5 ($p < 0.001$)	
Hand (^{0}C)	Mean ± SD	35.6 ± 1.3	35.0 ± 1.2	32.3 ± 1.6
	5th Percentile	33.6	33.1	29.4
	95th Percentile	38.0	36.7	34.7
	Skewness	0.2	−0.3	−0.3
	Kurtosis	0.3	0.2	−0.3
	F Value		424.6 ($p < 0.001$)	
Thigh (^{0}C)	Mean ± SD	35.6 ± 1.9	35.2 ± 1.3	31.7 ± 1.5
	5th Percentile	32.7	33.0	29.1
	95th Percentile	38.9	37.2	34.0
	Skewness	0.3	−0.1	−0.3
	Kurtosis	0.3	−0.4	0.8
	F Value		388.3 ($p < 0.001$)	
Foot (^{0}C)	Mean ± SD	35.2 ± 3.0	35.2 ± 1.4	28.9 ± 2.4
	5th Percentile	30.1	32.7	24.6
	95th Percentile	40.0	37.3	32.9
	Skewness	−0.1	−0.3	−0.1
	Kurtosis	0.1	−0.3	−0.1
	F Value		448.5 ($p < 0.001$)	
Weighted T_{sk} (^{0}C)	Mean ± SD	35.3 ± 1.3	35.0 ± 1.0	31.6 ± 1.4
	5th Percentile	33.0	33.3	29.2
	95th Percentile	37.4	36.6	33.8
	Skewness	−0.1	0.0	−0.3
	Kurtosis	−0.4	−0.3	−0.3
	F Value		264.4 ($p < 0.001$)	

rate in winter is due to decrease in environmental warmth and increase in physical load. The environmental load and heart rate responses differed significantly in summer and post-monsoon months of investigation [$F_{(2,931)} = 31.3$, $p < 0.001$]. About 85% of the workers in summer, 68% in post monsoon, and 79% in winter have working heart rates greater than 90 beats/min. The heart rate response and the prediction of oxygen uptakes at the range of 0.76–1.96 l/min for the workers, indicate that the severity of stone quarry work might be categorized as heavy to extremely heavy in summer and heavy to moderately heavy in post monsoon and winter. The systolic blood pressure in the month of winter was marginally higher (139 ± 15 mmHg) as compared to summer months (133 ± 17.1 mmHg). Also there was no significant difference in diastolic blood pressure during three seasons.

The average level of T_{cr} of the stone quarry workers during work in the months of summer, post monsoon and winter illustrates the dynamic equilibrium of heat transfer supposedly maintained between the body core and periphery, in regulating the buildup of body temperature. As given in **Table 3**, the 95th percentile value of T_{cr} in summer months reached 40.1°C. It was noted that nearly 10% of the workers, the T_{cr} level during their work in summer months crossed the critical limit value of heat tolerance (39°C) and these workers were at unsafe zone of exposure. This remains a challenge to recognize those vulnerable workers who might be at risk of heat disorders. None of the workers during post monsoon and winter crossed the heat tolerance criteria.

The workers had similar demographic and physical characteristics and they were engaged in equivalent nature of work. The physiological demand of work for the workers in the month of May to June was ∼14% higher, as compared to the strains during post monsoon and winter. The weighted T_{sk} and T_{cr} of the workers are grouped according to the WBGT range (**Figure 2**). There was a consistent increasing trend of T_{sk} and T_{cr}, however the gradient tend to decrease when the WBGT exceeded 32.9°C. This hallmarks the critical zone where the probably the thermoregulation mechanism of the body switched on to maintain the body haemostasis and further control build up of temperature at core so, that the workers body could adapt to the thermal environment. The cascades of event occurs to offload the produced heat is by increasing the cutaneous blood flow that bring the hot blood closer to the external environment

TABLE 3 | Physiological responses of workers during stone quarrying work.

Variable	Statistics	Summer ($N = 521$)	Post monsoon ($N = 214$)	Winter ($N = 199$)
Heart rate (beats/min)	Mean ± SD	108 ± 14.6	99 ± 14.6	109 ± 21.2
	5th Percentile	88	80	80
	95th Percentile	135	120	152
	Skewness	0.6	0.9	0.8
	Kurtosis	−0.1	2.4	0.5
	F Value		31.3 ($p < 0.001$)	
Systolic BP (mmHg)	Mean ± SD	133 ± 17.1	128 ± 13.4	139 ± 15.0
	5th Percentile	106	109	115
	95th Percentile	158	153	163
	Skewness	0.3	0.6	0.1
	Kurtosis	1.0	0.4	1.3
	F Value		21.9 ($p < 0.001$)	
Diastolic BP (mmHg)	Mean ± SD	78±12.7	79 ± 12.8	77 ± 10.7
	5th Percentile	60	60	60
	95th Percentile	98	101	94
	Skewness	1.7	0.6	−0.6
	Kurtosis	14.7	2.0	1.5
	F Value		1.5 (NS)	
T_{cr} (^{0}C)	Mean ± SD	37.3 ± 1.1	36.7 ± 0.4	36.8 ± 0.5
	5th Percentile	36.2	36.1	36.1
	95th Percentile	40.1	37.3	37.8
	Skewness	1.8	0.0	0.7
	Kurtosis	3.1	−0.7	0.3
	F Value		42.6 ($p < 0.001$)	
Sweat loss (gm/min)	Mean ± SD	15.6 ± 1.7	13.7 ± 1.5	6.5 ± 1.8
	5th Percentile	13.0	9.7	3.9
	95th Percentile	18.4	15.8	9.8
	Skewness	0.8	−1.1	0.4
	Kurtosis	1.2	1.4	−0.7
	F Value		2,099 ($p < 0.001$)	
Predicted tolerance time (min)	Mean ± SD	65 ± 12.7	83 ± 17.4	199 ± 42.7
	5th Percentile	46	62	131
	95th Percentile	88	132	266
	Skewness	−0.1	1.7	0.0
	Kurtosis	0.4	2.8	−0.7
	F Value		2,429.2 ($p < 0.001$)	

and loose the heat by radiation, convection, and evaporation of sweat into latent heat.

The segmental heat exchanges and the rate of body temperature build up were estimated and arrived at a time duration that corresponded to the limit of tolerance of 39°C and referred to as heat tolerance time (**Table 3**). During the summer season, the tolerance time was significantly less, in comparison to other two seasons. In post-monsoon season, the tolerance time was arrived at 83 ± 17 min at WBGT 32.2 ± 1.8°C; i.e., 18 min drop in tolerance time for 3.3°C increase in WBGT. For the winter season, the heat tolerance time was estimated as 199 ± 43 min at WBGT 23.1 ± 2.0°C. About 134 min drop in tolerance time for ∼12°C increase in WBGT in summer season.

The questionnaire surveyed the checkpoint that looked into the signs and symptoms of heat-related illnesses, as given in **Table 4** (Nag et al., 2013; Hanna and Tait, 2015). Corresponding to observations of physiological and subjective responses to heat stress, the workers were vulnerable to heat illnesses. Over 21.3% of the stone quarry workers complained of decreased urine output situation during the summer exposure, in comparison to only 7% workers in post monsoon and 17.6% in winter. Nearly 93.5% of the workers complained of excessive sweating and 88.7% feeling of excessive thirst/dry mouth and ∼58.7% workers reported elevated T_{cr} during the summer months. About 3/4th of the workers complained of decreased working capacity.

Perceived effort/exertion of an individual scored using Borg's scale corresponded closely to the severity of the tasks performed. The perceived effort levels remained in the range of 14–17 and for this level of subjective response, the heart rate variations might correspond to 140–170 beats/min. However, the 95th percentile values of heart rates for the workers in the months of summer, post monsoon and winter were 135, 120, and 152 beats/min, respectively. The subjective response to overall physical fatigue score remained at a high level, i.e., close to 9–10 in 13 point scale, however, the relative fatigue to different levels of environmental warmth could not be reflected. The self-reporting of perceived effort, physical fatigue, and any other heat-related symptoms by the illiterate workers have limitations and therefore, appropriate indoctrination of the workers and consistent recording by the field investigators was essential in establishing relationships between the symptoms and heat exposures.

Our study shows a need of break or rest rooms of the workers that may effective in reducing the thermal load of participants. Further, studies on stone quarry work may be advantageous in estimating the exact nature of thermal load experienced by workers and its discernible effects. Nevertheless, it will help in understanding India's burden of heat stress illness, both occupational and otherwise.

DISCUSSION

The stone quarry work as compared to other outdoor thermal environment occupation like steel plant, steel plant, power plant, and forge plant where it is difficult to control the environmental adversaries which becomes confounding variables in the study of such occupations. According to Indian Meteorology Department (IMD), a category of heat wave includes places where the normal maximum temperature is more than 40°C. Researchers had found that for the last 25 years the average global temperature rose by 0.6°C (De et al., 2005; IPCC, 2007). The conditions of the heat wave prevailed in the regions where the study was undertaken during the summer (May to June), as the 95th percentile value of dry bulb temperature was 43.2°C. The

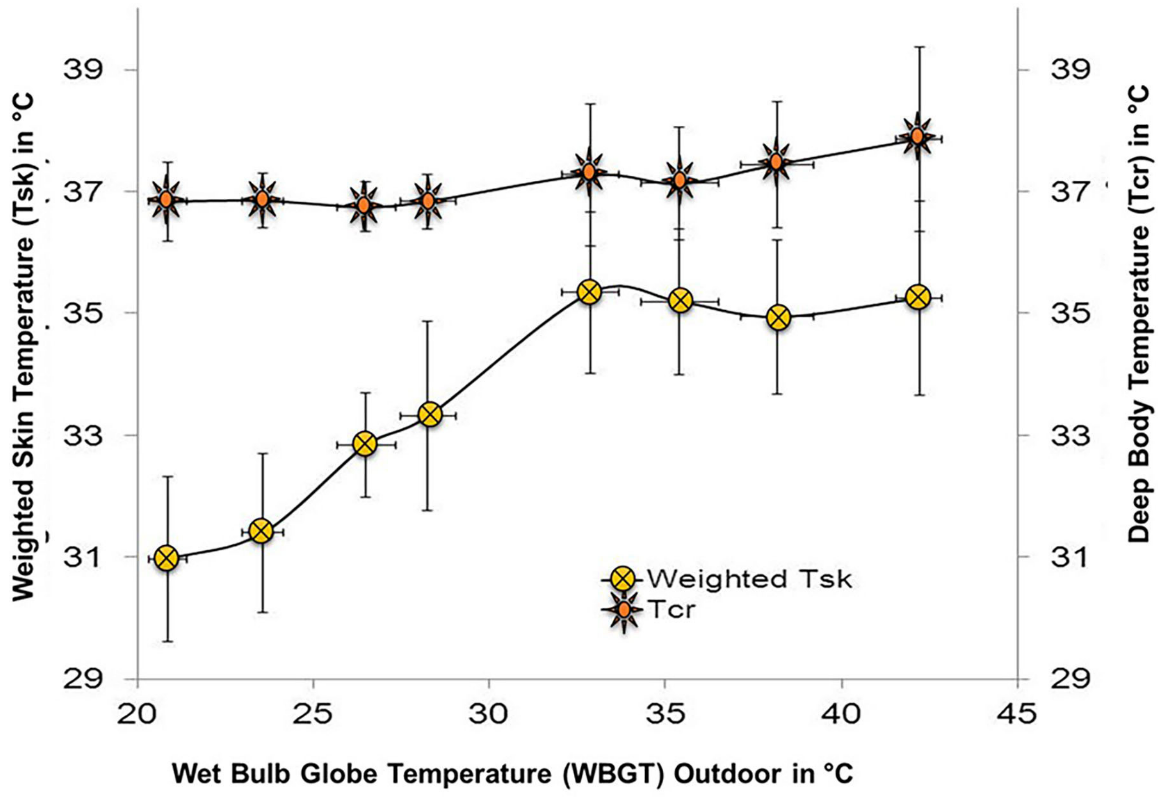

FIGURE 2 | Weighted average T_{sk} and T_{cr} at different environmental warmths.

environmental load in the month of winter was substantially less in comparison to conditions during the season summer and post monsoon.

The cardiovascular and thermoregulatory responses of the stone quarry workers differed significantly in the month of summer, post monsoon, and winter. The responses were the resultant of combined effect of environmental warmth and work strenuousness that ranged from heavy to extremely heavy in the month of summer, post monsoon and heavy to moderately heavy in the month of winter. The study observed a small increase in systolic blood pressure during the winter months. The trend of the results corroborates to the findings of Kristal-Boneh et al. (1995) that the average Systolic BP at work was higher in winter than in summer. The activation of the sympathetic nervous system and secretion of catecholamine might be increased in cooler environment, resulting in increase in blood pressure through an increased heart rate and peripheral vascular resistance (Alperovitch et al., 2009).

The relative effects of environmental stress on the physiological responses that would be expected beyond the level attributed to physical work, however, need to be ascertained. Data indicated that the environmental effects on local segmental T_{sk} and weighted average T_{sk} of workers were greater than the effects that might be attributed to work severity (Nag et al., 2013). The profile of segmental T_{sk} indicated deviation from the thermo-neutral reference, provoking distinctive peripheral response for feedback and regulation in building up of body temperature. For the range of environmental warmth from 25 to 43°C WBGT (ISO Standard 7243, 1989), the workers had an increasing trend of T_{sk} and T_{cr}, however the gradient tended to narrow down when the WBGT exceeded 32.9°C and the gradient was found to be < 3°C (Nag et al., 1997, 2013). The stone quarry works are performed directly under sun and the physiological demand of work in the month of summer was ∼14% higher, as compared to the demands in the months of post monsoon and winter.

However, the biophysical analysis of heat exchanges between the body core and skin surface yield the rate of body core temperature build up and accordingly, the tolerance time of heat exposure was arrived at, corresponding to the of T_{cr} 39°C (Hanna and Tait, 2015). Above 39°C of T_{cr}, serious heat stroke and neurological effects may occur to a worker (Parsons, 2003).

As observed, there was considerable difference in the tolerance time of stone quarry work in three different seasons, due to the differences in the environmental variables and workload. The tolerance time level in summer months (65 ± 13 min at WBGT 35 ± 2.3°C) was less than other two seasons (post monsoon and

TABLE 4 | Workers' subjective response to signs and symptoms of heat strains.

	Summer (N = 521)	Post monsoon (N = 214)	Winter (N = 199)
	% of workers expressed heat strain		
Heavy sweating	93.5	91.1	69.8
Elevated heart rate	76.0	59.8	61.3
Weakness or fatigue	75.2	78.5	62.3
Dizziness/nausea	40.5	31.8	41.2
Headache	51.1	43.5	44.2
Confused and irritated	44.5	20.1	19.1
Skin tanning	55.1	9.8	23.6
Excessive thirst/dry mouth	88.7	82.7	55.3
Decreased urine output	21.3	7.0	17.6
Loss of appetite	47.0	26.6	36.7
Blurred vision	44.5	37.4	25.1
Hot or dry skin (no sweating)	21.9	7.0	18.1
Red face	51.2	36.9	20.1
Chill feeling/shivers	45.5	31.8	23.6
Mental disorientation	43.8	15.4	27.6
Elevated body temperature	58.7	17.8	52.3
Seizure	13.4	0.0	6.5
Slurred speech	7.7	0.5	4.0
Abdominal spasms	35.9	32.7	31.2
Muscle pain/cramp (arms/legs)	48.2	57.9	64.3
Fainting/feel collapse	13.6	4.7	28.6
Pink or red bumps	35.3	25.2	10.1
Itching skin	39.2	24.3	14.1
Irritation or prickly sensation	29.6	31.8	13.1
Loss of work capacity	75.6	62.1	57.3

winter). From the cross-sectional data on stone quarry workers, it was estimated that there was ∼14% loss of tolerance time per degree increase of WBGT, from 33 to 35°C WBGT. The loss of tolerance time might also indicate loss of productivity due to heat exposure, which Kjellstrom (2016) referred to as High Occupational Temperature Health and Productivity Suppression (Hothaps) effect, for loss of working ability or working capacity. The relative workload was higher during winter season. It is likely that the workers might be adopting self-adjustment strategy in the pace of work distributing the work and workload as per the varying environmental exposures. The make-shift shelters where the workers take rest during the hottest hours. It was observed that the environmental effects on workers appeared to be greater than the effects of work severity, therefore consistent field investigators was essential in establishing relationships between the symptoms and heat exposures.

In repeated occupational exposures high heat load and strenuous physical activity, human's defense mechanism undergoes progressive changes for internal thermal stability (acclimatization), depending upon on physiological adaptive capacity (Morioka et al., 2006). Data amply suggest that the workers during the summer months were at unsafe zone of exposure and 14% of the workers were vulnerable to heat illnesses. Also, the workers lack awareness and measures to mitigate risks. This kind of data from a larger sample size is greatly important in the assessment of the health, safety and productivity impacts of climatic changes with seasonal variation, and therefore, might be useful to develop prevention programmes of the population at risk to heat waves.

STRENGTHS AND LIMITATIONS

The location of this cross-sectional study of stone quarry workers was the same in summer, post monsson and winter months but, the specific workers and worker tasks differed between the survey times. However, regardless of the possible difference in three seasons the survey participants and their ativities, perceived heat-related symptoms and environmental measurments of heat stress has supported our overall finding that heat stress is an important risk factor for worker health. Also of note is that this study may be conservative in its findings as responses related to heat disorders among stone quarry workers may be higher than those figures observed in the study due to a healthy worker bias (i.e., those most affected by the heat were absent or had stopped doing this type of work). Another possible explanation may be attributed to the fear of being reprimanded by the management for discussing issues that may portray them negatively.

A key strength of this study is that we surmised that the high exposure coupled with strenuous physical load are the major contributing factors. Further, there is lack of Indian heat exposure guidelines for determining ceiling limits of environmental exposure for tropical heat exposure of the population. Our study supports the establishment of separate tropical or India specific heat exposure guidelines and interventions that could simultaneously be worker protective but realistic in this climate.

CONCLUSION

The study bears considerable practical importance to assess the magnitude of thermal stress among stone quarry workers in the working environment and the worker's physiological reaction to it, and therefore to ensure optimal conditions for health and productivity. The study has a limitation of focusing only on three seasons, however, the basic premise was that the cardiovascular and thermoregulatory parameters are critical to manifest ones thermal environmental perceptive responses in a occupational situation. The habitual occupational involvement makes the workers naturally acclimatized to hot environment, however, even the habitual workers during peak summer months are at potential risk of developing heat-related illness. The comprehensive analysis of the physiological and thermoregulatory responses of workers to heat stress and strain would eventually ascertain the relative vulnerability of the stone quarry workers for their exposure to extreme hot environment.

DATA AVAILABILITY STATEMENT

The raw data supporting the conclusions of this article will be made available by the authors if required, without undue reservation. But, in that case the identity or the personal information of the participants will not be shared.

ETHICS STATEMENT

The studies involving human participants were reviewed and approved by Indian Council of Medical Research. The patients/participants provided their written informed consent to participate in this study.

AUTHOR CONTRIBUTIONS

All authors listed have made a substantial, direct and intellectual contribution to the work, and approved it for publication.

REFERENCES

Alperovitch, A., Lacombe, J. M., Hanon, O., Dartigues, J. F., Ritchie, K., Ducimetière, P., et al. (2009). Relationship between blood, pressure, and outdoor temperature in a large sample of elderly individuals the three-city, study. *Arch. Intern. Med.* 169, 75–80. doi: 10.1001/archinternmed.2008.512

Azhar, G. S., Mavalankar, D., Nori-Sarma, A., Rajiva, A., Dutta, P., Jaiswal, A., et al. (2014). Heat-related mortality in India: excess all-cause mortality associated with the 2010 Ahmedabad heat wave. *PLoS ONE* 9:*e*91831. doi: 10.1371/journal.pone.0091831

Bunker, A., Wildenhain, J., Vandenbergh, A., Henschke, N., Rocklöv, J., Hajat, S. et al. (2016). Effects of air temperature on climate-sensitive mortality and morbidity outcomes in the elderly: a systematic review and meta-analysis of epidemiological evidence. *EBioMedicine* 6, 258–268. doi: 10.1016/j.ebiom.2016.02.034

De, U. S., Dube, R. K., and Prakasa Rao, G. S. (2005). Extreme weather events over India in the last 100 years. *J. Ind. Geophys. Union* 9, 173–187.

Dutta, P., and Chorsiya, V. (2013). Scenario of climate change and human health in India. *Int. J. Innov. Res. Dev.* 2, 157–160.

Grecchi, A., Cristofolini, A., Correzzola, C., Piccioni, A., Buffa, C., and Pol, G. (2009). Ergonomic assessment of technical improvements in the work of manual laborers of a porphyry quarry. *Med. Lav.* 100, 142–150.

Griffin, M. J., Bovenzi, M., and Nelson, C. M. (2003). Dose-response patterns for vibration-induced white finger. *Occup. Environ. Med.* 60, 16–26. doi: 10.1136/oem.60.1.16

Hanna, E. G., and Tait, P. W. (2015). Limitations to thermoregulation and acclimatization challenge human adaptation to global warming. *Int. J. Environ. Res. Public Health* 12, 8034–8074. doi: 10.3390/ijerph.120708034

Indian Council of Medical Research (2000). *Ethical Guidelines for Biomedical Research on Human Subject*. New Delhi: Indian Council of Medical Research, 1–77.

IPCC (2007). *Fourth Assessment Report, Geneva, Inter-governmental Panel on Climate, C.hange.* Cambridge University Press: Cambridge. Available online at: http://www.ipcc.ch (accessed October 22, 2020).

ISO Standard 7243 (1989). *Hot Environments—Estimation of the Heat Stress On Working Man, Based on the WBGT-Index (Wet Bulb Globe Temperature)*. International Standards Organization, Geneva.

Kjellstrom, T. (2016). Impact of climate conditions on occupational health and related economic losses: a new feature of global and urban health in the context of climate change. *Asia Pacific J. Public Health* 28, 28S−37S. doi: 10.1177/1010539514568711

Krishnamurthy, M., Ramalingam, P., Perumal, K., Kamalakannan, L. P., Chinnadurai, J., Shanmugam, R., et al. (2017). Occupational heat stress impacts on health and productivity in a steel industry in southern India. *Saf. Health Work* 8, 99–104. doi: 10.1016/j.shaw.2016.08.005

Kristal-Boneh, K., Harari, G., Green, M. S., and Ribak, J. (1995). Seasonal changes in ambulatory blood pressure in employees under different indoor temperatures. *Occup. Environ. Med.* 52, 715–721. doi: 10.1136/oem.52.11.715

Liljegren, J. C., Carhart, R. A., Lawday, P., Tschopp, S., and Sharp, R. (2008). Modeling the Wet Bulb Globe Temperature using standard meteorological measurements. *J. Occup. Environ. Hyg.* 5, 645–655. doi: 10.1080/15459620802310770

Makoto, F., Masahora, S., Hisataka, S., Pham, Q. Q. (2005). Hand arm vibration syndrome among quarry workers in Vietnam. *J. Occup. Health* 47, 165–170. doi: 10.1539/joh.47.165

Mathur, M. L. (2005). Pattern and predictors of mortality in sandstone quarry workers. *Ind. J. Occup. Environ. Med.* 9, 80–85. doi: 10.4103/0019-5278.16747

Morioka, I., Miyai, N., and Kazuhisa, M. (2006). Hot environment and health problems of outdoor workers at a construction site. *Ind. Health* 44, 474–480. doi: 10.2486/indhealth.44.474

Nag, P. K., Ashtekar, S. P., Nag, A., Kothari, D., Bandyopadhyay, P., and Desai, H. (1997). Human heat tolerance in simulated environment. *Ind. J. Med. Res.* 105, 226–234.

Nag, P. K., Dutta, P., Chorsiya, V., and Nag, A. (2014). "GIS visualization of climate change and prediction of human responses," in *Computational Intelligence Techniques in Earth and Environmental Sciences,* eds T. Islam, P. K. Srivastava, M. Gupta, X. Zhu, and S. Mukherjee (Dordrecht: Springer), 93–105. doi: 10.1007/978-94-017-8642-3_5

Nag, P. K., Dutta, P., and Nag, A. (2013). Critical body temperature profile as indicator of heat stress vulnerability. *Ind. Health* 51, 113–122. doi: 10.2486/indhealth.2012-0108

Nag, P. K., Nag, A., and Ashtekar, S. P. (2007). Thermal limits of men in moderate to heavy work in tropical farming. *Ind. Health* 45, 107–117. doi: 10.2486/indhealth.45.107

Parsons, K. (2003). *Human Thermal Environment. The Effects of Hot, Moderate and Cold Temperatures on Human Health, Comfort and Performance*, *2nd Edn.* New York, NY: CRC Press.

Petitti, D. B., Hondula, D. M., Yang, S., Harlan, S. L., and Chowell, G. (2015). Multiple trigger points for quantifying heat-health impacts: new evidence from a hot climate. *Environ. Health Perspect.* 124, 176–183. doi: 10.1289/ehp.1409119

Saghiv, M. S., and Sagiv, M. S. (2020). "Thermoregulation," in *Basic Exercise, Physiology* (Cham: Springer), 437–463. doi: 10.1007/978-3-030-48806-2_9

Saiyed, H. N., and Tiwari, R. R. (2004). Occupational health research in India. *Ind. Health* 42, 141–148. doi: 10.2486/indhealth.42.141

Steeneveld, G. J., Koopmans, S., Heusinkveld, B. G., Van Hove, L. W. A., and Holtslag, A. A. M. (2011). Quantifying urban heat island effects and human comfort for cities of variable size and urban morphology in the Netherlands. *J. Geophys. Res. Atmos.* 116:JD015988. doi: 10.1029/2011JD015988

TaMrin, S. B. M., Jamalohdin, M. N., Ng, Y. G., Maeda, S., and Ali, N. A. M. (2012). The characteristics of vibrotactile perception threshold among shipyard workers in a tropical environment. *Ind. Health* 50, 156–163. doi: 10.2486/indhealth.MS1221

Varghese, B. M., Hansen, A., Bi, P., and Pisaniello, D. (2018). Are workers at risk of occupational injuries due to heat exposure? A comprehensive literature review. *Saf. Sci.* 110, 380–392. doi: 10.1016/j.ssci.2018.04.027

Conflict of Interest: The authors declare that the research was conducted in the absence of any commercial or financial relationships that could be construed as a potential conflict of interest.

frontiers in Sustainable Cities

ORIGINAL RESEARCH
published: 12 April 2021
doi: 10.3389/frsc.2021.648551

Elemental Characteristics and Source-Apportionment of $PM_{2.5}$ During the Post-monsoon Season in Delhi, India

Vaibhav Bangar[1], Amit Kumar Mishra[1], Manish Jangid[1] and Prashant Rajput[2]*

[1] School of Environmental Sciences, Jawaharlal Nehru University, New Delhi, India, [2] Centre for Environmental Health, Public Health Foundation of India, Gurugram, India

In this study, we have coupled measurements, modeling, and remote sensing techniques to better delineate the source characteristics and variability of air pollutants in Delhi primarily during the post-monsoon season in 2019. We show a comparison of ambient $PM_{2.5}$ (particulate matter having aerodynamic diameter $\leq 2.5\,\mu m$) levels and associated elements during the post-monsoon with those during a relatively clean season of monsoon (experiencing frequent wet precipitation). Air-mass back trajectories from Hybrid Single-Particle Lagrangian Integrated Trajectory (HYSPLIT) model have been used to infer the possible source pathways of $PM_{2.5}$ impacting at the receptor site in Delhi. The average concentrations of $PM_{2.5}$ during monsoon (June–July) and post-monsoon (October–November) were $42.2 \pm 15.5\ \mu g\ m^{-3}$ (range: 22–73 $\mu g\ m^{-3}$) and $121.4 \pm 53.6\ \mu g\ m^{-3}$ (range: 46–298 $\mu g\ m^{-3}$), respectively. The $PM_{2.5}$ samples were analyzed for heavy and trace elements (Si, S, Na, Mg, Al, Cl, Ca, K, Ti, V, Cr, Mn, Fe, Ni, Cu, Br, Rb, Zr, and Pb) using an Energy Dispersive X-ray Fluorescence (ED-XRF) technique and their concentrations have been used to carry out the source-apportionment utilizing principal component analysis (PCA) tool. The PCA analysis has identified three major sources of fine aerosols including contributions from the sources viz. vehicular emission, biomass burning, coal combustion, secondary aerosols formation, soil dust, solid-waste burning and industrial emission. The source involving biomass burning contributed largely to the $PM_{2.5}$ in post-monsoon season through long-range transport of large-scale agriculture-residue burning emissions (occurring in the states of Punjab, Haryana, and western part of Uttar Pradesh). The industrial emissions include primarily, medium- and small-scale metal processing industries (e.g. steel sheet rolling) in Delhi-National Capital Region. Traces of emission from coal based thermal power plants and waste incineration have also been observed in this study.

Keywords: atmospheric aerosols, trace metals, urban air-shed, source-apportionment, Delhi

OPEN ACCESS

Edited by:
Maria De Fatima Andrade,
University of São Paulo, Brazil

Reviewed by:
Jianlin Hu,
Nanjing University of Information Science and Technology, China
Imran Shahid,
Qatar University, Qatar
Evangelia Diapouli,
National Centre of Scientific Research Demokritos, Greece

****Correspondence:***
Amit Kumar Mishra
amit.mishra.jnu@gmail.com;
amitmishra@mail.jnu.ac.in

Specialty section:
This article was submitted to Climate Change and Cities, a section of the journal Frontiers in Sustainable Cities

Received: *31 December 2020*
Accepted: *10 March 2021*
Published: *12 April 2021*

Citation:
Bangar V, Mishra AK, Jangid M and Rajput P (2021) Elemental Characteristics and Source-Apportionment of $PM_{2.5}$ During the Post-monsoon Season in Delhi, India. Front. Sustain. Cities 3:648551. doi: 10.3389/frsc.2021.648551

INTRODUCTION

Clean and healthy air is essential to all life on earth and is crucial for the well-being of human beings and the optimum performance of its supporting ecosystems. However, industrialization and urbanization have severe detrimental effects on the natural environment, be it air, water, or the soil (Kushwaha et al., 2012). The atrocious levels of particulate matter (PM) pollution in the atmosphere has created a disconcerting situation across the world's scientific and political communities, especially in developing countries due to their climatic and human health impacts (Khodeir et al., 2012; World Health Organization, 2016). PM pollution alters the composition and chemistry of the lower atmosphere, degrades air quality, reduces visibility and impacts the global climate (Khain and Pinsky, 2018). Numerous harmful impacts of PM exposure such as pulmonary and cardiovascular diseases, allergies and premature deaths have been evinced in several epidemiological studies (Badyda et al., 2016; Ghude et al., 2016). A recent research has reported that more than 75% people in India are imperiled with $PM_{2.5}$ levels >40 $\mu g\ m^{-3}$, a limit set by the National Ambient Air Quality Standards (Balakrishnan et al., 2019). The study has also mentioned that exposure to ambient $PM_{2.5}$ resulted in ∼9.8 lakhs premature deaths in a year and is of the major concern to human health point of view. Another research has estimated that $PM_{2.5}$ exposures could lead to average loss of life expectancy (LLE) of 3.4 years for the country with the highest value of LLE of 6.3 years for Delhi (Ghude et al., 2016).

Recent studies have established that the impact of $PM_{2.5}$ on human health cannot be only connected directly to the total mass concentration but also to the toxicity of particulate matter constituents (Yadav and Phuleria, 2020), specifically trace metals (Lippmann and Chen, 2009; Stanek et al., 2011). It is also imperative to analyze the seasonal variation of $PM_{2.5}$ in the ambient air due to its high association with meteorological parameters such as relative humidity, wind speed, temperature, and precipitation (Das et al., 2020). Thus, a good understanding about chemical composition and emission sources of PM along with its seasonal variability is essential for attributing its major impacts and developing effective and efficient mitigation policy strategies (Bangar et al., 2020).

$PM_{2.5}$ has myriads of natural and anthropogenic sources and is known to originate from the combustion of fossil fuels, biomass burning, soil dust, coagulation of ultrafine particles, reactions in water droplets, and condensation of gaseous organic and inorganic molecules, among others (Sioutas et al., 2005; Edgerton et al., 2009). Studies on elemental composition associated with fine PM in India have revealed that the urban population is particularly exposed to elevated levels of elements including Na, K, Mg, Al, Ca, S, Si, Cl, Cr, Ti, As, Br, Pb, Fe, Zn, and Mn due to vehicular emissions, biomass burning, industrial emissions, and soil dust uplift (Kulshrestha et al., 2009; Murari et al., 2015; Sharma and Mandal, 2017). The extent of health impact and toxicity of PM varies as a function of its composition and source, thus making it essential to conduct source apportionment analysis to comprehend the sources contributing to the PM budget over a receptor site (Jain et al., 2020).

Receptor models use a multivariate statistical approach to identify and quantify the sources of air pollutants, assuming the mass conservation between the emission sources and receptor site (Hopke et al., 2006). In India, source apportionment studies for PM have been performed using different receptor models viz. chemical mass balance (CMB) (Sharma and Patil, 1994; Srivastava et al., 2005; Srivastava and Jain, 2008; Gummeneni et al., 2011), positive matrix factorization (PMF) (Jain et al., 2020; Tobler et al., 2020), and principal component analysis (PCA) (Karar and Gupta, 2007; Suman and Pal, 2010; Hazarika et al., 2015). Valuing the importance and possibility of identifying PM sources, the present study has been conducted using PCA. PCA can proficiently perform the source apportionment analysis without any prerequisite for source profile of constituents associated with PM (Karagulian and Belis, 2012).

The capital city of India (Delhi) is one of the most populous and drastically polluted cities on earth (Bhat, 2020). The rapid rise in demands for housing and infrastructure, production and manufacturing industries, motorized vehicles, and lack of adequate air pollution control programmes have exaggerated the health risks due to PM exposures in the city (Das et al., 2020). Sharma et al. (2016a), using a receptor model technique, identified that transport sector, biomass burning, and industry are the major contributors of $PM_{2.5}$ in Delhi during the winter season. For summer season, Sharma and Mandal (2017) identified long-range transport of soil dust from regional and transboundary areas as the key contributor of $PM_{2.5}$. Several other studies have also presented quite similar results; however, comprehensive studies comparing seasonal variation in PM concentrations, and elemental composition as well as confirming the sources of PM pollution (using modeling and remote sensing techniques) in India are scarce. The present work is an effort to distinguish the major sources of PM pollution in Delhi by incorporating measurements, modeling and remote sensing techniques with an aim to assist policymakers in developing improved and enhanced pollution control strategies to curb PM pollution. The current study emphasizes on analyzing the seasonal variations (monsoon and post-monsoon season) in the elemental composition of $PM_{2.5}$ and its source-apportionment during post-monsoon season in the year 2019. Samples of $PM_{2.5}$ were collected at Jawaharlal Nehru University, New Delhi, India and were assessed for elemental analysis using EDXRF (Energy Dispersive X-Ray Fluorescence). It is an extensively utilized method for the quantification of trace elements in airborne PM due to its non-destructive technique which provides elemental composition results quickly without any chemical pre-treatment (Nascimento Filho, 1999; Zucchi et al., 2000; Öztürk et al., 2011). The measured elemental composition was then used as an input to run the PCA model to quantify the sources contributing to $PM_{2.5}$ primarily for the post-monsoon season. Due to limited number of samples ($n = 20$) the PCA analysis was not performed for the monsoon season dataset. Moreover, the air-mass back-trajectories were also utilized in the study to understand the impact of distant sources regions on the $PM_{2.5}$ loading at the receptor site.

METHODOLOGY

Sampling Site

Samples of $PM_{2.5}$ were collected at Jawaharlal Nehru University (JNU), New Delhi (28.539°N, 77.167°E), India on the rooftop (16 m height) of the School of Environmental Sciences (SES) in the year 2019. The map of the sampling site is shown in **Figure 1** (source: Google maps and ArcGIS Pro version 1.2.0) and the locations of all the sites (sampling site and CPCB sites) have been marked. JNU is located in the south-west region of Delhi, in an environmentally sensitive area and extends over a large space of natural vegetation in an area of ∼800 acres. The sampling site is distant from any principal industrial activities; however, it is surrounded by major roads with high traffic density. Inside the campus the traffic density is relatively very low. The major landform features around Delhi are the Himalayas lying in north-northeast of Delhi approximately at a distance of 160 km, the Thar Desert of Rajasthan lying in the west and the alluvial plains in the south and east of Delhi. Delhi, with a population of more than 16 million people and over 10 million registered vehicles (Rai et al., 2020) remains choked with heavy air pollution, especially in the winter season due to temperature inversion and shallow boundary layer height which entraps a massive amount of pollutants near the ground level (Hazarika et al., 2015).

PM Sample Collection and Analysis

$PM_{2.5}$ sampling during the monsoon (21 June−13 July, 2019; $n = 20$) and the post-monsoon (11 October−20 November, 2019; $n = 40$) seasons was done using a Fine Particulate Air Sampler (APM 550, Envirotech, India). The mean flow rate of the sampler was maintained at 1 m^3 h^{-1} (accuracy ±2%). The sampler was operated for 24 h (8:00 a.m.−8:00 a.m.), and the volume of the air filtered during each sample collection was used to deduce the mass concentrations of PM in the ambient atmosphere. Standard protocol for the sample collection and storage until chemical analysis has been followed as prescribed by the Central Pollution Control Board (CPCB), India.

The samples were collected on the hydrophobic PTFE filter (Fluoropore, FHUP04700) of 47 mm diameter. The moisture of the filters (before and after sampling) was removed by desiccating them in a silica based desiccator. The initial and final weight of the filter substrate was determined on a microbalance and the $PM_{2.5}$ concentration was calculated using the standard gravimetric method. The meteorological data of temperature, humidity and wind speed was taken for both the seasons from Safdarjung airport (IMD: Indian Meteorological Department) site.

For the quantification of metals in $PM_{2.5}$, an Energy Dispersive X-ray fluorescence spectrometry (ED-XRF) was used for its non-destructive mechanism and quick analysis (Khodeir et al., 2012; Moriyama et al., 2014; Shaltout et al., 2017). In the present study, a total of 19 heavy and trace elements (Si, S, Na, Mg, Al, Cl, Ca, K, Ti, V, Cr, Mn, Fe, Ni, Cu, Br, Rb, Zr, and Pb) were analyzed using ED-XRF (PANalytical Epsilon 5 analyzer). The quality control and analysis (QC and QA) have been carried out during the elemental analysis on ED-XRF. The apparatus was set up with standard reference material (NIST SRM 2783). The instrument was pre-calibrated using the XRF standard BRPC3 and it performs a semi quantitative analysis. Semi-quantitative analysis allows the users to compare spectral data from samples in order to ascertain relative elemental concentration between samples. Accordingly, the uncertainty in the concentration of elements on ED-XRF was found to be within 10%. The lower limit of detection (LLD) of each element for ED-XRF is provided in **Supplementary Table 1**. The description of elemental analysis using ED-XRF and detailed methodology for calculating the concentration of individual elements are provided in the previous literatures (Maciejczyk et al., 2005; Hazarika et al., 2015). In the present study, the concentration of each element in ng/m^3 was calculated using the following equation (Hazarika et al., 2015):

$$\text{Conc. of element x in ng/m}^3 = \frac{\text{EDXRF value of x element} \times (\text{Difference in filter weight})}{\text{Volume of the air sampled}}$$

where EDXRF value denotes the concentration of element x in ppm, difference in filter weight (pre- and post-sampling) is in milligrams and the volume of air sampled is in m^3.

Air-Mass Backward Trajectory Analysis

The fine PM has relatively a high residence time, and it can undergo long-range transport in the ambient atmosphere (Maenhaut et al., 2016). Therefore, to understand the origin of $PM_{2.5}$ and its long-range transport pattern to the sampling site, the air-mass backward trajectory analysis was done using the Hybrid Single Particle Lagrangian Integrated Trajectory (HYSPLIT) model. Daily GDAS (1 degree, global) meteorological files were accessed to compute the 72-h back trajectories at 500 m and 1,000 m above the ground level (AGL) for each day and night of the sampling campaign. These heights were chosen to represent winds in the boundary layer and to eliminate local land cover and topographic effects. AIRS (Atmospheric Infrared Sounder) dust score data from NASA website (URL: https://earthdata.nasa.gov/labs/worldview/) and MODIS Moderate Resolution Imaging Spectroradiometer fire count data (URL: https://earthdata.nasa.gov/active-fire-data) was overlaid on a true color image to locate the geographical regions responsible for enhancing the aerosol concentrations at the sampling site. AIRS dust score layer shows the level of dust aerosols in the Earth's atmosphere and the areas affected by it. Whereas, the MODIS thermal anomalies data is a fire product in which active fires and other thermal anomalies are identified using thermal anomalies algorithm (Giglio et al., 2003).

Source Apportionment Using PCA

The source apportionment analysis of $PM_{2.5}$ was carried out only for the post-monsoon season using the Principal Component Analysis (PCA). PCA is a statistical tool which explains the variance of a large amount of data having inter-correlated variables and transforms it into a smaller dataset of independent variables called principal components (PC) (Thurston and Spengler, 1985; Sharma et al., 2016b). In PCA, the factor loadings or PC identify the sources associated with pollution based on the correlation of individual pollutant species with each component.

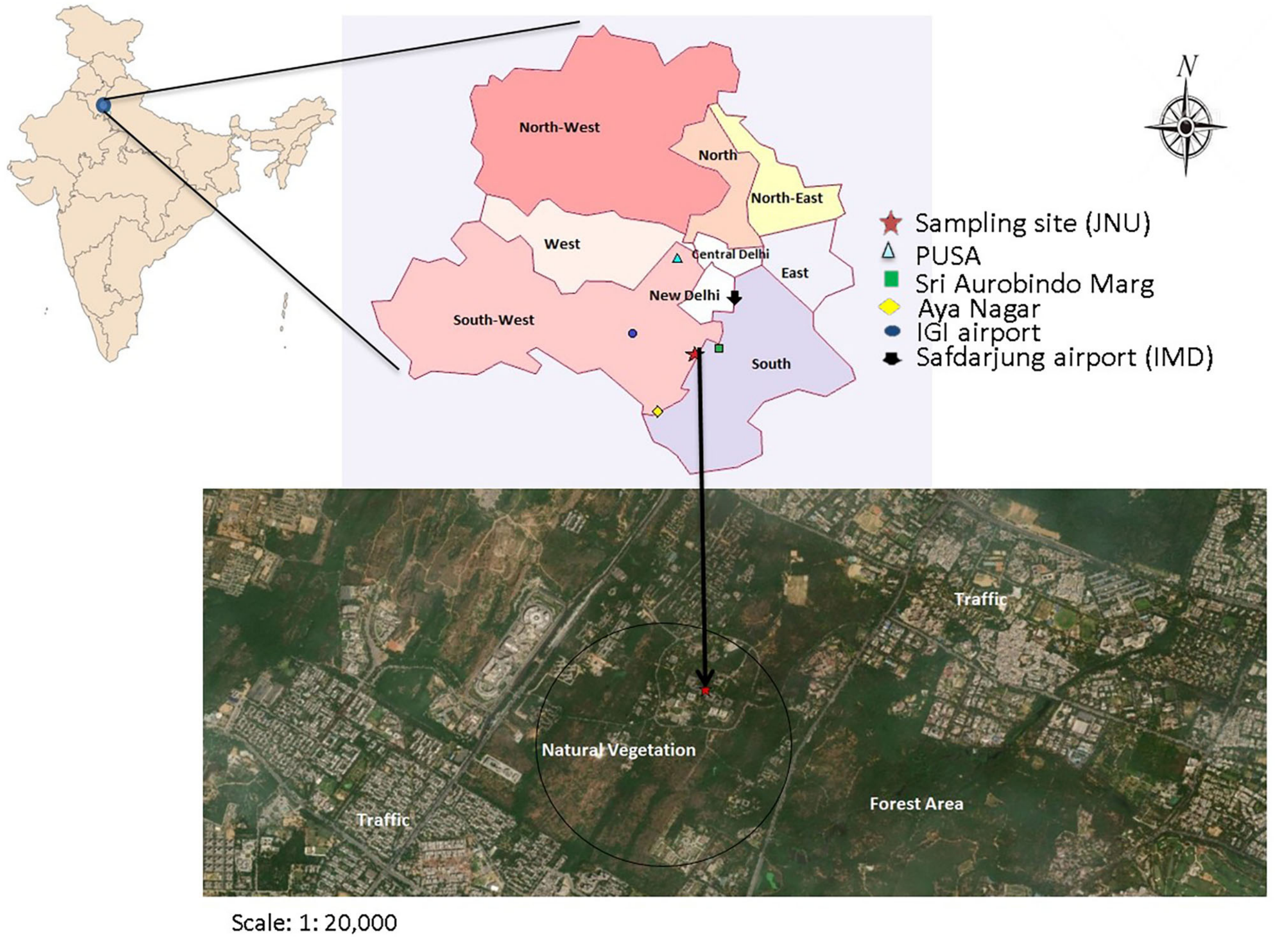

FIGURE 1 | Map of sampling site. All $PM_{2.5}$ measurement sites (JNU, PUSA, Sri Aurobindo Marg, Aya Nagar, IGI airport) and Meteorological measurement site (Safdarjung airport) are shown by legends on Delhi map. Google map of region (marked by vegetation and traffic locations) near the sampling site (JNU) is shown in the lower panel.

The pollutant species highly correlated with individual PCs indicates the association of that PC with the source emission composition (Johnson et al., 2015). In the present analysis, PCA has been performed with a statistical software SPSS (Version 25) following the Varimax Rotation method. This method maximizes the variance of the squared elements in the column of a factor matrix. In PCA, the first PC explains the most significant fraction of the original variables, while the second PC estimates a reduced fraction of the original variable in comparison with the first PC and so on (Sousa et al., 2007). PCA begins by normalizing the set of variables as Z_{ij} using equation (1), so that the variance of this set of variables is unity.

$$Z_{ij} = \frac{C_{ij} - \overline{C_j}}{\delta_j} \tag{1}$$

Where C_{ij} is the concentration of jth species in the ith sample; $\overline{C_j}$ and δ_j are the average concentration and standard deviation of that species j. The fundamental operation of PCA can be expressed by equation (2) indicating that it splits the data matrix into two matrices G_{ik} (factor loading) and H_{kj} (factor score), as shown below:

$$Z_{ij} = \sum_{k=1}^{p} G_{ik}H_{kj} + E_{ij} \tag{2}$$

Here, i, j, and k represent the index for sample, species and factors, respectively. E_{ij} represents the residual matrix. The two vectors G and E are unknown in the factor analysis (FA) and are obtained by assuming various covariance relationships between the vectors H and E and finally Varimax rotation of matrix is applied to minimize the datasets of elements having high loading factor (Kumar et al., 2001). As the factor load of the variable increases, the identification of the possible source of components also increases (Henry, 2003). The detailed methodology for air pollutant's source identification and apportionment using PCA is provided in Chavent et al. (2009). In the present study PCA was carried out utilizing elemental concentration data of 40 samples for the post-monsoon season. Numerous other studies have employed PCA for source apportionment using limited data points viz; Hazarika et al. (2015) utilized data from 12 samples for each season (summer, winter and monsoon) to perform PCA analysis, Liu et al. (2018) utilized data from 15 day samples, similarly Zhang et al. (2019) and Kanellopoulos et al. (2020) also utilized limited data set to carry out source apportionment analysis using PCA.

RESULTS AND DISCUSSION

Seasonal Variability of $PM_{2.5}$ and Air-Mass Back Trajectory Analysis

In total, 60 samples were collected to ascertain the seasonal variation in $PM_{2.5}$ concentrations during monsoon (n = 20 samples) and post-monsoon (n = 40 samples) seasons. Average mass concentrations were found to be 42.2 ± 15.5 μg m^{-3} (range: 21.8–72.5 μg m^{-3}) and 121.4 ± 53.6 μg m^{-3} (range: 45.9–298.1 μg m^{-3}) in monsoon and post-monsoon seasons, respectively. The $PM_{2.5}$ data monitored by the Central Pollution Control Board (CPCB) at four nearby sites (Aya Nagar, IGI Airport, PUSA and Sri Aurobindo Marg) was also taken into account to assess the spatial heterogeneity in $PM_{2.5}$ mass concentrations. **Figure 2** shows the temporal variability of $PM_{2.5}$ concentrations at the sampling site along with the mean concentration for the aforementioned nearby CPCB sites. The average $PM_{2.5}$ concentration at the sampling site i.e., JNU is lower than the other adjoining areas particularly in the post-monsoon season. The temporal variation of $PM_{2.5}$ mass concentrations for all sites during both the seasons are provided in **Supplementary Figure 1**. The average $PM_{2.5}$ mass concentrations at JNU and that integrated for the four CPCB sites were 42.2 μg m^{-3} and 44.3 μg m^{-3} in the monsoon season and 121.4 μg m^{-3} and 183.3 μg m^{-3} in the post-monsoon season. This can be attributed to the vast tract of natural vegetation and the low traffic density in the University campus site (JNU).

Figure 3 shows the daily variation of meteorological parameters (temperature, humidity and wind speed) during both the sampling seasons. It is apparent from the figure that the monsoon season was warmer than the post-monsoon season. The wind speed in the monsoon season was also higher than the post-monsoon season. However, the relative humidity appeared to be higher in the post-monsoon season as compared to the June–July period of the monsoon season. It is evident from **Figure 2** that the mean concentration of $PM_{2.5}$ was substantially higher in the post-monsoon season than the monsoon season. The previous studies conducted in Delhi assessing seasonal variations in $PM_{2.5}$ also showed an increased concentration in post-monsoon and winter season with respect to the monsoon season (Mandal et al., 2014; Gopalaswami, 2016; Panda et al., 2016; Sharma and Mandal, 2017; Jain et al., 2020). The most plausible explanation for lower $PM_{2.5}$ mass concentrations during the monsoon season relates to the high ventilation and dispersion of pollutants as well as occurrence of frequent precipitation leading to washout of the air pollutants during the monsoon (Jain et al., 2020). In the post-monsoon season, activities such as stubble (agriculture residues) burning in the fields of Haryana, Punjab, and western part of Uttar Pradesh, firecrackers burst during Diwali festival along with prevailing meteorological conditions such as minimal wind speed, shallow boundary layer height, and geographical settings (Himalayan range in the north and Deccan Plateau in the south) results into entrapment of a large amount of $PM_{2.5}$ near the ground level over the study region (Perrino et al., 2011; Rai et al., 2020). Kulshrestha and Kumar (2014) in their review report highlighted the need and significance of trajectory analysis for identifying the sources of PM pollution in South Asia.

The results from HYSPLIT back trajectory analysis indicating for the long-range transport of air masses at the sampling site are illustrated in **Figures 4A–E**. Air-mass back trajectories for a particular season do not look very different at two different altitudes, i.e., 500 and 1,000 m. During the monsoon season, the 72-h back trajectory indicated that the air masses traveled longer distances due to higher wind speed (**Figures 4A,B**). Most of the air masses in this period advanced to the receptor site from Indo-Gangetic Plain (IGP), Rajasthan, Gujarat, Pakistan, and the northern Arabian Sea, along with traces of air masses from Middle-East and the northern Bay of Bengal. The AIRS dust score overlaid on a true color image from MODIS shown for 24 June 2019 (**Figure 4C**) indicated for a strong dust layers in the atmosphere over Pakistan, Middle East and parts of the Arabian Sea which indicates that maybe the dust particles from these places would have transported over the receptor site. However, clean air mass from the Arabian Sea and Bay of Bengal would have diluted the overall dust load impact from these places at the receptor site. Sharma and Mandal (2017) made similar observations with the air-mass trajectory analysis during the monsoon season of 2013 over Delhi. Sharma et al. (2010) in their study of SO_2 variation over Delhi also highlighted the long-range transport of air-masses from sources pointing toward western and southwestern regions in the monsoon season.

In the post-monsoon season (**Figures 4D,E**), the back-trajectory showed that the air masses have covered shorter distance, attributable to the lower wind speed, before arriving at the receptor site. The air masses in this period were approaching the receptor site mainly from states of Haryana, Punjab, IGP region, Rajasthan, and Pakistan. The MODIS fire count data plot (**Figure 4F**) for 04 November 2019 exhibits an intensive stubble burning in Punjab, Haryana and western part Uttar Pradesh indicating that high concentration of PM (and gaseous pollutants) from biomass burning emission could severely impact the air quality at the receptor site. Moreover, emissions from numerous industries operating in Delhi would also contribute to PM loading at the receptor site. Therefore, higher concentration of $PM_{2.5}$ in the post-monsoon season can be attributed to the combined effect of lower wind speed, shallower boundary layer height, and the high incidence of stubble burning which increases the aerosol load over Delhi (Kanawade et al., 2020). For post-monsoon season similar results mentioning stable meteorological conditions leading to accumulation of local and transboundary pollutants have been mentioned in the previous studies conducted in Delhi (Tiwari et al., 2013; Panda et al., 2016; Cusworth et al., 2018; Kulkarni et al., 2020; Nair et al., 2020).

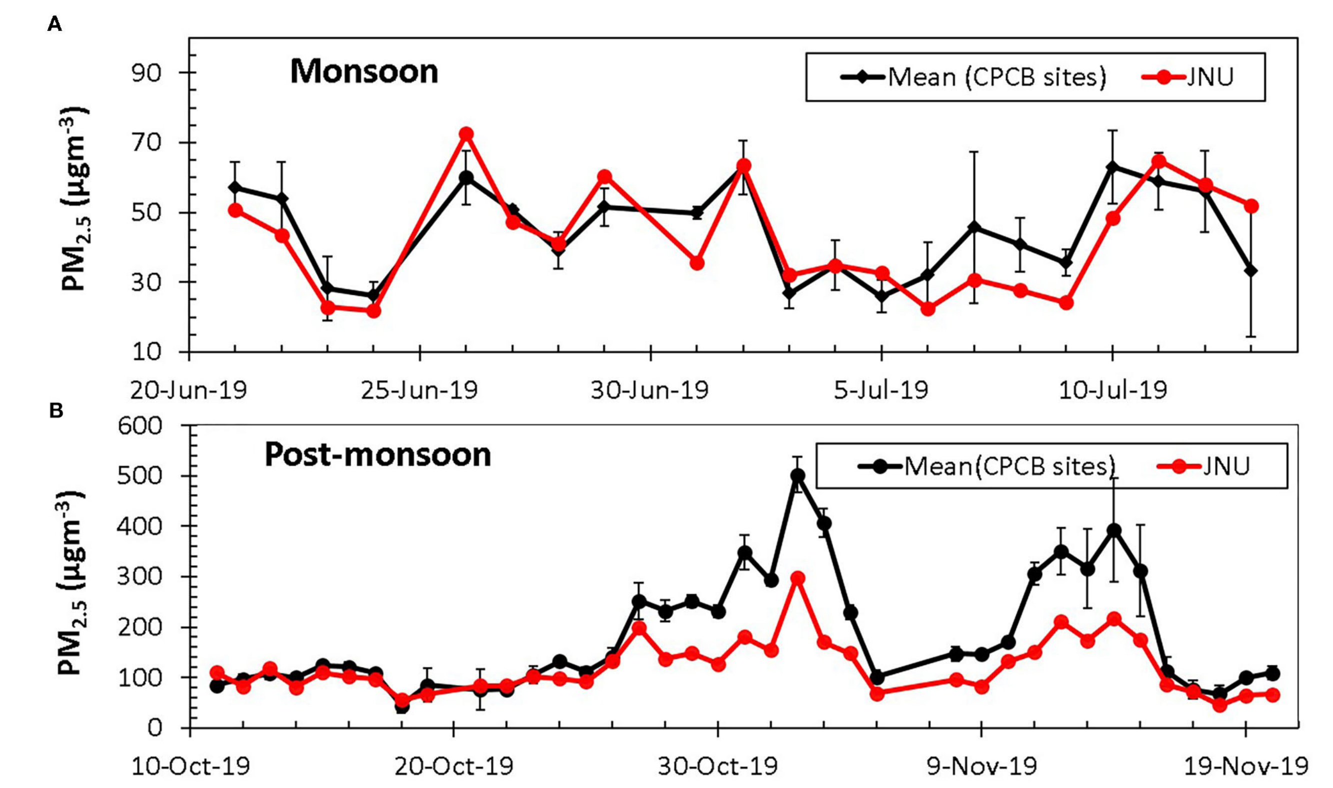

FIGURE 2 | Temporal variation of $PM_{2.5}$ concentrations ($\mu g\ m^{-3}$) at JNU (sampling site, shown by red color) and mean $PM_{2.5}$ concentrations for four CPCB sites (shown by black color, standard deviation is shown by vertical black lines) during **(A)** monsoon (21 Jun–13 July 2019) and **(B)** post-monsoon (11 Oct–20 Nov 2019) seasons.

In sharp contrast, the precipitation and high wind speed lead to lowering the concentration of atmospheric particles during the monsoon season (Sharma et al., 2016a). It is worth mentioning that the aerosols sampling was performed for 60 days, spread over both the seasons, and we found that the PM concentrations exceeded the NAAQS (National Ambient Air Quality Standard) standard value for more than 70% of the days. This is coherent with the other research work carried out over the Delhi (Pachauri et al., 2013; Tiwari et al., 2013; Sahu and Kota, 2016; Das et al., 2020; Jain et al., 2020).

Elemental Composition of $PM_{2.5}$

Figure 5 shows the percentage elemental composition of fine particulates for both seasons [(a) monsoon and (b) post-monsoon]. The daily variations in the percentage elemental composition of $PM_{2.5}$ for both the seasons are shown in **Supplementary Figure 2**. The temporal variations in concentration of the analyzed elements associated with $PM_{2.5}$ for both the seasons are depicted in **Supplementary Figures 3A–C**. The result of the current study showed that the average concentrations of elements were found in the decreasing order of Si>Al>Na>Mg>S>Ca>Cl>K>Fe for the monsoon season and S>Al>Na>Si>Cl>K>Mg>Ca>Fe for the post-monsoon season. The presence of Si, Al, Na, Mg, S, Ca, Fe and K as major elements associated with $PM_{2.5}$ is in agreement with other studies conducted in Delhi by Jain et al. (2017) and Sharma and Mandal (2017). Hazarika et al. (2015) also observed Na, Ca, Si and K as abundant elements in $PM_{2.5}$ followed by Ni, Cu and Pb. However, in the present study, the mean elemental concentration of individual elements was comparatively less than the previous studies conducted in Delhi. The relative contribution of elements associated with crustal or natural origin such as Si, Al, Na and Mg (Pipal et al., 2014; Ali et al., 2019; Rai et al., 2020) accounted for 87% of the elemental composition of $PM_{2.5}$ in the monsoon season, whereas in the post-monsoon season these elements accounted only for 57% (**Figure 5**). The element which contributed the most to the fine particulate was Silicon (Si) 39% in the monsoon season and Sulfur (S) 30% in the post-monsoon season. The high concentration of Si could be attributable to uplifted mineral dust contribution, whereas elevated S content may have contribution from coal combustion and agricultural-residue (biomass) burning (Sternbeck et al., 2002; Perrino et al., 2011). The sources of soil/road dust in the atmosphere include transboundary transport from deserts or entrainment from paved or unpaved roads, construction activities, and agricultural practices (Kulshrestha et al., 2009; Tiwari et al., 2013).

Moreover, the contribution of Potassium (K), Chlorine (Cl), and Lead (Pb) have been found to increase in the post-monsoon season due to different reasons. Higher concentration of K can

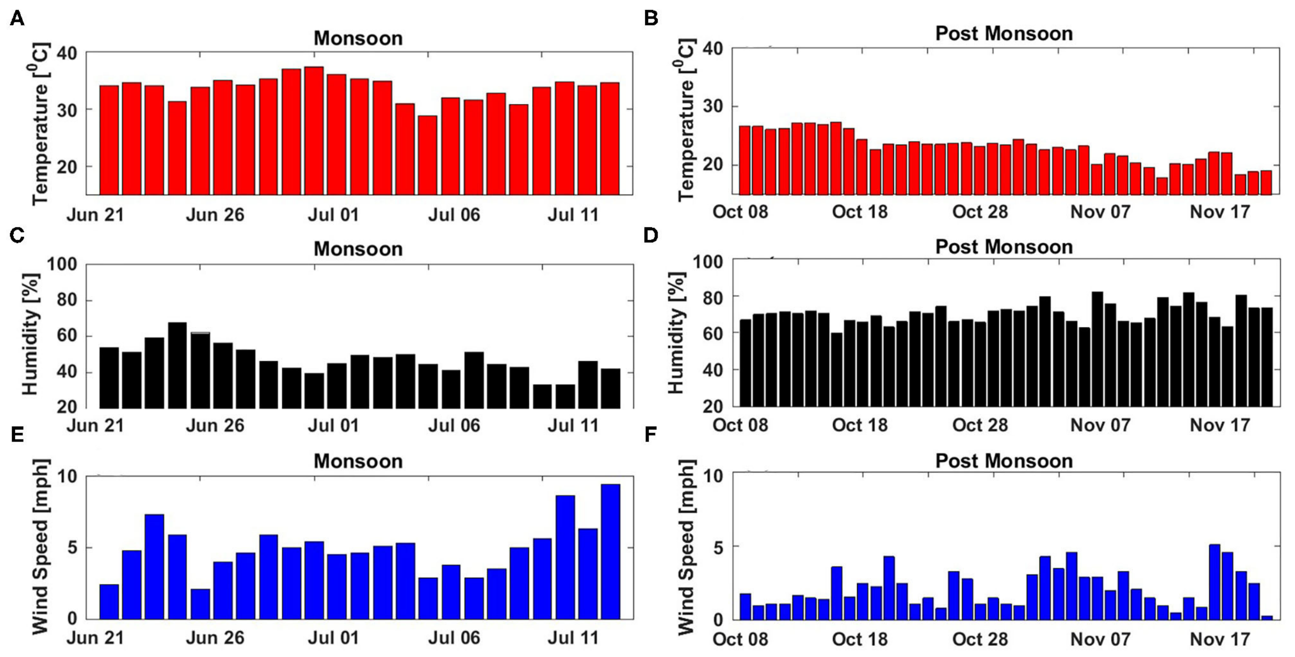

FIGURE 3 | Daily variation of meteorological parameters; **(A,B)** air temperature (in °C), **(C,D)** humidity (in %), and **(E,F)** wind speed (in mph) during the monsoon (21 June −13 July 2019) and post-monsoon (11 Oct−20 Nov 2019) seasons, respectively.

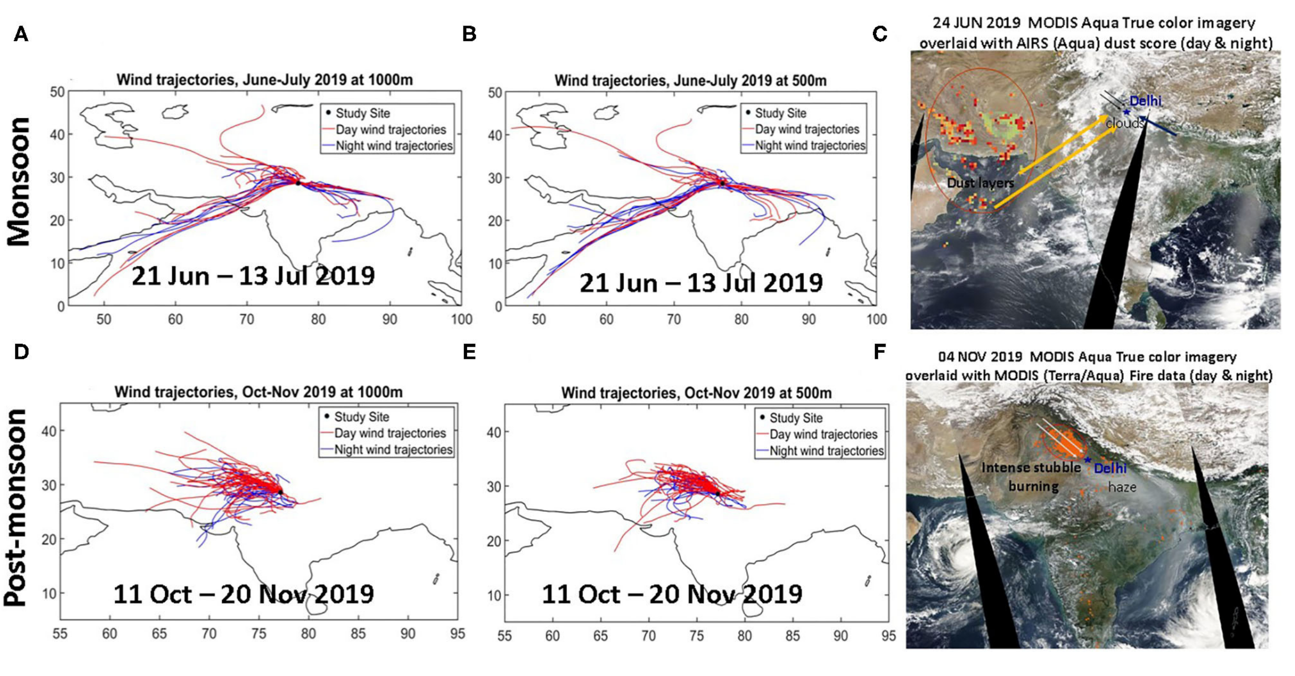

FIGURE 4 | HYSPLIT derived air-mass back trajectories during **(A,B)** monsoon (21 Jun−13 Jul 2019) season and, **(D,E)** post-monsoon (11 Oct−20 Nov 2019) season at 1,000 m and 500 m. Day time and night time wind trajectories are shown by red and blue colors, respectively. **(C)** MODIS aqua true color imagery overlaid with AIRS dust scores for 24 Jun, 2019 (major wind direction at receptor site are shown by arrows). **(F)** MODIS aqua true color imagery overlaid with MODIS fire counts for 4 Nov, 2019 (major wind direction at receptor site are shown by arrows).

be attributed to local biomass burning (in addition to some fraction from upper continental crust) for space heating and agricultural residue burning (Liu et al., 2018; Das et al., 2020); Cl can have contributions from lubricants, diesel fuels, coal combustion, biomass burning, and plastic and paper burning (Singhai et al., 2017; Chang et al., 2018); Pb to ore and metal

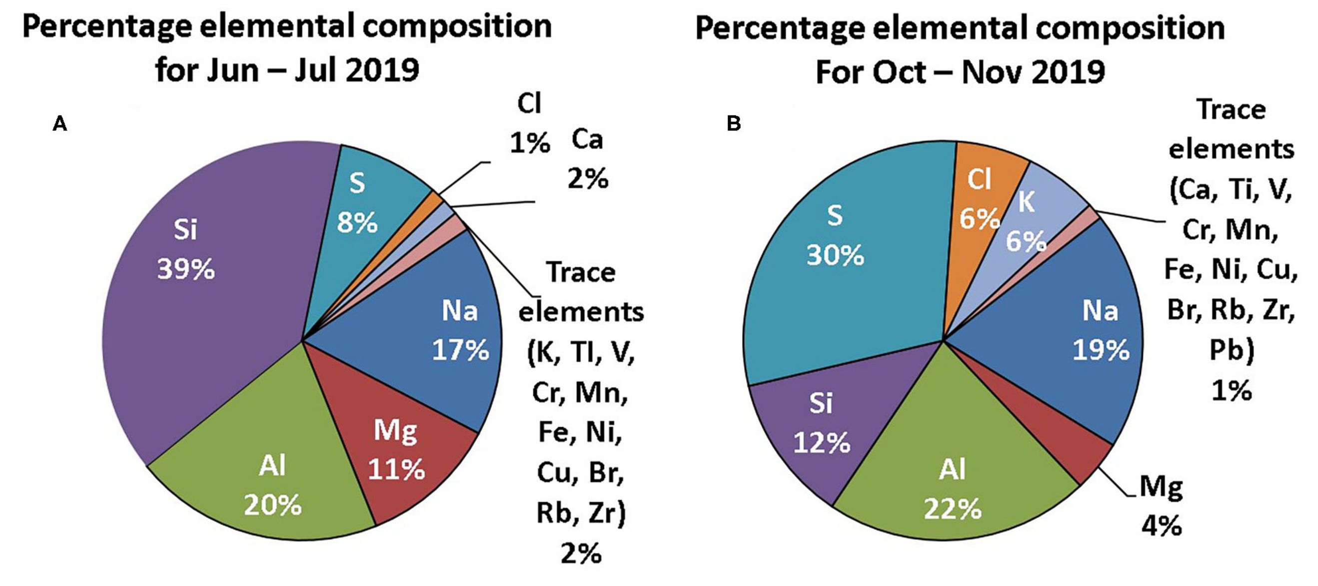

FIGURE 5 | Percentage elemental composition of $PM_{2.5}$ during **(A)** monsoon (21 Jun–13 July 2019) and **(B)** post-monsoon (11 Oct–20 Nov 2019) seasons.

processing, lead-acid battery production/recycling as well as waste incineration (Bukowiecki et al., 2009; Kothai et al., 2011). Summing up, the post-monsoon season witnessed a substantial increase in $PM_{2.5}$ concentrations predominantly due to the anthropogenic emissions (as suggested by elevated levels of S, K, Cl, Pb) with a relatively low contribution of mineral dust as compared to the scenario in monsoon season. Similar remarks have been noticed before in the previous research works (Khodeir et al., 2012; Das et al., 2020; Jain et al., 2020; Rai et al., 2020). Within the trace elements, three carcinogenic heavy metals were identified, i.e., Ni, Cr and Pb, that may pose substantial risk to humans (Liu et al., 2015). The estimated concentration of these elements is depicted in **Supplementary Figure 3B**. However, their concentration in this study was found well within the limits prescribed by the World Health Organization (WHO). The comprehensive details on source apportionment of $PM_{2.5}$ based on associated metals profile are discussed in the following section.

Source Apportionment

To distinguish the possible sources of fine fraction particulate matter, the principal component analysis (PCA) was carried out. Based on the eigenvalues >1, PCA segregates the data into several clusters known as principal components (PC), which also indicate the contribution of each dependent variable (which in this study is the element concentration) in terms of factor loadings. The PCA was performed using the data set consisting of 19 elemental species in 40 $PM_{2.5}$ samples (during the post-monsoon season) collected at JNU site in Delhi. **Table 1** shows the output of PCA analysis using SPSS (IBM, SPSS, version 25) software for the post-monsoon season. The correlation matrices for all 19 elements during both the seasons are shown in **Supplementary Tables 2, 3**. **Figure 6** shows the possible sources of $PM_{2.5}$ pollutions in the post-monsoon season as identified using PCA. The total variance explained for the sources of $PM_{2.5}$ during post-monsoon season (81.7%) using PCA are provided in **Supplementary Table 4**.

TABLE 1 | Summary of principal component analysis (PCA) of elements associated with $PM_{2.5}$ over Delhi during the post-monsoon season.

Species	Post-monsoon season		
	PC1	PC2	PC3
Na	**0.625**	**0.532**	0.490
Mg	**0.835**	0.460	0.165
Al	**0.924**	0.322	0.104
Cu	0.414	0.342	**0.822**
Ni	−0.009	**0.795**	−0.067
Zr	0.120	−0.155	**0.692**
Pb	0.140	**0.738**	0.049
Rb	0.302	0.320	**0.815**
Br	0.132	0.325	**0.840**
Fe	0.442	**0.852**	0.158
Mn	0.350	**0.850**	−0.101
Cr	−0.273	0.298	−0.473
V	**0.953**	0.046	0.050
Ti	**0.961**	0.172	0.081
Si	**0.829**	0.468	0.150
S	**0.536**	**0.725**	0.276
Ca	**0.694**	**0.589**	0.247
Cl	−0.191	−0.106	**0.761**
K	**0.888**	0.227	0.297
Variance (%)	**33.66**	**27.42**	**20.55**
Cumulative Variance (%)	**33.66**	**61.08**	**81.63**

The bold value shows the factor loadings greater than 0.5 indicating the inclusion of those elemental species into each Principal Component (i.e. PC1, PC 2, PC3).

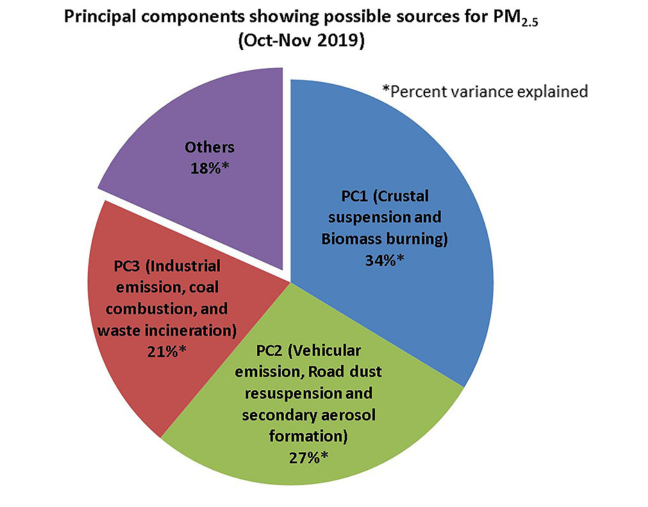

FIGURE 6 | Source-apportionment of $PM_{2.5}$ derived from PCA analysis during the post-monsoon (11 Oct–20 Nov 2019) season.

During the post-monsoon season, the PCA analysis revealed three factors, accounting for 81.7% of the total variance. The first PC explained 33.7% of the overall variance with an eigenvalue of 6.39 with high loadings of Na, Mg, Al, K, Ca, Ti, V and Si. Perrino et al. (2011) and Sharma et al. (2016a) reported that crustal dust is the major source of Si, Na, Mg, Ca, Ti, and Al in particulate matter. Therefore, this factor can be well-associated with crustal suspension. The % contribution of these elements (**Figure 5**) to fine particulate matter was relatively low in the post-monsoon season with respect to the monsoon season possibly due to low wind speed and boundary layer height leading to a lower resuspension of mineral dust in the ambient atmosphere. The Potassium (K) content, however, increased substantially owing to stubble/agriculture residue burning in the surrounding regions [as K is a tracer of biomass burning (Khare and Baruah, 2010)]. Similar results have been perceived in several other studies over Delhi (i.e., Jain et al., 2020; Rai et al., 2020). Therefore, this factor should be identified as crustal suspension and biomass burning. The second component with eigenvalue 5.21 represented 27.4% of the total variation with high loadings of S, Mn, Ni, Fe, and Pb. While Ni is related to vehicular emission especially with heavy diesel based vehicles (Khanna, 2015; Das et al., 2020), the elements such as Ni, Pb, Fe, and Mn are well associated with vehicular emissions mixed with road dust resuspension (Sternbeck et al., 2002; Khanna, 2015; Liu et al., 2015; Pant et al., 2015). The high concentration of S could be associated with coal combustion and secondary aerosols formation (Gummeneni et al., 2011). Therefore, this factor can be attributed to the vehicular emission, road dust resuspension, and secondary aerosols formation.

The third factor explains 20.6% of the overall variance with an eigenvalue of 3.9 and is strongly correlated with the elements Br, Cl, Cu, Rb, and Zr. These elements can have origin from industrial activities and solid-waste burning (Khodeir et al., 2012). Br in previous studies has been identified as the element associated with industrial emissions probably from various drug and chemical manufacturing industries (Kothai et al., 2011). Halogens can also be produced from solid-waste burning. In Delhi, most of the incineration of dumped waste occurs in three locations viz, Okhla (also a major industrial area in South Delhi), Bhalswa (North Delhi) and Ghazipur (East Delhi) (Ghosh et al., 2019). Moreover, in post-monsoon and winter season, brick kilns have been reported to function in areas encompassing Delhi, and they can possibly elevate the Cl concentrations in the atmosphere. These brick kilns are operating in large numbers around Delhi-NCR (National Capital Region) due to heavy demand in the infrastructure sector (Rai et al., 2020). These traditional kilns use coal and biomass as fuel to bake bricks which could emit a large amount of Cl and Br (Rai et al., 2020). Cu, Rb and Zr are associated with industrial emissions from different electroplating and other alloy manufacturing industries (Hazarika et al., 2015). Chowdhury et al. (2017) in their study in Delhi have indicated major point sources of emissions from coal based thermal power plants as well as major industrial areas located in central, northern, and eastern part of Delhi. The total number of coal based thermal power plants in Delhi-NCR is 6. These power plants and numerous industrial areas emit large amount of PM and other pollutants (Mittal et al., 2012). Therefore, this factor can be represented as coal combustion, industrial emissions, and waste incineration.

CONCLUSIONS

The seasonal variation in mass concentration and elemental composition of $PM_{2.5}$ was analyzed for the monsoon (June–July) and post-monsoon (October–November) seasons in 2019 at Delhi, India. The average $PM_{2.5}$ concentrations for the monsoon and post-monsoon season were 42.2 ± 15.5 $\mu g\ m^{-3}$ and 121.4 ± 53.6 $\mu g\ m^{-3}$, respectively. High wind speed and low relative humidity (%) were observed in the June–July months of monsoon season as compared to those during the post-monsoon season. The elements that contributed most to the $PM_{2.5}$ compositions were Si, Al, Na, and Mg in the monsoon season and S, Al, Na, Si, K and Cl in the post-monsoon season. Air-mass back trajectory analysis was performed to distinguish the major atmospheric pathways through which the air pollutants particularly $PM_{2.5}$ are impacting at the receptor site. High transboundary contribution to $PM_{2.5}$ was observed in the monsoon season, whereas in the post-monsoon season the contribution was by-and-large from the regional sources. PCA analyses, during the post-monsoon season, identified the major sources as (i) biomass burning and uplifted mineral dust, (ii) vehicular emissions, road dust resuspension, and secondary aerosols formation, and (iii) industrial emission, coal combustion, and solid-waste burning. These results were supported by the AIRS dust score and MODIS fire count data. The present study aims to assist the stakeholders and policymakers to better understand the characteristics of $PM_{2.5}$ during the post-monsoon season and to design and implement effective and efficient policy strategies to curb the problem of $PM_{2.5}$ pollution in Delhi.

DATA AVAILABILITY STATEMENT

The original contributions presented in the study are included in the article/**Supplementary Material**, further inquiries can be directed to the corresponding author/s.

AUTHOR CONTRIBUTIONS

AM and VB have designed the work and drafted the manuscript. VB, MJ, and AM have collected the required data. Data analysis, data interpretation and final editing is done by AM, VB, MJ, and PR.

ACKNOWLEDGMENTS

AM would also like to thank DST Purse grant and DST INSPIRE Faculty grant [DST/INSPIRE/04/2015/003253] to provide necessary funds for consumables and analysis cost. Authors would like to acknowledge the Advanced Instrumentation Research Facility (AIRF) at Jawaharlal Nehru University (JNU), New Delhi to facilitate ED-XRF analysis. Authors would like to thank three reviewers and editor for their valuable comments and suggestions.

SUPPLEMENTARY MATERIAL

The Supplementary Material for this article can be found online at: https://www.frontiersin.org/articles/10.3389/frsc.2021.648551/full#supplementary-material

REFERENCES

Ali, K., Acharja, P., Trivedi, D. K., Kulkarni, R., Pithani, P., Safai, P. D., et al. (2019). Characterization and source identification of PM2. 5 and its chemical and carbonaceous constituents during Winter Fog Experiment 2015–16 at Indira Gandhi International Airport, Delhi. *Sci. Total Environ.* 662, 687–696. doi: 10.1016/j.scitotenv.2019.01.285

Badyda, A. J., Grellier, J., and Dabrowiecki, P. (2016). "Ambient PM2. 5 exposure and mortality due to lung cancer and cardiopulmonary diseases in Polish cities," in *Respiratory Treatment and Prevention* ed Pokorski, M. (Cham: Springer), 9–17. doi: 10.1007/5584_2016_55

Balakrishnan, K., Dey, S., Gupta, T., Dhaliwal, R. S., Brauer, M., Cohen, A. J., et al. (2019). The impact of air pollution on deaths, disease burden, and life expectancy across the states of India: the Global Burden of Disease Study (2017). *Lancet Planetary Health* 3:e26–e39. doi: 10.1016/S2542-5196(18)30261-4

Bangar, V., Goyal, R., and Pandey, R. (2020). "Climate change responses and sustainable development: integration of mitigation and adaptation," in *Sustainable Development Goals* eds Hazra, S., and Bhukta, A. (Cham: Springer), 203–214. doi: 10.1007/978-3-030-42488-6_13

Bhat, M. Y. (2020). "Environmental problems of Delhi and Governmental Concern," in *Global Issues and Innovative Solutions in Healthcare, Culture, and the Environment* ed Mervio, M. (Hershey, PA: IGI Global), 133–67. doi: 10.4018/978-1-7998-3576-9.ch008

Bukowiecki, N., Lienemann, P., Hill, M., Figi, R., Richard, A., Furger, M., et al. (2009). Real-world emission factors for antimony and other brake wear related trace elements: size-segregated values for light and heavy duty vehicles. *Enviro. Sci. Tech.* 43, 8072–8078. doi: 10.1021/es9006096

Chang, Y., Huang, K., Xie, M., Deng, C., Zou, Z., Liu, S., et al. (2018). First long-term and near real-time measurement of trace elements in China's urban atmosphere: temporal variability, source apportionment and precipitation effect. *Atmos. Chem. Phys*. 18, 11793–11812. doi: 10.5194/acp-18-11793-2018

Chavent, M., Guegan, H., Kuentz, V., Patouille, B., and Saracco, J. (2009). PCA- and PMF-based methodology for air pollution sources identification and apportionment. *Environmetrics* 20, 928–942. doi: 10.1002/env.963

Chowdhury, S., Dey, S., Tripathi, S. N., Beig, G., Mishra, A. K., and Sharma, S. (2017). "Traffic intervention" policy fails to mitigate air pollution in megacity Delhi. *Environ. Sci. Policy* 74, 8–13. doi: 10.1016/j.envsci.2017.04.018

Cusworth, D. H., Mickley, L. J., Sulprizio, M. P., Liu, T., Marlier, M. E., DeFries, R. S., et al. (2018). Quantifying the influence of agricultural fires in northwest India on urban air pollution in Delhi, India. *Environ. Res. Lett.* 13:44018. doi: 10.1088/1748-9326/aab303

Das, A., Singh, G., Habib, G., and Kumar, A. (2020). Non-carcinogenic and carcinogenic risk assessment of trace elements of PM 2.5 during winter and pre-monsoon seasons in Delhi: a case study. *Exposure Health* 12, 63–77. doi: 10.1007/s12403-018-0285-y

Edgerton, E. S., Casuccio, G. S., Saylor, R. D., Lersch, T. L., Hartsell, B. E., Jansen, J. J., et al. (2009). Measurements of OC and EC in coarse particulate matter in the southeastern United States. *J. Air Waste Manage. Assoc.* 59, 78–90. doi: 10.3155/1047-3289.59.1.78

Ghosh, P., Shah, G., Chandra, R., Sahota, S., Kumar, H., Vijay, V. K., et al. (2019). Assessment of methane emissions and energy recovery potential from the municipal solid waste landfills of Delhi, India. *Bioresource Tech.* 272, 611–615. doi: 10.1016/j.biortech.2018.10.069

Ghude, S. D., Chate, D. M., Jena, C., Beig, G., Kumar, R., Barth, M. C., et al. (2016). Premature mortality in India due to $PM_{2.5}$ and ozone exposure. *Geophys. Res. Lett.* 43, 4650–4658. doi: 10.1002/2016GL068949

Giglio, L., Descloitres, J., Justice, C. O., and Kaufman, Y. J. (2003). An enhanced contextual fire detection algorithm for MODIS. *Remote Sens. Environ.* 87, 273–282. doi: 10.1016/S0034-4257(03)00184-6

Gopalaswami, P. (2016). A study on effects of weather, vehicular traffic and other sources of particulate air pollution on the city of Delhi for the year (2015). *J. Environ. Pollut. Human Health* 4, 24–41. doi: 10.12691/jephh-4-2-1

Gummeneni, S., Yusup, Y. B., Chavali, M., and Samadi, S. Z. (2011). Source apportionment of particulate matter in the ambient air of Hyderabad city, India. *Atmospheric Res.* 101, 752–764. doi: 10.1016/j.atmosres.2011.05.002

Hazarika, N., Jain, V. K., and Srivastava, A. (2015). Source identification and metallic profiles of size-segregated particulate matters at various sites in Delhi. *Environ. Monitoring Assessment* 187:602. doi: 10.1007/s10661-015-4809-7

Henry, R. C. (2003). Multivariate receptor modeling by N-dimensional edge detection. *Chemometr. Intelligent Lab. Syst.* 65, 179–189. doi: 10.1016/S0169-7439(02)00108-9

Hopke, P. K., Ito, K., Mar, T., Christensen, W. F., Eatough, D. J., Henry, R. C., et al. (2006). PM source apportionment and health effects: 1. Intercomparison of source apportionment results. *J. Exposure Sci. Environ. Epidemiol.* 16, 275–286. doi: 10.1038/sj.jea.7500458

Jain, S., Sharma, S. K., Choudhary, N., Masiwal, R., Saxena, M., Sharma, A., et al. (2017). Chemical characteristics and source apportionment of PM 2.5 using PCA/APCS, UNMIX, and PMF at an urban site of Delhi, India. *Environ. Sci. Pollut. Res.* 24, 14637–14656. doi: 10.1007/s11356-017-8925-5

Jain, S., Sharma, S. K., Vijayan, N., and Mandal, T. K. (2020). Seasonal characteristics of aerosols (PM2. 5 and PM10) and their source apportionment using PMF: a four years study over Delhi, India. *Environ. Pollut.* 262:114337. doi: 10.1016/j.envpol.2020.114337

Johnson, G. W., Ehrlich, R., Full, W., and Ramos, S. (2015). "Principal components analysis and receptor models in environmental forensics," in *Introduction to Environmental Forensics* eds Murphy, B. L. and Morrison, R. D. (Cambridge, MA: Academic Press), 609–653. doi: 10.1016/B978-0-12-404696-2.00018-7

Kanawade, V. P., Srivastava, A. K., Ram, K., Asmi, E., Vakkari, V., Soni, V. K., et al. (2020). What caused severe air pollution episode of November 2016 in New Delhi? *Atmospheric Environ.* 222:117125. doi: 10.1016/j.atmosenv.2019.117125

Kanellopoulos, P. G., Chrysochou, E., Koukoulakis, K., Vasileiadou, E., Kizas, C., Savvides, C., et al. (2020). Polar organic compounds in PM10 and PM2. 5 atmospheric aerosols from a background Eastern Mediterranean site during the winter period: Secondary formation, distribution and source apportionment. *atmosphere. Environ.* 237:117622. doi: 10.1016/j.atmosenv.2020.117622

Karagulian, F., and Belis, C. A. (2012). Enhancing source apportionment with receptor models to foster the air quality directive implementation. *Int. J. Environ. Pollut.* 50, 190–199. doi: 10.1504/IJEP.2012.051192

Karar, K., and Gupta, A. K. (2007). Source apportionment of PM10 at residential and industrial sites of an urban region of Kolkata, India. *Atmospheric Res.* 84, 30–41. doi: 10.1016/j.atmosres.2006.05.001

Khain, A. P., and Pinsky, M. (2018). *Physical Processes in Clouds and Cloud Modeling*. Cambridge: Cambridge University Press. doi: 10.1017/9781139049481

Khanna, I. (2015). Health risks associated with heavy metals in fine particulate matter: a case study in Delhi city, India. *J. Geosci. Environ. Protect.* 3:72. doi: 10.4236/gep.2015.32012

Khare, P., and Baruah, B. P. (2010). Elemental characterization and source identification of PM2. 5 using multivariate analysis at the suburban site of North-East India. *Atmospheric Res.* 98, 148–162. doi: 10.1016/j.atmosres.2010.07.001

Khodeir, M., Shamy, M., Alghamdi, M., Zhong, M., Sun, H., Costa, M., et al. (2012). Source apportionment and elemental composition of PM2. 5 and PM10 in Jeddah City, Saudi Arabia. *Atmospheric Pollut. Res.* 3, 331–340. doi: 10.5094/APR.2012.037

Kothai, P., Saradhi, I. V., Pandit, G. G., Markwitz, A., and Puranik, V. D. (2011). Chemical characterization and source identification of particulate matter at an urban site of Navi Mumbai, India. *Aerosol Air Quality Res.* 11, 560–569. doi: 10.4209/aaqr.2011.02.0017

Kulkarni, S. H., Ghude, S. D., Jena, C., Karumuri, R. K., Sinha, B., Sinha, V., et al. (2020). How much does large-scale crop residue burning affect the air quality in Delhi? *Environm. Sci. Tech.* 54, 4790–4799. doi: 10.1021/acs.est.0c00329

Kulshrestha, A., Satsangi, P. G., Masih, J., and Taneja, A. (2009). Metal concentration of PM2. 5 and PM10 particles and seasonal variations in urban and rural environment of Agra, India. *Sci. Total Environ.* 407, 6196–204. doi: 10.1016/j.scitotenv.2009.08.050

Kulshrestha, U., and Kumar, B. (2014). Airmass trajectories and long range transport of pollutants: review of wet deposition scenario in South Asia. *Adv. Meteorol.* 2014:596041. doi: 10.1155/2014/596041

Kumar, A. V., Patil, R. S., and Nambi, K. S. V. (2001). Source apportionment of suspended particulate matter at two traffic junctions in Mumbai, India. *Atmospheric Environ.* 35, 4245–4251. doi: 10.1016/S1352-2310(01)00258-8

Kushwaha, R., Lal, H., Srivastava, A., and Jain, V. K. (2012). Human exposure to particulate matter and their risk assessment over Delhi, India. *National Acad. Sci. Lett.* 35, 497–504. doi: 10.1007/s40009-012-0085-z

Lippmann, M., and Chen, L. C. (2009). Health effects of concentrated ambient air particulate matter (CAPs) and its components. *Crit. Rev. Toxicol.* 39, 865–913. doi: 10.3109/10408440903300080

Liu, K., Shang, Q., Wan, C., Song, P., Ma, C., and Cao, L. (2018). Characteristics and sources of heavy metals in PM2. 5 during a typical haze episode in rural and urban areas in Taiyuan, China. *Atmosphere* 9:2. doi: 10.3390/atmos9010002

Liu, X., Zhai, Y., Zhu, Y., Liu, Y., Chen, H., Li, P., et al. (2015). Mass concentration and health risk assessment of heavy metals in size-segregated airborne particulate matter in Changsha. *Sci. Total Environ.* 517, 215–221. doi: 10.1016/j.scitotenv.2015.02.066

Maciejczyk, P., Zhong, M., Li, Q., Xiong, J., Nadziejko, C., and Chen, L. C. (2005). Effects of subchronic exposures to concentrated ambient particles (CAPs) in mice: II. The design of a CAPs exposure system for biometric telemetry monitoring. *Inhalation Toxicol.* 17, 189–197. doi: 10.1080/08958370590912743

Maenhaut, W., Vermeylen, R., Claeys, M., Vercauteren, J., and Roekens, E. (2016). Sources of the PM10 aerosol in Flanders, Belgium, and re-assessment of the contribution from wood burning. *Sci. Total Environ.* 562, 550–560. doi: 10.1016/j.scitotenv.2016.04.074

Mandal, P., Sarkar, R., Mandal, A., and Saud, T. (2014). Seasonal variation and sources of aerosol pollution in Delhi, India. *Environmental Chem. Lett.* 12, 529–534. doi: 10.1007/s10311-014-0479-x

Mittal, M. L., Sharma, C., and Singh, R. (2012). "Estimates of emissions from coal fired thermal power plants in India," in *2012 International Emission Inventory Conference* (Tampa, FL), 13–16.

Moriyama, T., Morikawa, A., Doi, M., and Fess, S. (2014). Aerosol filter analysis using polarized optics EDXRF with thin-film FP method. *Powder Diffract.* 29:137. doi: 10.1017/S0885715614000207

Murari, V., Kumar, M., Barman, S. C., and Banerjee, T. (2015). Temporal variability of MODIS aerosol optical depth and chemical characterization of airborne particulates in Varanasi, India. *Environ. Sci. Pollut. Res.* 22, 1329–1343. doi: 10.1007/s11356-014-3418-2

Nair, M., Bherwani, H., Kumar, S., Gulia, S., Goyal, S., and Kumar, R. (2020). Assessment of contribution of agricultural residue burning on air quality of Delhi using remote sensing and modelling tools. *Atmospher. Environ.* 230:117504. doi: 10.1016/j.atmosenv.2020.117504

Nascimento Filho, V. F. (1999). *Nuclear analytical techniques of X-ray fluorescence by energy dispersion (EDXRF) and by total reflection (TXRF)*. Piracicaba: ESALQ/CENA/USP. (Handout), 33.

Öztürk, F., Zararsiz, A., Kirmaz, R., and Tuncel, G. (2011). An approach to measure trace elements in particles collected on fiber filters using EDXRF. *Talanta* 83, 823–831. doi: 10.1016/j.talanta.2010.10.038

Pachauri, T., Singla, V., Satsangi, A., Lakhani, A., and Kumari, K. M. (2013). Characterization of carbonaceous aerosols with special reference to episodic events at Agra, India. *atmosphere. Res.* 128, 98–110. doi: 10.1016/j.atmosres.2013.03.010

Panda, S., Sharma, S. K., Mahapatra, P. S., Panda, U., Rath, S., Mahapatra, M., et al. (2016). Organic and elemental carbon variation in PM 2.5 over megacity Delhi and Bhubaneswar, a semi-urban coastal site in India. *Natural Hazards* 80, 1709–1728. doi: 10.1007/s11069-015-2049-3

Pant, P., Shukla, A., Kohl, S. D., Chow, J. C., Watson, J. G., and Harrison, R. M. (2015). Characterization of ambient PM2. 5 at a pollution hotspot in New Delhi, India and inference of sources. *atmosphere. Environ.* 109, 178–189. doi: 10.1016/j.atmosenv.2015.02.074

Perrino, C., Tiwari, S., Catrambone, M., Dalla Torre, S., Rantica, E., and Canepari, S. (2011). Chemical characterization of atmospheric PM in Delhi, India, during different periods of the year including Diwali festival. *atmosphere. Pollut. Res.* 2, 418–427. doi: 10.5094/APR.2011.048

Pipal, A. S., Jan, R., Satsangi, P. G., Tiwari, S., and Taneja, A. (2014). Study of surface morphology, elemental composition and origin of atmospheric aerosols (PM2. 5 and PM10) over Agra, India. *Aerosol Air Qual. Res.* 14, 1685–1700. doi: 10.4209/aaqr.2014.01.0017

Rai, P., Furger, M., El Haddad, I., Kumar, V., Wang, L., Singh, A., et al. (2020). Real-time measurement and source apportionment of elements in Delhi's atmosphere. *Sci. Total Environ.* 742:140332. doi: 10.1016/j.scitotenv.2020.140332

Sahu, S. K., and Kota, S. H. (2016). Significance of PM2. 5 air quality at the Indian capital. *Aerosol Air Qual. Res. 17*, 588–597. doi: 10.4209/aaqr.2016.06.0262

Shaltout, A. A., Boman, J., and Alsulimane, M. E. (2017). Identification of elemental composition of PM2. 5 collected in Makkah, Saudi Arabia, using EDXRF. *X-Ray Spectrometry* 46, 151–163. doi: 10.1002/xrs.2732

Sharma, S. K., Datta, A., Saud, T., Saxena, M., Mandal, T. K., Ahammed, Y. N., et al. (2010). Seasonal variability of ambient NH3, NO, NO2 and SO2 over Delhi. *J. Environ. Sci.* 22, 1023–1028. doi: 10.1016/S1001-0742(09)60213-8

Sharma, S. K., and Mandal, T. K. (2017). Chemical composition of fine mode particulate matter (PM2. 5) in an urban area of Delhi, India and its source apportionment. *Urban Climate* 21, 106–122. doi: 10.1016/j.uclim.2017.05.009

Sharma, S. K., Mandal, T. K., Jain, S., Sharma, A., and Saxena, M. (2016b). Source apportionment of PM 2.5 in Delhi, India using PMF model. *Bull. Environ. Contaminat. Toxicol.* 97, 286–293. doi: 10.1007/s00128-016-1836-1

Sharma, S. K., Mandal, T. K., Srivastava, M. K., Chatterjee, A., Jain, S., Saxena, M., et al. (2016a). Spatio-temporal variation in chemical characteristics of PM 10 over Indo Gangetic Plain of India. *Environ. Sci. Pollut. Res.* 23, 18809–18822. doi: 10.1007/s11356-016-7025-2

Sharma, V. K., and Patil, R. S. (1994). Chemical mass balance model for source apportionment of aerosols in Bombay. *Environ. Monitor. Assessment* 29, 75–88. doi: 10.1007/BF00546780

Singhai, A., Habib, G., Raman, R. S., and Gupta, T. (2017). Chemical characterization of PM 1.0 aerosol in Delhi and source apportionment using positive matrix factorization. *Environ. Sci. Pollution Res.* 24, 445–462. doi: 10.1007/s11356-016-7708-8

Sioutas, C., Delfino, R. J., and Singh, M. (2005). Exposure assessment for atmospheric ultrafine particles (UFPs) and implications in epidemiologic research. *Environ. Health Perspect.* 113, 947–955. doi: 10.1289/ehp.7939

Sousa, S. I. V., Martins, F. G., Alvim-Ferraz, M. C. M., and Pereira, M. C. (2007). Multiple linear regression and artificial neural networks based on principal components to predict ozone concentrations. *Environ. Modell. Softw.* 22, 97–103. doi: 10.1016/j.envsoft.2005.12.002

Srivastava, A., and Jain, V. K. (2008). Source apportionment of suspended particulate matters in a clean area of Delhi: a note. *Transportat. Res. Part D* 13, 59–63. doi: 10.1016/j.trd.2007.09.001

Srivastava, A., Sengupta, B., and Dutta, S. A. (2005). Source apportionment of ambient VOCs in Delhi City. *Sci. Total Environ.* 343, 207–220. doi: 10.1016/j.scitotenv.2004.10.008

Stanek, L. W., Brown, J. S., Stanek, J., Gift, J., and Costa, D. L. (2011). Air pollution toxicology—a brief review of the role of the science in shaping the current understanding of air pollution health risks. *Toxicol. Sci.* 120(suppl_1), S8–S27. doi: 10.1093/toxsci/kfq367

Sternbeck, J., Sjödin, Å., and Andréasson, K. (2002). Metal emissions from road traffic and the influence of resuspension—results from two tunnel studies. *atmosphere. Environ.* 36, 4735–4744. doi: 10.1016/S1352-2310(02)00561-7

Suman, G. S., and Pal, A. K. (2010). Source apportionment of respirable particulate matter using principal component analysis: a case study from India. *Int. J. Appl. Environm. Sci.* 5, 909–921.

Thurston, G. D., and Spengler, J. D. (1985). A quantitative assessment of source contributions to inhalable particulate matter pollution in metropolitan Boston. *atmosphere. Environ.* (1967) 19, 9–25. doi: 10.1016/0004-6981(85)90132-5

Tiwari, S., Pervez, S., Cinzia, P., Bisht, D. S., Kumar, A., and Chate, D. M. (2013). Chemical characterization of atmospheric particulate matter in Delhi, India, Part II: source apportionment studies using PMF 3.0. *Sustain. Environ. Res.* (2013) 23:295–306.

Tobler, A., Bhattu, D., Canonaco, F., Lalchandani, V., Shukla, A., Thamban, N. M., et al. (2020). Chemical characterization of PM2. 5 and source apportionment of organic aerosol in New Delhi, India. *Sci. Total Environ.* 745:140924. doi: 10.1016/j.scitotenv.2020.140924

World Health Organization (2016). *Ambient Air Pollution: A Global Assessment of Exposure and Burden of Disease*. doi: 10.17159/2410-972X/2016/v26n2a4

Yadav, S., and Phuleria, H. C. (2020). "Oxidative potential of particulate matter: a prospective measure to assess PM toxicity," in *Measurement, Analysis and Remediation of Environmental Pollutants* eds Gupta, T., Singh, S. P., Rajput, P., and Agarwal, A. K. (Singapore: Springer), 333–56. doi: 10.1007/978-981-15-0540-9_16

Zhang, X., Zhao, X., Ji, G., Ying, R., Shan, Y., and Lin, Y. (2019). Seasonal variations and source apportionment of water-soluble inorganic ions in PM 2.5 in Nanjing, a megacity in southeastern China. *J. Atmospher. Chem.* 76:73–88. doi: 10.1007/s10874-019-09388-z

Zucchi, O. D., Dias, A. D., Nascimento Filho, V. F., and Salvador, M. J. (2000). Characterization of two medicinal plants by X-ray spectrometry. *J. Trace Microprobe Techniques* 18, 441–450. doi: 10.1385/BTER:103:3:277

Conflict of Interest: The authors declare that the research was conducted in the absence of any commercial or financial relationships that could be construed as a potential conflict of interest.

frontiers in Sustainable Cities

ORIGINAL RESEARCH
published: 24 June 2021
doi: 10.3389/frsc.2021.672428

Assessment of Health Impact of $PM_{2.5}$ Exposure by Using WRF-Chem Model in Kathmandu Valley, Nepal

*Avalokita Tuladhar, Palistha Manandhar and Kundan Lal Shrestha**

Department of Environmental Science and Engineering, Kathmandu University, Dhulikhel, Nepal

$PM_{2.5}$ is one of the major air pollutants in Kathmandu Valley, and its emission and the unique atmospheric condition of the valley make it significantly hazardous to human health. The air pollution due to particulate matter is a major health issue with numerous negative impacts on us. This research aims to quantify the health impacts of $PM_{2.5}$ exposure on the population of Kathmandu Valley. The ambient $PM_{2.5}$ concentration of Kathmandu Valley was simulated using WRF-Chem model by using a horizontal grid resolution of 3 × 3 km. The concentration obtained from WRF-Chem was used as input in the health equation of an intervention model to quantify the health impacts. This quantitative assessment of atmospheric pollution was applied to evaluate the human exposure to $PM_{2.5}$ in Kathmandu Valley. $PM_{2.5}$ concentration and its distribution in the valley along with the ward-wise population distribution were used to find the health impact of the particulate matter in December 2019 in Kathmandu Valley. Exposure analysis using the model showed that 19 people could die due to lung cancer and 175 people could die due to all cause diseases except accidents due to $PM_{2.5}$ exposure in December 2019. It was estimated that the reduction in the $PM_{2.5}$ level by half in the valley reduces the monthly mortality by 51.4%. Hence, the exposure analysis of the particulate matter on the urban population could be improved by using air quality models in order to solve the health problems arising from air pollution.

Keywords: air quality, exposure, health impact model, Kathmandu Valley, WRF-Chem model, $PM_{2.5}$

OPEN ACCESS

Edited by:
Atinderpal Singh,
University of Delhi, India

Reviewed by:
Pallavi Saxena,
Hindu College, University of Delhi, India
Mohd Talib Latif,
National University of Malaysia, Malaysia

****Correspondence:***
Kundan Lal Shrestha
kundan@ku.edu.np

Specialty section:
This article was submitted to Climate Change and Cities, a section of the journal Frontiers in Sustainable Cities

Received: *25 February 2021*
Accepted: *10 May 2021*
Published: *24 June 2021*

Citation:
Tuladhar A, Manandhar P and Shrestha KL (2021) Assessment of Health Impact of $PM_{2.5}$ Exposure by Using WRF-Chem Model in Kathmandu Valley, Nepal. Front. Sustain. Cities 3:672428. doi: 10.3389/frsc.2021.672428

1. INTRODUCTION

$PM_{2.5}$ in the ambient atmosphere is hazardous and detrimental to both the environment and human health. The amount of particulate matter can determine some of the impacts of air pollution on human health. If we consider the World Health Organization's recommended limits for the air pollution, the quality of Nepalese air is very poor with an annual mean $PM_{2.5}$ concentration of 44.5 $\mu g/m^3$, which exceeds the recommended threshold of 10 $\mu g/m^3$ (IQAir, 2019).

Studies have found that the major contributing factors of air pollution in the valley are the vehicles, residential combustion, brick kilns, the manufacturing and construction industries, biowaste burning, and dust particles (Stone et al., 2010; Kim et al., 2015; Sarkar et al., 2017; Shakya et al., 2017). Out of them, vehicular emission is the primary contributing factor due to consumption of fossil fuels (Sarkar et al., 2017; Shakya et al., 2017). The unusually high pollution levels from the vehicles are mainly due to the haphazard traffic system, poor maintenance of the vehicles, and ineffective control of vehicle emissions (CEN and ENPHO, 2003).

The Kathmandu Valley is the capital city of Nepal and has the largest number of population. One of the main reasons for the highly polluted state of Kathmandu Valley is the highly dense concentration of people coming from all over the country (Bakrania, 2015). Nepal has one of the highest rates of urbanization rates in the world that can steadily keep on increasing in the long run as well (Bakrania, 2015). Most of the development work has been concentrated in the Kathmandu Valley and the subsequent economic activities as well as the consumption of fossil fuel have aggravated the pollution and health-related problems in the city.

The traffic scenario in Kathmandu Valley is deteriorating steadily with the constant influx of people. A projection has estimated this increase in the number of vehicles in the valley from 461,927 in 2009 to 895,802 in 2021 (ADB, 2010). The increase in vehicular air pollution affects the human respiratory system. As the vehicular traffic grows, so does the production of $PM_{2.5}$ that results in adverse health impacts like respiratory and pulmonary diseases (US EPA, 2020). Ghimire and Shrestha (2014) showed that the total estimated $PM_{2.5}$ was 9646.40 tons/year from vehicular emission in Kathmandu Valley.

The InMAP model has been used to estimate the annual average primary and secondary $PM_{2.5}$ related to changes in emissions. This model provides marginal health damages based on source–receptor relationships calculated by the WRF-Chem chemical transport model. Inputs to the model include precursor emissions (NH_3, SO_2, $PM_{2.5}$, NOx, and VOCs), annual average meteorology, air quality, deposition information, annual gridded surface emissions, and point sources. InMAP model uses population and health incidence data that can be used to estimate health impacts (IEc, 2019). EASIUR is another model that calculates the monetized health impacts of emissions changes in the contiguous United States. The EASIUR model follows a standard method for estimating mortality burden, which is an impact pathway analysis of estimating ambient $PM_{2.5}$ from precursor emissions and then quantifying associated premature deaths based on epidemiological studies (Heo et al., 2016). This method achieves detailed spatial resolution according to the location of the emission source, accounting for differences in the exposed population downwind. EASIUR can quantify the benefits of the air quality policy scenarios and can be normalized per ton of emissions. Using chemical transport model simulations, the model builds a large dataset of air quality public health impacts from marginal emissions throughout the United States, taking into account the exposed population distribution throughout the country (Heo et al., 2016). APEEP model also follows a similar format of quantifying the health impacts. The model begins with calculating emissions using an air quality model. Next, APEEP computes exposures of people to ambient air pollution to determines the resulting human health impacts. APEEP calculates human exposures to the predicted concentrations by multiplying county-level pollution concentrations by the county-level population data. The model translates exposures into physical effects using concentration–response functions published in peer-reviewed studies in the epidemiological literature (Groosman et al., 2011).

The relationship between the change in concentration of the pollutant (Δx), and the corresponding change in the population health response (Δy) derived from a concentration response relationship is the health impact function (US EPA, 2010). Many epidemiological studies report some measure of the change in the population health response associated with a specific change in the pollutant concentration, which is called the relative risk.

Pope et al. (2002) assessed the relationship between long-term exposure to fine particulate air pollution and all-cause, lung cancer, and cardiopulmonary mortality. The study found that each 10 $\mu g/m^3$ elevation in fine particulate air pollution was associated with 4, 6, and 8% increased risk of all-cause, cardiopulmonary, and lung cancer mortality, respectively. The findings are based on 16 years of research involving about 500,000 people and 116 metropolitan areas in the United States. Similarly another study by Krewski et al. (2009) consisted of approximately 360,000 participants residing in areas of the country that have adequate monitoring information on levels of $PM_{2.5}$ analyzed the relative risks of all causes, cardiopulmonary disease (CPD), ischemic heart disease, lung cancer, and all remaining causes. The study showed 6% increase in overall mortality for every 10 $\mu g/m^3$ increase in $PM_{2.5}$ concentration. Lepeule et al. (2012) found significant associations between $PM_{2.5}$ exposure and increased risk of all-cause, cardiovascular and lung cancer mortality, and reported that each increase in $PM_{2.5}$ (10 $\mu g/m^3$) was associated with an increased risk of all-cause mortality of 14%, along with 26 and 37% increase in cardiovascular and lung cancer mortality, respectively.

The health impact of $PM_{2.5}$ exposure in Nepal has been conducted using concentration–response relations from various other regions (Gurung and Bell, 2013). Giri et al. (2007) have estimated the mortality due to the PM_{10} pollution in Kathmandu Valley as 17,132 premature deaths/year. Shah and Nagpal (1997) estimated the impact of PM on mortality and morbidity and found the impact of 84 deaths, 506 cases of chronic bronchitis, 475,298 restricted activity days, and 1.5 million respiratory symptom days in Kathmandu Valley in 1990. In this study, the $PM_{2.5}$ pollution exposure in Kathmandu Valley and its health impacts have been evaluated using the distributed approach of simulating the air quality by employing WRF-Chem modeling.

The annual $PM_{2.5}$ concentration of Nepal is 10 times the limit set by WHO. The strongest predictor for deaths caused by ambient air pollution is chronic $PM_{2.5}$ exposure (Künzli et al., 2001; Pope and Dockery, 2006). $PM_{2.5}$ is capable of traveling long distances and can also be highly spatially variable near emission sources. To date, limited studies have been conducted to analyze the $PM_{2.5}$ emission and its health impacts in Kathmandu Valley. This study aims to use a high-resolution WRF-Chem simulation to test and support the research on $PM_{2.5}$ emission and its health impact.

2. MATERIALS AND METHODS

2.1. Study Area

The research was conducted for Kathmandu Valley as shown in **Figure 1**, having a population of 1,376,000 in 2019, and 665 km^2 area (Macrotrends, 2020). The valley stands at 1,425 m (4,675

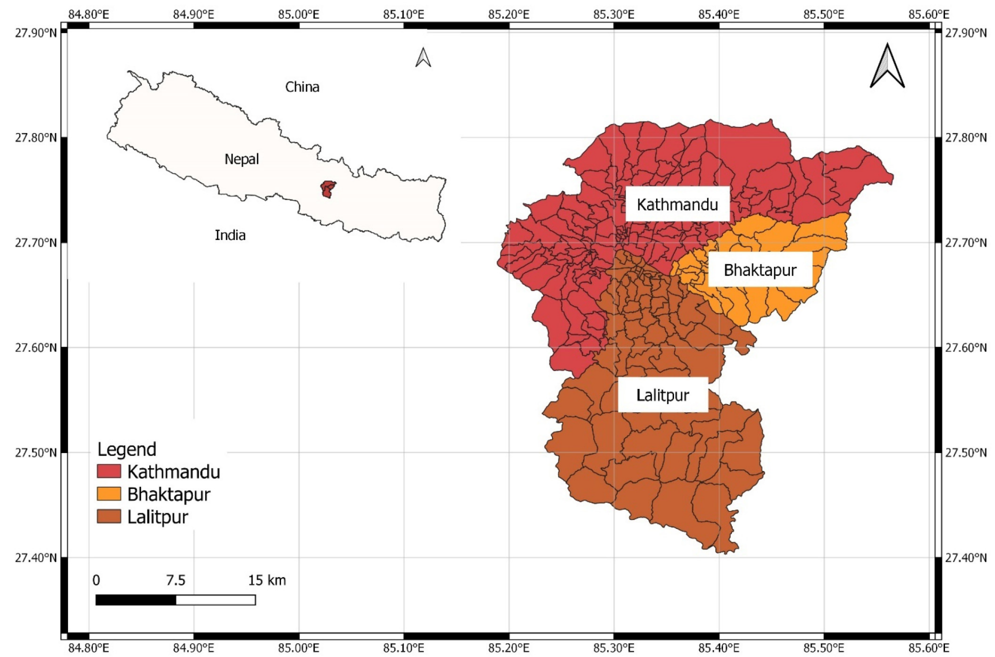

FIGURE 1 | Map of Kathmandu Valley.

ft) above sea level. It comprises three main districts of Nepal: Kathmandu, Lalitpur, and Bhaktapur District. The total number of wards in each district are 71 wards in Lalitpur, 38 in Bhaktapur, 138 in Kathmandu. The temperature in Kathmandu valley is around 20–35°C in the summer and −3 to 20°C in winter.

2.2. Study Period

In order to select the time period for the study, US embassy station data were analyzed. Upon analyzing the PM concentrations throughout the year of 2019, we observed that PM peaks in the driest winter month of December. In December, the average temperature ranges between min 3.7°C (38.7°F) and max 20.2°C (68.4°F), during which PM concentration is the maximum (IQAir, 2019; Weather Atlas, 2020). The pollution stations of Government of Nepal started operating only from 2016, and US Embassy stations operated after a year in 2017. During this research, only 3-year data were available but the data were very limited with lots of missing data. In a comparison of monthly data, we found that December, January, and February usually have high PM concentrations. For example, in US embassy station data of 2018, December had the highest $PM_{2.5}$ concentration of 101.6 $\mu g/m^3$ followed by January and February with 99.9 and 94.8 $\mu g/m^3$, respectively. The $PM_{2.5}$ exposure analysis of this study was done in very high spatial resolution of 3 × 3 km. Some papers (Heo et al., 2016; Thind et al., 2019) have used 36 × 36 km and 48 × 48 km resolution. Being a high-resolution simulation with a time period representing the highest $PM_{2.5}$ pollution in Kathmandu Valley, the time period from December 1, 2019 to December 30, 2019 was selected for the study.

2.3. Population Data

The baseline population data from Central Bureau of Statistics (CBS), Nepal (https://cbs.gov.np/population/) was used for the study. Using the Ratio method as used by CBS reports for population projection, this ward-wise population data were projected from the baseline year 2011 to year 2019.

The equation of this method is:

$$\mathit{Sub\ area\ Projected\ Population} = \frac{\mathit{Sub\ area\ Population}}{\mathit{Parent\ Population}} \times \mathit{Parent\ Population\ Projection}$$

where,

Sub area Projected Population is the required ward-wise projected population for 2019,

Sub area Population is the ward-wise population of baseline year 2011,

Parent Population is the Population of Nepal in baseline year 2011,

Parent Population Projection is the projected population of Nepal in 2019.

The *Parent Population* was taken from the Population Projection Report prepared by CBS (2014).

2.4. Mortality Data

The mortality rate for lung cancer and all-cause mortality data to quantify the health impacts were taken from the reports published by Nepal Health Research Council (NHRC). The all-cause mortality rate for the valley is found to be 607.8 per 100,000 people (NHRC, 2018).

TABLE 1 | WRF-WPS model setup.

WRF-Chem parameters	Value
Horizontal grid resolution	3 km
Grid	66 × 58 cells
Vertical resolution	38 levels
Projection	Mercator

2.5. WRF-Chem Modeling

The Weather Research and Forecasting (WRF) model (Skamarock et al., 2008) is a widely used distributed model to simulate the atmospheric process and it is able to model meteorological processes and atmospheric transport.

WRF-Chem is a numerical weather and atmospheric simulation model that is coupled with chemistry (Grell et al., 2005). It can simulate and predict the atmospheric emission of pollutants, the chemical transport, and transformation at multiple spatial scales. The interaction between meteorology and chemical processes is also modeled by WRF-Chem.

2.6. Modeling Setup

Version 4.0 of Weather Research and Forecasting Model coupled with Chemistry was used for simulating the meteorology and chemistry over the model domain shown in **Table 1**. The model domain is defined on the mercator projection. The model contains 3 km grid resolution and of 38 vertical layers.

The data required for the model run were downloaded from different sources.

NCEP FNL Operational Global Analysis was used for the initial and lateral boundary conditions for meteorological field. Fire Inventory from the National Centre for Atmospheric Research (NCAR) (FINN) version 1.5 was used for biomass burning data. The anthropogenic emission required for running the model is taken from Emission Database for Global Atmospheric Research (EDGAR-HTAP v2) inventory. The biogenic emissions were from Model of Gases and Aerosols from Nature (MEGAN). WSM 5-class microphysics scheme, Grell 3-D cumulus parameterization, RRTM longwave option, Dudhia shortwave scheme, Yonsei University planetary boundary layer parameterization, MOZCART chemistry scheme, and Madronich F-TUV photolysis option were used for running the WRF-Chem model.

2.7. Estimation of $PM_{2.5}$ Pollution-Related Deaths

Health impact function was used to estimate the number of deaths and illnesses associated with $PM_{2.5}$ attributable to each of the 247 wards of Kathmandu Valley. One of the input parameters is the $PM_{2.5}$ concentration from the WRF-Chem model.

Various reduced complexity models (RCMs) have been developed to quantify and value the health impacts of changes in air quality. The reduced form models employ simpler methods to approximate the more complex analyses with a lower computational burden (IEc, 2019). Health benefit results from the models can be obtained by the use of Chemical Transport Models (CTMs) to estimate the impact of emissions on ambient concentrations, and the health effects from exposure to these concentrations can be quantified by using concentration–response functions (Gilmore et al., 2019). Several RCMs such as EASIUR (Heo et al., 2016), InMAP (Tessum et al., 2017), and APEEP (Muller and Mendelsohn, 2007) use health impact function from BenMAP (US EPA, 2010) to determine the mortality due to pollutant exposure. The function calculates the number of death resulted per year due to PM exposure by taking a certain concentration response relation (Pope et al., 2002; Krewski et al., 2009). All three RCMs use the same equation to predict the mortality burden caused by $PM_{2.5}$ pollution.

TABLE 2 | Relative risk for the diseases from epidemiological study done by Pope et al. (2002).

Cause of mortality	Relative risk (*R*)
Lung cancer	1.14
All cause	1.06

The log-linear relationship is the most common form of health impact function used in these types of studies (US EPA, 2010). A typical health impact function specifying a log-linear relationship between risk and air quality change is as follows (US EPA, 2010):

$$y_i = \left\{ \exp\left(\frac{\log R}{10} \cdot c \right) - 1 \right\} \times \textit{Total Population} \times \textit{Mortality Rate} \quad (1)$$

where

c is the average $PM_{2.5}$ concentration,

Total Population is the ward-wise population,

Mortality Rate is the mortality rate for certain diseases per 100,000 people,

R is the relative risk reported from various published epidemiological studies,

y_i is the estimated number of $PM_{2.5}$-related total deaths for each ward.

In this study, the value of R is different for lung cancer and all-cause mortality (**Table 2**). Since Nepal does not have a reliable published source of relative risk, we have taken it from the study conducted by Pope et al. (2002), which states that an increase of 10 $\mu g/m^3$ in fine PM concentration in the atmosphere contributes about 6 and 14% increase in the risk of all cause and lung cancer mortality, respectively. Due to lack of mortality data for Kathmandu Valley, only two factors—lung cancer and all cause disease—could be considered.

The input and output of the model were plotted in the Kathmandu Valley map by using the QGIS software.

3. RESULTS

3.1. Projected Population

The ward-wise population of Kathmandu Valley for the year 2019 was estimated using the Ratio method. The baseline population was taken from Central Bureau of Statistics (2011). **Figure 2** shows the projected population of the valley for 2019.

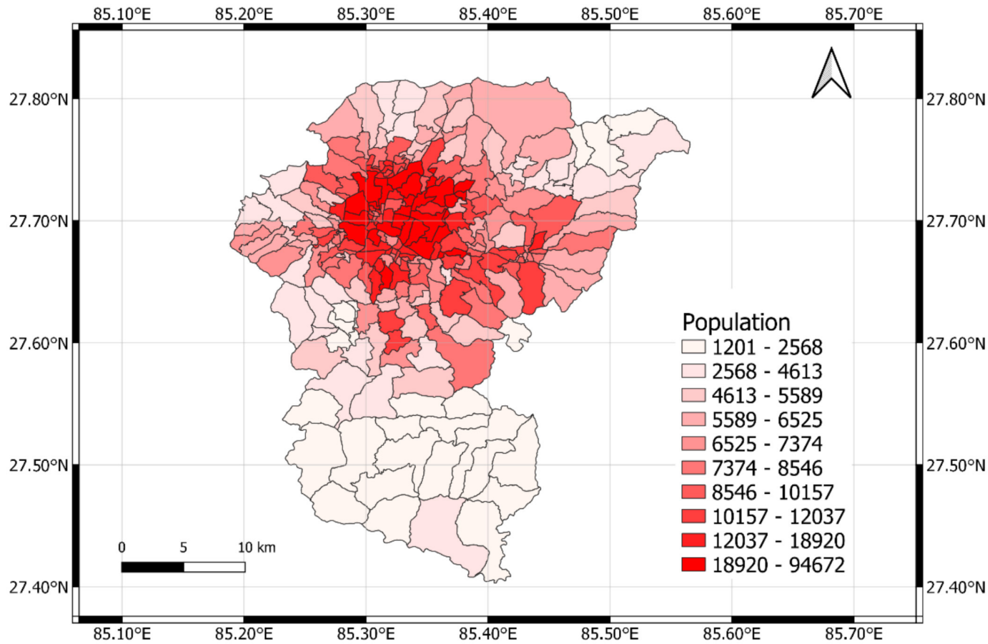

FIGURE 2 | Ward-wise population of Kathmandu Valley for the year 2019.

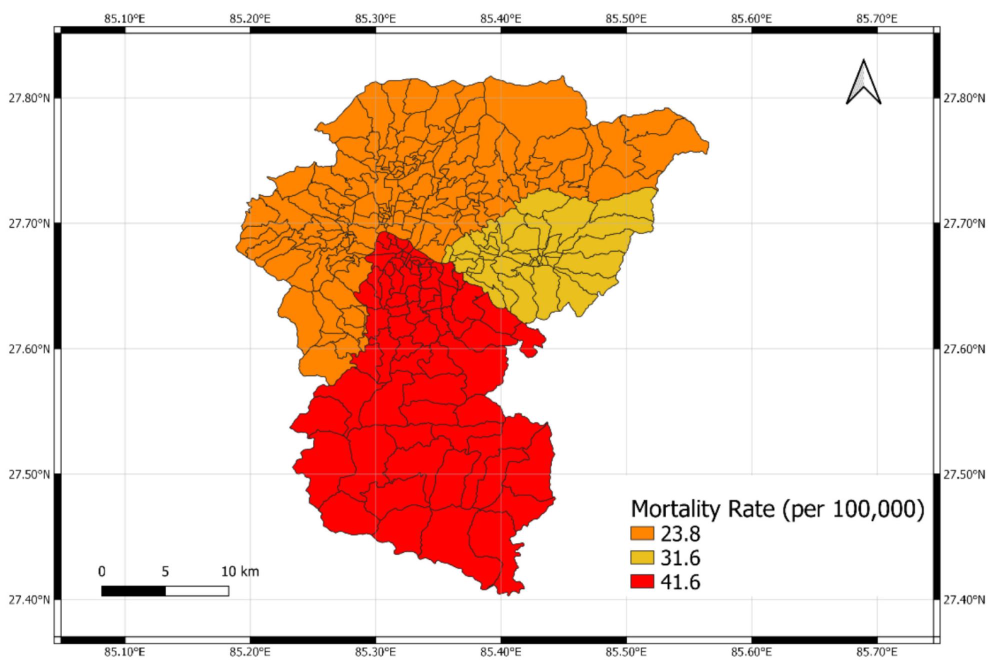

FIGURE 3 | Mortality rate (per 100,000 people) due to lung cancer in Kathmandu Valley in 2018.

Kathmandu Valley at 2019 has approximately 2.7 million people. The densely populated urban centers comprise the Kathmandu and Patan cities and Bhaktapur city in the eastern edge of the valley. Urbanization can be seen increasing throughout the valley, agricultural field are also present over the flat valley floor, and substantial area is found to be used for brickfields especially in the Bhaktapur district.

3.2. Mortality Rate

Figure 3 shows the mortality rate of Kathmandu Valley for lung cancer (NHRC, 2018). Mortality rate (per 100,000 people) due to all cause (except accidents) diseases in Kathmandu valley was taken as 607.8 (NHRC, 2018). We projected the rate from 2018, using Ratio method, to 2019 but no significant changes were observed. So we used mortality rate of 2018.

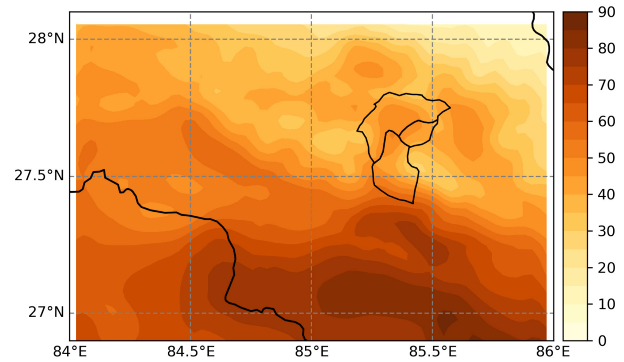

FIGURE 4 | Average $PM_{2.5}$ emission ($\mu g/m^3$) in the valley obtained from WRF-Chem for December 2019.

3.3. Emission Concentration From WRF-Chem

In **Figure 4**, the 1 month (December, 2019) average spatial distribution of calculated $PM_{2.5}$ is shown along with the population distribution in the Kathmandu valley. The maximum $PM_{2.5}$ concentration is seen in Kathmandu district. This region of Kathmandu, being the main urban center, holds the maximum population density along with maximum traffic congestion, with large development activities resulting in high air pollution. Largely protected from any winds, the pollutants are not dispersed and hang heavy over the local population especially during the dry winter months. Wards including Nagarjun 4, Nagarjun 9, Nagarjun 10, Chandragiri 13, and Chandragiri 14 experience the greatest $PM_{2.5}$ concentrations. The lowest concentration was found to be at Bagmati 4. There is less $PM_{2.5}$ concentration in the outskirts of Kathmandu, lower region of Lalitpur and Bhaktapur district.

3.3.1. Health Impact of $PM_{2.5}$ Exposure

The cumulative deaths due to $PM_{2.5}$ induced lung cancer and all cause is found to be 19 and 175, respectively, for December 2019, which was obtained using Equation (2) that estimates the number of $PM_{2.5}$-related total deaths (Y) for each ward i ($i = 1,2,3\ldots 247$).

$$Y = \sum_{i=1}^{247} y_i \tag{2}$$

where y_i is the ward-wise $PM_{2.5}$-related death (see Equation 1) and Y is the total $PM_{2.5}$-related death of entire Kathmandu Valley.

The health impact function was applied to the 247 wards individually to calculate the mortality burden per ward. The summation of all the ward results provided us with the total number of deaths in the entire valley. **Table 3** shows that the death number for lung cancer and all cause disease are 19 and 175, respectively. Different relative risks were applied for lung cancer and all cause, along with different mortality data input to provide the mortality results.

TABLE 3 | $PM_{2.5}$ related premature deaths attributable to emissions in December 2019.

	Total no. of death	Average mortality rate (per 100,000)
Lung cancer	19	0.71
All cause	175	6.37

4. DISCUSSION

Figure 5 shows maximum and minimum mortality values for lung cancer to be 0.403 and 1.081 per 100,000 people, respectively. The highest $PM_{2.5}$ induced lung cancer mortality rates are seen in Lalitpur district. The mortality rate for lung cancer is 41.6 (per 100,000) as provided by NHRC (2018), which explains the higher $PM_{2.5}$ induced lung cancer mortality rates than the other two districts. Although the population density of Kathmandu is greater, the lung cancer mortality rate for Lalitpur district is greater than that of both Kathmandu and Bhaktapur districts. The topmost region of Lalitpur district has the maximum mortality rates due to high emission concentration as well as large population.

The maximum and minimum mortality rate burden for all cause is shown in **Figure 6** to be 4.31 and 6.93 per 100,000 people, respectively. The highest $PM_{2.5}$ induced all cause mortality rates are seen in Kathmandu district. The mortality rate for all cause is 607.8 (per 100,000) for the entire valley. It is evident that the high emission concentration and population cause maximum mortality burden due to $PM_{2.5}$ in Kathmandu district. Therefore, $PM_{2.5}$-related mortality burden is highest where population concentration and $PM_{2.5}$ emission is maximum.

The estimated mortality is higher than that reported by Regmi and Kitada (2003). Regmi and Kitada (2003) estimated 226 deaths per year, whereas this study estimates around 175 deaths during the month of December (**Table 4**). Increase of both the population and pollutant concentration has contributed toward this trend. The health impact functions (Ostro and Chestnut, 1998) used by Regmi and Kitada (2003) provides very less relative risk compared to ours, and the target population for the valley was also 50% less than the target population of this study. This change in the health impact constant and the population distribution predicted lesser mortality results.

Similar study was done by Shah and Nagpal (1997), who estimated similar results as that of Regmi and Kitada (2003). Shah and Nagpal (1997) had also used the same health impact equation for similar target population as that of Regmi and Kitada (2003). The main reasons for the difference in the results are the increases in population and pollutant concentration.

The mortality results due to $PM_{2.5}$ emission was calculated after reducing the concentration of every ward by half. The hourly $PM_{2.5}$ concentration data are not compared with the observed station data since the model provides average of the grid (3 km) while the stations provide point wise data. The grid value and the station point data are not comparable. The monthly data obtained for the individual wards got reduced by nearly 50% and

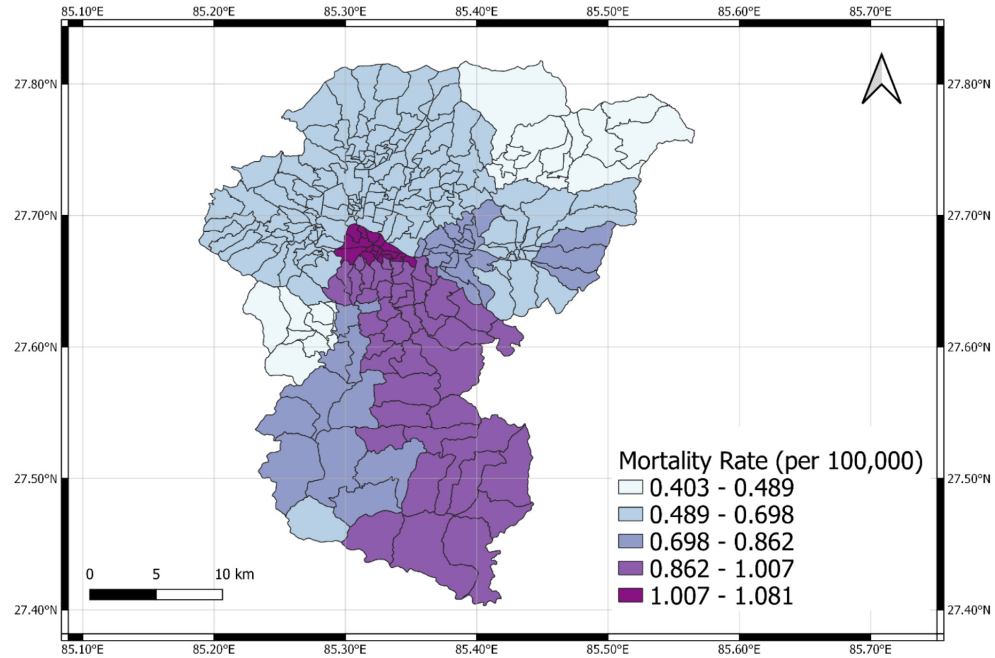

FIGURE 5 | $PM_{2.5}$ induced lung cancer mortality rate (per 100,000 people) for December 2019.

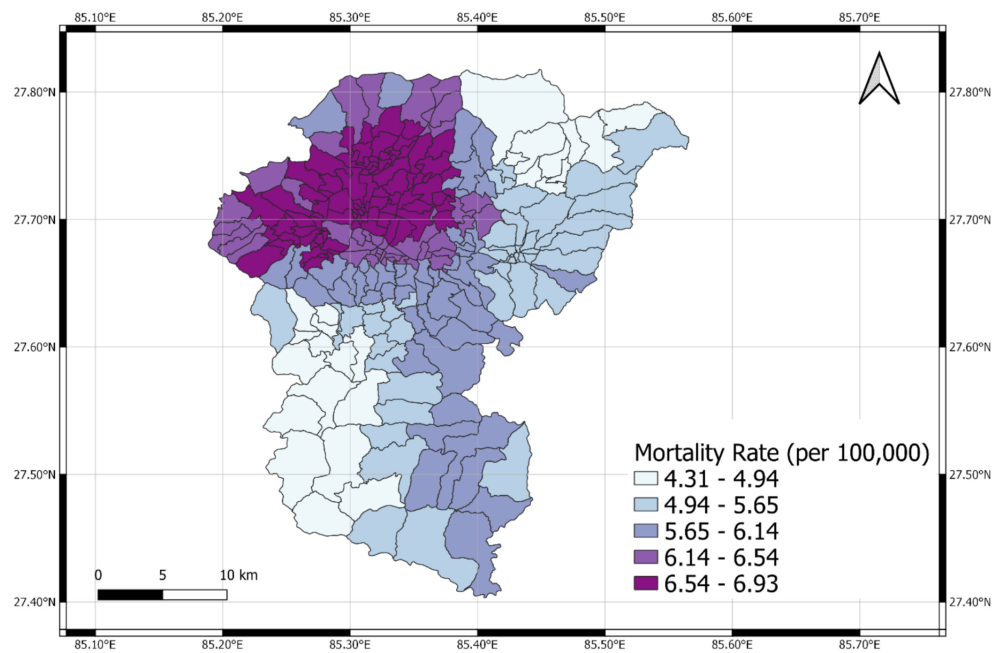

FIGURE 6 | $PM_{2.5}$ induced all cause mortality rate (per 100,000 people) for December 2019.

the results were obtained (**Table 5**). Upon analyzing the result before and after the emission reduction, it is seen that the death result also significantly reduced by half. Thus, it is estimated that reduction in $PM_{2.5}$ level in the valley will reduce the monthly mortality by approximately 50%.

Taking into account the exposure map, high concentration of exposure seems to be prevalent in the cities of Kathmandu district. To reduce adverse health outcome stringent emission control measures should be implemented (Regmi and Kitada, 2003). Nepal is regularly ranked poorly in the air quality

TABLE 4 | Comparison of the results with previous studies for Kathmandu Valley.

	Death	Time period
This study	175	December 2019
Regmi and Kitada (2003)	226	Annual 2003
Shah and Nagpal (1997)	84	Annual 1996

TABLE 5 | Comparison between $PM_{2.5}$ resulted death after reducing the emission by half in December 2019.

	$PM_{2.5}$ resulted death	$PM_{2.5}$ resulted death after reducing emission	Percentage decreased (%)
Lung cancer	19	9	52.6
All cause	175	85	51.4

indices. Considering the mortality burden, the places affected by $PM_{2.5}$ pollution should be identified and effective air pollution mitigation plan should be enforced.

4.1. Conclusion and Recommendations

In this research, numerical simulation of particulate matter of Kathmandu Valley was done using Chemical Transport Model, WRF-Chem for December, 2019. Values of simulated 24-h mean $PM_{2.5}$ concentration ranges from 30 μ to 65 $\mu g/m^3$. The values of $PM_{2.5}$ obtained from the model simulation exceeds the WHO standard, which is 25 $\mu g/m^3$ 24-h mean. The level of $PM_{2.5}$ in Kathmandu's air is extremely high, especially in the dry winter month (December). In this month, the air in urban Kathmandu can be classified as " very unhealthy."

Human $PM_{2.5}$ pollution exposure has been studied utilizing the numerically simulated $PM_{2.5}$ concentration value and residential distribution of population over Kathmandu valley. Human-$PM_{2.5}$ pollution-exposure maps for Kathmandu valley have been analyzed and various health outcomes due to the prevalence of $PM_{2.5}$ are evaluated. Spatial exposure strength, i.e., population times concentration for $PM_{2.5}$, occurs in the main urban area of Kathmandu, Patan, Thimi, and Bhaktapur cities due to the large population living in these cities. From the model, we calculated the total number of deaths for the month of December, 2019 to be 19 from lung cancer and 175 from all cause disease, both $PM_{2.5}$ induced. The results obtained showed that greater the emission and population concentration, greater is the mortality rate in the region. From our calculations, mortality burden was highest in central Kathmandu with a value of 1.081 and 6.93 per 100,000 people for lung cancer and all cause diseases, respectively. The highest $PM_{2.5}$ concentration is seen in the central region of Kathmandu Valley where the population density is also high, thereby contributing to highest mortality in that area. If the monthly average emissions are reduced by 50%, the total number of deaths are also approximately reduced by 50%, implying that $PM_{2.5}$ is directly related to total number of deaths in this case. Finally, the results indicate that $PM_{2.5}$ is dangerous to human health and can even be fatal.

This research plays a role in understanding the health impacts caused by $PM_{2.5}$ based on quantitative analysis. Since annual time period was not possible for this study, a future study with a longer time period could be proposed. Other air pollutants can also be studied in the future along with their health impacts. Moreover, study including whole Nepal as study area can also be proposed to further understand the relation between $PM_{2.5}$ and its human health impact. There are evidences that link air pollution and health impacts and further studies are required on the health effects of air pollution in Kathmandu valley. The result from these studies can be used by policymakers to improve the air quality in Nepal. We also recommend the simulation for a longer time period at high resolution to better understand the relation between $PM_{2.5}$ concentration and number of death attributable to it.

DATA AVAILABILITY STATEMENT

The raw data supporting the conclusions of this article will be made available by the authors, without undue reservation.

AUTHOR CONTRIBUTIONS

PM carried out the GIS processing of input and output data in the exposure maps. AT performed the population projection analysis. KS performed the simulations of WRF-Chem and coordinated the entire research. All authors contributed to the article and approved the submitted version.

REFERENCES

ADB (2010). *Kathmandu Sustainable Urban Transport Project (RRP NEP 44058-01)*. Technical report, Asian Development Bank.

Bakrania, S. (2015). *Urbanisation and Urban Growth in Nepal*. Report, GSDRC, University of Birmingham, Birmingham.

CBS (2014). *National Population and Housing Census 2011 (Population Projection 2011 - 2031)*. Technical report, Central Bureau of Statistics, Government of Nepal.

CEN and ENPHO (2003). *Health Impacts of Kathmandu's Air Pollution*. Technical Report September, Clean Energy Nepal (CEN) Environment and Public Health Organization (ENPHO). Submitted to Kathmandu Electric Vehicle Alliance, Prepared for KEVA Secretariat under USAID/Nepal.

Ghimire, K., and Shrestha, S. (2014). Estimating vehicular emission in Kathmandu Valley, Nepal. *Int. J. Environ*. 3:143. doi: 10.3126/ije.v3i4.11742

Gilmore, E. A., Heo, J., Muller, N. Z., Tessum, C. W., Hill, J. D., Marshall, J. D., et al. (2019). An inter-comparison of the social costs of air quality from reduced-complexity models. *Environ. Res. Lett*. 14, 3–6. doi: 10.1088/1748-9326/ab1ab5

Giri, D., Murthy, V. K., Adhikary, P. R., and Khanal, S. N. (2007). Estimation of number of deaths associated with exposure to excess ambient PM10 air pollution. *Int. J. Environ. Sci. Technol*. 4, 183–188. doi: 10.1007/BF03326272

Grell, G. A., Peckham, S. E., Schmitz, R., McKeen, S. A., Frost, G., Skamarock, W. C., et al. (2005). Fully coupled "online" chemistry within the WRF model. *Atmos. Environ*. 39, 6957–6975. doi: 10.1016/j.atmosenv.2005.04.027

Groosman, B., Muller, N. Z., and O'Neill-Toy, E. (2011). The ancillary benefits from climate policy in the United States. *Environ. Resour. Econ*. 50, 585–603. doi: 10.1007/s10640-011-9483-9

Gurung, A., and Bell, M. L. (2013). The state of scientific evidence on air pollution and human health in Nepal. *Environ. Res*. 124, 54–64. doi: 10.1016/j.envres.2013.03.007

Heo, J., Adams, P. J., and Gao, H. O. (2016). Reduced-form modeling of public health impacts of inorganic PM2.5 and precursor emissions. *Atmos. Environ*. 137, 80–89. doi: 10.1016/j.atmosenv.2016.04.026

IEc (2019). *Evaluating Reduced-Form Tools for Estimating Air Quality Benefits*. Technical report, Industrial Economics, Incorporated, Cambridge, MA.

IQAir (2019). *2019 World Air Quality Report*. Technical report, IQAir.

Kim, B. M., Park, J.-S., Kim, S.-W., Kim, H., Jeon, H., Cho, C., et al. (2015). Source apportionment of PM10 mass and particulate carbon in the Kathmandu Valley, Nepal. *Atmos. Environ*. 123, 190–199. doi: 10.1016/j.atmosenv.2015.10.082

Krewski, D., Jerrett, M., Burnett, R. T., Ma, R., Hughes, E., Shi, Y., et al. (2009). Extended follow-up and spatial analysis of the American Cancer Society study linking particulate air pollution and mortality. *Health Effects Inst*. 5–114; discussion: 115–36.

Künzli, N., Medina, S., Kaiser, R., Quénel, P., Horak, F. Jr., and Studnicka, M. (2001). Assessment of deaths attributable to air pollution: should we use risk estimates based on time series or on cohort studies? *Am. J. Epidemiol*. 153, 1050–1055. doi: 10.1093/aje/153.11.1050

Lepeule, J., Laden, F., Dockery, D., and Schwartz, J. (2012). Chronic exposure to fine particles and mortality: an extended follow-up of the Harvard six cities study from 1974 to 2009. *Environ. Health Perspect*. 120, 965–970. doi: 10.1289/ehp.1104660

Macrotrends (2020). *Kathmandu, Nepal Metro Area Population 1950-2021*. Available online at: https://www.macrotrends.net/cities/21928/kathmandu/population

Muller, N. Z., and Mendelsohn, R. (2007). Measuring the damages of air pollution in the United States. *J. Environ. Econ. Manage*. 54, 1–14. doi: 10.1016/j.jeem.2006.12.002

NHRC (2018). *Population Based Cancer Registries at Kathmandu, Bhaktapur, Lalitpur, Siraha, Saptari, Dhanusha, Mohattari, West Rukum and East Rukum Districts, Nepal, 2018*. Technical report, Nepal Health Research Council, Government of Nepal.

Ostro, B., and Chestnut, L. (1998). Assessing the health benefits of reducing particulate matter air pollution in the United States. *Environ. Res*. 76, 94–106. doi: 10.1006/enrs.1997.3799

Pope, C. A. III., Burnett, R. T., Thun, M. J., Calle, E. E., Krewski, D., Ito, K., et al. (2002). Lung cancer, cardiopulmonary mortality, and long-term exposure to fine particulate air pollution. *JAMA* 287, 1132–1141. doi: 10.1001/jama.287.9.1132

Pope, C. A. III., and Dockery, D. W. (2006). Health effects of fine particulate air pollution: lines that connect. *J. Air Waste Manage. Assoc*. 56, 709–742. doi: 10.1080/10473289.2006.10464485

Regmi, R. P., and Kitada, T. (2003). Human-air pollution exposure map of the Kathmandu valley, Nepal: assesment based on chemical transport simulation. *J. Glob. Environ. Eng*. 9, 89–109. Available online at: https://ci.nii.ac.jp/naid/10024474542/en/

Sarkar, C., Sinha, V., Sinha, B., Panday, A. K., Rupakheti, M., and Lawrence, M. G. (2017). Source apportionment of NMVOCs in the Kathmandu Valley during the SusKat-ABC international field campaign using positive matrix factorization. *Atmos. Chem. Phys*. 17, 8129–8156. doi: 10.5194/acp-17-8129-2017

Shah, J. J., and Nagpal, T. (1997). *Urban Air Quality Management Strategy in Asia*. Kathmandu Valley report. The World Bank. doi: 10.1596/0-8213-4032-8

Shakya, K. M., Rupakheti, M., Shahi, A., Maskey, R., Pradhan, B., Panday, A., et al. (2017). Near-road sampling of PM2.5, BC, and fine-particle chemical components in Kathmandu Valley, Nepal. *Atmos. Chem. Phys*. 17, 6503–6516. doi: 10.5194/acp-17-6503-2017

Skamarock, W. C., Klemp, J. B., Dudhia, J., Gill, D. O., Barker, D. M., Duda, M. G., et al. (2008). *A Description of the Advanced Research WRF Version 3*. Technical report, Mesoscale and Microscale Meteorology Division, National Center for Atmospheric Research (NCAR), Boulder, CO.

Stone, E. A., Schauer, J. J., Pradhan, B. B., Dangol, P. M., Habib, G., Venkataraman, C., et al. (2010). Characterization of emissions from South Asian biofuels and application to source apportionment of carbonaceous aerosol in the Himalayas. *J. Geophys. Res. Atmos*. 115, 1–2. doi: 10.1029/2009JD011881

Tessum, C. W., Hill, J. D., and Marshall, J. D. (2017). InMAP: a model for air pollution interventions. *PLoS ONE* 12:e0176131. doi: 10.1371/journal.pone.0176131

Thind, M. P., Tessum, C. W., Azevedo, I. L., and Marshall, J. D. (2019). Fine particulate air pollution from electricity generation in the US: health impacts by race, income, and geography. *Environ. Sci. Technol*. 53, 14010–14019. doi: 10.1021/acs.est.9b02527

US EPA (2010). *Quantitative Health Risk Assessment for Particulate Matter*. U. S. Environmental Protection Agency.

US EPA (2020). *Health and Environmental Effects of Particulate Matter (PM)*. US EPA. Available online at: https://www.epa.gov/pm-pollution/health-and-environmental-effects-particulate-matter-pm

Weather Atlas (2020). *Monthly Weather Forecast of Kathmandu*. Available online at: https://www.weather-atlas.com/en/nepal/kathmandu-climate

Conflict of Interest: The authors declare that the research was conducted in the absence of any commercial or financial relationships that could be construed as a potential conflict of interest.

frontiers in Sustainable Cities

ORIGINAL RESEARCH
published: 19 July 2021
doi: 10.3389/frsc.2021.681759

Long-Term (2003–2019) Air Quality, Climate Variables, and Human Health Consequences in Dhaka, Bangladesh

Md Riad Sarkar Pavel†, Shahid Uz Zaman, Farah Jeba, Md Safiqul Islam and Abdus Salam†*

Department of Chemistry, University of Dhaka, Dhaka, Bangladesh

Long-term trends in air quality by studying the criteria pollutants ($PM_{2.5}$, PM_{10}, CO, O_3, NO_2, and SO_2) and climate variables (temperature, surface pressure, and relative humidity) were depicted in this study. The 17-year (2003–2019) average values of $PM_{2.5}$, PM_{10}, CO, O_3, NO_2, and SO_2 were 88.69 ± 9.76 μg/m^3, 124.57 ± 12.75 μg/m^3, 0.69 ± 0.06 ppm, 51.42 ± 1.82 ppb, 14.87 ± 2.45 ppb, and 8.76 ± 2.07 ppb, respectively. The trends among the ambient pollutants were increasingly significant ($p < 0.05$) except for O_3 with slopes of 1.83 ± 0.15 μg/m^3/year, 2.35 ± 0.24 μg/m^3/year, 0.01 ± 0.002 ppm/year, 0.47 ± 0.03 ppb/year, and 0.40 ± 0.02 ppb/year for $PM_{2.5}$, PM_{10}, CO, NO_2, and SO_2, respectively. Pearson correlations revealed a significant association among the pollutants while a noteworthy correlation was observed between ambient pollutants and surface temperature. Principal component analysis (PCA) and positive matrix factorization (PMF) have been employed collectively to examine the main sources of the pollutants. PCA revealed similar trends for PMs and CO, as well as NO_2 and SO_2 being equally distributed variables. PMF receptor modeling resulted in attributing four sources to the pollutants. The factors inferred from the PMF modeling were signified as vehicular emissions, road/soil dust, biomass burning, and industrial emissions. The hazard quotient (HQ) values were not antagonistic (HQ $<$ 1) in acute exposure levels for the three age groups (infants, children, and adults) while showing significant health risk (HQ $>$ 1) in chronic exposure for infants and children. Children are identified as the worst sufferers among the age groups, which points to low breathing levels and high exposure to traffic pollution in Dhaka, Bangladesh.

Keywords: air quality, climate variables, positive matrix factorization, hazard quotient, Kendall and Spearman's correlations, Pearson correlations, principal component analysis

OPEN ACCESS

Edited by:
Jai Prakash,
Washington University in St. Louis,
United States

Reviewed by:
Sarkawt Hama,
University of Surrey, United Kingdom
Ashraf Dewan,
Curtin University, Australia

***Correspondence:**
Abdus Salam
asalam@gmail.com;
asalam@du.ac.bd

†These authors have contributed equally to this work and share first authorship

Specialty section:
This article was submitted to Climate Change and Cities, a section of the journal Frontiers in Sustainable Cities

Received: *17 March 2021*
Accepted: *26 May 2021*
Published: *19 July 2021*

Citation:
Pavel MRS, Zaman SU, Jeba F, Islam MS and Salam A (2021) Long-Term (2003–2019) Air Quality, Climate Variables, and Human Health Consequences in Dhaka, Bangladesh. Front. Sustain. Cities 3:681759. doi: 10.3389/frsc.2021.681759

HIGHLIGHTS

- Long-term trends of criteria air pollutants and climate variables were analyzed.
- Significant positive trends were observed for the pollutants except ozone.
- Four factors were characterized as estimated sources from PMF modeling.
- HQ exceeded the acceptable limit ($>$1) for chronic exposure to children and infants.

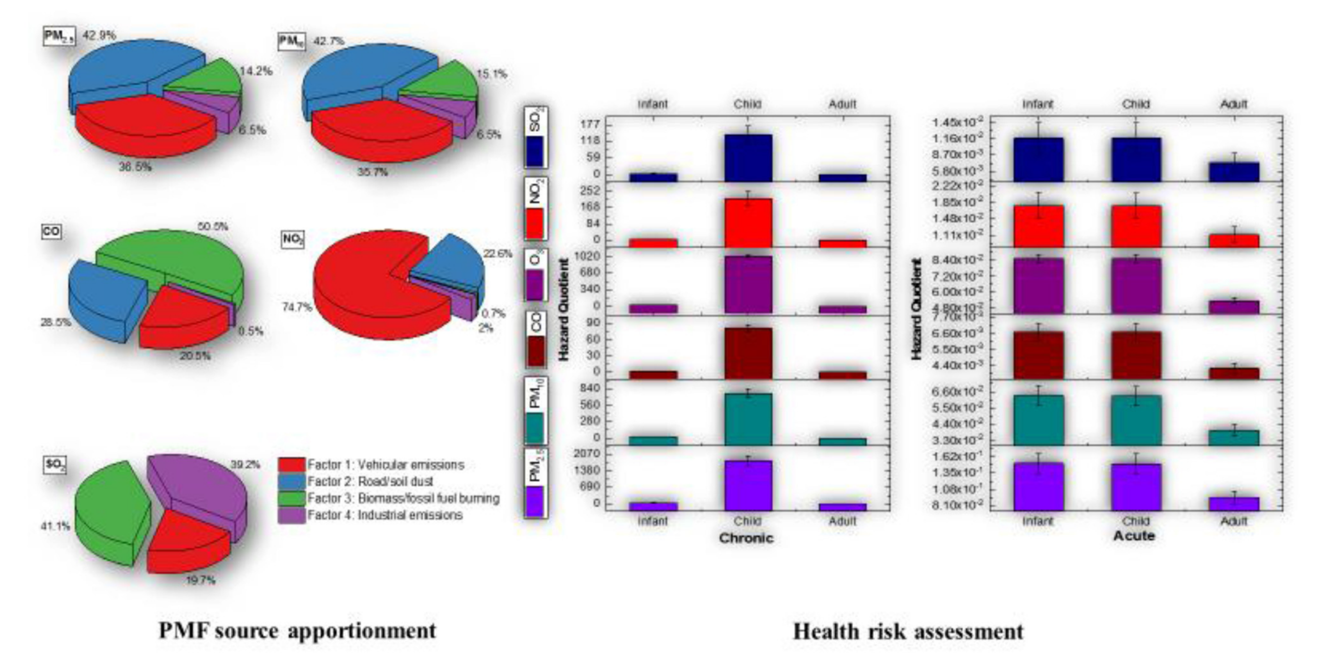

GRAPHICAL ABSTRACT | Source apportionment and hazard quotients of ambient air pollutants in Dhaka.

INTRODUCTION

Air pollution and climate change are the two most significant and interconnected challenges plaguing the 21st century. If existing policies remain unchanged, air pollution would be the most important environmental factor affecting premature deaths by 2050 (OECD, 2012). Global warming has culminated in a 43% increase in anthropogenic radiative forcing (RF) since 2005, according to the new IPCC report, focusing on human behavior as the most significant influencer (Stocker et al., 2013). The urban heat-island effect causes towns to be far warmer than their neighboring rural area due to enhanced anthropogenic activities. Owing to associations between warming and air emissions, this effect would pose extreme health problems for cities around the world by 2050 (Schmale et al., 2014). Lancet Commission on Pollution and Health reported 6.5 million deaths in 2015 due to atmospheric air pollution (Landrigan et al., 2017). while mortality due to past climate change on air quality was much lower: ∼1500 and ∼2200 deaths per year due to ozone and $PM_{2.5}$, respectively (Silva et al., 2013). The global air quality scenarios are unlikely to change anytime soon, and the crisis in the megacities of developing countries is expected to worsen. As a result, it is important to continue tackling air quality problems in tandem with climate change mitigation initiatives (Williams, 2012).

Approximately 91% of the world's population live in areas where WHO air quality standards have been exceeded. However, due to its large population, Bangladesh is one of the most polluted countries in terms of air quality, with Dhaka ranking as one of the world's two most polluted cities (AirVisual, 2018). In Bangladesh, there had been little to no effort and administrative works to track or mitigate ambient air pollution before 1999. In 1999, the government began establishing frameworks and regulations to meet US EPA and Bangladesh National Air Quality Standards, especially in Dhaka. In this regard, a number of controls have been implemented, including the prohibition of leaded gasoline in July 1999 and the replacement of old two-stroke engine three-wheelers with compressed natural gas (CNG)-powered four-stroke three-wheelers beginning in January 2003; introducing CNG-powered cars, buses, and trucks; and regulating brick kiln emanations, which resulted in a reduction of airborne Pb concentrations and improved air quality than before (Salam et al., 2013; Begum and Hopke, 2019). However, since the introduction of CNG and the prohibition of two-stroke engines, traffic congestion in Dhaka city has greatly worsened air quality, and numerous brick kilns using crude oil, fossil fuel, coal, natural gas, electricity, and biomass as a source of energy have sprung up all over the city and have been discharging many air pollutants including black carbon and organic carbon (Salam et al., 2013). In addition, research on the results of CNG conversion in other megacities (Rio de Janeiro, Mexico City, and New Delhi) and the greenhouse gas (GHG) benefits of such conversion showed that switching from diesel vehicles increased high-emission particulates and black carbon, which are more potent as GHGs than CO_2 or CH_4. Thus, large-scale conversion of petrol vehicles embodies the risk of reduced GHG benefit or even negative GHG impacts (Wadud and Khan, 2013). Furthermore, permanent wetlands have been disappearing at an unprecedented pace as a result of unplanned urbanization to accommodate the huge population, with more than 49% of wetland areas disappearing in Dhaka city between 1960 and

2008 (Rai et al., 2017). As a result of such adverse situations, Dhaka had very high (>1) toxicity potential (TP) values of $PM_{2.5}$ and PM_{10} (Zaman et al., 2021) and recorded the highest mortality and morbidity rates (hospital admissions) among the megacities studied, with about 7,000 deaths and 2,100 excess cases (cardiovascular and respiratory) each year (Gurjar et al., 2010). **Table 1** reports several previous researches on ambient air quality and climate impact in Dhaka, Bangladesh, undertaken after 2003.

Carbon monoxide, lead, ground-level ozone, particulate matter (PM), nitrogen dioxide, and sulfur dioxide have been designated as criteria air contaminants by the Environmental Protection Agency (EPA) and the World Health Organization (WHO), and national and global ambient air quality standards (NAAQS) have been developed for these six pollutants (EPA). These contaminants, which are made up of various materials, have a broad range of sources of pollution and varying degrees of health impacts and toxicity, dictating the use of source apportionment studies to understand the formation processes and their sources. On source apportionment, two chemometric techniques, principal component analysis (PCA) and positive matrix factorization (PMF) receptor model, were employed collectively. PCA is utilized to relate the air pollutants and their overall changes in the aerosol composition while PMF is used to determine the different sources of pollution and the temporal variability of each pollutant without considering their correlations (Padoan et al., 2020).

Dhaka is one of the most contaminated cities in the world and is in dire need of effective mitigation policies to attain national and global air quality standards. Unfortunately, there is limited information for the criteria air pollutants levels, sources apportionment, impact on human health, and climate variables based on long-term datasets. Therefore, the objective of this study is to understand the long-term (2003–2019) evolution of major atmospheric contaminants ($PM_{2.5}$, PM_{10}, CO, O_3, NO_2, and SO_2) and the effect of meteorological parameters (temperature, pressure, and relative humidity) on these pollutants following the January 2003 ban on old two-stroke engine three-wheelers in favor of CNG-powered four-stroke three-wheelers. Although there have been recent comparative studies for fine and coarse fractions of PM in terms of source attribution in the seasonal and short-term periods, long-term studies for all of the criteria contaminants and their health effects, as well as their origins, have been scarce. This study will help evaluate the aftermath of implementing the CNG-powered vehicles and how the vehicles and other sources might be regulated in the future to improve the ambient air quality in Dhaka, Bangladesh.

Description of the Study Area

Dhaka, Bangladesh's capital and most populous city, is situated at the northeastern end of the Indo-Gangetic Plain (IGP). Dhaka is the center of Bangladesh with an elevation of ∼9 m above sea level (**Figure 1**). Dhaka encompasses a total area of 1463.60 square kilometers (565.10 square miles) and possesses a population of 12.5 million and, hence, is one of the most densely populated cities in the world with a density of 8,229 per square kilometer. Dhaka has a population growth rate of 3.48% per year due to ever-growing urbanization (urbanization rate = 77.36%), which drives a huge chunk of the population toward urban life every year from rural/suburban areas (www.dhaka.gov.bd). As

TABLE 1 | Recent studies concerning air quality and climate variables in Dhaka, Bangladesh.

Studied variables	Observation	Model/study methods	References
$PM_{2.5}$, its precursors, and climate variables	Air quality changes from the CNG conversion scheme in 2010 resulted in around 2045 (1665) avoided premature deaths and a savings of around USD 400 million in greater Dhaka. Climate expenses (∼USD 17.7 million) were in the order of magnitude less than the air quality gains.	GIS-based modeling	Wadud and Khan, 2013
Climate variables (monthly rainfall and temperature)	Daily energy usage in Dhaka city rises by 6.46–11.97 and 2.37–6.25 MkWh per unit increase in temperature and rainfall, respectively, while daily gross residential energy demand and peak demand will rise by 5.9–15.6% and 5.1–16.7% by the end of the century, depending on climate change scenarios.	An ensemble of six GCMs of CMIP5 under four RCP scenarios	Shourav et al., 2018
PM_{10}, $PM_{2.5}$, BC, and Pb	Dhaka's air quality has remained steady over the last decade, despite increased economic development and the number of sources such as passenger cars and brick kilns.	EEL-type Smoke Stain Reflectometer	Begum and Hopke, 2018
$PM_{2.5}$	Wood burning, soil dust, brick kilns, fugitive Pb, road dust, Zn sources, motor vehicles, and sea salt have been reported as sources.	Ion Beam Analysis (IBA) and EEL-type Smoke Stain Reflectometer	Begum and Hopke, 2019
NO_2, CO, O_3, SO_2, and $PM_{2.5}$ and PM_{10}	The presence of a seasonal pattern of air quality implies that the air is highly toxic and polluted.	Seasonal Autoregressive Integrated Moving Average (SARIMA) model	Islam et al., 2020
$PM_{2.5}$	Metal(oid) contamination in dust and soil at school compounds was primarily caused by traffic-related events, natural causes, and manufacturing operations.	Ion Beam Analysis (IBA) methods and PCA-APCS-MLR receptor model	Rahman et al., 2021

GCM, global circulation models; CMIP5, coupled model intercomparison project phase 5; RCP, representative concentration pathway.

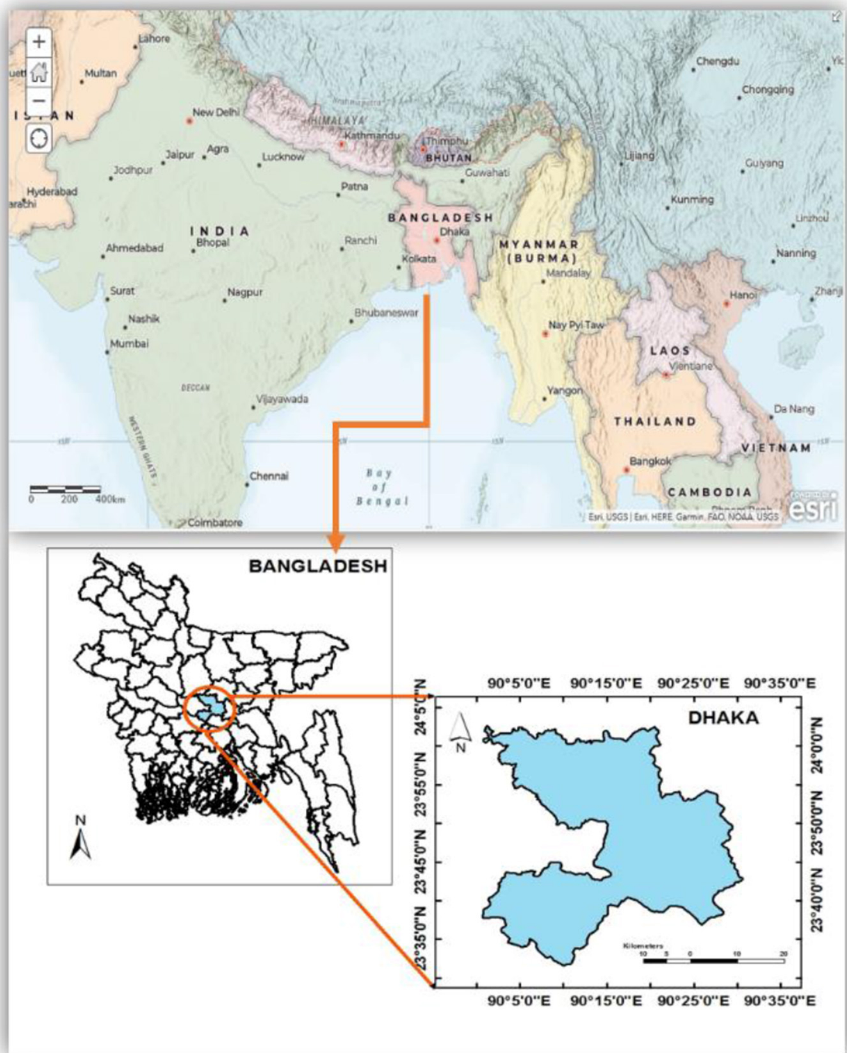

FIGURE 1 | Location of Bangladesh and the district of Dhaka.

a result, Bangladesh with a mean $PM_{2.5}$ concentration of 77.1 $\mu g/m^3$ and megacity Dhaka with the same mean concentration of that of Bangladesh has emerged as the 1st and 2nd most polluted country and capital city in the world (Amato et al., 2020).

Air Pollution and Meteorological Data

Although the Department of Environment (DoE) has some ground-based monitoring stations for atmospheric pollutants, long-term datasets are still scarce for Dhaka. As a result, 24-h ambient concentrations of the air pollutants ($PM_{2.5}$, PM_{10}, CO, O_3, NO_2, and SO_2) and meteorological data (temperature, surface pressure, and relative humidity) were collected from the EAC4 (ECMWF Atmospheric Composition Reanalysis 4) global reanalysis dataset produced by the European Centre for Medium-Range Weather Forecasts (ECMWF) from Copernicus Atmosphere Monitoring Service (CAMS) for the period January 2003 to December 2019. The dataset contains gridded global data with 0.75° × 0.75° horizontal resolution and has the following vertical coverage: surface, total column, model levels, and pressure levels. This period was chosen to depict long-term air quality and its consequences on climate variables and human health in Dhaka, Bangladesh.

CAMS Reanalysis Data

Reanalysis combines model data with measurements from around the world to construct a globally robust and coherent resource using a physics and chemistry-based model of the atmosphere. The data integration is defined as a technique used by numerical weather prediction centers and air quality forecasting centers, in which a preceding prediction is merged with currently available measurements in an optimized way every so many hours (12 h at ECMWF) to create a new best estimate of the atmospheric situation, known as analysis, from which an updated, enhanced forecast is produced (ads.atmosphere.copernicus.eu). The CAMS reanalysis is the most recent global reanalysis data collection of atmospheric composition (AC) developed by the Copernicus Atmosphere Monitoring Service, and it consists of three-dimensional time-consistent AC fields, including aerosols, chemical species, and greenhouse gases, through the CAMS global greenhouse gas reanalysis (EGG4). The dataset improves on the knowledge obtained during the development of the Monitoring Atmospheric Composition and Climate (MACC) reanalysis and the CAMS interim reanalysis. The assimilation method estimates observational biases and separates high-quality data from low-quality data. Estimates are made using the atmosphere model in places where data collection is limited or for pollutants for which no direct measurements are possible. Reanalysis is a very easy and common dataset to work with since it provides forecasts at each grid point across the world at each daily production time, over a long period of time, and in the same format.

The CAMS reanalysis was created with 60 hybrid sigma/pressure (model) levels in the vertical, with the top level at 0.1 hPa, using 4DVar data assimilation in ECMWF's Integrated Forecast System (IFS) CY42R1. The 4DVar data assimilation employs 12-h assimilation periods spanning 09 UTC to 21 UTC and 21 UTC to 09 UTC, respectively. The IFS model documentation for various model cycles can be found at https://www.ecmwf.int/en/forecasts/documentation-and-support/changes-ecmwf-model/ifs-documentation. On these levels, atmospheric data are available, which are also interpolated to 25 strain, 10 potential temperature, and 1 potential vorticity level(s). Data on the "surface" or "single stage" are also available.

EAC4 is the fourth-generation ECMWF global reanalysis of AC. Monthly surface data were utilized to study human exposure to the selected pollutants and the effect of the climate variables. Monthly means for assessments and instantaneous predictions are calculated using data with a valid time in the month, ranging from 00 to 23 UTC, except the time 00 UTC on the first day of the next month. Data with a prediction date that falls within the month are used to establish monthly means for accumulations and mean rates.

However, there have been some issues associated with assimilation of the CAMS global reanalysis (EAC4). During 2003 and between March and August 2004, the ozone analysis has a degraded quality, while from 2013 onwards, there is a larger seasonally varying bias in ozone in the free troposphere, particularly in the Arctic and Antarctic that is not seen in the control run. Furthermore, NO_2 in the CAMS reanalysis is mainly influenced by prescribed emissions (e.g., anthropogenic MACCity, GFAS biomass burning) and only to a lesser extent by assimilated findings due to its short lifespan. As a result, patterns or deviations derived from NO_2 reanalysis fields will primarily represent trends in underlying pollution. More details about the EAC4 data products, i.e., the observation techniques, data assimilation methods, bias correction, etc. have been described by Inness et al. (2019) and Flemming et al. (2015).

TABLE 2 | Observations used in the assimilation and validation of CAMS, ordered by species.

Species, Vertical range	Assimilation	Validation
Aerosol mass (PM_{10}, $PM_{2.5}$)	MODIS Aqua/Terra	European Airbase stations
O_3, PBL/surface		Surface ozone: WMO/GAW, NOAA/ESRL-GMD, AIRBASE
CO, PBL/surface	IASI, MOPITT	Surface CO: WMO/GAW, NOAA/ESRL
NO_2, troposphere	OMI, GOME-2, partially constrained due to short lifetime	TROPOMI, SCIAMACHY, GOME-2, MAX-DOAS, TROPOMI
SO_2	GOME-2 (Volcanic eruptions)	

MODIS, Moderate Resolution Imaging Spectroradiometer; IASI, Infrared Atmospheric Sounding Interferometer; MOPITT, Measurements of Pollution in the Troposphere; WMO/GAW, World Meteorological Organization/Global Atmosphere Watch; NOAA/ESRL-GMD, National Oceanic and Atmospheric Administration/Earth System Research Laboratory-Ground-based midcourse defense; GOME-2, Global Ozone Monitoring Experiment-2; TROPOMI, Tropospheric Monitoring Instrument; SCIAMACHY, Scanning Imaging Absorption Spectrometer for Atmospheric Cartography; MAX-DOAS, Multi-Axis Differential Optical Absorption Spectroscopy.

Validation of the Reanalysis Data

The CAMS-84 is a sub-project of CAMS that deals with service product validation. The validation reports for the global and regional services are updated every 3 months by CAMS-84. The validation is focused on a variety of measurements and measuring methods, including *in situ* observations, surface remote sensing, airplane observations, balloon sounding, ship observations, and satellite observations. With a deadline of $\sim$1 month after sensing, the validation reports' three-monthly interval adds restrictions on the timely availability of the findings. **Table 2** represents the assimilation and validation products for specific species along with their vertical range. The validation reports and the verification websites can be found at http://atmosphere.copernicus.eu/user-support/validation/verification-global-services.

For this study, the selected reanalysis products were validated with the monthly average air pollution concentration data overlapping the months of the analysis period obtained from the Department of the Environment (DoE, CASE project) in Dhaka, Bangladesh. Validation of $PM_{2.5}$ and PM_{10} NO_2, and SO_2 with the DoE data has been depicted in the following figure and the concentrations showed R^2 values of 0.93, 0.85, 0.58, and 0.76, which confirms that the reanalysis data are capable of reflecting the ground-based air pollution data (**Figure 2**). Validation for the other pollutants was not done due to temporal anomalies between the reanalysis and ground-based data.

Source Apportionment Using PCA and PMF Modeling

Correlations among the variables were studied through Pearson correlation coefficients instead of non-parametric tests as non-parametric tests are better suited for datasets having no linear relationships or violating normality (Hauke and Kossowski,

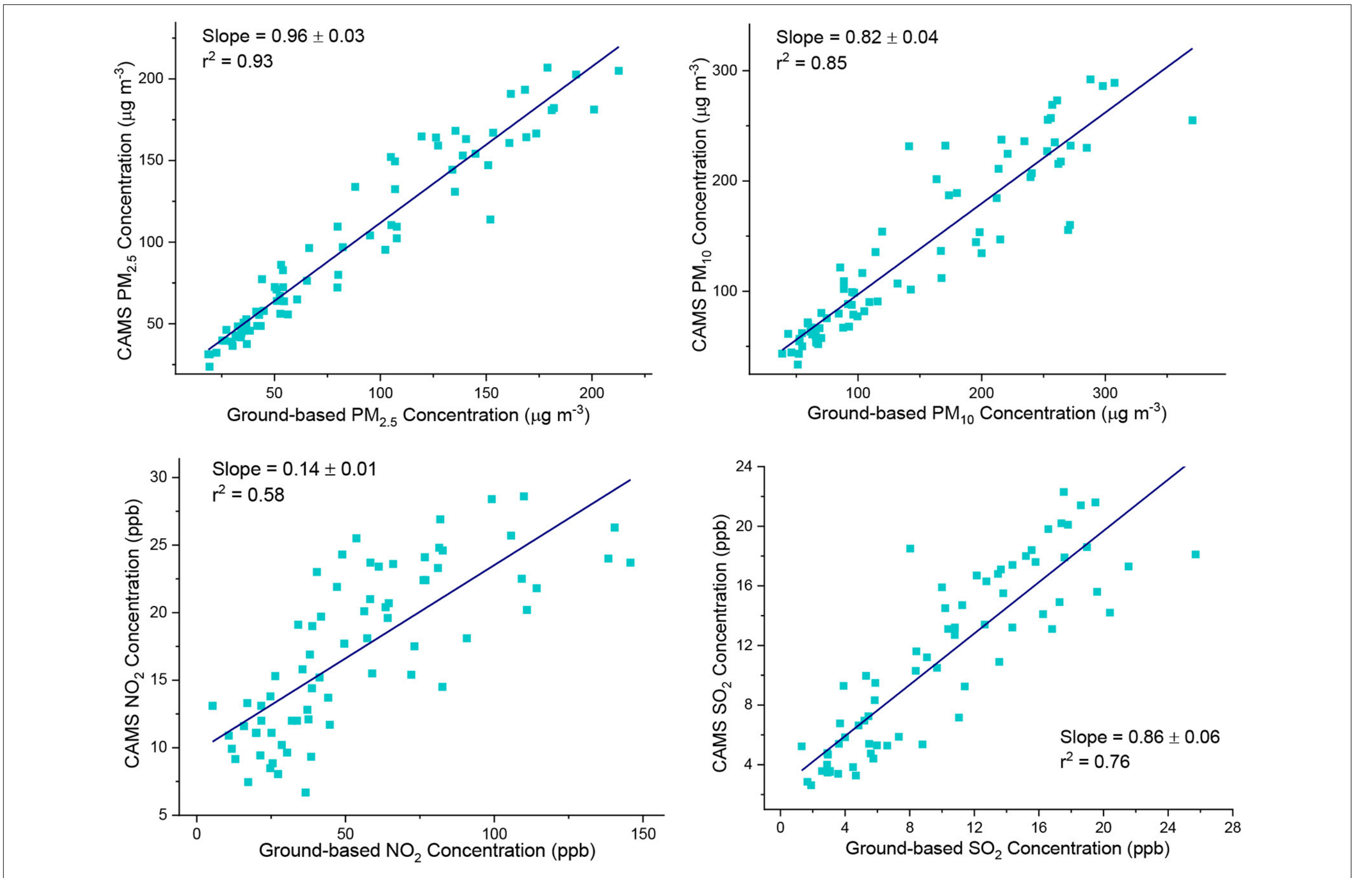

FIGURE 2 | Validation of the Copernicus Atmosphere Monitoring Service (CAMS) products with ground-based products obtained from the Department of Environment (DoE), Bangladesh.

2011). Source apportionment has always been tricky in the case of environmental datasets (Gao et al., 2016). PCA has been used robustly (Cotta et al., 2020) and coupled with other techniques (Sun and Sun, 2017; Franceschi et al., 2018; Gao et al., 2020; Liu et al., 2020). On the other hand, the contribution of various sources to PM and other contaminants around the world have been studied by PMF analysis, as well as references therein (Cesari et al., 2016, 2018; Sharma et al., 2016a,b; Crilley et al., 2017; Liu et al., 2017; Ryou et al., 2018; Jain et al., 2019, 2020). Although PCA is useful for evaluating the association between variables and measurements, it can also be used to describe each observation independently, whereas PMF is more based on the overall dataset definition. As a result, PCA can be used to explain how each attribute affects the observations, as well as whether certain observations or classes of observations have unusual characteristics. Instead of focusing on each observation or indicator, PMF explores the temporal pattern of all variables to find a potential common source. As a result, combining PCA and PMF to achieve an aggregate statistical summary of data is a safe way to view each observation as "independent" and as part of a temporal pattern (Padoan et al., 2020).

Firstly, the distribution of the variables over the studied period was evaluated through PCA, a widely used chemometric technique (Jollife and Cadima, 2016). PCA allows rotating the space spanned by the original variables to a new space spanned by the principal components (PCs), in which the first (generally two or three) PCs report the majority of the details found in the original data. As a result, analyzing the behavior of samples (in the scores plot) and variables is made easier by visualizing the two- or three-dimensional plot of PC1 vs. PC2 (and/or PC3) (in the loading plot).

Then, PMF modeling was employed for the allocation of sources and the inner characteristics of ambient air pollutants ($PM_{2.5}$, PM_{10}, CO, O_3, NO_2, and SO_2) on a monthly basis using EPA PMF (version 5.0). PMF also rotates space spanned by the original variables but the calculated factors are not orthogonal to each other like PCA. This way, a better or worse solution can be obtained by PMF modeling by rotating the variables. Standard deviations associated with each measurement are also required to choose the most suitable number of factors and to evaluate the rotational stability of the obtained solution in the PMF analysis (Paatero and Tapper, 1994). PMF allows for the visualization of diverse sources of air contaminants as well as their contributions to specific pollutant concentrations. Several previous research and related sources enumerated in those publications had detailed explanations of PMF algorithms and their use (EPA PMF 5.0 guide; Sharma et al., 2016a; Cesari et al., 2018; Jain et al., 2020). Therefore, only the compulsory information to elucidate PMF modeling has been described here.

The PMF decomposes a matrix composed of the factors (p), source profiles (f), and the contribution (g) of each source to individual samples based on the following equation (Liu et al., 2017):

$$X_{ij} = \sum_{k=1}^{p} g_{ik} f_{kj} + e_{ij} \tag{1}$$

where ij signifies species residuals, i is the number of concentrations, j is the number of chemical components, and X denotes i by j matrix.

Monthly average concentrations of the ambient air pollutants were utilized in the PMF modeling. To attain acceptable results reducing the uncertainties of online datasets, the following precautions were employed: (1) purging of the outliers (far-off values compared to the average value); (2) apportionment of the sources from monthly datasets (using daily mean concentrations obtained from hourly values); and (3) employment of multiple receptor model (Belis et al., 2015; Cesari et al., 2016). Photochemical oxidation of carbon monoxide (CO) and volatile organic compounds (VOCs) in the presence of nitrogen oxides ($NO_x = NO + NO_2$) and sunlight is the primary source of ozone (Lu et al., 2018). Thus, including O_3 concentrations could bias the source apportionment of the receptor models by using PMF. Therefore, O_3 was excluded from the input dataset in the modeling.

Standard deviations for each month were included to account for uncertainties of each data point and ease the model to estimate results with a significant confidence level for each pollutant. PMF has the establishment of considering uncertainties accompanying each chemical component of the data (EPA PMF 5.0 guide).

$$Uncertainty = \sqrt{(Error\ fraction \times Concentration)^2 + (0.5 \times MDL)^2} \tag{2}$$

where Error fraction is defined as a measure of the standard deviation of particular pollutants divided by the square root of the total number of concentrations. The signal-to-noise (S/N) ratio is utilized to categorize quality of data and the S/N ratios found in this study fall within the acceptable range of those presented in many PMF studies (Sharma et al., 2016a; Cesari et al., 2018; Amato et al., 2020; Jain et al., 2020). The data used in the modeling were specifically divided into three groups based on S/N ratios, with variables with S/N ratios of >2 being labeled as "strong variables," variables with S/N ratios of 0.2–2 being labeled as "weak variables," and the model employing three-fold uncertainty with them. Variables that had S/N ratios <0.2 were disregarded from further analysis and denoted as "bad variables" (Amato et al., 2020). The S/N ratio of all the variables of the air pollutants has been reported in **Supplementary Table 1**.

PMF modeling was employed to run in robust mode, and the Q robust and Q true values were found to be in good agreement with the base run for a four-factor solution. **Supplementary Table 2** displays the Q robust and Q true values for the base runs. The little discrepancies between the two Q-values indicate that the models were able to achieve a satisfactory fit for the data and outliers. Furthermore, 100% convergence rate for all analytical runs was obtained in the model runs, which also affirms the steadiness of the model and the ability to fit all the variables suitably (Nayebare et al., 2018). Extra modeling uncertainty is an additional important parameter that pronounces the fitness of the model. No (0%) error constant (extra modeling uncertainty) was found for all the air pollutants. The results obtained for the air pollutants by PMF modeling had a significant agreement between measured and modeled concentrations specified by R^2 that further confirmed that the concentrations were well-reconstructed (Cusack et al., 2013). R^2 values [from the one-way analysis of variance (ANOVA) F-test] for all the air pollutants were detected to be higher than 0.98, and p-values [from the two-sample Kolmogorov–Smirnov (KS) test] were close to 0 (**Supplementary Table 2**). The performance factor profiles' uncertainties were also assessed using error estimation methods, namely, the Bootstrap (BS) and Displacement (DISP) methods. Details about error estimation methods used in EPA PMF software, 5.0, have been described by Brown et al. (2015). A strong mapping of the PMF species was observed for all datasets in the BS study, with unmapped cases accounting for <5% of the total. Furthermore, the findings are consistent since no factor profile swap was observed in DISP for any of the datasets (Manousakas et al., 2017).

Human Health Risk Assessment

Adverse effects due to exposure to toxic agents can be inclusively estimated through health risk assessment (USEPA, 1989). This procedure predicts effects on human health caused by a particular pollutant utilizing existing exposure data (WHO, 1996). Exposure to $PM_{2.5}$, PM_{10}, CO, O_3, NO_2, and SO_2 and their adverse effects has been studied in this study through the US EPA human health risk assessment framework. This method has been employed in several previous studies to assess non-carcinogenic risk due to the criteria pollutants (Megido et al., 2017; Piersanti et al., 2018; Embiale et al., 2020; Mundackal and Ngole-jeme, 2020; Edlund et al., 2021; Morakinyo et al., 2021). The four steps involved in the HHRA are depicted below:

Hazard Identification

Firstly, $PM_{2.5}$, PM_{10}, CO, O_3, NO_2, and SO_2 have been identified as criteria air pollutants by the WHO as well as USEPA (World Health Organization, 2005; USEPA, 2016).

Dose–Response Assessment

Secondly, the amount of pollutants absorbed by the body was calculated as a function of concentration and exposure time. This research did not have a dose–response analysis. Rather, WHO and the DoE environmental quality guidelines for these air contaminants were used as a benchmark in this study (depicted in **Table 3**).

Exposure Assessment

Then, identification of the exposed population and the magnitude of hazard and duration of exposure are estimated

TABLE 3 | Comparison of ambient guideline values of the criteria pollutants in Bangladesh.

Criteria pollutants	Averaging time	Guideline values		
		Bangladesh[a]	USEPA[b]	WHO[c]
$PM_{2.5}$ (μg/m^3)	24 h	65	35	25
	Annual	15	15	10
PM_{10} (μg/m^3)	24 h	150	150	50
	Annual	50	-	15
CO (ppm)	1 h	35	35	26.25
	8 h	9	9	9
O_3 (ppm)	1 h	0.12	0.12	-
	8 h	0.08	0.08	0.051
NO_2 (ppm)	Annual	0.053	0.053	-
SO_2 (ppm)	24 h	0.014	0.14	0.0077
	Annual	0.03	0.029	-

[a] *case.doe.gov.bd.*
[b] *www.epa.gov/criteria-air-pollutants.*
[c] *www.who.int/news-room/fact-sheets/detail/ambient-(outdoor)-air-quality-and-health.*

through exposure assessment. Inhalation is considered the major route of exposure to pollutants. Chronic (annual) and acute (1-h) exposure assessments were determined for three different age groups, namely, infants (birth to a year), children (6–12 years), and adults (19–75 years).

The acute exposure assessment for the non-carcinogenic pollutants ($PM_{2.5}$, PM_{10}, CO, O_3, NO_2, and SO_2) was based on the rate equation as follows:

$$AHD = \frac{C \times IR}{BW} \tag{3}$$

where AHD stands for average hourly dosage for inhalation (μg/kg/h), C stands for chemical concentration (μg/m^3), IR stands for inhalation rate (m^3/hour), and BW stands for bodyweight (kg) (WHO, 1999).

The rate equation for the chronic exposure assessment for the non-carcinogenic pollutants ($PM_{2.5}$, PM_{10}, CO, O_3, NO_2, and SO_2) was:

$$ADD = \frac{C \times IR \times ED}{BW \times AT} \tag{4}$$

where ADD represents the average daily dosage of the chemical of interest (μg/kg/day), C represents the volume of the chemical in ambient air (μg/m^3), IR represents the inhalation rate (m^3/day), ED represents the exposure period (days), BW represents the exposed group's body weight (kg), and AT represents the averaging time (days) (WHO, 1999). ED is defined by the following equation:

$$ED = ET \times EF \times DE \tag{5}$$

where ET denotes exposure time (h/day), EF denotes exposure frequency (days/year), and DE denotes exposure period (year). **Table 4** shows the estimated values of each variable used in this assessment for each population group in terms of acute and chronic exposure periods (Morakinyo et al., 2017, 2021; Embiale et al., 2020).

Risk Characterization

Finally, using the hazard quotient (HQ), the potential non-carcinogenic consequences of exposure to a known pollutant are quantified *via* the "Risk characterization" process (Morakinyo et al., 2017). HQ expresses the likelihood of a negative health outcome among stable and/or sensitive people. The adverse health outcome occurring among different individuals of different age groups is reflected by this process. Thus, non-cancer risks associated with the air pollutants were estimated through HQ. Acute and chronic non-cancer risks were calculated according to the following equations:

$$HQ = \frac{ADD}{RfC} \ \left(chronic\ exposure\right) \tag{6}$$

$$HQ = \frac{AHD}{RfC} \ \left(acute\ exposure\right) \tag{7}$$

where RfC is an approximation containing uncertainty of considerable scale of an incessant inhalation exposure to the human population (including sensitive subgroups) that possesses a substantial risk of lethal effects during a lifetime (www.epa.gov). The chemical identifications, RfC values, and affecting organs are presented in **Supplementary Table 2**.

An HQ value of 1.0 indicates no risk to human health, while an HQ value of 1.0 indicates a marginal risk, indicating that the considered contaminant is not a potential health risk, to even a sensitive person. However, an HQ > 1.0 signifies risks to some extent upon exposure to different individuals, adults, and/or children (USEPA, 1989).

RESULTS AND DISCUSSION

Ambient PM Trends in Dhaka

Long-term yearly as well as monthly trends of $PM_{2.5}$ and PM_{10} have been depicted in **Figure 3**. **Supplementary Table 4** shows the statistics of $PM_{2.5}$ and PM_{10} during the studied period. Both $PM_{2.5}$ and PM_{10} showed normal distribution for the studied period with mean yearly concentrations of 88.69 ± 9.76 and 124.57 ± 12.75 μg/m^3, respectively. The yearly values of $PM_{2.5}$ and PM_{10} exceeded the national air quality standards respectively by nearly 6.0 and 2.5 times while exceeding WHO standards by 9.0 and 6.0 times. The linear regression analysis has been performed to determine the trends and statistical significances of $PM_{2.5}$ and PM_{10}. Increasing trends have been observed for $PM_{2.5}$ and PM_{10} over the years with slopes of 1.83 ± 0.15 and 2.35 ± 0.24 μg/m^3/year, respectively. One-way ANOVA showed that the increasing trends were statistically significant ($p < 0.05$) for both the PMs (**Figure 3**). Rana et al. (2016) reported similar findings in Dhaka that showed that $PM_{2.5}$ concentrations exceeded the WHO guideline value by 8–13 times. Begum and Hopke (2018) also showed that long-term trends for $PM_{2.5}$ and PM_{10} exceed the USEPA standards in Dhaka.

Monthly variations were identical for the PMs with the highest values observed in winter (November–February) and the lowest

TABLE 4 | The variables used in the calculation of exposure rate and risk assessment factors for different age groups.

Variable	Description	Value						Unit
		Infant (Birth to 1 Year)		Child (6–12 years)		Adult (19–75 years)		
		Acute	Chronic	Acute	Chronic	Acute	Chronic	
C	Contaminant concentration in ambient air							$\mu g/m^3$
IR	Mean inhalation rate	0.30	6.80	1.20	13.50	1.20	13.30	m^3/h
BW	Mean body weight	11.30		45.30		71.80		kg
ET	Exposure time	1.00	14.60 [(350/24) × 1]	1.00	1050.00 [(4200/24) × 6]	1.00	1312.50 [(10,500/24) × 3]	h
EF	Exposure frequency	350.00		350.00		350.00		days
DE	Exposure duration	1.00		12.00		30.00		years
AT	Averaging time	365.00 (1 × 365)		4380.00 (12 × 365)		10,950.00 (30 × 365)		days

in monsoon (June–August). Previous studies also supported such seasonality of PMs with the highest values being associated with the dry season compared to the wet season (Rana et al., 2016; Rahman et al., 2020).

Gaseous Pollutants' Trends in Dhaka

Trace gases CO, O_3, NO_2, and SO_2 showed yearly concentrations of 0.69 ± 0.06 ppm, 51.42 ± 1.82 ppb, 14.87 ± 2.45 ppb, and 8.76 ± 2.07 ppb, respectively for 2003–2019. Normal distribution was observed for all the trace gases over the studied period (**Supplementary Figure 1**). NO_2 and SO_2 were below the annual national guideline values set by DoE. Yearly trends of CO, O_3, NO_2, and SO_2 showed slopes of 0.01 ± 0.002 ppm/year, 0.13 ± 0.09 ppb/year, 0.47 ± 0.03 ppb/year, and 0.40 ± 0.02 ppb/year for the studied period. One-way ANOVA showed that the trends of the trace gases were statistically significant ($p < 0.05$) except for O_3 (**Figure 4**). Rahman M. M. et al. (2019) showed similar significant positive trends for SO_2 and CO in Dhaka, Bangladesh for 2013–2017.

Monthly observations showed that CO, NO_2, and SO_2 followed an almost similar pattern over the year with the highest values in winter (November–February) and the lowest in monsoon (June–August). On the contrary, O_3 showed the maximum values in March–May and the minimum in July–September. The seasonal trends of ozone in Dhaka differed from those of other contaminants, which all exhibited distinct seasonal variation with a peak in the winter and a trough in the monsoon (Rahman M. M. et al., 2019).

Meteorological Parameters' Trends in Dhaka

The air quality of an urban area is heavily influenced by meteorological factors (Rahman M. S. et al., 2019; Afrin et al., 2021). Long-term trends of the meteorological parameters have been depicted in **Figure 5**. Surface temperature, pressure, and relative humidity showed yearly values of 25.99 ± 0.750°C, 1006.46 ± 0.54 hPa, and 71.30 ± 1.36%, respectively, over the studied period. Monthly variation of temperature showed the highest values in April–June and lowest in December–January. Surface pressure showed opposite monthly variation with the highest values observed in June–July and lowest in December–January. Relative humidity, on the other hand, showed the highest values in June–September and lowest in February–March. Linear regression of the parameters showed slopes of 0.12 ± 0.02°C/year, 0.03 ± 0.02 hPa/year, and 0.11 ± 0.07%/year, respectively, for temperature, pressure, and RH. The one-way ANOVA study revealed that the trends were statistically insignificant except for temperature.

Correlation Among the Pollutants and Meteorological Parameters

Pearson correlation analyses were employed to quantify relationships among the ambient air pollutants and meteorological parameters as the variables did not violate the normality test (**Table 5**; **Supplementary Figure 1**). $PM_{2.5}$ and PM_{10} showed significant positive values with PMs, NO_2, and SO_2. Furthermore, NO_2 and SO_2 also showed significant positive values with each other, PMs, and CO. The significant positive correlations among the air pollutants suggested similar production pathways for them.

Previous studies also investigated associations among the air pollutants and meteorological parameters. Ozone had non-significant associations with the other pollutants, according to Rahman M. M. et al. (2019). Although not significant, O_3 has a positive association with PMs, CO, NO_2 ($R^2 > 0.37$), suggesting that the other pollutants could play important roles in the development of O_3. Besides, O_3 showed a negative correlation with RH but a positive correlation with temperature.

In the case of the meteorological parameters, temperature showed significantly positive correlations with all the pollutants but not in the case of the other meteorological variables. Surface pressure did not show any significant association with any other variables other than RH. Lastly, RH did not exhibit any significant connection with the variables. However, according to Afrin et al.

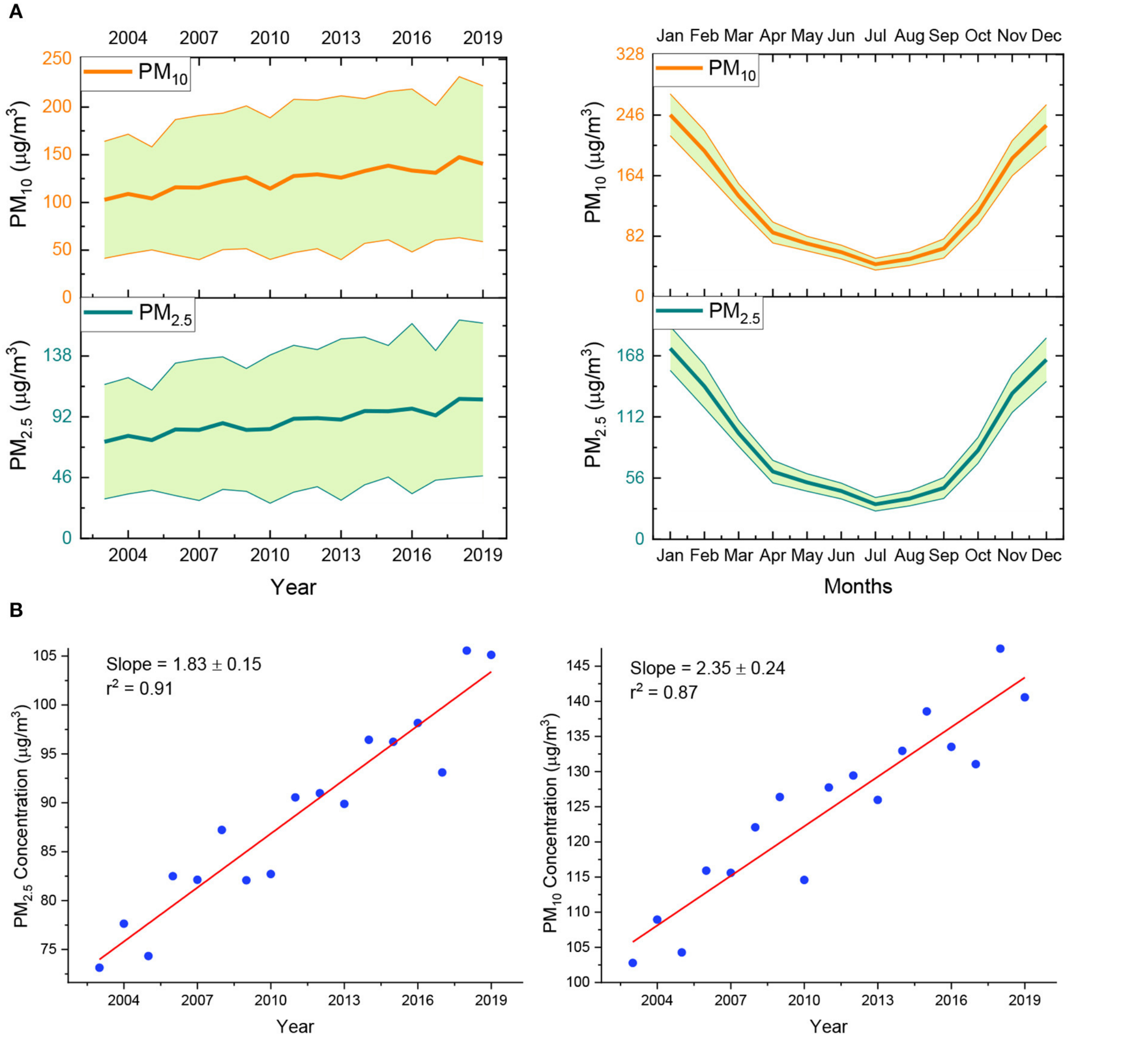

FIGURE 3 | Yearly and monthly trends **(A)** of particulate matters ($PM_{2.5}$ and PM_{10}) and the long-term evolution of $PM_{2.5}$ and PM_{10} **(B)** for 2003–2019 (the shaded regions represent the standard deviations).

(2021), air temperature, wind speed, and wind direction could account for more than 90% of $PM_{2.5}$ variability.

Source Apportionment

Principal Component Analysis

PCA was employed on the monthly datasets of the air pollutants. The datasets were auto-scaled before the analysis. This indicates that the column mean has been subtracted from each digit of the dataset, and the result has been separated by the column standard deviation. **Figure 6** shows the bi-plots obtained by the PCA carried out on the datasets. It reports both scores and loadings in the same PC1 vs. PC2 graph. PC1 and PC2 loadings account for 98.88% of the total variance of the pollutants. PC1 carries 45.20, 45.20, 45.02, 44.09, and 44.09% of explained variance for $PM_{2.5}$, PM_{10}, CO, NO_2, and SO_2 and PC2 carries 55.32 and 55.25% of explained variance for NO_2 and SO_2 (**Figure 6**). The two PMs, CO, NO_2, and SO_2 have the same characteristics as they are distributed evenly along the *x*-axis, which accounts for almost ∼45% of the variance. Thereby, PC1 can be inferred to be vehicular emissions according to the component variance test, whereas NO_2 and SO_2 showed similar discrimination along the *y*-axis, contributing ∼55% of these variables. Thus, PC2 can be attributed to the industrial emissions enriched in NO_2 and SO_2. Furthermore, the variables are almost evenly distributed in the positive and negative regions of PC1 and PC2. It indicates that the chemical composition of the studied compounds has similar concentrations in the case of these two variables.

PMF Modeling

The factor profiles of all the sources of the air pollutants ($PM_{2.5}$, PM_{10}, CO, NO_2, and SO_2) are depicted in **Supplementary Figure 2**. Four factors were attributed to be

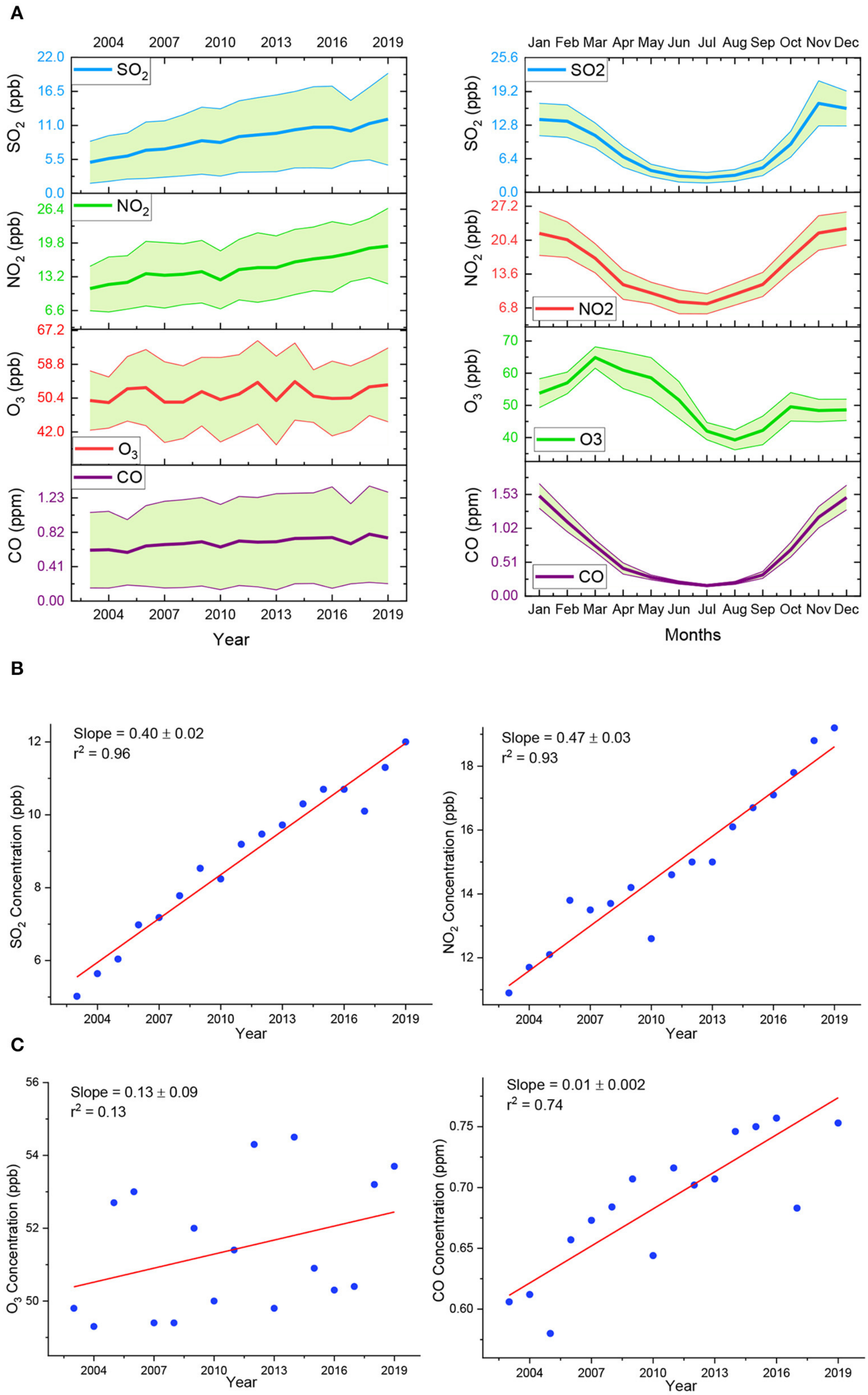

FIGURE 4 | Yearly and monthly trends **(A)** of the gases (SO_2, NO_2, O_3, and CO) and the long-term evolution of SO_2, NO_2, **(B)** O_3, and CO **(C)** for 2003–2019 (the shaded regions represent the standard deviations).

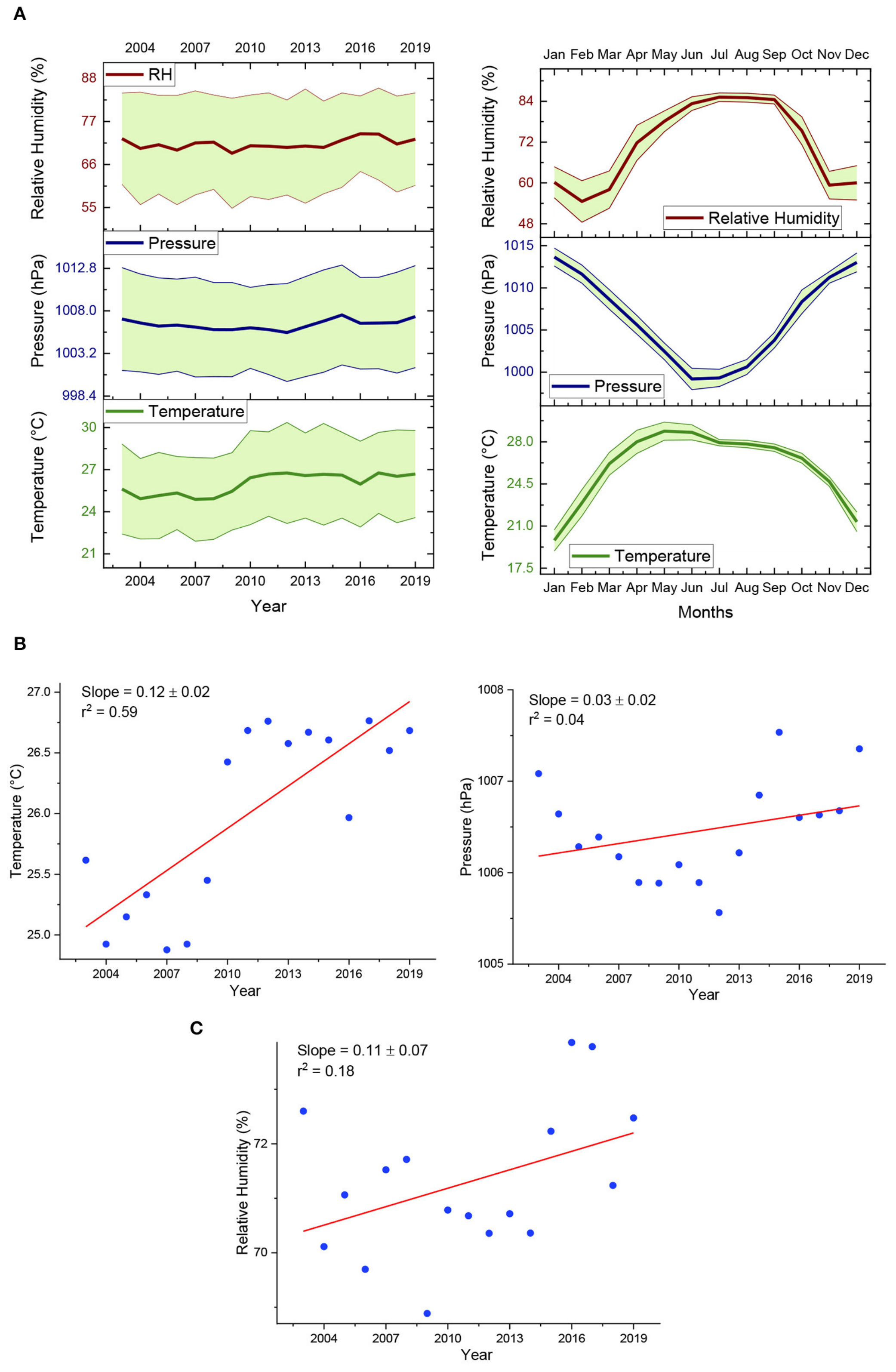

FIGURE 5 | Yearly and monthly trends **(A)** of temperature, pressure, and relative humidity and the long-term evolution of temperature, pressure, **(B)** and relative humidity **(C)** for 2003–2019 (the shaded regions represent the standard deviations).

TABLE 5 | Pearson correlation coefficients among the air pollutants ($PM_{2.5}$, PM_{10}, CO, NO_2, and SO_2) and the meteorological parameters (surface temperature, pressure, and relative humidity).

Pearson correlation	$PM_{2.5}$	PM_{10}	CO	O_3	NO_2	SO_2	T	P	RH
$PM_{2.5}$	1.00	0.96**	0.93**	0.42	0.96**	0.96**	0.69**	0.33	0.34
PM_{10}	0.96**	1.00	0.96**	0.43	0.94**	0.96**	0.68	0.25	0.22
CO	0.93**	0.96**	1.00	0.37	0.87**	0.92**	0.61*	0.22	0.18
O_3	0.42	0.43	0.37	1.00	0.42	0.41	0.41	0.05	−0.31
NO_2	0.96**	0.94**	0.87**	0.42	1.00	0.95**	0.66**	0.37	0.40
SO_2	0.96**	0.96**	0.92**	0.41	0.95**	1.00	0.78**	0.25	0.29
T	0.69**	0.68**	0.61*	0.41	0.66**	0.78**	1.00	0.22	0.22
P	0.33	0.25	0.22	0.05	0.37	0.25	0.22	1.00	0.50*
RH	0.34	0.22	0.18	−0.31	0.40	0.29	0.22	0.50*	1.00

**Significant at the 95% confidence level.*
***Significant at the 99% confidence level.*

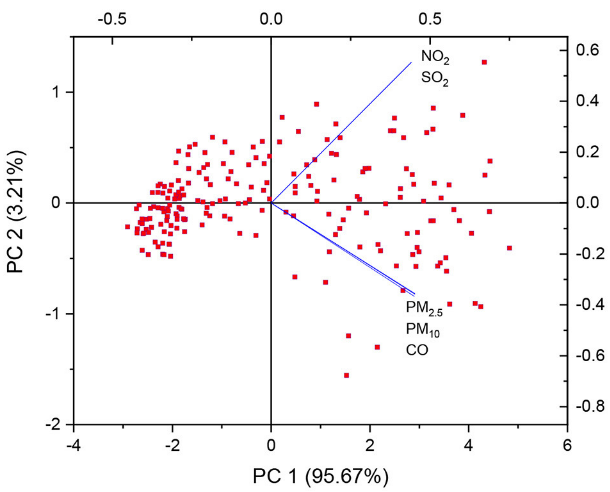

FIGURE 6 | PCA bi-plot of the monthly datasets of the pollutants ($PM_{2.5}$, PM_{10}, CO, NO_2, and SO_2).

the estimated sources contributing to the aforementioned ambient air pollutants. The percent contributions of the factors influencing the air pollutants have been depicted in **Figure 7**.

Factor 1: The first factor is characterized by the highest contribution (74.7%) to NO_2 followed by the signature of 36.5, 35.7, 20.5, and 19.7%, respectively, for $PM_{2.5}$, PM_{10}, CO, and SO_2 (**Figure 7**). Thus, factor 1 is inferred to be vehicular emissions as these pollutants were significantly correlated, suggesting similar sources. Despite the fact that many buses in Dhaka have been converted to CNG engines, heavy-duty trucks that are limited continue to run on diesel between the hours of 10 p.m. and 6 a.m. However, the lower contribution to SO_2 suggests that the conversion of most light-duty vehicles and buses to CNG has resulted in significant reductions in light-duty vehicle and bus emissions (Begum and Hopke, 2018).

Factor 2: PM loadings appeared to be highest (42.9 and 42.7%, respectively, for $PM_{2.5}$ and PM_{10}) for factor 2 with contributions of 28.5 and 22.5% for CO and NO_2, suggesting that this factor can be inferred to be road/soil dust or secondary sources. Elemental characterization is needed to correctly attribute this factor to the ambient pollutants. Spearman correlation revealed that PMs have significant correlations with CO, NO_2, and SO_2 that further affirms traces of the same factor in the case of these pollutants. Due to both anthropogenic and natural sources, dust has been identified as a significant contributor to measure $PM_{2.5}$ in Dhaka, accounting for 11% of total $PM_{2.5}$ (Weagle et al., 2018).

Factor 3: This factor is characterized by the highest contribution (50.5%) to CO with significant contributions to SO_2. PMs are also influenced by this factor with loadings of 14.2 and 15.1%, respectively, for $PM_{2.5}$ and PM_{10}. This factor can be inferred to biomass or fossil fuel burning as suggested by the high loading of CO. Ommi et al. (2017) reported the transboundary influence of biomass burning from the IGP to be an important factor in Dhaka, mainly arising from the preparations of the lands through field burning. Furthermore, Salam et al. (2008) reported that the higher concentration of SO_2 in the city center is possibly due to the high content of sulfur in fossil fuel.

Factor 4: Factor 4 can be inferred as industrial emissions as it contributes mostly (39.2%) to SO_2 with traces in the case of CO (0.5%) and NO_2 (2.0%). Both $PM_{2.5}$ and PM_{10} are associated with about 6.5% for factor 2. The high contribution to SO_2 from this factor signifies the effect of industrialization centered in Dhaka, which has increased exponentially in the last decade or so. The commercial areas of Dhaka had the highest SO_2 concentration (76.8 $\mu g/m^3$) (Salam et al., 2008).

However, since sources of atmospheric pollutants are extremely complicated and diverse, particularly for unorganized emission sources, ambient pollutants cannot be apportioned perfectly through receptor modeling, and some factors remain unknown (Liu et al., 2016, 2017). Furthermore, the dearth of element analysis for metals limits the capability of receptor models to categorize all the sources present regionally. Moreover, the transboundary effects are also significant for ambient regional pollutants in Bangladesh that might affect the ambient air quality as reported by many previous studies (Rana et al., 2016; Rahman et al., 2020).

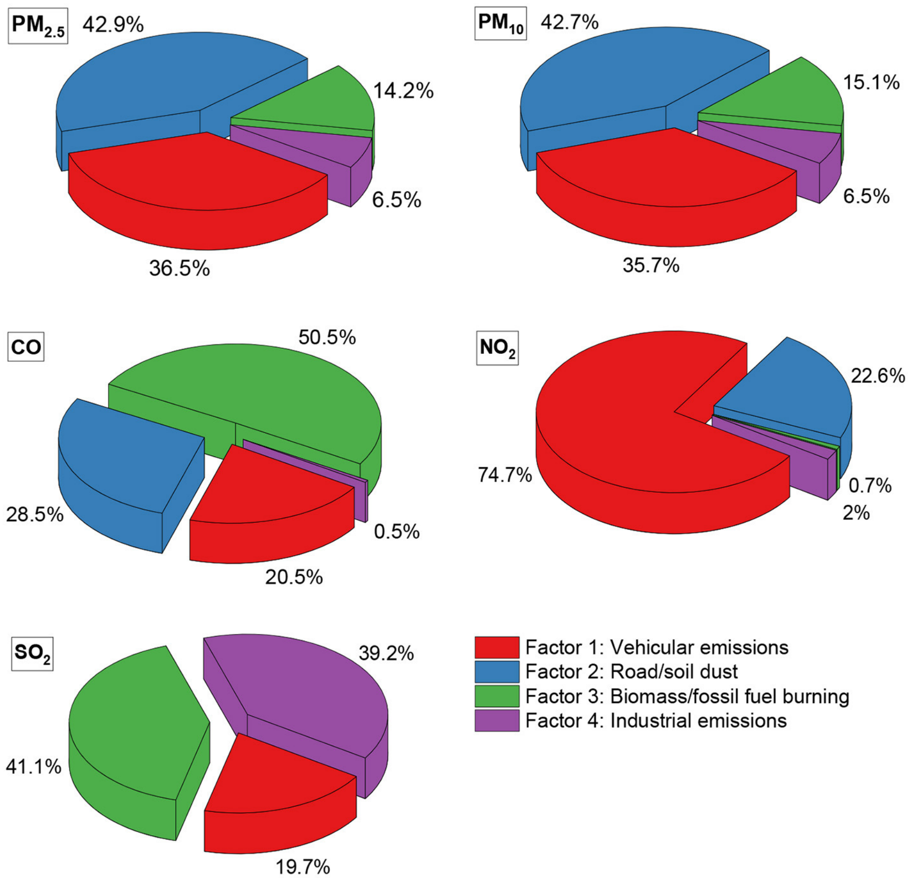

FIGURE 7 | Contribution of the sources to the air pollutants ($PM_{2.5}$, PM_{10}, CO, NO_2, and SO_2) obtained from PMF modeling.

Human Health Risk Assessment

The HQ was calculated for three age groups (infant, child, and adult) in acute and intermediate level exposures, which have been reported in **Figure 8**. At the acute exposure level, no pollutants showed an adverse effect, that is, HQ values were below 1, for any of the age groups. On the other hand, the HQ values posed significant health risk (HQ > 1) at the chronic exposure level for infants and children while no antagonistic health effects risk (HQ < 1) were observed for the pollutants in the case of the adults. Among the pollutants, $PM_{2.5}$ ($1.81 \times 10^3 \pm 2.00 \times 10^2$) and O_3 ($1.03 \times 10^3 \pm 3.65 \times 10^1$) were observed to be the most harmful pollutants affecting the studied age groups, especially the children. In terms of the studied age groups, children were observed to be affected far more than infants and adults at the chronic exposure level. These results suggest that the air pollutants affect all age groups significantly when considered at the chronic level with children being the worst sufferers while negligible effects are observed at the acute level. Owing to a variety of factors, including their comparatively higher level of air inhalation (a resting infant's air consumption per weight unit is double that of an adult), their immune system and lungs not being fully grown, children are the population most impaired by indoor air contamination (Lina Thabethe et al., 2014). Morakinyo et al. also demonstrated a similar adverse impact on children when compared to other age groups. These results essentially signify that low breathing heights could be the main factor along with other indoor and outdoor air pollution sources behind this phenomenon in children who are particularly susceptible to ground-level pollution. In a study conducted at a local school, Sharma and Kumar (2020) found that in-pram babies are exposed to up to 44% higher fine particle concentrations than adults. **Table 6** lists some more previous studies comparing health risks associated with ambient air pollutants.

DISCUSSION AND FUTURE IMPLICATIONS

The air pollutant ($PM_{2.5}$, PM_{10}, CO, NO_2, and SO_2) concentrations except O_3 showed significantly increasing trends in this study. However, an analysis of Dhaka's air quality over two decades (1996–2015) found that the city's air quality has remained constant over the last decade, despite increased economic development and the number of sources such as passenger cars and brick kilns (Begum and Hopke, 2018). On the contrary, a recent analysis found that $PM_{2.5}$ concentrations in Dhaka decreased slightly (statistically non-significant) from 2013 to 2017, but fine PM concentrations remained elevated and

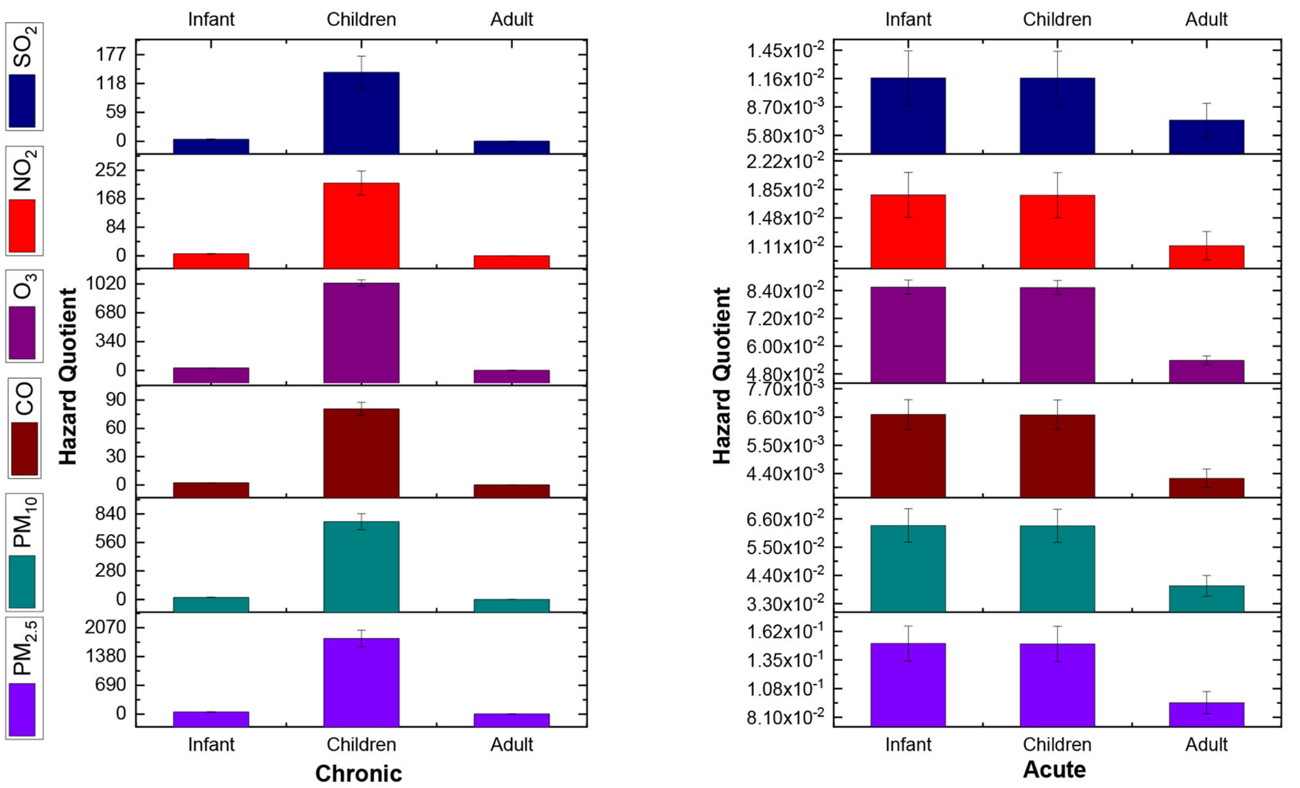

FIGURE 8 | Hazard quotients associated with the ambient pollutants ($PM_{2.5}$, PM_{10}, CO, O_3, NO_2, and SO_2) for infants, children, and adults in chronic and acute levels.

TABLE 6 | Human health risk assessments in various samples and sites according to the USEPA method.

Study area	Studied variables	Findings	References
Gijón, Spain	PM_{10} samples	Cancer and non-cancer risk values were within tolerable limits for both adults and children while the health risk was predicted to be higher for children	Megido et al., 2017
Cordoba city, Argentina	PM samples	HI < 1 for all age groups and land use areas	Mateos et al., 2018
Beihai and Shanghai, China	Heavy metals in street dust	Non-carcinogenic risks due to Cr for children in both the sites were relatively higher than other metals (HI < 1)	Chen et al., 2019
Dhaka, Bangladesh	Heavy metals in street dust	Children may have a slight non-cancer health risk as a result of exposure to street dust (HI > 1).	Rahman M. S. et al., 2019
Dhaka, Bangladesh	Heavy metals in road dust and roadside soil from different school buildings	Children are more susceptible to non-cancer risks than adults and ingestion was identified as the dominant pathway (HI < 1).	Rahman et al., 2021
This study	$PM_{2.5}$, PM_{10}, CO, O_3, NO_2, and SO_2	HQ < 1 at acute levels but HQ > 1 for infants and children at chronic level	

presumably continue to affect human health (Rahman M. M. et al., 2019). Therefore, there remains a need for further study into long-term seasonal cycles, as well as their assessment concerning actions taken by relevant bodies.

Among the meteorological parameters, the temperature seemed to significantly correlate with the air pollutants ($PM_{2.5}$, PM_{10}, CO, NO_2, and SO_2) except O_3. However, according to Afrin et al. (2021), meteorological factors (temperature, relative humidity, etc.) account for about 57% and 35% of the variations in $PM_{2.5}$ and $PM_{2.5-10}$ concentrations, respectively, implying that the finer PM fraction is affected more by meteorology than the coarser fraction. Thus, more quantitative approaches to how climate change affects urban air quality may provide further insights into contaminant reduction policies.

This study estimates four probable main sources contributing to the emission of the six air pollutants in Dhaka, Bangladesh, which are vehicular emissions, road/soil dust, biomass burning, and industrial emissions. In a study on NO_x pollution from vehicular emissions in Dhaka, Iqbal et al. (2019) found that, while a critical urban health ecosystem already exists, the current pattern of vehicular expansion, combined with current vehicle technology and on-road traffic management systems, may soon lead to an unbecoming situation. As a result of these findings, the vehicular management system in Dhaka should be strengthened, and further research into PMs, CO, and NO_x emissions caused by them should be conducted. Furthermore, according to Rahman M. S. et al. (2019), ingestion of dust particles increases the risk of heavy metals (Cr, Cd) in children and adults in Dhaka City, where children were facing a possible health risk. Dhaka is witnessing several infrastructure schemes, such as the Dhaka Metrorail Project and the Dhaka Elevated Expressway Project, which have raised the risk of dust contamination by a factor of many. So, heavy metal contamination caused by dust particles should be investigated more thoroughly in Dhaka, as it poses a threat to children in particular. Rahman et al. (2020) suggested that air pollution in Dhaka is influenced by both local and transboundary sources, but biomass-related $PM_{2.5}$ was found to be the most prevalent during cycles of crop-burning in the IGP. Thus, biomass burning is a major contributor to Dhaka's poor air quality, necessitating further study into the source's impact and mitigation. Finally, the rising pattern of SO_2 in this study and previous studies (Rahman M. M. et al., 2019) indicates that industrial operations in Dhaka, especially brick kiln operations and high sulfur diesel usages, are still contributing significantly to detrimental air quality. More studies encompassing the brick kiln operations and other industrial usage of high sulfur materials in Dhaka are also of paramount importance. Begum et al. (2011) described vehicular emissions and emissions from brick kilns as the two major sources of air pollution in Dhaka and stated that the government of Bangladesh is exploring various measures to minimize emissions from those sources through the adoption of regional policies. However, the pollutant patterns in this study indicate that effective implementation of such measures is still scarce in Dhaka, Bangladesh.

CONCLUSION

In this study, monthly ambient concentrations of the air pollutants ($PM_{2.5}$, PM_{10}, CO, O_3, NO_2, and SO_2) and meteorological data (temperature, surface pressure, and relative humidity) were utilized to explore long-term variations of these parameters and their association with each other. Long-term trends of the ambient pollutants were observed to be increasing significantly in the one-way ANOVA test except for surface ozone while the meteorological parameters showed no significant trends over the studied period. Pearson correlation studies revealed that the ambient pollutants were significantly (CI $>$ 95%) correlated with each other, suggesting probably the same sources. The PCA bi-plot revealed that the PMs and CO demonstrated similar variance while NO_2 and SO_2 followed an analogous pattern. However, four factors emerged as estimated sources of the pollutants in PMF receptor modeling, which were vehicular emissions, road/soil dust, biomass burning, and industrial emissions. PMs were dominated ($\sim$42%) by the road/soil dust along with emissions from vehicles. Biomass burning played a major role in CO (50.5%) and SO_2 (41.1%) production while industrial emissions were another prominent factor (39.2%) in the case of SO_2. On the contrary, NO_2 was identified to be mainly emitted from vehicular emissions (74.7%).

Health risk assessment of the pollutants for three age groups (infant, child, and adult) in acute level exposures indicated no adverse effect (HQ $<$ 1) for any of the age groups. On the other hand, the HQ values posed significant health risk (HQ $>$ 1) at the chronic exposure level for infants and children while no antagonistic health effects risk (HQ $<$ 1) were observed for the pollutants in the case of the adults.

This study reveals that the implementation of CNG wheelers in 2003 might have reduced Pb emissions in megacity Dhaka, but vehicular emissions along with road dust, biomass burning, and industrial emissions remain the most prominent sources that have a significant hazard risk on children and infants particularly. However, since most studies have focused on Dhaka, there is still room to assess long-term possible health risks and the effect of climate variables on air quality at the divisional and district levels in Bangladesh.

DATA AVAILABILITY STATEMENT

The raw data supporting the conclusions of this article will be made available by the authors, without undue reservation.

AUTHOR CONTRIBUTIONS

All authors listed have made a substantial, direct and intellectual contribution to the work, and approved it for publication.

ACKNOWLEDGMENTS

The authors acknowledge the support of the Department of Chemistry, University of Dhaka, Bangladesh. The authors also acknowledge the Department of Environment (DoE), Bangladesh, and the EAC4 (ECMWF Atmospheric Composition Reanalysis 4) global reanalysis dataset produced by the European Centre for Medium-Range Weather Forecasts (ECMWF) from Copernicus Atmosphere Monitoring Service (CAMS) for data support.

SUPPLEMENTARY MATERIAL

The Supplementary Material for this article can be found online at: https://www.frontiersin.org/articles/10.3389/frsc.2021.681759/full#supplementary-material

REFERENCES

Afrin, S., Islam, M. M., and Ahmed, T. (2021). A meteorology based particulate matter prediction model for megacity dhaka. *Aerosol. Air. Qual. Res.* 21, 1–14. doi: 10.4209/aaqr.2020.07.0371

AirVisual (2018). *2018 World Air Quality Report $PM_{2.5}$ Ranking*. Available online at: https://www.iqair.com/us/blog/press-releases/IQAir-AirVisual-2018-World-Air-Quality-Report-Reveals-Worlds-Most-Polluted-Cities (accessed March 15).

Amato, F., Alastuey, A., Karanasiou, A., Lucarelli, F., and AirVisual (2020). *2020 World Air Quality Report $PM_{2.5}$ Ranking*. Available online at: https://www.iqair.com/us/blog/press-releases/IQAir-AirVisual-2020-World-Air-Quality-Report-Reveals-Worlds-Most-Polluted-Cities (accessed March 15).

Begum, B. A., Biswas, S. K., and Hopke, P. K. (2011). Key issues in controlling air pollutants in Dhaka, Bangladesh. *Atmos. Environ.* 45, 7705–7713. doi: 10.1016/j.atmosenv.2010.10.022

Begum, B. A., and Hopke, P. K. (2018). Ambient air quality in dhaka bangladesh over two decades: impacts of policy on air quality. *Aerosol. Air Qual. Res.* 18, 1910–1920. doi: 10.4209/aaqr.2017.11.0465

Begum, B. A., and Hopke, P. K. (2019). Identification of sources from chemical characterization of fine particulate matter and assessment of ambient air quality in Dhaka, Bangladesh. *Aerosol. Air Qual. Res.* 19, 118–128. doi: 10.4209/aaqr.2017.12.0604

Belis, C. A., Karagulian, F., Amato, F., Almeida, M., Artaxo, P., Beddows, D. C. S., et al. (2015). A new methodology to assess the performance and uncertainty of source apportionment models II: the results of two European intercomparison exercises. *Atmos. Environ.* 123, 240–250. doi: 10.1016/j.atmosenv.2015.10.068

Brown, S. G., Eberly, S., Paatero, P., and Norris, G. A. (2015). Science of the total environment methods for estimating uncertainty in pmf solutions: examples with ambient air and water quality data and guidance on reporting PMF results. *Sci. Total Environ.* 518–519, 626–635. doi: 10.1016/j.scitotenv.2015.01.022

Cesari, D., De Benedetto, G. E., Bonasoni, P., Busetto, M., Dinoi, A., Merico, E., et al. (2018). Seasonal variability of PM2.5 and PM10 composition and sources in an urban background site in Southern Italy. *Sci. Total Environ.* 612, 202–213. doi: 10.1016/j.scitotenv.2017.08.230

Cesari, D., Donateo, A., Conte, M., and Contini, D. (2016). Inter-comparison of source apportionment of PM10 using PMF and CMB in three sites nearby an industrial area in central Italy. *Atmos. Res.* 182, 282–293. doi: 10.1016/j.atmosres.2016.08.003

Chen, X., Guo, M., Feng, J., Liang, S., Han, D., and Cheng, J. (2019). Characterization and risk assessment of heavy metals in road dust from a developing city with good air quality and from Shanghai. *Environ. Sci. Pollut. Res.* 26, 11387–11398. doi: 10.1007/s11356-019-04550-2

Cotta, H. H. A., Reisen, V. A., Bondon, P., and Filho, P. R. P. (2020). Identification of redundant air quality monitoring stations using robust principal component analysis. *Environ. Model. Assess.* 25, 521–530. doi: 10.1007/s10666-020-09717-7

Crilley, L. R., Lucarelli, F., Bloss, W. J., Harrison, R. M., Beddows, D. C., Calzolai, G., et al. (2017). Source apportionment of fine and coarse particles at a roadside and urban background site in London during the 2012 summer ClearfLo campaign. *Environ. Pollut.* 220, 766–778. doi: 10.1016/j.envpol.2016.06.002

Cusack, M., Pérez, N., Pey, J., Alastuey, A., and Querol, X. (2013). Source apportionment of fine PM and sub-micron particle number concentrations at a regional background site in the western Mediterranean: a 2.5 year study. *Atmos. Chem. Phys.* 13, 5173–5187. doi: 10.5194/acp-13-5173-2013

Edlund, K. K., Killman, F., Moln, P., Boman, J., Stockfelt, L., and Wichmann, J. (2021). Health risk assessment of PM 2.5 and PM 2.5-bound trace elements in thohoyandou, South Africa. *Int. J. Environ. Res. Public Health* 18:1359. doi: 10.3390/ijerph18031359

Embiale, A., Chandravanshi, B. S., Zewge, F., and Sahle-Demessie, E. (2020). Health risk assessment of total volatile organic compounds, particulate matters and trace elements in PM10 in typical living rooms in Addis Ababa, Ethiopia. *Int. J. Environ. Anal. Chem*. doi: 10.1080/03067319.2020.1814266. [Epub ahead of print].

EPA. *Criteria Air Pollutants*. Washington, DC: EPA.

Flemming, J., Huijnen, V., Arteta, J., Bechtold, P., Beljaars, A., Blechschmidt, A. M., et al. (2015). Tropospheric chemistry in the integrated forecasting system of ECMWF. *Geosci. Model Dev.* 8, 975–1003. doi: 10.5194/gmd-8-975-2015

Franceschi, F., Cobo, M., and Figueredo, M. (2018). Discovering relationships and forecasting PM10 and PM2.5 concentrations in Bogotá Colombia, using Artificial Neural Networks, Principal Component Analysis, and k-means clustering. *Atmos. Pollut. Res.* 9, 912–922. doi: 10.1016/j.apr.2018.02.006

Gao, J., Peng, X., Chen, G., Xu, J., Shi, G. L., Zhang, Y. C., et al. (2016). Insights into the chemical characterization and sources of PM2.5 in Beijing at a 1-h time resolution. *Sci. Total Environ.* 542, 162–171. doi: 10.1016/j.scitotenv.2015.10.082

Gao, S., Zhao, H., Bai, Z., Han, B., Xu, J., Zhao, R., et al. (2020). Combined use of principal component analysis and artificial neural network approach to improve estimates of PM2.5 personal exposure: a case study on older adults. *Sci. Total Environ.* 726:138533. doi: 10.1016/j.scitotenv.2020.138533

Gurjar, B. R., Jain, A., Sharma, A., Agarwal, A., Gupta, P., Nagpure, A. S., et al. (2010). Human health risks in megacities due to air pollution. *Atmos. Environ.* 44, 4606–4613. doi: 10.1016/j.atmosenv.2010.08.011

Hauke, J., and Kossowski, T. (2011). Comparison of values of pearson's and spearman's correlation coefficients on the same sets of data. *Quaest. Geogr.* 30, 87–93. doi: 10.2478/v10117-011-0021-1

Inness, A., Ades, M., Agustí-Panareda, A., Barr, J., Benedictow, A., Blechschmidt, A. M., et al. (2019). The CAMS reanalysis of atmospheric composition. *Atmos. Chem. Phys.* 19, 3515–3556. doi: 10.5194/acp-19-3515-2019

Iqbal, A., Afroze, S., and Rahman, M. (2019). Probabilistic health risk assessment of vehicular emissions as an urban health indicator in Dhaka City. *Sustainability* 11:6427. doi: 10.3390/su11226427

Islam, M. M., Sharmin, M., and Ahmed, F. (2020). Predicting air quality of Dhaka and Sylhet divisions in Bangladesh: a time series modeling approach. *Air Qual. Atmos. Heal.* 13, 607–615. doi: 10.1007/s11869-020-00823-9

Jain, S., Sharma, S. K., Srivastava, M. K., Chaterjee, A., Singh, R. K., Saxena, M., et al. (2019). Source apportionment of PM 10 over three tropical urban atmospheres at indo-gangetic plain of india: an approach using different receptor models. *Arch. Environ. Contam. Toxicol.* 76, 114–128. doi: 10.1007/s00244-018-0572-4

Jain, S., Sharma, S. K., Vijayan, N., and Mandal, T. K. (2020). Seasonal characteristics of aerosols (PM2.5 and PM10) and their source apportionment using PMF: a four year study over Delhi, India. *Environ. Pollut.* 262:114337. doi: 10.1016/j.envpol.2020.114337

Jollife, I. T., and Cadima, J. (2016). Principal component analysis: a review and recent developments. *Philos. Trans. R. Soc. A Math. Phys. Eng. Sci.* 374:20150202. doi: 10.1098/rsta.2015.0202

Landrigan, P. J., Fuller, R., Acosta, N. J. R., Adeyi, O., Arnold, R., Basu, N. N., et al. (2017). The lancet commission on pollution and health. *Lancet* 391, 462–512. doi: 10.1016/S0140-6736(17)32345-0

Lina Thabethe, N. D., Engelbrecht, J. C., Wright, C. Y., and Oosthuizen, M. A. (2014). Human health risks posed by exposure to PM10 for four life stages in a low socio-economic community in South Africa. *Pan Afr. Med. J.* 18, 1–12. doi: 10.11604/pamj.2014.18.206.3393

Liu, B., Song, N., Dai, Q., Mei, R., Sui, B., Bi, X., et al. (2016). Chemical composition and source apportionment of ambient PM2.5 during the non-heating period in Taian, China. *Atmos. Res.* 170, 23–33. doi: 10.1016/j.atmosres.2015.11.002

Liu, B., Yang, J., Yuan, J., Wang, J., Dai, Q., Li, T., et al. (2017). Source apportionment of atmospheric pollutants based on the online data by using PMF and ME2 models at a megacity, China. *Atmos. Res.* 185, 22–31. doi: 10.1016/j.atmosres.2016.10.023

Liu, D., Deng, Q., Ren, Z., Zhou, Z., Song, Z., Huang, J., et al. (2020). Variation trends and principal component analysis of nitrogen oxide emissions from motor vehicles in Wuhan City from 2012 to 2017. *Sci. Total Environ.* 704:134987. doi: 10.1016/j.scitotenv.2019.134987

Lu, X., Hong, J., Zhang, L., Cooper, O. R., Schultz, M. G., Xu, X., et al. (2018). Severe surface ozone pollution in china: a global perspective. *Environ. Sci. Technol. Lett.* 5, 487–494. doi: 10.1021/acs.estlett.8b00366

Manousakas, M., Papaefthymiou, H., Diapouli, E., Migliori, A., Karydas, A. G., Bogdanovic-Radovic, I., et al. (2017). Assessment of PM2.5 sources and their corresponding level of uncertainty in a coastal urban area using EPA PMF 5.0 enhanced diagnostics. *Sci. Total Environ.* 574, 155–164. doi: 10.1016/j.scitotenv.2016.09.047

Mateos, A. C., Amarillo, A. C., Carreras, H. A., and González, C. M. (2018). Land use and air quality in urban environments : Human health risk assessment due to inhalation of airborne particles. *Environ. Res.* 161, 370–380. doi: 10.1016/j.envres.2017.11.035

Megido, L., Suárez-peña, B., Negral, L., and Castrillón, L. (2017). Suburban air quality: human health hazard assessment of potentially toxic elements in PM10. *Chemosphere* 177, 284–291. doi: 10.1016/j.chemosphere.2017.03.009

Morakinyo, O. M., Adebowale, A. S., Mokgobu, M. I., and Mukhola, M. S. (2017). Health risk of inhalation exposure to sub-10 μm particulate matter and gaseous pollutants in an urban-industrial area in South Africa: an ecological study. *BMJ Open* 7, 1–9. doi: 10.1136/bmjopen-2016-013941

Morakinyo, O. M., Mukhola, M. S., and Mokgobu, M. I. (2021). Health risk analysis of elemental components of an industrially emitted respirable particulate matter in an urban area. *Int. J. Environ. Res. Public Health* 18:3653. doi: 10.3390/ijerph18073653

Mundackal, A., and Ngole-Jeme, M. V. (2020). Evaluation of indoor and outdoor air quality in university academic buildings and associated health risk. *Int. J. Environ. Health Res*. (2020). doi: 10.1080/09603123.2020.1828304. [Epub ahead of print].

Nayebare, S. R., Aburizaiza, O. S., Siddique, A., Carpenter, D. O., Hussain, M., Zeb, J., et al. (2018). Ambient air quality in the holy city of Makkah: a source apportionment with elemental enrichment factors (EFs) and factor analysis (PMF). *Environ. Pollut.* 243, 1791–1801. doi: 10.1016/j.envpol.2018.09.086

OECD (2012). *OECD Environmental Outlook to 2050*. Available online at: http://www.oecd-ilibrary.org/environment/oecd-environmental-outlook-to-2050_9789264122246-en (accessed March 15).

Ommi, A., Emami, F., Zíková, N., Hopke, P. K., and Begum, B. A. (2017). Trajectory-based models and remote sensing for biomass burning assessment in Bangladesh. *Aerosol. Air Qual. Res.* 17, 465–475. doi: 10.4209/aaqr.2016.07.0304

Paatero, P., and Tapper, U. (1994). Positive matrix factorization: a non-negative factor model with optimal utilization of error estimates of data values. *Environmetrics* 5, 111–126. doi: 10.1002/env.3170050203

Padoan, S., Zappi, A., Adam, T., Melucci, D., Gambaro, A., Formenton, G., et al. (2020). Organic molecular markers and source contributions in a polluted municipality of north-east Italy: extended PCA-PMF statistical approach. *Environ. Res.* 186:109587. doi: 10.1016/j.envres.2020.109587

Piersanti, A., Adani, M., Briganti, G., Cappelletti, A., Ciancarella, L., Cremona, G., et al. (2018). Science of the Total Environment Air quality modeling and inhalation health risk assessment for a new generation coal- fi red power plant in Central Italy. *Sci. Total Environ.* 644, 884–898. doi: 10.1016/j.scitotenv.2018.06.393

Rahman, M. M., Begum, B. A., Hopke, P. K., Nahar, K., and Thurston, G. D. (2020). Assessing the PM2.5 impact of biomass combustion in megacity Dhaka, Bangladesh. *Environ. Pollut.* 264, 1–11. doi: 10.1016/j.envpol.2020.114798

Rahman, M. M., Mahamud, S., and Thurston, G. D. (2019). Recent spatial gradients and time trends in Dhaka, Bangladesh, air pollution and their human health implications. *J. Air Waste Manag. Assoc.* 69, 478–501. doi: 10.1080/10962247.2018.1548388

Rahman, M. S., Khan, M. D. H., Jolly, Y. N., Kabir, J., Akter, S., and Salam, A. (2019). Assessing risk to human health for heavy metal contamination through street dust in the Southeast Asian Megacity: Dhaka, Bangladesh. *Sci. Total Environ.* 660, 1610–1622. doi: 10.1016/j.scitotenv.2018.12.425

Rahman, M. S., Kumar, S., and Saha, N. (2021). Deciphering the origin of Cu, Pb, and Zn contamination in school dust and soil of Dhaka, a megacity in Bangladesh. *Environ. Sci. Pollut. Res.* doi: 10.1007/s11356-021-13565-7. [Epub ahead of print].

Rai, R., Zhang, Y., Paudel, B., Li, S., and Khanal, N. R. (2017). A synthesis of studies on land use and land cover dynamics during 1930–2015 in bangladesh. *Sustainability* 9, 1–20. doi: 10.3390/su9101866

Rana, M. M., Sulaiman, N., Sivertsen, B., Khan, M. F., and Nasreen, S. (2016). Trends in atmospheric particulate matter in Dhaka, Bangladesh, and the vicinity. *Environ. Sci. Pollut. Res.* 23, 17393–17403. doi: 10.1007/s11356-016-6950-4

Ryou, H., gon, Heo, J., and Kim, S. Y. (2018). Source apportionment of PM10 and PM2.5 air pollution, and possible impacts of study characteristics in South Korea. *Environ. Pollut.* 240, 963–972. doi: 10.1016/j.envpol.2018.03.066

Salam, A., Hossain, T., Siddique, M. N. A., and Shafiqul Alam, A. M. (2008). Characteristics of atmospheric trace gases, particulate matter, and heavy metal pollution in Dhaka, Bangladesh. *Air Qual. Atmos. Heal.* 1, 101–109. doi: 10.1007/s11869-008-0017-8

Salam, A., Ullah, B., and Islam, S. (2013). Carbonaceous species in total suspended particulate matters at different urban and suburban locations in the Greater Dhaka region, Bangladesh. *Air Qual. Atmos. Heal.* 11, 925–935. doi: 10.1007/s11869-011-0166-z

Schmale, J., Shindell, D., Von Schneidemesser, E., Chabay, I., and Lawrence, M. (2014). Air pollution: clean up our skies. *Nature* 515, 335–337. doi: 10.1038/515335a

Sharma, A., and Kumar, P. (2020). Quantification of air pollution exposure to in-pram babies and mitigation strategies. *Environ. Int.* 139:105671. doi: 10.1016/j.envint.2020.105671

Sharma, S. K., Mandal, T. K., Jain, S., Saraswati, Sharma A., and Saxena, M. (2016a). Source apportionment of PM2.5 in Delhi, India using PMF model. *Bull. Environ. Contam. Toxicol.* 97, 286–293. doi: 10.1007/s00128-016-1836-1

Sharma, S. K., Mandal, T. K., Srivastava, M. K., Chatterjee, A., Jain, S., Saxena, M., et al. (2016b). Spatio-temporal variation in chemical characteristics of PM10 over Indo Gangetic Plain of India. *Environ. Sci. Pollut. Res.* 23, 18809–18822. doi: 10.1007/s11356-016-7025-2

Shourav, M. S. A., Shahid, S., Singh, B., Mohsenipour, M., Chung, E. S., and Wang, X. J. (2018). Potential impact of climate change on residential energy consumption in Dhaka City. *Environ. Model. Assess.* 23, 131–140. doi: 10.1007/s10666-017-9571-5

Silva, R. A., West, J. J., Zhang, Y., Anenberg, S. C., Lamarque, J. F., Shindell, D. T., et al. (2013). Global premature mortality due to anthropogenic outdoor air pollution and the contribution of past climate change. *Environ. Res. Lett.* 8:034005. doi: 10.1088/1748-9326/8/3/034005

Stocker, T. F., Qin, D., Plattner, G. K., Tignor, M. M. B., Allen, S. K., Boschung, J., et al. (2013). *Climate Change 2013 the Physical Science Basis: Working Group I Contribution to the Fifth Assessment Report of the Intergovernmental Panel on Climate Change*. Cambridge, New York, NY: Cambridge University Press, 1–1535.

Sun, W., and Sun, J. (2017). Daily PM2.5 concentration prediction based on principal component analysis and LSSVM optimized by cuckoo search algorithm. *J. Environ. Manage.* 188, 144–152. doi: 10.1016/j.jenvman.2016.12.011

USEPA (1989). *Risk Assessment Guidance for Superfund. Volume I Human Health Evaluation Manual (Part A). I 289*. Washington, DC: USEPA.

USEPA (2016). Criteria air pollutants. *Encycl. Immunotoxicol.* 218–218. doi: 10.1007/978-3-642-54596-2_200326

Wadud, Z., and Khan, T. (2013). Air quality and climate impacts due to CNG conversion of motor vehicles in Dhaka, Bangladesh. *Environ. Sci. Technol.* 47, 13907–13916. doi: 10.1021/es402338b

Weagle, C. L., Snider, G., Li, C., Van Donkelaar, A., Philip, S., Bissonnette, P., et al. (2018). Global sources of fine particulate matter: interpretation of PM2.5 chemical composition observed by SPARTAN using a global chemical transport model. *Environ. Sci. Technol.* 52, 11670–11681. doi: 10.1021/acs.est.8b01658

WHO (1996). *Linkage Methods for Environment and Health Analysis. General Guidelines*. Geneva: WHO.

WHO (1999). *Environmental health criteria 210 principles for the assessment of risks to human health from exposure to chemicals*. Geneva: WHO, 76–87.

Williams, M. (2012). Tackling climate change: what is the impact on air pollution? *Carbon Manag.* 3, 511–519. doi: 10.4155/cmt.12.49

World Health Organization, W. (2005). *WHO Air Quality Guidelines for Particulate Matter, Ozone, Nitrogen Dioxide and Sulfur Dioxide: Global Update 2005*. Geneva: World Health Organization, 1–21.

Zaman, S. U., Yesmin, M., Pavel, M. R. S., Jeba, F., and Salam, A. (2021). Indoor air quality indicators and toxicity potential at the hospitals' environment in Dhaka, Bangladesh. *Environ. Sci. Pollut. Res.* doi: 10.1007/s11356-021-13162-8. [Epub ahead of print].

Conflict of Interest: The authors declare that the research was conducted in the absence of any commercial or financial relationships that could be construed as a potential conflict of interest.

The reviewer SH declared a past co-authorship with the authors FJ and AS to the handling Editor.

frontiers in Sustainable Cities

REVIEW
published: 13 August 2021
doi: 10.3389/frsc.2021.705131

Air Pollution, Climate Change, and Human Health in Indian Cities: A Brief Review

*Rajveer Kaur and Puneeta Pandey**

Department of Environmental Science and Technology, School of Environment and Earth Sciences, Central University of Punjab, Bathinda, India

Climate change and air pollution have been a matter of serious concern all over the world in the last few decades. The present review has been carried out in this concern over the Indian cities with significant impacts of both the climate change and air pollution on human health. The expanding urban areas with extreme climate events (high rainfall, extreme temperature, floods, and droughts) are posing human health risks. The intensified heat waves as a result of climate change have led to the elevation in temperature levels causing thermal discomfort and several health issues to urban residents. The study also covers the increasing air pollution levels above the prescribed standards for most of the Indian megacities. The aerosols and PM concentrations have been explored and hazardous health impacts of particles that are inhaled by humans and enter the respiratory system have also been discussed. The air quality during COVID-2019 lockdown in Indian cities with its health impacts has also been reviewed. Finally, the correlation between climate change, air pollution, and urbanizations has been presented as air pollutants (such as aerosols) affect the climate of Earth both directly (by absorption and scattering) and indirectly (by altering the cloud properties and radiation transfer processes). So, the present review will serve as a baseline data for policy makers in analyzing vulnerable regions and implementing mitigation plans for tackling air pollution. The adaptation and mitigation measures can be taken based on the review in Indian cities to reciprocate human health impacts by regular air pollution monitoring and addressing climate change as well.

Keywords: air pollution, climate change, aerosols, urban, India, health

OPEN ACCESS

Edited by:
*Prashant Rajput,
Banaras Hindu University, India*

Reviewed by:
*Atinderpal Singh,
University of Delhi, India
Pallavi Saxena,
Hindu College, University of Delhi, India*

***Correspondence:**
*Puneeta Pandey
puneetapandey@gmail.com*

Specialty section:
This article was submitted to Climate Change and Cities, a section of the journal Frontiers in Sustainable Cities

Received: *04 May 2021*
Accepted: *09 July 2021*
Published: *13 August 2021*

Citation:
Kaur R and Pandey P (2021) Air Pollution, Climate Change, and Human Health in Indian Cities: A Brief Review. Front. Sustain. Cities 3:705131. doi: 10.3389/frsc.2021.705131

INTRODUCTION

Air pollution and climate change are major threats to rapidly growing cities in present times. The developing nations like India, which are switching from predominantly rural country to increasingly urban, have to face critical challenges in terms of climate action and sustainable development (Van Duijne, 2017; Singh C. et al., 2021). India is projected to have 53% of the national population as urban population by addition of 416 million urban dwellers by the year 2050 (UNDESA, 2018).

The change in land use land cover patterns in urban areas due to ongoing urbanization affects regional climate by altering the surface and boundary layer atmospheric properties (Shepherd, 2005; Ren et al., 2008; Yang et al., 2012). Further, the urbanization by changing land use land cover affects climate via increased anthropogenic emissions, extreme precipitation (that may cause urban flooding), higher temperatures, and frequent heat waves with heat related human health impacts (Chestnut et al., 1998; Ramanathan et al., 2001; Shastri et al., 2015). The regional climate changes are reflected by different meteorological conditions such as changes in temperature and precipitation. The anthropogenic emissions such as greenhouse gas (GHG) emissions trigger these local climate changes.

In addition to the impact of urbanization on climate, the increasing urban population and vehicular traffic increases the pollutant emissions and aerosol load in the atmosphere. The increasing urbanization alongwith growing population and industrialization has been stated as one of the key reasons for high aerosol loading in the Indian sub-continent (Kaskaoutis et al., 2011; Ramachandran et al., 2012; Krishna Moorthy et al., 2013). Thus, the climate change and air pollution remain one of the biggest threats to human health and well-being in cities and are interlinked with each other as discussed later in this study.

According to a report by World Health Organization (WHO) more than seven million people across the world lose their lives due to diseases linked with $PM_{2.5}$ pollution (WHO, 2015). India, being a rapidly developing country with increasing population is suffering from severe air pollution; as among the world's 10 most polluted cities, nine of them lie in India [WHO Global Urban Ambient Air Pollution Database (Update 2016), 2016]. The increasing air pollution in most of the Indian megacities over last few decades and its consequential human health impacts (such as asthma and cardio-respiratory illness) have drawn prominent attention in recent years (Sarath and Ramani, 2014; Gautam et al., 2020; Shaw and Gorai, 2020).

CLIMATE CHANGE

The global change in climate has been reported by various workers in the last few decades. The natural process of climate change because of volcanic eruptions, continental drift, and astronomical cycles is now accelerated by human activities (IPCC, 2007). The emission of greenhouse gases (GHGs) is one of the major factors in altering climate by changing atmospheric concentration of certain gases. Further, the role of water vapors in altering the climate is also being well looked into by scientists (Jacob, 2001; Forster and Collins, 2004). Not only this, scientists are also looking into the role of black carbon in climate change due to their ability to strongly absorb incoming solar radiations (Jacobson, 2001; Ramanathan and Carmichae, 2008; Surendran et al., 2013). Menon et al. (2002) used a global climate model to investigate the role of aerosols in altered climate in India and China and reported that precipitation and temperature changes in the model could be correlated to large load of absorbing black carbon in the aerosols. Also, due to heating of air by black carbon aerosols, atmospheric stability is altered leading to changes in hydrologic cycle and large-scale circulations.

Climate change is known to alter the temperature, precipitation pattern and solar insolation over the planet. According to IPCC (2007) report, about 0.65°C increase has been observed in global average surface temperature over last 50 years and is projected to increase by 1.1–6.4°C. The rise in sea level has been observed with ongoing warming trend. Annual sea level rise between 2.5 and 3 mm along the coastline of Mumbai has been reported (Pramanik, 2017). Also, according to a study by NASA, this region has possessed increase in average temperatures by 2.4°C for the period from 1881 to 2015 (NASA, 2015). Further, an increase in frequency of extreme rainfall was analyzed that can cause flooding. This can also be seen in Mumbai, one of the Indian mega-city and home to the largest population threatened by coastal flooding (Intergovernmental Panel on Climate Change IPCC-SREX, 2012). Mumbai has been recognized as one of the world's most vulnerable cities to climate change according to UN-HABITAT, 2010 (Mehta et al., 2019). The changes in rainfall in the past century (1901–2019) were observed over India by Kuttippurath et al. (2021). In the study of 119 years of rainfall measurements, a significant change in the rainfall pattern has been confirmed after 1973 with the declining trend of about 0.42 ± 0.024 mm dec^{-1}. The study shows that in recent decades, the wettest place of the world has shifted from Cherrapunji to Mawsynram.

Besides, the increasing temperature due to climate change can trigger melting of glaciers. A study conducted by Kumar et al. (2021) for monitoring glacier changes in Nanda Devi region of Central Himalaya, India, for three decades, shows the loss of about 26 km^2 (10%) of the glaciated area between 1980 and 2017. Additionally, the climate change causing extreme weather events causes increase in frequency and intensity of floods, storms, torrential rains, and droughts etc. that take thousands of lives and affect millions of people (Haines et al., 2006; Majra and Gur, 2009). The projected climate change estimates from 2036 to 2060 for 57 Indian cities show that 33 cities are likely to experience rise in extreme rainfall and exacerbated flood risk. The remaining 24 cities will observe precipitation declines, reflecting higher drought risk (Ali et al., 2014; Singh C. et al., 2021).

The land use land cover being an important factor in climate change has been focused in many studies over Indian cities such as Nath et al. (2021) that shows rapid expansion of built-up areas in Guwahati with an overall increase of 103% in area over the last 30 years (1990–2020). The expansion in urban areas causes decline in vegetated areas, cropland, and fallow land thereby contributing to climate change. Paul et al. (2021) also showed expansion in urban areas at annual rates of 38.6% with decline in agricultural area at rate of 2.1% for peripheral Delhi during the 1973–2017. So, climate change is one of the emerging threats to human health in Indian cities. With the increase in climate variability, there is an associated increase in health issues (Bush et al., 2011). Cities, due to UHI occurrence, are supposed to have higher effect of climate extremes such as precipitation extremes and heat waves than rural regions (Shepherd, 2005; Shastri et al., 2017; Chauhan and Singh, 2020).

Human Health Impacts Associated With Climate Change

The adverse impacts of climate change on human health have been documented in several studies and these effects are expected to increase with future climate change (Luber and McGeehin, 2008; Bell et al., 2018; Filippelli et al., 2020). The climate change affects human health by problems induced from notable extreme weather conditions such as increased temperature, precipitation, increased intensity and frequency of heat waves, floods, droughts, strong winds, and landslides (Orimoloye et al., 2019). The change in temperature and precipitation causing severe heat, extreme cold, and unpredictable rain linked with climate change increases health related issues; as these climatic changes further induces water and air-borne infections, vector borne-infections, malnutrition, incidence of diarrhoeal diseases, and heat related morbidity and mortality (Haines et al., 2006; Dutta and Chorsiya, 2013).

Children, elderly people, and urban residents are more vulnerable to these health impacts (Haines et al., 2006; Ebi and Paulson, 2010; Filippelli et al., 2020). Nearly 150,000 deaths and about 5 million illnesses have been reported per year due to climate change (Dutta and Chorsiya, 2013).

The respiratory infections, chronic obstructive pulmonary disease, pneumothorax, asthma, allergies, hyperthermia, and dehydration are some of human health issues associated with climate change either directly or indirectly (D'Amato et al., 2011; Filippelli et al., 2020). About 6% of children in India are prone to respiratory tract infections and 2% of adults in India are also trapped in asthma disease (International Institute for population sciences (IIPS) Macro International, 2007).

Thus, these extreme weather conditions have adverse health impacts that can also result in loss of lives. If we look at the extreme heat related human health effects, it becomes imperative to understand the effects of rising temperature on biota.

The increase in temperature due to climate change is a major cause of heat-related diseases in cities such as skin cancer, heat stroke, heart disease, diarrhea, and increased mortality (Changnon et al., 1996; Hondula and Barnett, 2014; Orimoloye et al., 2019). The heat related human health impacts also include dehydration, heat cramps, heat exhaustion, heat stroke, loss of fluids, heat injuries, eye, and skin diseases (Dutta and Chorsiya, 2013). The increase in urban temperature or the urban heat island (UHI) effect is an important implication of climate change. The UHI effect have been reported in many Indian cities (Ambinakudige, 2011; Kikon et al., 2016; Mathew et al., 2016; Kaur and Pandey, 2020) causing thermal discomfort to urban residents. This effect is linked with certain respiratory problems due to deterioration of air quality by cooling agents (Liu and Zhang, 2011).

Besides, the heat waves along with other frequent weather events are reported as significant evidence of climate change in eastern India (Patil and Deepa, 2007). The heat wave during 1998 and 2015 has taken lives of more than 2000 people each in India (Mukherjee and Mishra, 2018). Approximately 1,625 people lost their lives in Rajasthan, followed by Bihar, Uttar Pradesh, and Odisha during 1978 to 1999 due to heat wave (De, 2000); while the toll increased to 3,442 heat-related deaths during 1999–2003 (Chaudhury et al., 2000; Centers for Disease Control Prevention, 2006). The statistical data documented in a study by Dutta and Chorsiya (2013) states that more than 600 people have died due to heat wave in India in 2013. Besides, about 1,400 deaths were caused by high ambient temperature (50°C) in Andhra Pradesh in 2002. Similarly, in Ahmadabad high ambient temperature (46.8°C) took lives of many urban residents in 2010. Further, the heat waves significantly affected dozens of Indian states such as Rajasthan and Uttarakhand in 2009 (Dutta and Chorsiya, 2013). The climate variability and its relation with mortality due to heat in India were documented by Akhtar (2007), Dholakia et al. (2015) for Ahmedabad, Murari K. K. et al. (2015), and Mazdiyasni et al. (2017). Further, following the increasing frequency of hot days and nights during the period 1951–2016, 4-fold increase has been projected by 2050 and 12-fold by 2,100 that will lead to increased heat-related mortality (Mukherjee and Mishra, 2018; Singh C. et al., 2021).

The climate change is known to trigger other extreme events such as drought, floods, tsunamis, and cyclones that are associated with negative human health impacts. Urban drought and floods caused by changing climate due to scarcity or excess of rainfall indirectly affects human health. Drowning, hypothermia, and trauma are some physical effects of floods on human health (Ahern et al., 2005; Du et al., 2010). Severe drought conditions resulting in scarcity of food caused high number of deaths due to starvation in India (Dutta and Chorsiya, 2013). Also, the high rainfall causing floods lead to destruction of crops that in turn causes shortage of food leading to malnutrition and public health issues. The malnutrition is a severe issue in India with about 47% of the children prone to this problem according to World Bank Report on Malnutrition in India (2009). The malnutrition can further cause anemia from which about 70% children, 55% women, and 25% of men population are suffering, in India (Majra and Gur, 2009).

The rising sea level due to climate change may cause flooding that can cause death (Dutta and Chorsiya, 2013). Moreover, the drought and flood conditions also decrease the availability of fresh water. The increase in risk of diarrheal diseases linked with floods has been reported for India (Mondal et al., 2001). The contaminated water can cause transmission of various water-borne infections leading to *E. coli* infection, cholera, typhoid, cryptosporidium, shigella, giardia, and viruses such as hepatitis A (Gabastou et al., 2002; Kovats and Akhtar, 2008; Majra and Gur, 2009). Besides, floods also lead to certain rodent-borne diseases such as including tularemia, leptospirosis, and viral hemorrhagic diseases. Lyme disease, Hantavirus pulmonary syndrome, and tick-borne encephalitis are some other diseases linked with climatic variability for Baltimore and London (Wilson et al., 2001; Majra and Gur, 2009).

Besides, the extreme weather events due to climate change such as cyclones, tsunamis, and floods have taken thousands of lives and affected millions of population in many Indian states such as Assam, Bihar, West Bengal, Odisha, Uttar Pradesh, Himachal Pradesh, Rajasthan, and Gujarat (World Health Organization (WHO), 2005; Majra and Gur, 2009). These events also cause adverse health impacts on surviving population. Some of these extreme weather events reported in the past few years are:

Heat wave in Odisha in 1998 and 2004, Super cyclone in Odisha with wind speed over 300 km/h in October 1999, Heat wave in Andhra Pradesh in 2003, Cold wave in Uttar Pradesh and Uttaranchal in 2004, Tsunami affecting Tamil Nadu, Andhra Pradesh, Kerala, and the Andaman-Nicobar Islands in 2004, Heaviest rainfall in Indian metropolitan city of Mumbai in 2005, Cyclone in Andhra Pradesh in 2005, Floods in Gujarat and Madhya Pradesh in 2005 and cloudburst and flood in Uttarakhand in June 2013.

These disasters enhances the incidence and spread of diseases by increasing transmission of infectious vectors such as plague, Japanese encephalitis, malaria, dengue fever, chikungunya, and filariasis (Bhattacharya et al., 2006; Devi and Jauhari, 2006; Dhiman et al., 2008; Bush et al., 2011). Additionally, these calamities have badly affected Indian states such as Plague in Surat, malaria in Odisha, West Bengal, Jharkhand, Chattisgarh, Madhya Pradesh, and North East (Kumar et al., 2007). The coastal regions of India are prone to tsunamis and cyclones (Dutta and Chorsiya, 2013).

These disasters also lead to occurrence of water-borne diseases such as amoebiasis, crytosporidiosis, giardiasis, typhoid, cholera, and other infections. According to The World Health Organization (WHO), 900,000 Indians die each year from drinking contaminated water and breathing polluted air (World Health Organization and United Nations Children's Fund (WHO and UNICEF), 2000). Also, Indian Ministry of Health estimated 1.5 million deaths annually between 0- and 5-year-old children. Every year in India around 0.6–0.7 million children under 5 years of age die from diarrhea.

So, the potential health impacts related with climate change can be categorized as:

a) Direct factors: The factors such as thermal stress, death/injury in floods and storms are direct implication of climate change that affects human health.
b) Indirect factors: The indirect factors include vectors-borne diseases, water-borne pathogens, water and air quality, and food availability and quality that are indirectly caused by climate change.

AIR POLLUTION

Air pollution is a matter of serious concern in megacities where the pollution levels often exceed the permissible limits due to its associated health risks for city residents (Chattopadhyay et al., 2010; Debone et al., 2020). The metropolitan cities of India are exposed to unhealthy and unhygienic conditions due to air pollution (Dutta et al., 2021). The continuous and alarming increase of urban air pollution is an emerging environmental issue in the Indian megacities for the last few decades (Faheem et al., 2021).

Major outdoor and indoor air pollutants in urban areas can be primary or secondary air pollutants. Primary air pollutants that are emitted directly include particulate matter {$PM_{2.5}$, PM_{10}, suspended particulate matter (SPM), respirable particulate matter (RPM)}, SOx, NOx, CO, ammonia, and dust particles while the secondary air pollutants involve ozone, smog, Peroxyacyl nitrates (PANs) etc.

The developing nations like India with ongoing urbanization are suffering from increased air pollution issues due to the lack of services such as adequate transportation management, suitable roads, and unplanned distribution of industries (Rumana et al., 2014). The congested roads in cities reduce average vehicular speed resulting in higher vehicular emissions adding to air pollution levels (West Bengal Pollution Control Board, 2010). The increasing and unplanned urbanization coupled with industrialization and population growth are posing threat to human health by increasing air pollution levels leading to number of health issues (Dutta et al., 2021). Additionally, the complex and intensive human activities in these urban areas are fueling the problem by increasing emission of pollutants.

In Indian cities, the air pollutants are either emitted from natural sources such as long-range transport of desert dust influx originated from the western arid regions of Africa, Middle-East, and Thar (Rajasthan) regions, predominately during summer and pre-monsoon season (El-Askary et al., 2006) or they can be of anthropogenic origin as given in **Figure 1** (Ghose et al., 2005; Habib et al., 2006; Prasad and Singh, 2007; Badarinath et al., 2010; Sharma et al., 2010; Kharol et al., 2011; Dandotiya et al., 2020).

Vehicular emissions (95%) have been identified as prevalent source of high NO_2 concentrations followed by industries and fuel burning, thereby increasing air pollution in urban areas of India (Mondal et al., 2000; Ghose et al., 2004; ARAI, 2010). The combustion of low-quality fuel in Indian cities causes SO_2 emissions (Zou et al., 2007). Air pollutants are also emitted from crude oil wells and flared natural gas (Amakiri et al., 2009). Besides, open burning and landfill fires of municipal solid waste were recognized as chief source of air pollution for Mumbai, India in a study reported by National Environmental Engineering Research Institute (Central Pollution Control Board (CPCB), 2010). Open coal liming, fluoride mining, lime stone mining, thermal power plant, natural and domestic burning of coal, cement industry, and road dust were another primary source of air pollution in India (MPCB, 2010; Maji et al., 2016). Road dust (61%) was identified as major source of high particulate matter concentration followed by vehicular emissions, industrial emissions, vegetation, and solid fuel burning for another Indian city (Pune). Plastic industry, domestic waste burning, and food processing factories were the main sources of air pollution in Nashik city (Maji et al., 2016). Diesel generators, coal based industrial emissions, oil refinery emissions were major source of PM in Agra (Maji et al., 2016). Also, thermal power plants in most of the cities in addition to large- and small-scale industries are contributing to high air pollution levels. For Kolkata, 51.4% of the air pollution is contributed by motor vehicles followed by 24.5% emissions from industries and 21.1% dust particles (West Bengal Pollution Control Board, 2005).

The deterioration of air quality has been further aggravated by emission of toxic pollutants such as particulate matter, greenhouse gases like SOx, NOx, and O_3 (Rumana et al., 2014). Emission of aerosols from deserts, oceans, forest fires, and volcanoes into the atmosphere also adds to air quality depletion. Increase in population, urbanization, and industrialization has depleted air quality and hence adversely affects human health (Rumana et al., 2014).

Besides, Particulate matter, Black carbon (BC) has been studied by various workers around the globe. Singh A. et al. (2014) reported mass concentrations of BC in Indo-Gangetic Plains (IGP) that varied from 8.5 to 19.6, 2.4 to 18.2, and

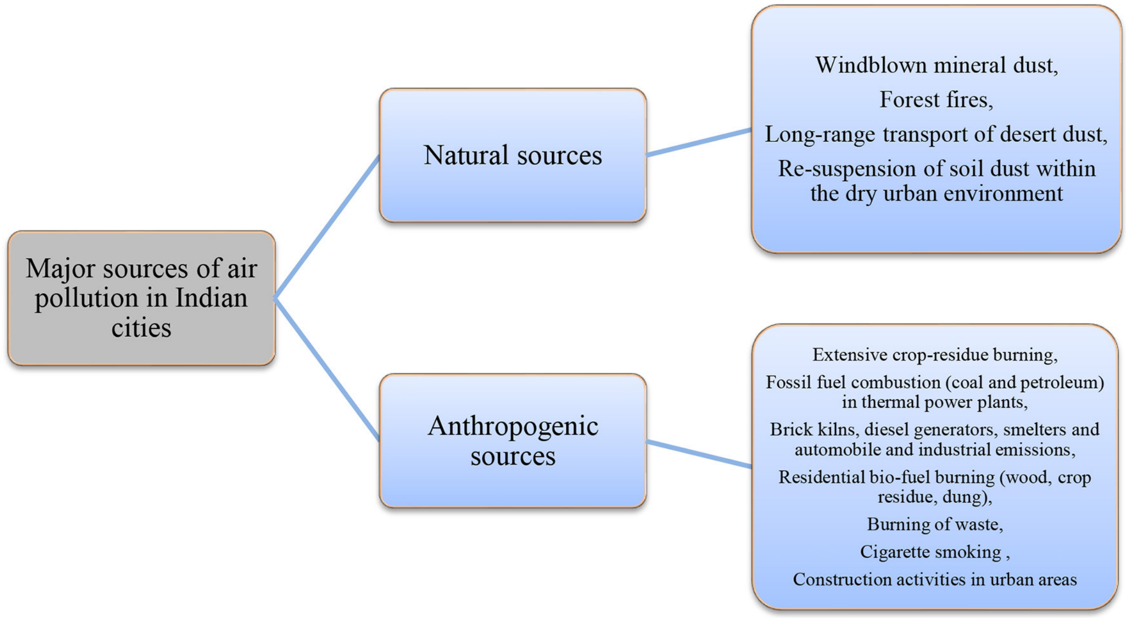

FIGURE 1 | Major sources of air pollution in Indian cities.

2.2 to 9.4 μg m^{-3} during paddy-residue burning emission in the month of October-November, emission from bio- and fossil-fuel combustion during December–March months and wheat-residue burning emissions duringApril-May, respectively. In contrast, the mass concentrations of Elemental Carbon (EC) varied from 3.8 to 17.5, 2.3 to 8.9, and 2.0 to 8.8 μg m−3 during these emissions, respectively. Not only this, polycyclic aromatic hydrocarbons (PAHs) have been studied by Rajput et al. (2011) during paddy and wheat biomass burning emissions of Indo-Gangetic plains and reported 40 ng m^{-3} of total PAHs are reported from paddy residue burning and 7 ngm^{-3} during wheat burning season.

Human Health Impacts by Air Pollution

Since last few decades, there has been signification degradation of air quality in most of the Indian cities as many of the Indian cities are in grip of serious air pollution issue such as Kolkata, Delhi (Ghose et al., 2005) with the air quality above the standards provided by CPCB and WHO. The daily and annual average values were high for most of the gaseous pollutants in Indian cities (Dandotiya et al., 2020). The literature suggests the high load of ambient air pollution (specifically in the Indo-Gangetic plain) (Satheesh et al., 2002; Kharol et al., 2011; Ramachandran et al., 2012) has been identified as one of the important contributors to the air pollution related diseases burden in India (Prabhakaran et al., 2020). Rajput et al. (2016) assessed temporal variability and source contributions of PM1, trace metals, five major elements, and four water-soluble inorganic species (WSIS) in the Indo-Gangetic Plains (IGP). Total WSIS contributes about 26% to PM_1 mass concentration. Secondary aerosols (contributing as high as) were predominantly derived from stationary combustion sources and contributed ~60% to PM_1 loading. Further, atmospheric fog prevalent during wintertime can have a severe impact on atmospheric chemistry in the air-shed of IGP.

The health issues linked with air pollution is a topic of major concern specially for developing Indian cities. In India, the outdoor air pollution has become fifth eminent reason of death after high blood pressure, indoor air pollution, poor nutrition and tobacco smoking in 2012 causing about 0.62 million premature excess number of death cases (NYT, 2014; Maji et al., 2016).

Air pollution is linked with short term, medium, or long term impacts on human health (Gumashta and Bijlwan, 2020). Several studies have been conducted regarding the short-term health effects of exposure to air pollution. Short term impacts include irritation to eyes, throat, and nose, and some respiratory infections such as pneumonia and bronchitis, while long term air pollution impacts involve chronic respiratory diseases, heart related problems, lung cancer, and even damage to the brain, liver, kidneys, or nerves (Faheem et al., 2021). Meanwhile Prabhakaran et al. (2020) reported that both short- and long-term exposure to air pollutants contributed to higher blood pressure and increased risk of incident hypertension. The associations between gaseous pollutants and health outcomes have also been discussed (Samoli et al., 2008, 2013; Stafoggia et al., 2013). The higher gaseous and particulate matter concentrations in air are significantly connected with premature mortality and hospitalizations for respiratory and post respiratory illnesses in cities (Burnett et al., 1997; Yang et al., 2004). Rajput et al. (2019) reported that coarse particles exhibited higher mass deposition fraction in extrathoracic region, whereas fine particles deposited significantly in pulmonary region. Intensification of biomass and biofuel burning emissions during post-monsoon and wintertime have implications to deeper penetration and higher mass deposition fraction of fine-particles in the PUL region.

The air pollution impacts are different in different people such as some individuals are more sensitive to air pollutants than others. Children, elderly people and pregnant women are more prone to health risks related with air pollutants. The studies revealed that the children on exposure to air pollution are highly affected as compared to adults as the lungs of children are comparatively less developed at birth and are not proper functional until about 6–8 years of age (Burri, 1984; Lee, 2010; Smith, 2013). Also, the people who are already suffering from health issues like heart, lung disease, asthma etc are having higher probability to suffer more. Moreover, the extent of impacts depends on duration of exposure and concentration of air pollutants as studied in the city of Agra (Faheem et al., 2021).

Various epidemiological studies conducted in this concern states that poor quality of air poses significant risk to human health creating problems such as decreased lung function, respiratory symptoms and increased asthma incidence, allergy, and cardio-respiratory illness [Ghose et al., 2005; Pope et al., 2009; Beckerman et al., 2012; Portnov et al., 2012; WHO, 2013; Cheng et al., 2014; Tsai and Yang, 2014; Carosino et al., 2015; Global Initiative for Asthma (GINA), 2015; Shaw and Gorai, 2020] with higher concentration of air pollutants. Chronic obstructive pulmonary diseases, influenza, bronchitis, asthma, upper track respiratory infection, and acute respiratory infections were some other health impacts observed for Indian cities due to air pollution (Haque and Singh, 2017). Further, air pollution is linked with several disease and even premature death. The air pollutants dispersed to a long distance and they react or damage the mechanisms by chemical reaction with the molecules of respiratory system and bringing about adverse chemical changes. The health issues such as genetic changes, impaired liver function, hematological abnormalities, and neurobehavioral problems were also associated with air pollution especially for the people exposed to higher vehicular emissions. These include traffic policeman, auto, and taxi drivers and roadside hawkers (Mukhopadhyay, 2009). Besides, detrimental health effects, such as lung cancer, cardiovascular disease risk, cardiopulmonary mortality, and pulmonary inflammation have been reported on exposure to particulate matter in several epidemiological studies (Pope et al., 2009; Huang et al., 2012; Gorai et al., 2014; Prabhakaran et al., 2020).

Furthermore, the health impacts of NO_2 involve irritation of the alveoli and resistance in airways and pulmonary function and decrease in pulmonary capacity reported for cities such as Agra and Taiwan (Mudgal et al., 2000; Yang et al., 2005; Saini et al., 2008). Respiratory health effects, lower birth rates, lower birth weights, and chronic bronchitis are health impacts associated with exposure to high SO_2 concentrations (Ciccone et al., 1995; Dejmek et al., 2000; Rogers et al., 2000). Although gaseous air pollutants such as NO_2 and SO_2 are matter of increasing concern for human health; but particulate matter was observed as prominent reason for air pollution related mortality and morbidity rather than gaseous pollutants (Maji et al., 2016). High particulate matter concentration was observed in India with more than 50% of the population exposed to these higher concentrations (above NAAQs) (Ramya et al., 2021). The premature death due to SPM is reported to be very high and the children are the worst effected groups in Kolkata (Haque and Singh, 2017). Besides, abundance and variability of viable bioaerosols was reported by Rajput et al. (2017) in Indo-Gangetic Plains with very high concentration of Gram-positive bacteria (GPB), Gram-negative bacteria (GNB), and Fungi; having implications for human health.

The monitoring of ambient air quality for selected cities in India is conducted by The Central Pollution Control Board (CPCB). In 1984, CPCB initiated National Ambient Air Quality Monitoring (NAAQM) for monitoring air quality that was later renamed as National Air Monitoring Programme (NAMP). Also, the Government of India has prescribed The National Ambient Air Quality Standards (NAAQS). Health risk assessment has been conducted in various studies using formulae given by USEPA.

About 91% of world's population has been found to be residing in areas with air quality higher than permissible limits according to WHO (Mostafavi et al., 2021). Air pollution has led to death of about 3.8 million people throughout the globe as reported by WHO, due to certain human health issues such as ischemic heart disease (27%), pneumonia (27%), chronic obstructive pulmonary disease (20%), stroke (18%), and lung cancer (8%) (Ramya et al., 2021). In India, about 1.24 million deaths have occurred due to air pollution. Out of this, 0.67 million cases were attributed to ambient air pollution and remaining 0.48 million cases were linked with household air pollution (Rumana et al., 2014; Balakrishnan et al., 2019). In India, about 0.62 million in 2005 and 0.69 million in 2010 premature death cases have occurred due to outdoor air pollution (OECD, 2014).

About 1.67 million (95% uncertainty interval) deaths were attributable to air pollution in India in 2019, accounting for 17.8% (15.8–19.5) of the total deaths in the nation. The majority of these deaths were due to ambient particulate matter pollution (0.98 million) and household air pollution (0.61 million). There was a decrease in death rate due to household air pollution by 64.2% from 1990 to 2019, whereas an increase was observed in death rate due to ambient particulate matter pollution by 115.3 and 139.2% increase in death rate due to ambient ozone pollution (GBD 2015 Risk Factors Collaborators).

Air pollution has led to respiratory diseases in about 70% of people in an Indian city, Kolkata as reported jointly by Chittaranjan National Cancer Institute, West Bengal Department of Environment and the Central Pollution Control Board (CPCB) (Mukhopadhyay, 2009). About 10,647 premature deaths were caused due to air pollution in Kolkata in 1995 (Ghose, 2002; Schwela et al., 2006). Adverse lung diseases and genetic abnormalities in exposed lung tissues were reported for children exposed to polluted air in Kolkata (Lahiri et al., 2000). The people residing in Kolkata city were facing seven times higher burden on their lungs due to air pollution as compared to their rural counterparts and about 47% of Kolkata's residents were suffering from lower respiratory tract symptoms Roy et al., 2001; West Bengal Pollution Control Board (WBPCB), 2003; Schwela et al., 2006. Rajeev et al. (2018) reported health risk assessment of PM1-bound carcinogenic hexavalent chromium [Cr (VI)] from central part of Indo-Gangetic plain (IGP) by assessing excess cancer risk (ECR) which was found to be 57 and 14.3 (in one million) for adults and children, respectively.

The human health impacts caused by air pollution result in high economic cost of about USD 80 billion in 2010, that is almost equal to 5.7% of India's gross domestic product (GDP) (Maji et al., 2016).

Various studies have been conducted regarding air pollution and their associated health impacts for Indian cities such as for Delhi (Gurjar et al., 2010; HEI, 2011; Rizwan et al., 2013; Nagpure et al., 2014); Chandigarh (Gupta et al., 2001); Kolkata (Ghose et al., 2005; Gurjar et al., 2016; Haque and Singh, 2017); Rajasthan (Rumana et al., 2014); Lucknow (Lawrence and Fatima, 2014); Mumbai (Joseph et al., 2003; Maji et al., 2016); Maharashtra (Maji et al., 2016), Agra (Maji et al., 2017); Gwalior City (Dandotiya et al., 2020); Chennai (Jayanthi and Krishnamoorthy, 2006; HEI, 2011). Agarwal et al. (2018) studied mutagenicity and cytotoxicity of PM from biodiesel-fueled engines that were relatively higher compared to their diesel counterparts, indicating the need for exhaust gas after-treatment. The exhaust of chemical characterization revealed that biodiesel-fueled engines contained several harmful PAHs and trace metals, which affected the biological activity of PM.

Aerosols and Particulate Matter

Aerosols have been considered as one of the key air pollutants that significantly influence the air quality and affects public health (Xu et al., 2014). Aerosol optical depth (AOD), an optical property, have been determined in several studies using either ground based observations or satellite data to monitor the concentration of aerosols in the atmosphere. The AOD values are extensively used to represent air pollution level, reflect atmospheric conditions and define climatic effects as these values are closely linked with air pollutants such as $PM_{2.5}$, PM_{10}, NO_2, SO_2, and O_3 (Chu et al., 2003; Xu et al., 2014; Li et al., 2016; Awais et al., 2018; Ahmad et al., 2020). The monitoring of aerosols has been carried out in many of the Indian cities, as India has been recognized as one of the regional hot spots of aerosols because of increasing anthropogenic activities in the country. The high aerosols load in the atmosphere causes adverse human health impacts and reduces visibility due to poor air quality (Davidson et al., 2005). The exposure to particulate matter (especially $PM_{2.5}$ i.e., particles $<2.5\ \mu m$ in diameter) has been recognized as fifth leading risk factor throughout the globe and the third leading risk factor in India with about 1 million premature mortality per year across the nation (Chowdhury and Dey, 2016; GBD 2015 Risk Factors Collaborators, 2016; Conibear et al., 2018; Chen et al., 2020). The $PM_{2.5}$ can penetrate deep into the human body and hence can cause greater risk among all other air pollutants (Xing et al., 2016). In India, industrial and vehicular emissions, dust, emissions from biomass burning, open waste burning, household and power sector are major sources of high $PM_{2.5}$ concentrations (Guo et al., 2017; Conibear et al., 2018; Venkataraman et al., 2018). Domestic cooking and heating, dust from construction activities and industrial emissions are major urban sources of $PM_{2.5}$ (Guttikunda et al., 2019). Rajput et al. (2014) reported the PM2.5 mass concentrations in Patiala region of Punjab during paddy-residue burning in the months of October and November in the range of 60–390 μgm^{-3} with organic carbon (OC≈33%) contributing significantly; while, mass concentration of $PM_{2.5}$ during wheat-residue burning period of April–May varies from 18 to 123 μgm^{-3}.

Besides, emissions in the surrounding rural areas, also contribute to the urban pollution in India (Guttikunda et al., 2019; Ravindra et al., 2019), such as local sources (like traffic, power plants, industries) account for ∼70% of total $PM_{2.5}$, but the non-local sources (agricultural crop burning in the neighboring states) contribute over 30% in Delhi (Guo et al., 2017; Prabhakaran et al., 2020). Moreover, the burning of firecrackers during Diwali festival in Delhi worsens the situation by adding more pollutants (Ganguly et al., 2019). With the ongoing urbanization, $PM_{2.5}$ pollution is expected to further increase in the coming decades (Chowdhury et al., 2018; Conibear et al., 2018).

The important studies conducted over Indian cities regarding aerosols and particulate matter are discussed in this section and average AOD values for some of the Indian cities are given in **Table 1**.

Kaskaoutis et al. (2012) conducted a decadal study (2001–2010) for analysis of variations and trends in aerosol properties over Kanpur, India using AERONET data. The study showed overall increase in column-integrated AOD on a yearly basis with significant increase in AOD during the months of November and December as well as for the months of March and April. The increase has been attributed to continuous increase in anthropogenic emissions during which are primarily due to fossil-fuel and biomass combustion over the IGP. Choudhary et al. (2021) studied the seasonal and spatial variability of Brown Carbon (BrC) and reported that water soluble organic carbon (WSOC) aerosols during winter exhibited ∼1.6 times higher light absorption capacity than in the monsoon season at Kanpur, a central site in Indo-Gangetic Plains.

Further, the aerosols optical properties have been examined during the period 2010–2012 for Greater Noida, Delhi region, using ground-based sun photometer data by Sharma et al. (2014).

In a study conducted for Varanasi, India by Murari V. et al. (2015), the annual mean concentration of particulate matter ($PM_{2.5}$ and PM_{10}) was higher than annual permissible limit (PM_{10}: 80%; $PM_{2.5}$: 84%) in a range of 8–9 times over than the approved standard values. The study states that high PM values pose a risk of developing cardiovascular and respiratory diseases as well as lung cancer. Further, Sahu and Kota (2017) showed 0.69% increase in non-accidental mortality per 10 μgm^{-3} increase of $PM_{2.5}$ over Delhi in a study conducted during 2011–2014. Rajeev et al. (2016) attempted to characterize fine-mode ambient aerosols, and individual rain waters during the South-west monsoon (July–September 2015) in the central Indo-Gangetic Plain (IGP). Not only this, water-soluble ionic species (WSIS) were measured and characteristic mass ratios suggested that below-cloud scavenging was predominant mechanism of aerosols wash-out.

TABLE 1 | PM values for some Indian cities during different years.

Study area	PM values ($\mu g/m^3$)	References
Jorhat, Northeast India	24 h mean concentration $PM_{2.5} = 121 \pm 49$ $PM_{10} = 153 \pm 45$	Islam and Saikia, 2020
Delhi (ITO)	24-h mean concentration $PM_{2.5} = 71.9$	Shaw and Gorai, 2020
Banglore (S. G. Halli)	24-h mean concentration $PM_{10} = 11.90$	
Kolkata	24-h mean concentration $PM_{10} = 97.00$	
Bhubaneswar	Annual mean concentration $PM_{2.5} = 30.6 \pm 22.1$ $PM_{10} = 88.3 \pm 30.6$	Mahapatra et al., 2018
Kanpur	PM_1 average mass concentration During non-foggy conditions = 247 ± 113 During foggy conditions = 107 ± 58	Rajput et al., 2018
Patiala	$PM_{2.5}$ mass concentration= 60-390 (October–November) $PM_{2.5}$ mass concentration = 18–123 (April–May)	Rajput et al., 2016
Patiala	Average concentration $PM_{2.5} = 55.4 \pm 13.5$	Sen et al., 2016
Lucknow	Average concentration $PM_{2.5} = 51.5 \pm 17.7$ $PM_{10} = 182.2 \pm 58.0$	
Kolkata	Average concentration $PM_{2.5} = 47.6 \pm 9.3$ $PM_{10} = 66.7 \pm 17.0$	
New Delhi	Average concentration $PM_{2.5} = 61.8 \pm 18.6$ $PM_{10} = 127.4 \pm 62.2$	
Nagpur	Average concentration $PM_{2.5} = 35.2 \pm 18.4$ $PM_{10} = 53.9 \pm 23.7$	
Varanasi	Average concentration $PM_{2.5} = 52.5 \pm 28.6$ $PM_{10} = 139.6 \pm 68.0$	
Mid-IGP region	Annual mean PM_{10} concentration = 206.2 ± 77.4	Sharma et al., 2016
Varanasi	Annual mean concentration $PM_{2.5} = 100.0 \pm 29.6$ $PM_{10} = 176.1 \pm 85.0$ Monthly average concentration PM_{10} = 43.6–318.5 μg/m3 $PM_{2.5}$ = 50.1–154.0 μg/m3	Murari V. et al., 2015
Delhi	Mean mass concentrations $PM_{2.5} =118.3 \pm 81.7$ $PM_{10} =232.1 \pm 131.1$	Tiwari et al., 2015
Vishakhapatnam	Annual average concentration $PM_{10} = 70.4 \pm 29.7$	Guttikunda et al., 2015
Chennai	Annual average concentration $PM_{10} = 121.5 \pm 45.5$	
Delhi	$PM_{2.5} = 130.0 \pm 103.0$ $PM_{10} = 222.0 \pm 142.0$	Tiwari et al., 2014
Pune	Average mass concentration $PM_{2.5=} 72.3 \pm 31.3$ $PM_{10} =113.8 \pm 51.6$	Yadav and Satsangi, 2013
Barapani, foot–hills of NE–Himalaya	Wintertime concentration of $PM_{2.5}$ = 39–348	Rajput et al., 2013
Raipur	Annual average concentrations (July 2009 to June 2010) PM2.5 = 150.9 ± 78.6 PM10 = 270.5 ± 105.5 PM1 = 72.5 ± 39.0	Deshmukh et al., 2013

(Continued)

TABLE 1 | Continued

Study area	PM values (μg/m^3)	References
Mumbai	Average concentration PM $_{2.5}$ = 42	Kothai et al., 2011
Agra	PM 2.5 = 104.9 PM10 = 154.2	Kulshrestha et al., 2009
Kolkata	PM_{10} = 140	Karar and Gupta, 2006

Adding to PM studies, Singh V. et al. (2021) analyzed particulate matter ($PM_{2.5}$) in five Indian megacities (Chennai, Kolkata, New Delhi, Hyderabad and Mumbai) for 6 years period (2014–2019). Among all cities, Delhi is found to be the most polluted city followed by Kolkata, Mumbai, Hyderabad, and Chennai. Chakraborty et al. (2017) reported high levels of water-soluble organic aerosols (WSOA) and total organic aerosols (OA) using Aerosol Mass Spectrometer in two cities of Indo-Gangetic Plains.

In addition, Chen et al. (2020) discussed the long-term and short-term effects of $PM_{2.5}$ over four Indian megacities (Delhi, Chennai, Hyderabad and Mumbai) during 2015–2018. The results depict annual averaged $PM_{2.5}$ concentration of 110 μg/m^3 (Delhi), 60 μg/m^3 (Mumbai), 56 μg/m^3 (Hyderabad), and 33 μg/m^3 (Chennai) during study period with worst air quality for Delhi. The study showed 75% increase in $PM_{2.5}$ concentration during Diwali due to burning of firecrackers that causes 20 extra daily mortality. The long-term exposure to $PM_{2.5}$ causes 17,200–39,400 premature mortality and 428,900–935,200 years of life lost each year in these four Indian cities. About 10,200, 2,800, 5,200, and 9,500 premature deaths occur each year in Delhi, Chennai, Hyderabad, and Mumbai, respectively, on long-term ambient $PM_{2.5}$ exposures. Among the major diseases, **c**ardiovascular diseases were dominant with ischaemic heart disease (IHD) contributing about 40% and cerebrovascular disease contributing about 30% in each city.

Dutta and Jinsart, 2020 analyzed the PM concentration over Guwahati city during three-year period (2016–2018) and observed high PM levels (>100 μg m $^{-3}$) during winter season causing high air pollution. The study showed acute health risk to city residents during winter as analyzed from computed hazard quotients (>1). Sorathia et al. (2018) reported diurnal variability of Dicarboxylic Acids (DCAs) and levoglucosan in PM10 during winter over IGP indicating biomass burning emission and secondary transformations to be predominant sources of DCA during wintertime.

Meanwhile, Delhi has been recognized as one of the most heavily polluted cities of India suffering from air pollution caused by industrial and vehicular emissions, thereby possessing high levels of anthropogenic aerosols (Mishra et al., 2013; Singh B. P. et al., 2014). The dust aerosols during pre-monsoon period further worsens the air quality, reduces visibility and increases radiative forcing (Singh et al., 2005, 2010). According to urban air database by WHO in September 2011, high PM 10 (above permissible limits) was observed in Delhi. The high particulate matter concentration causes several respiratory issues that may lead to chronic diseases in Indian cities (Jayaraman, 2007). Tiwari et al. (2009) also reported that $PM_{2.5}$ concentration (97 $\pm$ 56 μg m^{-3}) was nine times higher than the air quality guidelines given by World Health Organization (WHO) (2005) over Delhi in 2007.

Besides, particulate matter concentration for Indian megacities during 2010 and 2016 has been discussed in **Figure 2** depicting % increase in almost all the Indian megacities during 6 year period in cities such as Varanasi (Singh et al., 2017; Kumar A. et al., 2020). The increasing PM concentration is correlated with the rising urban population (Kumar P. et al., 2020).

Meanwhile, toxicological studies have established that the toxic effects of particulate matter arise from combined effects of PM size and chemical composition. The modifications in PM composition due to several factors also impart changes in health effects (Peng et al., 2005). These results suggesting that besides mass concentration, chemical composition of PM is also important in evaluation of toxicity on exposure to PM, were supported by Oeder et al. (2012), Kelly and Fussell (2012), and Mirowsky et al. (2013). Further, the source apportionment of aerosols during wintertime has been looked into by various researchers. Rajput et al. (2018) studied secondary formation processes, fog-processing and source-apportionment of PM_1-bound species in IGP and reported that the foggy conditions were associated with higher contribution of PM_1-bound organic matter alongwith approximately equal decrease in SO_4^{2-}, NO_3^-, and NH_4^+ and mineral dust fractions.

COVID-19 and Air Quality

Besides the deteriorating air pollution conditions, the improvement in air quality has been reported globally during lockdown imposed due to COVID-19. The restrictions lead to reduction in anthropogenic emissions and hence decrease in PM and gaseous concentrations in most of the cities throughout the globe (Adams, 2020; Berman and Ebisu, 2020; Menut et al., 2020). The similar trend was observed in Indian cities such as for Delhi, Kolkata (Bera et al., 2020; Mahato et al., 2020; Sharma et al., 2020; Singh and Chauhan, 2020; Srivastava et al., 2020; Maji et al., 2021). According to the data provided by NASA, there has been 30% reduction in global NO_2 emissions with 70% decrease in NO_2 emissions in India (Gautam, 2020).

A lockdown period study was conducted by Vadrevu et al. (2020) for analysis of spatio-temporal variations of air pollution (Singh B. P. et al., 2014) (using NO_2 and AOD) for 41 Indian cities. The study revealed about 13% reduction in NO_2 levels during the lockdown as compared to pre-lockdown period. The

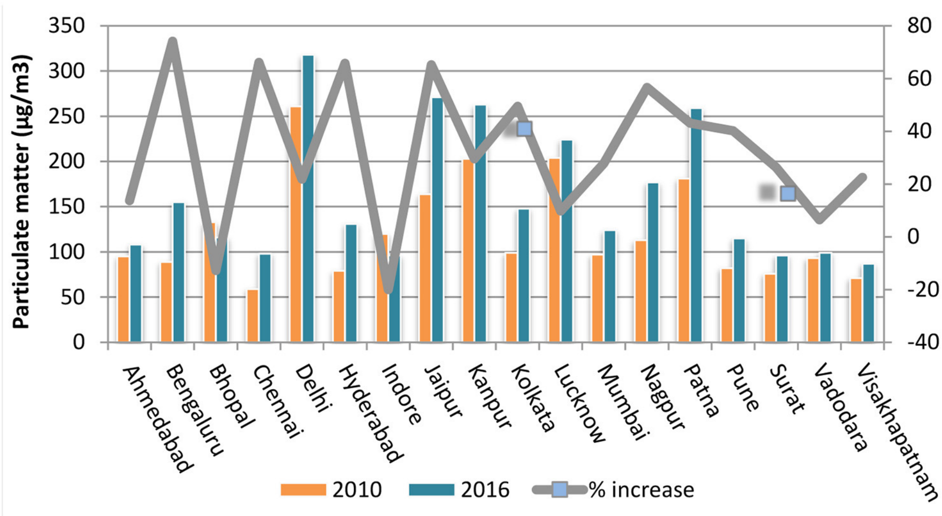

FIGURE 2 | The % increase in particulate matter concentrations for Indian megacities.

NO_2 levels were reduced by 19% as compared to same duration of previous year. Further, Siddiqui et al. (2020) found 27% improvement in air quality index over 8 five million plus cities of India with an average decrease of 46% in NO_2 levels. The closures of industrial and construction activities during lockdown were reason for improved air quality.

Adding to the research in this field, Srivastava et al. (2020) conducted air pollution study over Lucknow and New Delhi during 21-day lockdown in India by analyzing available data for primary air pollutants ($PM_{2.5}$, NO_2, SO_2, and CO). Significant decrease in air pollutants with an improvement in air quality was observed for both the Indian cities. Further, Bera et al. (2020) in a study conducted for Kolkata city stated the reduction in air pollutants such as CO, NO_2, and SO_2 along with particulate matter for the study area as shown in **Table 2**. The decrease in fossil fuel combustion, vehicular and industrial emissions contributed to significant reduction in air pollutants (CO, NO_2, and SO_2) levels during Covid-19 lockdown. The study further stated the decrease in biomass burning, construction activities and vehicular movement contributed to about 17.5% decrease in PM concentration during Covid-19 lockdown. The improvements in air quality with 30–40% reduction in CO_2 levels with significant temporal variation were observed for Kolkata also by Mitra et al. (2020).

Moreover, the improvement in air quality ($PM_{2.5}$, NO_2, and AQI) during Covid-19 lockdown was reported by Karuppasamy et al. (2020) revealing improved mortality rates with less number of deaths in India and worldwide due to air pollution. Further, Kant et al. (2020) analyzed decrease in AOD levels during the COVID-19 lockdown period for Eastern Indo-Gangetic planes, peninsular India and North India. On comparison of $PM_{2.5}$ levels over five Indian cities, Kumar A. et al. (2020) observed 50% reduction in $PM_{2.5}$ concentrations over five Indian cities during this period. Goel et al. (2020) in a study conducted for Ludhiana city of India revealed decline in $PM_{2.5}$, PM_{10}, NH_3, SO_2 concentrations with an overall improvement in air quality index.

TABLE 2 | Percent reduction in air pollutants for Indian cities during COVID-19 lockdown.

Parameter	Location	% reduction	References
NO_2	New Delhi	61.74%	Vadrevu et al., 2020
	Delhi	60.37%	
	Bangalore	48.25%	
$PM_{2.5}$, PM_{10}	Ahmedabad	46.20%	Bera et al., 2020
	Nagpur	46.13%	
	Gandhinagar	45.64%	
	Mumbai	43.08%	
	Kolkata	17.5%	
AOD	Eastern Indo-Gangetic planes, peninsular India and North India	20–37%	Kant et al., 2020
$PM_{2.5}$	Ghaziabad	85.1%	Lokhandwala and Gautam, 2020
$PM_{2.5}$	Delhi	35%	Chauhan and Singh, 2020
	Mumbai	14%	

Meanwhile, Delhi, the most polluted megacities of India was focused in many of the lockdown period studies. Gupta et al. (2020) reported decrease in CO, SO_2, and ozone levels over Delhi that was supported by significant improvement in air quality over Delhi reported by Kotnala et al. (2020). Significant decrease in PM concentrations was observed for Delhi even in the initial days of lockdown (Maji et al., 2021). Goel V. et al. (2021) analyzed 78% decrease in black carbon during the lockdown and unlock phases for Delhi as compared to the pre-lockdown period. Mahato et al. (2020) also discussed the reduction in the concentration of seven pollutants (PM_{10}, $PM_{2.5}$, SO_2, NO_2, CO, O_3, and NH_3 gases) over Delhi during lockdown period. The study revealed more than 50% reduction in PM_{10} and $PM_{2.5}$ concentrations. About 40–50% improvement in air quality was observed using the data collected from 34 monitoring stations. The reduction in levels of various air pollutants for more Indian cities during COVID-19 lockdown period have been presented in **Table 2**.

Such reduction in air pollutant concentration during COVID-19 lockdown is associated with several health benefits. The study conducted by Goel A. et al. (2021) in this concern over Indian cities stated highest health benefits during phase 1 of the lockdown (initial 21 days) due to least $PM_{2.5}$ concentrations during this period. The average pollutant reduction of 44.6% was observed in Uttar Pradesh and about 58.5% decline in Delhi-NCR as compared with year 2019. The tracheobronchial particle deposition was reduced by 30.14% during lockdown. The mortality reduction of 29.85 per 100,000 persons was observed due to declined PM concentrations during 1st phase of lockdown. Also, the decrease in mortality of 8.01 per 100,000 people was analyzed during phase 1 in comparison with the pre-lockdown period in Ghaziabad.

NEXUS BETWEEN URBANIZATION, CLIMATE CHANGE, AIR POLLUTION AND HUMAN HEALTH

The interactions between urban climate, air pollution, and human health in cities need to be explored. The cities in developing nations like India are facing high pressure due to air pollution and climate change. Limited studies have been performed on the combined effects of weather, climate variability, increased air pollution, and health impacts in India (Agarwal et al., 2006; Karar et al., 2006).

Climate plays a considerable role in spatial and temporal distribution of air pollutants. Greenhouse warming and ozone depletion in stratosphere are vital factors of climate change. Climate change can influence the air pollutant concentration and catalyze the formation of secondary pollutants. Also, the climatic conditions in addition to atmospheric parameters, topography and urban settlements influence the dispersion, accumulation and transformation of pollutants in the atmosphere. The dispersal of these air pollutants may cause respiratory disorders such as emphysema, asthma, allergy problems and chronic bronchitis (D'Amato et al., 2002).

According to the World Health Organisation (WHO) estimation, in past 30 years, the precipitation and warming trends due to anthropogenic climate change had taken 150,000 lives annually. The alterations in climate had caused many prevalent human diseases such as cardiovascular mortality and respiratory illnesses due to heat waves etc.

Besides, the nexus between urbanization, climate change and air pollution lies in a way such that some of the atmospheric pollutants (aerosols) can enhance the climate change because of their direct and in-direct effects (Ramachandran and Cherian, 2008). These air pollutants not only degrade the air quality with certain human health impacts but also have a considerable impact on climate by heating lower and mid troposphere, causing sea-land temperature gradients, monsoon circulation, distribution of rainfall solar dimming and cloud microphysics (Lau et al., 2006; Gautam et al., 2010; Sharma et al., 2014) thereby modifying the heat wave frequency, intensity of storms and precipitation patterns. These small sized particles can weaken the UHI effect by up to 1 K under heavily polluted conditions (Wu et al., 2017). So, the increased concentrations of air pollutants (such as aerosols) have an impact on global climate change as the increased air pollution (aerosol load) in the atmosphere is associated with the climate system and hydrological cycle (Ramanathan et al., 2001; Jirak and Cotton, 2006). In addition to this, the indirect effect of aerosols can also be seen on optical properties of clouds. Aerosols can affect the surface energy balance by either scattering or absorbing the incoming solar radiations that may cause surface cooling and atmospheric heating (Kaufman et al., 2002; Wu et al., 2017). This influences the radiation equilibrium of Earth via radiative forcing and chemical perturbations (Rosenfeld et al., 2007; Wang et al., 2009; Zhu et al., 2010; Zhang S. et al., 2016; Zhang W. et al., 2016).

Besides, the atmospheric structure and climate is influenced by concentration of atmospheric pollutants that are emitted by human activities (Fischer et al., 2003; Jaffe and Ray, 2007; Yan et al., 2008).

Commercial and high traffic regions have higher concentration of gaseous pollutants than vegetated areas. Also, the concentration of pollutants varies with the seasons and other atmospheric parameters (Dandotiya et al., 2020). The estimation of pollutant concentration is influenced by atmospheric conditions of that urban area such as temperature, relative humidity and wind speed etc.

The greenhouse gases (GHGs) emissions are estimated mainly by consumption patterns in cities of the developed world that causes climate change. According to IPCC report, ∼20% of global emissions were attributed by buildings. Further, transportation was estimated to contribute to 13% of GHG emissions (Diarmid Campbell-Lendrum and Corvala). It can be seen that both buildings and transportation are eminent factors of cities. Also, the cities face higher pollution issues than rural areas with higher vegetation due to higher emissions from transportation and fossil fuel burning in highly populated regions with high vehicular traffic (Dandotiya et al., 2019).

Further, it is notable that the urbanization phenomenon plays important role in both climate change and air pollution either directly or indirectly. The increase in air pollutant emissions and their concentration in the atmosphere increases with the urbanization. The urban characteristics, materials used, vegetation, vehicular traffic etc alters the climatic conditions of an urban area thus leading to formation of strong spatial gradients of heat and air pollution. These conditions exacerbate the risks for human health.

The expanding urban areas with inadequate or improper management accompanied by land use land cover changes, deforestation and decrease in vegetation cover and alterations in climate variables can influence or modify urban climate by transformation of natural land surface to impervious surfaces (Balica et al., 2012; Jha et al., 2012). The urban heat island effect by increased urban temperature due to climate change increases the demand of energy requirement for cooling in cities. The air conditioners used for reducing the high temperature in cities in turn emits harmful GHGs that cause urban air pollution. Also, the concentration of certain pollutants, such as ozone, is influenced by atmospheric conditions and tends to be higher on warmer days. Moreover, the higher demand of electricity consumption leads to higher burning of fossil fuels that also increases air pollution. Certain respiratory issues can be caused by UHI effect due to depleted air quality by certain cooling agents (Liu and Zhang, 2011). The city residents also suffer from thermal discomfort due to elevated urban temperature by UHI effect resulting in exacerbation of heat-waves (Ohashi et al., 2007). The UHI effect influences air quality as the differential heating generates mesoscale winds that facilitate pollutant movement and circulation causing urban air pollution issues (Agarwal and Tandon, 2010). So, air pollution and climate change are interlinked with adverse impacts on human health in cities.

CONCLUSION

The present review highlights high air pollution levels over most of the Indian megacities with air pollutant levels lying above the permissible limits. The continuous emissions from both anthropogenic as well as natural sources causing high PM concentration with adverse human health impacts highlight the necessity of continuous monitoring of air pollutants over the Indian subcontinent using measurements and remote sensing satellite data.

The essential information regarding air pollutant levels in different megacities of India, provided in this review can help in design of effective mitigation strategies for each city by analyzing vulnerable regions. The data can facilitate a baseline data for air quality modeling studies to predict air pollution levels for effective preparedness, adaption and mitigations plans in tackling air pollution. The high disease burden and mortality linked with air pollution in Indian cities should be emphasized to effectively control air pollutant concentration throughout the nation. Besides, the results depicting reduction in air pollution during COVID-19 lockdown period suggest adoption of such short-time restrictions for pollution mitigation across different cities of India to improve the air quality and thus benefit human health.

Further, as stated in the review, India being a developing country is experiencing adverse human health impacts due to climate change. Indian cities are exposed to extreme weather events such as high precipitation, floods, droughts, heat waves with increased temperatures induced by climate change. The increase in health surveillance for heat waves, floods and for vector-borne diseases linked with climate change can help in combating severe human health impacts in near future in Indian cities. Also, the high population density with ongoing urbanization and industrialization are some of the primary factors to be considered to avoid negative health impacts associated with climate change in India. So, essential mitigation and adaptation strategies are required for current and projected climate change impacts mentioned in the review to avoid myriad human health effects in Indian cities because of climate change.

To conclude, the use of advanced technologies such as satellite data with geospatial techniques can be of great help in monitoring and mapping of spatial-temporal distribution patterns of the air pollution and climate change and associated health impacts. So, while focusing on building smart cities in developing nations like India, proper urban planning and sustainable measures should be taken for sustainable urban environment to avoid adverse health impacts.

AUTHOR CONTRIBUTIONS

RK was involved in review of the chapter and preparation of the manuscript. PP was involved in overall supervision of the manuscript and manuscript review and editing. Both authors contributed to the article and approved the submitted version.

REFERENCES

Adams, M. D. (2020). Air pollution in Ontario, Canada during the COVID-19 state of emergency. *Sci. Total Environ.* 742:140516. doi: 10.1016/j.scitotenv.2020.140516

Agarwal, A. K., Singh, A. P., Gupta, T., Agarwal, R. A., Sharma, N., Rajput, P., et al. (2018). Mutagenicity and cytotoxicity of particulate matter emitted from biodiesel-fueled engines. *Environ. Sci. Technol*. 52, 14496–14507. doi: 10.1021/acs.est.8b03345

Agarwal, M., and Tandon, A. (2010). Modeling of the urban heat island in the form of mesoscale wind and of its effect on air pollution dispersal. *Appl. Mathematic. Modell.* 34, 2520–2530. doi: 10.1016/j.apm.2009.11.016

Agarwal, R., Jayaraman, G., Anand, S., and Marimuthu, P. (2006). Assessing respiratory morbidity through pollution status and meteorological conditions for Delhi. *Environ. Monit. Assess.* 114, 489–504. doi: 10.1007/s10661-006-4935-3

Ahern, M., Kovats, R. S., Wilkinson, P., Few, R., and Matthies, F. (2005). Global health impacts of floods: epidemiologic evidence. *Epidemiol. Rev.* 27, 36–46. doi: 10.1093/epirev/mxi004

Ahmad, M., Tariq, S., Alam, K., Anwar, S., and Ikram, M. (2020). Long-term variation in aerosol optical properties and their climatic implications over major cities of Pakistan. *J. Atmos. Solar-Terrestrial Phys.* 210:105419. doi: 10.1016/j.jastp.2020.105419

Akhtar, R. (2007). Climate change and health and heat wave mortality in India. *Glob. Environ. Res.* 11, 51–57.

Ali, H., Mishra, V., and Pai, D. S. (2014). Observed and projected urban extreme rainfall events in India. *J. Geophysical Res.* 119, 12–621. doi: 10.1002/2014JD022264

Amakiri, A. O., Monsi, A., Teme, S. C., Ede, P. N., Owen, O. J., and Ngodigha, E. M. (2009). Air quality and micro-meterological monitoring of gaseous pollutants/flame emissions from burning crude petroleum in poultry house. *Toxicol. Environ. Chem.* 91, 225–232. doi: 10.1080/02772240802131551

Ambinakudige, S. (2011). Remote sensing of land cover's effect on surface temperatures: a case study of the urban heat island in Bangalore, India. *Appl. GIS* 7, 1–12.

ARAI (2010). *Air Quality Monitoring and Emission Source Apportionment Study for City of Pune*. Pune: The Automotive Research Association of India, [ARAI/IOCLAQM/R-12/2009-10]. Retrieved from: https://www.mpcb.gov.in/sites/default/files/focus-area-reports-documents/pune_report_cpcb.pdf (accessed April 15, 2021).

Awais, M., Shahzad, M. I., Nazeer, M., Mahmood, I., Mehmood, S., Iqbal, M. F., et al. (2018). Assessment of aerosol optical properties using remote sensing over highly urbanised twin cities of Pakistan. *J. Atmos. Solar-Terrestrial Phys.* 173, 37–49. doi: 10.1016/j.jastp.2018.04.008

Badarinath, K. V. S., Kharol, S. K., Kaskaoutis, D. G., Sharma, A. R., Ramaswamy, V., and Kambezidis, H. D. (2010). Long-range transport of dust aerosols over the Arabian Sea and Indian region—A case study using satellite data and ground-based measurements. *Glob. Planetary Change* 2, 164–181. doi: 10.1016/j.gloplacha.2010.02.003

Balakrishnan, K., Dey, S., Gupta, T., Dhaliwal, R. S., Brauer, M., Cohen, A. J., et al. (2019). The impact of air pollution on deaths, disease burden, and life expectancy across the states of India: the Global Burden of Disease Study 2017. *Lancet Planetary Health* 3, e26–e39. doi: 10.1016/S2542-5196(18)30261-4

Balica, S. F., Wright, N. G., and Van der Meulen, F. (2012). A flood vulnerability index for coastal cities and its use in assessing climate change impacts. *Nat. Hazards* 64, 73–105. doi: 10.1007/s11069-012-0234-1

Beckerman, B. S., Jerrett, M., Finkelstein, M., Kanaroglou, P., Brook, J. R., Arain, M. A., et al. (2012). The association between chronic exposure to traffic-related air pollution and ischemic heart disease. *J. Toxicol. Environ. Health A* 75, 402–411. doi: 10.1080/15287394.2012.670899

Bell, J. E., Brown, C. L., Conlon, K., Herring, S., Kunkel, K. E., Lawrimore, J., et al. (2018). Changes in extreme events and the potential impacts on human health. *J. Air Waste Manage. Assoc.* 68, 265–287. doi: 10.1080/10962247.2017.1401017

Bera, B., Bhattacharjee, S., Shit, P. K., Sengupta, N., and Saha, S. (2020). Significant impacts of COVID-19 lockdown on urban air pollution in Kolkata (India) and amelioration of environmental health. *Environ. Dev. Sustain*. 23, 1–28. doi: 10.1007/s10668-020-00898-5

Berman, J. D., and Ebisu, K. (2020). Changes in US air pollution during the COVID-19 pandemic. *Sci. Total Environ.* 739:139864. doi: 10.1016/j.scitotenv.2020.139864

Bhattacharya, S., Sharma, C., Dhiman, R. C., and Mitra, A. P. (2006). Climate change and malaria in India. *Curr. Sci.* 90:369–375.

Burnett, R. T., Dales, R. E., Brook, J. R., Raizenne, M. E., and Krewski, D. (1997). Association between ambient carbon monoxide levels and hospitalizations for congestive heart failure in the elderly in 10 Canadian cities. *Epidemiology* 8, 162–167. doi: 10.1097/00001648-199703000-00007

Burri, P. H. (1984). Lung development and histogenesis. *Handbook Physiol.* 4, 1–46. doi: 10.1146/annurev.ph.46.030184.003153

Bush, K. F., Luber, G., Kotha, S. R., Dhaliwal, R. S., Kapil, V., Pascual, M., et al. (2011). Impacts of climate change on public health in India: future research directions. *Environ. Health Perspect.* 119, 765–770. doi: 10.1289/ehp.1003000

Carosino, C. M., Bein, K. J., Plummer, L. E., Castañeda, A. R., Zhao, Y., Wexler, A. S., et al. (2015). Allergic airway inflammation is differentially exacerbated by daytime and nighttime ultrafine and submicron fine ambient particles: heme oxygenase-1 as an indicator of PM-mediated allergic inflammation. *J. Toxicol. Environ. Health A* 78, 254–266. doi: 10.1080/15287394.2014.959627

Centers for Disease Control and Prevention (2006). Heat-related deaths–United States, 1999-2003. *MMWR: Morbidity Mortal. Weekly Rep.* 55, 796–798.

Central Pollution Control Board (CPCB) (2010). *Air Quality Assessment, Emissions Inventory and Source Apportionment Studies*. Mumbai. Central Pollution Control Board. Retrieved from: https://www.mpcb.gov.in/sites/default/files/focus-area-reports-documents/Mumbai_report_cpcb.pdf (accessed April 15, 2021).

Chakraborty, A., Rajeev, P., Rajput, P., and Gupta, T. (2017). Water soluble organic aerosols in Indo-Gangetic Plain (IGP): insights from aerosol mass spectrometry. *Sci. Total Environ.* 599–600, 1573–1582. doi: 10.1016/j.scitotenv.2017.05.142

Changnon, S. A., Kunkel, K. E., and Reinke, B. C. (1996). Impacts and responses to the 1995 heat wave: a call to action. *Bull. Am. Meteorol. Soc.* 77, 1497–1506. doi: 10.1175/1520-0477(1996)077<1497:IARTTH>2.0.CO;2

Chattopadhyay, S., Gupta, S., and Saha, R. N. (2010). Spatial and temporal variation of urban air quality: a GIS approach. *J. Environ. Prot.* 1, 264–277. doi: 10.4236/jep.2010.13032

Chaudhury, S. K., Gore, J. M., and Ray, K. S. (2000). Impact of heat waves over India. *Curr. Sci.* 79, 153–155.

Chauhan, A., and Singh, R. P. (2020). Decline in PM2. 5 concentrations over major cities around the world associated with COVID-19. *Environ. Res.* 187:109634. doi: 10.1016/j.envres.2020.109634

Chen, Y., Wild, O., Conibear, L., Ran, L., He, J., Wang, L., et al. (2020). Local characteristics of and exposure to fine particulate matter (PM2. 5) in four Indian megacities. *Atmosp. Environ.* X 5:100052. doi: 10.1016/j.aeaoa.2019.100052

Cheng, Y., Li, X., Li, Z., Jiang, S., and Jiang, X. (2014) "Fine-grained air quality monitoring based on gaussian process regression," in *Neural Information Processing. ICONIP 2014. Lecture Notes in Computer Science, Vol. 8835*, eds C. K. Loo, K. S. Yap, K. W. Wong, A. Teoh, and K. Huang (Cham: Springer). doi: 10.1007/978-3-319-12640-1_16

Chestnut, L. G., Breffle, W. S., Smith, J. B., and Kalkstein, L. S. (1998). Analysis of differences in hot-weather-related mortality across 44 US metropolitan areas. *Environ. Sci. Policy* 1, 59–70. doi: 10.1016/S1462-9011(98)00015-X

Choudhary, V., Rajput, P., and Gupta, T. (2021). Absorption properties and forcing efficiency of light-absorbing water-soluble organic aerosols: Seasonal and spatial variability. *Environ. Pollut.* 272:115932. doi: 10.1016/j.envpol.2020.115932

Chowdhury, S., and Dey, S. (2016). Cause-specific premature death from ambient PM2. 5 exposure in India: estimate adjusted for baseline mortality. *Environ. Int.* 91, 283–290. doi: 10.1016/j.envint.2016.03.004

Chowdhury, S., Dey, S., and Smith, K. R. (2018). Ambient PM2.5 exposure and expected premature mortality to 2100 in India under climate change scenarios. *Nat. Commun.* 9:318. doi: 10.1038/s41467-017-02755-y

Chu, D. A., Kaufman, Y. J., Zibordi, G., Chern, J. D., Mao, J., Li, C., et al. (2003). Global monitoring of air pollution over land from the Earth Observing System-Terra Moderate Resolution Imaging Spectroradiometer (MODIS). *J. Geophys. Res.* 108. doi: 10.1029/2002JD003179

Ciccone, G., Faggiano, F., and Falasca, P. (1995). SO2 air pollution and hospital admissions in Ravenna: a case-control study. *Epidemiol. Prevenzione* 19, 99–104.

Conibear, L., Butt, E. W., Knote, C., Arnold, S. R., and Spracklen, D. V. (2018). Residential energy use emissions dominate health impacts from exposure to ambient particulate matter in India. *Nat. Commun.* 9:617. doi: 10.1038/s41467-018-02986-7

D'Amato, G., Liccardi, G., D'amato, M., and Cazzola, M. (2002). Outdoor air pollution, climatic changes and allergic bronchial asthma. *Europ. Respir. J.* 20, 763–776. doi: 10.1183/09031936.02.00401402

D'Amato, G., Rottem, M., Dahl, R., Blaiss, M. S., Ridolo, E., Cecchi, L., et al. (2011). Climate change, migration, and allergic respiratory diseases: an update for the allergist. *World Allergy Organ. J.* 4, 121–125. doi: 10.1097/WOX.0b013e3182260a57

Dandotiya, B., Sharma, H. K., and Jadon, N. (2019). Role of urban vegetation in particulate pollution control in urban areas of Gwalior City with special reference to SPM. *Adv. Biores.* 10, 97–103. doi: 10.15515/abr.0976-4585.10.1.97103

Dandotiya, B., Sharma, H. K., and Jadon, N. (2020). Ambient air quality and meteorological monitoring of gaseous pollutants in urban areas of Gwalior City India. *Environ. Claims J.* 32, 248–263. doi: 10.1080/10406026.2020.1744854

Davidson, C. I., Phalen, R. F., and Solomon, P. A. (2005). Airborne particulate matter and human health: a review. *Aerosol Sci. Technol.* 39, 737–749. doi: 10.1080/02786820500191348

De, U. S. (2000). Weather and climate related impacts on health in megacities. *WMO Bull.* 49, 340–348.

Debone, D., Leirião, L. F. L., and Miraglia, S. G. E. K. (2020). Air quality and health impact assessment of a truckers' strike in Sáo Paulo state, Brazil: a case study. *Urban Climate* 34:100687. doi: 10.1016/j.uclim.2020.100687

Dejmek, J., Jelinek, R., Solansky, I., Benes, I., and Sram, R. (2000). Fecundability and parental exposure to ambient sulphur dioxide. *Environ. Health Perspect.* 108, 647–654 doi: 10.1289/ehp.00108647

Deshmukh, D. K., Deb, M. K., and Mkoma, S. L. (2013). Size distribution and seasonal variation of size-segregated particulate matter in the ambient air of Raipur city, India. *Air Qual. Atmosp. Health* 6, 259–276. doi: 10.1007/s11869-011-0169-9

Devi, N. P., and Jauhari, R. K. (2006). Climatic variables and malaria incidence in Dehradun, Uttaranchal, India. *J. Vector Borne Dis.* 43:21–28.

Dhiman, R. C., Pahwa, S., and Dash, A. P. (2008). Climate change and Malaria in India: interplay between temperature and mosquitoes. *Regional Health Forum* 12:27–31.

Dholakia, H. H., Mishra, V., and Garg, A. (2015). *Predicted Increases in Heat Related Mortality Under Climate Change in Urban India*.

Du, W., FitzGerald, G. J., Clark, M., and Hou, X. Y. (2010). Health impacts of floods. *Prehosp. Disaster Med.* 25, 265–272. doi: 10.1017/S1049023X00008141

Dutta, A., and Jinsart, W. (2020). Risks to health from ambient particulate matter (PM2. 5) to the residents of Guwahati city, India: an analysis of prediction model. *Human Ecol. Risk Assess. Int. J.* 27, 1094–1111. doi: 10.1080/10807039.2020.1807902

Dutta, P., and Chorsiya, V. (2013). Scenario of climate change and human health in India. *Int. J. Innovat. Res. Dev.* 2, 157–160.

Dutta, S., Ghosh, S., and Dinda, S. (2021). Urban Air-quality assessment and inferring the association between different factors: a comparative study among Delhi, Kolkata and Chennai Megacity of India. *Aerosol Sci. Eng.* 5, 93–111. doi: 10.1007/s41810-020-00087-x

Ebi, K. L., and Paulson, J. A. (2010). Climate change and child health in the United States. *Curr. Prob. Pediatric Adoles. Health Care* 40, 2–18. doi: 10.1016/j.cppeds.2009.12.001

El-Askary, H., Gautam, R., Singh, R. P., and Kafatos, M. (2006). Dust storms detection over the Indo-Gangetic basin using multi sensor data. *Adv. Space Res.* 37, 728–733. doi: 10.1016/j.asr.2005.03.134

Faheem, M., Danish, M., and Ansari, N. (2021). *Impact of Air Pollution on Human Health in Agra District.*

Filippelli, G. M., Freeman, J. L., Gibson, J., Jay, S., Moreno-Madriñán, M. J., Ogashawara, I., et al. (2020). Climate change impacts on human health at an actionable scale: a state-level assessment of Indiana, USA. *Climatic Change* 163, 1985–2004. doi: 10.1007/s10584-020-02710-9

Fischer, H., Kormann, R., Klupfel, T., Gurk, C., K € onigstedt, R., Parchatka, U., et al. (2003). Ozone production and trace gas correlations during the June (2000). *MINATROC intensive measurement campaign at Mt. Cimone. Atmosph. Chem. Phys.* 3, 725–738. doi: 10.5194/acp-3-725-2003

Forster, P. M. de. F., and Collins, M. (2004). Quantifying the water vapour feedback associated with post-Pinatubo global cooling. *Climate Dynam.* 23, 207–214. doi: 10.1007/s00382-004-0431-z

Gabastou, J., Pesantes, C., Escalente, S., Narvez, Y., Vela, E., Garcia, L., et al. (2002). Caracteristicas de la epidemia de colera de 1998 en Ecuador durante el fenomeno de El Niño" (Characteristics of the cholera epidemic of 1998 in Ecuador during El Niño). *Revista Panamerica de Salud Publica* 12, 157–164. doi: 10.1590/S1020-49892002000900003

Ganguly, N. D., Tzanis, C. G., Philippopoulos, K., and Deligiorgi, D. (2019). Analysis of a severe air pollution episode in India during Diwali festival-a nationwide approach. *Atmósfera* 32, 225–236. doi: 10.20937/ATM.2019.32.03.05

Gautam, R., Hsu, N. C., and Lau, K. M. (2010). Premonsoon aerosol characterization and radiative effects over the Indo-Gangetic Plains: implications for regional climate warming. *J. Geophys. Res.* 115. doi: 10.1029/2010JD013819

Gautam, S. (2020). COVID-19: air pollution remains low as people stay at home. *Air Qual. Atmos. Health* 13, 853–857. doi: 10.1007/s11869-020-00842-6

Gautam, S., Talatiya, A., Patel, M., Chabhadiya, K., and Pathak, P. (2020). Personal exposure to air pollutants from winter season bonfires in rural areas of Gujarat, India. *Exposure Health* 12, 89–97. doi: 10.1007/s12403-018-0287-9

GBD 2015 Risk Factors Collaborators (2016). Global, regional, and national comparative risk assessment of 79 behavioural, environmental and occupational, and metabolic risks or clusters of risks, 1990–2015: a systematic analysis for the Global Burden of Disease Study 2015. *Lancet* 388:1659. doi: 10.1016/S0140-6736(16)31679-8

Ghose, K. M., Paul, R., and Banerjee, S. K. (2004). Assessment of the impacts of vehicular emissions on urban air quality and its management in Indian context: the case of Kolkata (Calcutta). *Environ. Sci. Policy* 7, 345–351. doi: 10.1016/j.envsci.2004.05.004

Ghose, M. K. (2002). Controlling of motor vehicle emissions for a sustainable city. *TERI Informat. Digest Energy Environ.* 1, 273–288.

Ghose, M. K., Paul, R., and Banerjee, R. K. (2005). Assessment of the status of urban air pollution and its impact on human health in the city of Kolkata. *Environ. Monitor. Assess.* 108, 151–167. doi: 10.1007/s10661-005-3965-6

Global Initiative for Asthma (GINA) (2015). *GINA Report. The Global Strategy for Asthma Management and Prevention*. Global Initiative forAsthma (GINA). Available online at: https://www.slideshare.net/cristobalbunuel/-report-2015 (accessed April 20, 2021).

Goel, A., Saxena, P., Sonwani, S., Rathi, S., Srivastava, A., Bharti, A. K., et al. (2021). Health benefits due to reduction in respirable particulates during COVID-19 Lockdown in India. *Aerosol Air Qual. Res.* 21:129435. doi: 10.4209/aaqr.200460

Goel, P., Kaur, H., Kumar, R., Bilga, P. S., and Aggarwal, N. (2020). "Analysis of air quality index during lockdown: a case of Ludhiana District-Punjab," in *Sustainable Development Through Engineering Innovations: Select Proceedings of SDEI*, 671–681. doi: 10.1007/978-981-15-9554-7_60

Goel, V., Hazarika, N., Kumar, M., Singh, V., Thamban, N. M., and Tripathi, S. N. (2021). Variations in Black Carbon concentration and sources during COVID-19 lockdown in Delhi. *Chemosphere* 270:129435. doi: 10.1016/j.chemosphere.2020.129435

Gorai, A. K., Tuluri, F., and Tchounwou, P. B. (2014). A GIS based approach for assessing the association between air pollution and asthma in New York State, USA. *Int. J. Environ. Res. Public Health* 11, 4845–4869. doi: 10.3390/ijerph110504845

Gumashta, R., and Bijlwan, A. (2020). Public health threat assessment of vehicular load index-induced urban air pollution indices near traffic intersections in Central India. *Cureus* 12:e11142. doi: 10.7759/cureus.11142

Guo, H., Kota, S. H., Sahu, S. K., Hu, J., Ying, Q., Gao, A., et al. (2017). Source apportionment of PM2. 5 in North India using source-oriented air quality models. *Environ. Pollut.* 231, 426–436. doi: 10.1016/j.envpol.2017.08.016

Gupta, D., Boffetta, P., Gaborieau, V., and Jindal, S. K. (2001). Risk factors of lung cancer in Chandigarh, India. *Indian J. Med. Res.* 113, 142–150.

Gupta, N., Tomar, A., and Kumar, V. (2020). The effect of COVID-19 lockdown on the air environment in India. *Global J. Environ. Sci. Manage.* 6, 31–40. doi: 10.22034/GJESM.2019.06.SI.04

Gurjar, B. R., Jain, A., Sharma, A., Agarwal, A., Gupta, P., Nagpure, A. S., et al. (2010). Human health risks in megacities due to air pollution. *Atmosp. Environ.* 44, 4606–4613. doi: 10.1016/j.atmosenv.2010.08.011

Gurjar, B. R., Ravindra, K., and Nagpure, A. S. (2016). Air pollution trends over Indian megacities and their local-to-global implications. *Atmos. Environ.* 142, 475–495. doi: 10.1016/j.atmosenv.2016.06.030

Guttikunda, S. K., Goel, R., Mohan, D., Tiwari, G., and Gadepalli, R. (2015). Particulate and gaseous emissions in two coastal cities—Chennai and Vishakhapatnam, India. *Air Qual. Atmos. Health* 8, 559–572. doi: 10.1007/s11869-014-0303-6

Guttikunda, S. K., Nishadh, K. A., Gota, S., Singh, P., Chanda, A., Jawahar, P., et al. (2019). Air quality, emissions, and source contributions analysis for the Greater Bengaluru region of India. *Atmos. Pollut. Res.* 10, 941–953. doi: 10.1016/j.apr.2019.01.002

Habib, G., Venkataraman, C., Chiapello, I., Ramachandran, S., Boucher, O., and Reddy, M. S. (2006). Seasonal and interannual variability in absorbing aerosols over India derived from TOMS: relationship to regional meteorology and emissions. *Atmos. Environ.* 40, 1909–1921. doi: 10.1016/j.atmosenv.2005.07.077

Haines, A., Kovats, R. S., Campbell-Lendrum, D., and Corvalán, C. (2006). Climate change and human health: impacts, vulnerability and public health. *Public Health* 120, 585–596. doi: 10.1016/j.puhe.2006.01.002

Haque, M., and Singh, R. B. (2017). Air pollution and human health in Kolkata, India: a case study. *Climate* 5:77. doi: 10.3390/cli5040077

HEI (2011). *Public Health and Air Pollution in Asia (PAPA): Coordinated Studies of Short-Term Exposure to Air Pollution and Daily Mortality in Two Indian Cities*. Research Report 157. Boston, MA: Health Effects Institute.

Hondula, D. M., and Barnett, A. G. (2014). Heat-related morbidity in Brisbane, Australia: spatial variation and area-level predictors. *Environ. Health Perspect.* 122, 831–836. doi: 10.1289/ehp.1307496

Huang, W., Cao, J., Tao, Y., Dai, L., Lu, S. E., Hou, B., et al. (2012). Seasonal variation of chemical species associated with shortterm mortality effects of PM2.5 in Xi'an, a Central City in China. *Am. J. Epidemiol.* 175, 556–566. doi: 10.1093/aje/kwr342

Intergovernmental Panel on Climate Change IPCC-SREX (2012). "Managing the risks of extreme events and disasters to advance climate change adaptation. a special report of working groups I and II of the Intergovernmental panel on climate change," in *Field*, eds C. B. V. Barros, T. F. Stocker, D. Qin, D. J. Dokken, K. L. Ebi, M. D. Mastrandrea, et al. (Cambridge, New York, NY: Cambridge University Press), 1–582.

International Institute for population sciences (IIPS) and Macro International (2007). *National Family Health survey (NFHS-3). 2005-06*: *Volume 1.* Mumbai: IIPS.

IPCC (2007). "Summary for policymakers," in *Climate change 2007: Impacts, Adaptation and Vulnerability. Contribution of Working Group II to the IV Assessment Report of the Intergovernmental Panel on Climate. Intergovernmental Panel on Climate Change (IPCC)* (Cambridge: Cambridge University Press).

Islam, N., and Saikia, B. K. (2020). Atmospheric particulate matter and potentially hazardous compounds around residential/road side soil in an urban area. *Chemosphere* 259:127453. doi: 10.1016/j.chemosphere.2020.127453

Jacob, D. (2001). The role of water vapour in the atmosphere. A short overview from a climate modeller's point of view. *Phys. Chem. Earth A Solid Earth Geodesy* 26, 523–527. doi: 10.1016/S1464-1895(01)00094-1

Jacobson, M. (2001), Strong radiative heating due to the mixing state of BC in atmospheric aerosols, *Nature* 409, 695–697. doi: 10.1038/35055518

Jaffe, D., and Ray, J. (2007). Increase in surface ozone at rural sites in the western US. *Atmos. Environ.* 41, 5452–5463. doi: 10.1016/j.atmosenv.2007.02.034

Jayanthi, V., and Krishnamoorthy, R. (2006). Key airborne pollutants–impact on human health in Manali, Chennai. *Curr. Sci.* 405–413.

Jayaraman, G. (2007). Air quality and respiratory health in Delhi. *Environ. Monitor. Assess.* 135, 313–325. doi: 10.1007/s10661-007-9651-0

Jha, A. K., Bloch, R., and Lamond, J. (2012). *Cities and Flooding: A Guide to Integrated Urban Flood Risk Management for the 21st Century*. The World Bank. doi: 10.1596/978-0-8213-8866-2

Jirak, I. L., and Cotton, W. R. (2006). Effect of air pollution on precipitation along the Front Range of the Rocky Mountains. *J. Appl. Meteorol. Climatol.* 45, 236–245. doi: 10.1175/JAM2328.1

Joseph, A., Sawant, A. D., and Srivastava, A. (2003). PM10 and its impacts on health-a case study in Mumbai. *Int. J. Environ. Health Res.* 13, 207–214. doi: 10.1080/0960312031000098107

Kant, Y., Mitra, D., and Chauhan, P. (2020). Space-based observations on the impact of COVID-19-induced lockdown on aerosols over India. *Curr. Sci.* 119, 539–544.

Karar, K., and Gupta, A. K. (2006). Seasonal variations and chemical characterization of ambient PM10 at residential and industrial sites of an urban region of Kolkata (Calcutta), India. *Atmosp. Res.* 81, 36–53. doi: 10.1016/j.atmosres.2005.11.003

Karar, K., Gupta, A. K., Kumar, A., and Biswas, A. K. (2006). Seasonal variations of PM10 and TSP in residential and industrial sites in an urban area of Kolkata, India. *Environ. Monitor. Assess.* 118, 369–381. doi: 10.1007/s10661-006-1503-9

Karuppasamy, M. B., Seshachalam, S., Natesan, U., Ayyamperumal, R., Karuppannan, S., Gopalakrishnan, G., et al. (2020). Air pollution improvement and mortality rate during COVID-19 pandemic in India: global intersectional study. *Air Quali. Atmos. Health* 13, 1375–1384. doi: 10.1007/s11869-020-00892-w

Kaskaoutis, D. G., Kharol, S. K., Sinha, P. R., Singh, R. P., Badarinath, K. V. S., Mehdi, W., et al. (2011). Contrasting aerosol trends over South Asia during the last decade based on MODIS observations. *Atmosp. Measure. Techniq. Discuss.* 4, 5275–5323. doi: 10.5194/amtd-4-5275-2011

Kaskaoutis, D. G., Singh, R. P., Gautam, R., Sharma, M., Kosmopoulos, P. G., and Tripathi, S. N. (2012). Variability and trends of aerosol properties over Kanpur, northern India using AERONET data (2001–10). *Environ. Res. Lett.* 7:024003. doi: 10.1088/1748-9326/7/2/024003

Kaufman, Y. J., Tanré, D., and Boucher, O. (2002). A satellite view of aerosols in the climate system. *Nature* 419, 215–223. doi: 10.1038/nature01091

Kaur, R., and Pandey, P. (2020). Monitoring and spatio-temporal analysis of UHI effect for Mansa district of Punjab, India. *Adv. Environ. Res.* 9, 19–39. doi: 10.12989/aer.2020.9.1.019

Kelly, F. J., and Fussell, J. C. (2012). Size, source and chemical composition as determinants of toxicity attributable to ambient particulate matter. *Atmosp. Environ.* 60, 504–526. doi: 10.1016/j.atmosenv.2012.06.039

Kharol, S. K., Badarinath, K. V. S., Sharma, A. R., Kaskaoutis, D. G., and Kambezidis, H. D. (2011). Multiyear analysis of Terra/Aqua MODIS aerosol optical depth and ground observations over tropical urban region of Hyderabad, India. *Atmosp. Environ.* 45, 1532–1542. doi: 10.1016/j.atmosenv.2010.12.047

Kikon, N., Singh, P., Singh, S. K., and Vyas, A. (2016). Assessment of urban heat islands (UHI) of Noida City, India using multi-temporal satellite data. *Sustain. Citiesd Soc.* 22, 19–28. doi: 10.1016/j.scs.2016.01.005

Kothai, P., Saradhi, I. V., Pandit, G. G., Markwitz, A., and Puranik, V. D. (2011). Chemical characterization and source identification of particulate matter at an urban site of Navi Mumbai, India. *Aerosol Air Qual. Res.* 11, 560–569. doi: 10.4209/aaqr.2011.02.0017

Kotnala, G., Mandal, T. K., Sharma, S. K., and Kotnala, R. K. (2020). Emergence of blue sky over Delhi due to Coronavirus disease (COVID-19) lockdown implications. *Aerosol Sci. Eng.* 4, 228–238. doi: 10.1007/s41810-020-00062-6

Kovats, S., and Akhtar, R. (2008). Climate, climate change and human health in Asian cities. *Environ. Urbaniz.* 20, 165–175. doi: 10.1177/0956247808089154

Krishna Moorthy, K., Suresh Babu, S., Manoj, M. R., and Satheesh, S. K. (2013). Buildup of aerosols over the Indian Region. *Geophys. Res. Lett.* 40, 1011–1014. doi: 10.1002/grl.50165

Kulshrestha, A., Satsangi, P. G., Masih, J., and Taneja, A. (2009). Metal concentration of PM2.5 and PM10 particles and seasonal variations in urban and rural environment of Agra, India. *Sci. Total Environ.* 407, 6196–6204. doi: 10.1016/j.scitotenv.2009.08.050

Kumar, A., Pratap, V., Kumar, P., and Singh, A. K. (2020). "Frequency distribution of aerosol optical depth over Varanasi during 2011," in *2020 URSI Regional Conference on Radio Science (URSI-RCRS)* (IEEE), 1–2. doi: 10.23919/URSIRCRS49211.2020.9113642

Kumar, A., Valecha, N., Jain, T., and Dash, A. P. (2007). Burden of malaria in India: retrospective and prospective view. *Am. J. Tropic. Med. Hygiene* 77(6_Suppl), 69–78. doi: 10.4269/ajtmh.2007.77.69

Kumar, P., Hama, S., Omidvarborna, H., Sharma, A., Sahani, J., Abhijith, K. V., et al. (2020). Temporary reduction in fine particulate matter due to 'anthropogenic emissions switch-off'during COVID-19 lockdown in Indian cities. *Sustain. Cities Soc.* 2:102382. doi: 10.1016/j.scs.2020.102382

Kumar, V., Shukla, T., Mehta, M., Dobhal, D. P., Bisht, M. P. S., and Nautiyal, S. (2021). Glacier changes and associated climate drivers for the last three decades, Nanda Devi region, Central Himalaya, India. *Quaternary Int.* 575, 213–226. doi: 10.1016/j.quaint.2020.06.017

Kuttippurath, J., Murasingh, S., Stott, P. A., Sarojini, B. B., Jha, M. K., Kumar, P., et al. (2021). Observed rainfall changes in the past century (1901–2019) over the wettest place on Earth. *Environ. Res. Lett.* 16:024018. doi: 10.1088/1748-9326/abcf78

Lahiri, T., Roy, S., Basu, C., Ganguly, S., Ray, M. R., and Lahiri, P. (2000). Air pollution in Calcutta elicits adverse pulmonary reaction in children. *Indian J. Med. Res.* 112, 21–26.

Lau, K. M., Kim, M. K., and Kim, K. M. (2006). Asian summer monsoon anomalies induced by aerosol direct forcing: the role of the Tibetan Plateau. *Climate Dynam.* 26, 855–864. doi: 10.1007/s00382-006-0114-z

Lawrence, A., and Fatima, N. (2014). Urban air pollution & its assessment in Lucknow City—the second largest city of North India. *Sci. Total Environ.* 488, 447–455. doi: 10.1016/j.scitotenv.2013.10.106

Lee, B. K. (2010). "Sources, distribution and toxicity of polyaromatic hydrocarbons (PAHs) in particulate matter," in *Air Pollution*, ed V. Villanyi (Rijeka: In Tech).

Li, R., Li, J. W., Liu, Z. J., Hua, J. J., Wang, Y., and Wang, W. Y. (2016). Satellite observational study on correlations among aerosol optical depth, NO2 and SO2 over China. *Chinese Sci. Bullet.* 61, 2524–2535. doi: 10.1360/N972016-00149

Liu, L., and Zhang, Y. (2011). Urban heat island analysis using the Landsat TM data and ASTER data: a case study in Hong Kong. *Remote Sensing* 3, 1535–1552. doi: 10.3390/rs3071535

Lokhandwala, S., and Gautam, P. (2020). Indirect impact of COVID-19 on environment: a brief study in Indian context. *Environ. Res.* 188:109807. doi: 10.1016/j.envres.2020.109807

Luber, G., and McGeehin, M. (2008). Climate change and extreme heat events. *Am. J. Prevent. Med.* 35, 429–435. doi: 10.1016/j.amepre.2008.08.021

Mahapatra, P. S., Sinha, P. R., Boopathy, R., Das, T., Mohanty, S., Sahu, S. C., et al. (2018). Seasonal progression of atmospheric particulate matter over an urban coastal region in peninsular India: role of local meteorology and long-range transport. *Atmosp. Res.* 199, 145–158. doi: 10.1016/j.atmosres.2017.09.001

Mahato, S., Pal, S., and Ghosh, K. G. (2020). Effect of lockdown amid COVID-19 pandemic on air quality of the megacity Delhi, India. *Sci. Total Environ.* 730:139086. doi: 10.1016/j.scitotenv.2020.139086

Maji, K. J., Dikshit, A. K., and Deshpande, A. (2016). Human health risk assessment due to air pollution in 10 urban cities in Maharashtra, India. *Cogent Environ. Sci.* 2:1193110. doi: 10.1080/23311843.2016.1193110

Maji, K. J., Dikshit, A. K., and Deshpande, A. (2017). Assessment of city level human health impact and corresponding monetary cost burden due to air pollution in India taking Agra as a model city. *Aerosol Air Qual. Res.* 17, 831–842. doi: 10.4209/aaqr.2016.02.0067

Maji, K. J., Namdeo, A., Bell, M., Goodman, P., Nagendra, S. S., Barnes, J. H., et al. (2021). Unprecedented reduction in air pollution and corresponding short-term premature mortality associated with COVID-19 Lockdown in Delhi, India. *J. Air Waste Manage. Assoc*. 1–17. doi: 10.1080/10962247.2021.1905104

Majra, J. P., and Gur, A. (2009). Climate change and health: why should India be concerned? *Indian J. Occupat. Environ. Med.* 13, 11–16. doi: 10.4103/0019-5278.50717

Mathew, A., Khandelwal, S., and Kaul, N. (2016). Spatial and temporal variations of urban heat island effect and the effect of percentage impervious surface area and elevation on land surface temperature: study of Chandigarh city, India. *Sustain. Cities Soc.* 26, 264–277. doi: 10.1016/j.scs.2016.06.018

Mazdiyasni, O., AghaKouchak, A., Davis, S. J., Madadgar, S., Mehran, A., Ragno, E., et al. (2017). Increasing probability of mortality during Indian heat waves. *Sci. Adv.* 3:e1700066. doi: 10.1126/sciadv.1700066

Mehta, L., Srivastava, S., Adam, H. N., Bose, S., Ghosh, U., and Kumar, V. V. (2019). Climate change and uncertainty from 'above'and 'below': perspectives from India. *Region. Environ. Change* 19, 1533–1547. doi: 10.1007/s10113-019-01479-7

Menon, S., Hansen, J., Nazarenko, L., and Luo, Y. (2002). Climate effects of black carbon aerosols in China and India. *Science* 297, 2250–2253. doi: 10.1126/science.1075159

Menut, L., Bessagnet, B., Siour, G., Mailler, S., Pennel, R., and Cholakian, A. (2020). Impact of lockdown measures to combat Covid-19 on air quality over western Europe. *Sci. Total Environ.* 741:140426. doi: 10.1016/j.scitotenv.2020.140426

Mirowsky, J., Hickey, C., Horton, L., Blaustein, M., Galdanes, K., Peltier, R. E., et al. (2013). The effect of particle size, location and season on the toxicity of urban and rural particulate matter. *Inhalat. Toxicol.* 25, 747–757. doi: 10.3109/08958378.2013.846443

Mishra, A. K., Srivastava, A., and Jain, V. K. (2013). Spectral dependency of aerosol optical depth and derived aerosol size distribution over Delhi: an implication to pollution source. *Sustain. Environ. Res.* 23, 113–128.

Mitra, A., Chaudhuri, T. R., Mitra, A., Pramanick, P., Zaman, S., Mitra, A., et al. (2020). Impact of COVID-19 related shutdown on atmospheric carbon dioxide level in the city of Kolkata. *Parana J. Sci. Educ.* 6, 84–92.

Mondal, N. C., Biswas, R., and Manna, A. (2001). Risk factors of diarrhoea among flood victims: a controlled epidemiological study. *Indian J. Public Health* 45, 122–127.

Mondal, R., Sen, G. K., Chatterjee, M., Sen, B. K., and Sen, S. (2000). Ground-level concentration of nitrogen oxides (NOx) at some traffic intersection points in Calcutta. *Atmosp. Environ.* 34, 629–633. doi: 10.1016/S1352-2310(99)00216-2

Mostafavi, S. A., Safikhani, H., and Salehfard, S. (2021). Air pollution distribution in Arak city considering the effects of neighboring pollutant industries and urban traffics. *Int. J. Energy Environ. Eng.* 12, 307–333. doi: 10.1007/s40095-020-00379-5

MPCB (2010). *Action Plane for Industrial Cluster: Chandrapur*. Maharashtra Pollution Control Board. Available online at: http://cpcb.nic.in/divisionsofheadoffice/ess/Action%20plan%20CEPI-Chandrapur.pdf (Retrieved February 14, 2015).

Mudgal, R., Sharma, B., Upadhyay, R., and Taneja, A. (2000). *Seasonal Variation of Ambient Air Quality at Selected Sites in Agra City*.

Mukherjee, S., and Mishra, V. (2018). A sixfold rise in concurrent day and night-time heatwaves in India under 2 C warming. *Sci. Rep.* 8:16922. doi: 10.1038/s41598-018-35348-w

Mukhopadhyay, K. (2009). *Air Pollution in India and Its Impact on the Health of Different Income Groups*. Nova Science Publishers.

Murari, K. K., Ghosh, S., Patwardhan, A., Daly, E., and Salvi, K. (2015). Intensification of future severe heat waves in India and their effect on heat stress and mortality. *Region. Environ. Change* 15, 569–579. doi: 10.1007/s10113-014-0660-6

Murari, V., Kumar, M., Barman, S. C., and Banerjee, T. (2015). Temporal variability of MODIS aerosol optical depth and chemical characterization of airborne particulates in Varanasi, India. *Environ. Sci. Pollut. Res.* 22, 1329–1343. doi: 10.1007/s11356-014-3418-2

Nagpure, A. S., Gurjar, B. R., and Martel, J. C. (2014). Human health risks in national capital territory of Delhi due to air pollution. *Atmosp. Pollut. Res.* 5, 371–380. doi: 10.5094/APR.2014.043

NASA (2015). *GISS Surface Temperature Analysis*. Available online at: https://www.nytimes.com/2014/02/14/opinion/indias-air-pollution-emergency.html (accessed April 1, 2021).

Nath, B., Ni-Meister, W., and Choudhury, R. (2021). Impact of urbanization on land use and land cover change in Guwahati city, India and its implication on declining groundwater level. *Groundwater Sustain. Dev.* 12:100500. doi: 10.1016/j.gsd.2020.100500

NYT (2014). *India's Air Pollution Emergency [online]*. The New York Times. Retrieved from: http://www.nytimes.com/2014/02/14/opinion/indias-airpollutionemergency.html?_r=0

OECD (2014). *The Cost of Air Pollution: Health Impacts of Road Transport*. Paris: OECD Publishing. doi: 10.1787/9789264210448-en

Oeder, S., Dietrich, S., Weichenmeier, I., Schober, W., Pusch, G., Jörres, R. A., et al. (2012). Toxicity and elemental composition of particulate matter from outdoor and indoor air of elementary schools in Munich, Germany. *Indoor Air* 22, 148–158. doi: 10.1111/j.1600-0668.2011.00743.x

Ohashi, Y., Genchi, Y., Kondo, H., Kikegawa, Y., Yoshikado, H., and Hirano, Y. (2007). Influence of air conditioning waste heat on air temperature in Tokyo during summer: numerical experiments using an urban canopy model coupled with a building energy model. *J. Appl. Meteorol. Climatol.* 46, 66–81. doi: 10.1175/JAM2441.1

Orimoloye, I. R., Mazinyo, S. P., Kalumba, A. M., Ekundayo, O. Y., and Nel, W. (2019). Implications of climate variability and change on urban and human health: a review. *Cities* 91, 213–223. doi: 10.1016/j.cities.2019.01.009

Patil, R. R., and Deepa, T. M. (2007). Climate change: the challenges for public health preparedness and response-an Indian case study. *Indian J. Occup. Environ. Med.* 11, 113–115. doi: 10.4103/0019-5278.38460

Paul, S., Saxena, K. G., Nagendra, H., and Lele, N. (2021). Tracing land use and land cover change in peri-urban Delhi, India, over 1973–2017 period. *Environ. Monit. Assess.* 193, 1–12. doi: 10.1007/s10661-020-08841-x

Peng, R. D., Dominici, F., Pastor-Barriuso, R., Zeger, S. L., and Samet, J. M. (2005). Seasonal analyses of air pollution and mortality in 100 US cities. *Am. J. Epidemiol.* 161, 585–594. doi: 10.1093/aje/kwi075

Pope, C. A. III., Ezzati, M., and Dockery, D. W. (2009). Fine-particulate air pollution and life expectancy in the United States. *N. Engl. J. Med.* 360, 376–386. doi: 10.1056/NEJMsa0805646

Portnov, B. A., Reiser, B., Karkabi, K., Cohen-Kastel, O., and Dubnov, J. (2012). High prevalence of childhood asthma in Northern Israel is linked to air pollution by particulate matter: evidence from GIS analysis and Bayesian Model Averaging. *Int. J. Environ. Health Res.* 22, 249–269. doi: 10.1080/09603123.2011.634387

Prabhakaran, D., Mandal, S., Krishna, B., Magsumbol, M., Singh, K., Tandon, N., et al. (2020). Exposure to particulate matter is associated with elevated blood pressure and incident hypertension in urban India. *Hypertension* 76, 1289–1298. doi: 10.1161/HYPERTENSIONAHA.120.15373

Pramanik, M. K. (2017). Impacts of predicted sea level rise on land use/land cover categories of the adjacent coastal areas of Mumbai megacity, India. *Environ. Dev. Sustain.* 19, 1343–1366. doi: 10.1007/s10668-016-9804-9

Prasad, A. K., and Singh, R. P. (2007). Changes in aerosol parameters during major dust storm events (2001–2005) over the Indo-Gangetic Plains using AERONET and MODIS data. *J. Geophys. Res.* 112:D9. doi: 10.1029/2006JD007778

Rajeev, P., Rajput, P., and Gupta, T. (2016). Chemical characteristics of aerosol and rain water during an El Niño and PDO influenced Indian summer monsoon. *Atmos. Environ.* 145, 192–200. doi: 10.1016/j.atmosenv.2016.09.026

Rajeev, P., Rajput, P., Singh, D, K., Singh, A, K., and Gupta, T. (2018). Risk assessment of submicron PM-bound hexavalent chromium during wintertime. *Human Ecol. Risk Assess. Int. J.* 24, 1453–1463. doi: 10.1080/10807039.2017.1414581

Rajput, P., Anjum, M, H., and Gupta, T. (2017). One year record of bioaerosols and particles concentration in Indo-Gangetic Plain: implications of biomass burning emissions to high-level of endotoxin exposure. *Environ. Pollut.* 224, 98–106. doi: 10.1016/j.envpol.2017.01.045

Rajput, P., Izhar, S., and Gupta, T. (2019). Deposition modeling of ambient aerosols in human respiratory system: health implication of fine particles penetration into pulmonary region. *Atmos. Pollut. Res.* 10, 334–343. doi: 10.1016/j.apr.2018.08.013

Rajput, P., Mandaria, A., Kachawa, L., Singh, D, K., Singh, A, K., and Gupta, T. (2016). Chemical characterisation and source apportionment of PM1 during massive loading at an urban location in Indo-Gangetic Plain: impact of local sources and long-range transport. *Tellus B Chem. Phys. Meteorol.* 68, 1–10. doi: 10.3402/tellusb.v68.30659

Rajput, P., Sarin, M., and Kundu, S. S. (2013). Atmospheric particulate matter (PM2. 5), EC, OC, WSOC and PAHs from NE–Himalaya: abundances and chemical characteristics. *Atmosp. Pollut. Res.* 4, 214–221. doi: 10.5094/APR.2013.022

Rajput, P., Sarin, M., Sharma, D., and Singh, D. (2014). Characteristics and emission budget of carbonaceous species from post-harvest agricultural-waste burning in source region of the Indo-Gangetic Plain. *Tellus B Chem. Phys. Meteorol.* 66:121026. doi: 10.3402/tellusb.v66.21026

Rajput, P., Sarin, M. M., Rengarajan, R., and Singh, D. (2011). Atmospheric polycyclic aromatic hydrocarbons (PAHs) from post-harvest biomass burning emissions in the Indo-Gangetic Plain: isomer ratios and temporal trends. *Atmosp. Environ.* 45, 6732–6740. doi: 10.1016/j.atmosenv.2011.08.018

Rajput, P., Singh, D, K., Singh, A, K., and Gupta, T. (2018). Chemical composition and source-apportionment of sub-micron particles during wintertime over Northern India: new insights on influence of fog-processing. *Environ. Pollut.* 233, 81–91. doi: 10.1016/j.envpol.2017.10.036

Ramachandran, S., and Cherian, R. (2008). Regional and seasonal variations in aerosol optical characteristics and their frequency distributions over India during 2001–2005. *J. Geophys. Res.* 113:D8. doi: 10.1029/2007JD008560

Ramachandran, S., Kedia, S., and Srivastava, R. (2012). Aerosol optical depth trends over different regions of India. *Atmos. Environ.* 49, 338–347. doi: 10.1016/j.atmosenv.2011.11.017

Ramanathan, V., and Carmichael, G. (2008). Global and regional climate changes due to black carbon. *Nat. Geosci.* 1, 221–227. doi: 10.1038/ngeo156

Ramanathan, V. C. P. J., Crutzen, P. J., Kiehl, J. T., and Rosenfeld, D. (2001). Aerosols, climate, and the hydrological cycle. *Science* 294, 2119–2124. doi: 10.1126/science.1064034

Ramya, A., Nivetha, A., and Dhevagi, P. (2021). "Overview of indoor air pollution: a human health perspective," in *Spatial Modeling and Assessment of Environmental Contaminants* (Cham: Springer), 495–514. doi: 10.1007/978-3-030-63422-3_25

Ravindra, K., Singh, T., Mor, S., Singh, V., Mandal, T. K., Bhatti, M. S., et al. (2019). Real-time monitoring of air pollutants in seven cities of North India during crop residue burning and their relationship with meteorology and transboundary movement of air. *Sci. Total Environ.* 690, 717–729. doi: 10.1016/j.scitotenv.2019.06.216

Ren, G., Zhou, Y., Chu, Z., Zhou, J., Zhang, A., Guo, J., et al. (2008). Urbanization effects on observed surface air temperature trends in North China. *J. Climate* 21, 1333–1348. doi: 10.1175/2007JCLI1348.1

Rizwan, S. A., Nongkynrih, B., and Gupta, S. K. (2013). Air pollution in Delhi: its magnitude and effects on health. *Indian J. Community Med.* 38, 4–8. doi: 10.4103/0970-0218.106617

Rogers, J. F., Thompson, S. J., Addy, C. L., McKeown, R. E., Cowen, D. J., and Decoufle, P. (2000). Association of very low birth weight with exposures to environmental sulfur dioxide and total suspended particulates. *Am. J. Epidemiol.* 151, 602–613. doi: 10.1093/oxfordjournals.aje.a010248

Rosenfeld, D., Dai, J., Yu, X., Yao, Z., Xu, X., Yang, X., et al. (2007). Inverse relations between amounts of air pollution and orographic precipitation. *Science* 315, 1396–1398. doi: 10.1126/science.1137949

Roy, S., Ray, M. R., Basu, C., Lahiri, P., and Lahiri, T. (2001). Abundance of siderophages in sputum: indicator of an adverse lung reaction to air pollution. *Acta Cytol.* 45, 958–964. doi: 10.1159/000328371

Rumana, H. S., Sharma, R. C., Beniwal, V., and Sharma, A. K. (2014). A retrospective approach to assess human health risks associated with growing air pollution in urbanized area of Thar Desert, western Rajasthan, India. *J. Environ. Health Sci. Eng.* 12, 1–9. doi: 10.1186/2052-336X-12-23

Sahu, S. K., and Kota, S. H. (2017). Significance of PM2. 5 air quality at the Indian capital. *Aerosol Air Qual. Res.* 17, 588–597. doi: 10.4209/aaqr.2016.06.0262

Saini, R., Satsangi, G. S., and Taneja, A. (2008). *Concentrations of Surface O3, NO_2 and CO During Winter Seasons at a Semi-arid Region–Agra, India*.

Samoli, E., Peng, R., Ramsay, T., Pipikou, M., Touloumi, G., Dominici, F., et al. (2008). Acute effects of ambient particulate matter on mortality in Europe and North America: results from the APHENA study. *Environm. Health Perspect.* 116, 1480–1486. doi: 10.1289/ehp.11345

Samoli, E., Stafoggia, M., Rodopoulou, S., Ostro, B., Declercq, C., Alessandrini, E., et al. (2013). Associations between fine and coarse particles and mortality in Mediterranean cities: results from the MEDPARTICLES project. *Environ. Health Perspect.* 121, 932–938. doi: 10.1289/ehp.1206124

Sarath, K. G., and Ramani, V. K. (2014). Source emissions and health impacts of urban air pollution in Hyderabad, India. *Air Qual. Atmosp. Health* 7, 195–207. doi: 10.1007/s11869-013-0221-z

Satheesh, S. K., Ramanathan, V., Holben, B. N., Moorthy, K. K., Loeb, N. G., Maring, H., et al. (2002). Chemical, microphysical, and radiative effects of Indian Ocean aerosols. *J. Geophys. Res.* 107, AAC—20. doi: 10.1029/2002JD002463

Schwela, D., Haq, G., Huizenga, C., Han, W. J., Fabian, H., and Ajero, M. (2006). *Urban Air Pollution in Asian Cities: Status, Challenges and Management*. Routledge.

Sen, A., Ahammed, Y. N., Banerjee, T., Chatterjee, A., Choudhuri, A. K., Das, T., et al. (2016). Spatial variability in ambient atmospheric fine and coarse mode aerosols over Indo-Gangetic plains, India and adjoining oceans during the onset of summer monsoons, 2014. *Atmos. Pollut. Res.* 7, 521–532. doi: 10.1016/j.apr.2016.01.001

Sharma, A. R., Kharol, S. K., Badarinath, K. V. S., and Singh, D. (2010). Impact of agriculture crop residue burning on atmospheric aerosol loading–a study over Punjab State, India. *Annal. Geophys.* 28, 367–379. doi: 10.5194/angeo-28-367-2010

Sharma, M., Kaskaoutis, D. G., Singh, R. P., and Singh, S. (2014). Seasonal variability of atmospheric aerosol parameters over Greater Noida using ground sunphotometer observations. *Aerosol Air Qual. Res.* 14, 608–622. doi: 10.4209/aaqr.2013.06.0219

Sharma, S., Zhang, M., Gao, J., Zhang, H., and Kota, S. H. (2020). Effect of restricted emissions during COVID-19 on air quality in India. *Sci. Total Environ.* 728:138878. doi: 10.1016/j.scitotenv.2020.138878

Sharma, S. K., Mandal, T. K., Srivastava, M. K., Chatterjee, A., Jain, S., Saxena, M., et al. (2016). Spatio-temporal variation in chemical characteristics of PM10 over Indo Gangetic Plain of India. *Environ. Sci. Pollut. Res*. 23, 18809–18822. doi: 10.1007/s11356-016-7025-2

Shastri, H., Barik, B., Ghosh, S., Venkataraman, C., and Sadavarte, P. (2017). Flip flop of day-night and summer-winter surface urban heat island intensity in India. *Sci. Rep.* 7:40178. doi: 10.1038/srep40178

Shastri, H., Paul, S., Ghosh, S., and Karmakar, S. (2015). Impacts of urbanization on Indian summer monsoon rainfall extremes. *J. Geophysic. Res.* 120, 496–516. doi: 10.1002/2014JD022061

Shaw, N., and Gorai, A. K. (2020). Study of aerosol optical depth using satellite data (MODIS Aqua) over Indian Territory and its relation to particulate matter concentration. *Environ. Dev. Sustain.* 22, 265–279. doi: 10.1007/s10668-018-0198-8

Shepherd, J. M. (2005). A review of current investigations of urban-induced rainfall and recommendations for the future. *Earth Interact.* 9, 1–27. doi: 10.1175/EI156.1

Siddiqui, A., Halder, S., Chauhan, P., and Kumar, P. (2020). COVID-19 pandemic and city-level nitrogen dioxide (NO 2) reduction for urban centres of India. *J. Indian Soc. Remote Sensing* 48, 999–1006. doi: 10.1007/s12524-020-01130-7

Singh, A., Rajput, P., Sharma, D., Sarin, M. M., and Singh, D. (2014). Black carbon and elemental carbon from postharvest agricultural-waste burning emissions in the Indo-Gangetic Plain. *Adv. Meteorol.* 2014, 1–10, doi: 10.1155/2014/179301

Singh, B. P., Srivastava, A. K., Tiwari, S., Singh, S., Singh, R. K., Bisht, D. S., et al. (2014). Radiative impact of fireworks at a tropical Indian location: a case study. *Adv. Meteorol.* 2014. doi: 10.1155/2014/197072

Singh, C., Madhavan, M., Arvind, J., and Bazaz, A. (2021). Climate change adaptation in Indian cities: a review of existing actions and spaces for triple wins. *Urban Climate* 36:100783. doi: 10.1016/j.uclim.2021.100783

Singh, R., Sharma, C., and Agrawal, M. (2017). Emission inventory of trace gases from road transport in India. *Transport. Res. Part D Transp. Environ.* 52, 64–72. doi: 10.1016/j.trd.2017.02.011

Singh, R. P., and Chauhan, A. (2020). Impact of lockdown on air quality in India during COVID-19 pandemic. *Air Qual. Atmosp. Health* 13, 921–928. doi: 10.1007/s11869-020-00863-1

Singh, S., Nath, S., Kohli, R., and Singh, R. (2005). Aerosols over Delhi during pre-monsoon months: Characteristics and effects on surface radiation forcing. *Geophys. Res. Lett.* 32:L13808. doi: 10.1029/2005GL023062

Singh, S., Soni, K., Bano, T., Tanwar, R. S., Nath, S., and Arya B. C. (2010). Clear-sky direct aerosol radiative forcing variations over mega-city Delhi. *Ann. Geophys.* 28, 1157–1166. doi: 10.5194/angeo-28-1157-2010

Singh, V., Singh, S., and Biswal, A. (2021). Exceedances and trends of particulate matter (PM2. 5) in five Indian megacities. *Sci. Total Environ.* 750:141461. doi: 10.1016/j.scitotenv.2020.141461

Smith, K. R. (2013). *Biofuels, Air Pollution, and Health: A Global Review*.

Sorathia, F., Rajput, P., and Gupta, T. (2018). Dicarboxylic acids and levoglucosan in aerosols from Indo-Gangetic Plain: Inferences from day night variability during wintertime. *Sci. Total Environ.* 624, 451–460. doi: 10.1016/j.scitotenv.2017.12.124

Srivastava, S., Kumar, A., Bauddh, K., Gautam, A. S., and Kumar, S. (2020). 21-Day lockdown in India dramatically reduced air pollution indices in Lucknow and New Delhi, India. *Bull. Environ. Contamin. Toxicol.* 105, 9–17. doi: 10.1007/s00128-020-02895-w

Stafoggia, M., Samoli, E., Alessandrini, E., Cadum, E., Ostro, B., Berti, G., et al. (2013). Short-term associations between fine and coarse particulate matter and hospitalizations in Southern Europe: results from the MED-PARTICLES project. *Environ. Health Perspect.* 121, 1026–1033. doi: 10.1289/ehp.1206151

Surendran, D. E., Beig, G., Ghude, S. D., Panicker, A. S., Manoj, M. G., Chate, D. M., et al. (2013). Radiative forcing of black carbon over Delhi. *Int. J. Photoenergy* 2013:313652. doi: 10.1155/2013/313652

Tiwari, S., Bisht, D. S., Srivastava, A. K., Pipal, A. S., Taneja, A., Srivastava, M. K., et al. (2014). Variability in atmospheric particulates and meteorological effects on their mass concentrations over Delhi, India. *Atmos. Res.* 145, 45–56. doi: 10.1016/j.atmosres.2014.03.027

Tiwari, S., Hopke, P. K., Pipal, A. S., Srivastava, A. K., Bisht, D. S., Tiwari, S., et al. (2015). Intra-urban variability of particulate matter (PM2.5 and PM10) and its relationship with optical properties of aerosols over Delhi, India. *Atmos. Res.* 166, 223–232. doi: 10.1016/j.atmosres.2015.07.007

Tiwari, S., Srivastava, A. K., Bisht, D. S., Bano, T., Singh, S., Behura, S., et al. (2009). Black carbon and chemical characteristics of PM10 and PM2.5 at an urban site of North India. *J. Atmosp. Chem.* 62, 193–209. doi: 10.1007/s10874-010-9148-z

Tsai, S.-S., and Yang, C.-H. (2014). Fine particulate air pollution and hospital admissions for pneumonia in a subtropical city: Taipei, Taiwan. *J. Toxicol. Environ. Health A* 77, 192–201. doi: 10.1080/15287394.2013.853337

UNDESA (2018). *2018 Revision of World Urbanization Prospects*.

UN-HABITAT (2010). *State of the World's Cities 2010/2011: Bridging the Urban Divide.* London: Earthscan. doi: 10.4324/9781849774864

Vadrevu, K. P., Eaturu, A., Biswas, S., Lasko, K., Sahu, S., Garg, J. K., et al. (2020). Spatial and temporal variations of air pollution over 41 cities of India during the COVID-19 lockdown period. *Sci. Rep.* 10:16574. doi: 10.1038/s41598-020-72271-5

Van Duijne, R. J. (2017). What is India's urbanisation riddle. *Econ. Politic. Weekly* 52, 76–77.

Venkataraman, C., Brauer, M., Tibrewal, K., Sadavarte, P., Ma, Q., Cohen, A., et al. (2018). Source influence on emission pathways and ambient PM2.5 pollution over India (2015–2050). *Atmosp. Chem. Phys.* 18, 8017–8039. doi: 10.5194/acp-18-8017-2018

Wang, K., Dickinson, R. E., and Liang, S. (2009). Clear sky visibility has decreased over land globally from 1973 to 2007. *Science* 323, 1468–1470. doi: 10.1126/science.1167549

West Bengal Pollution Control Board (2005). Air Quality Management: Final Report. New Delhi: WBPCB in Collaboration with Asian Development Bank; Intercontinental Consultant and Technocrats Pvt. Ltd.

West Bengal Pollution Control Board (2010). *Annual Report 2008–2010; Government of West Bengal*. Kolkata.

West Bengal Pollution Control Board (WBPCB) (2003). A *Quinqueenniel Report, April 1998 to March 2003*. Kolkata: West Bengal Pollution Control Board.

WHO (2013). *Review of Evidence on Health Aspects of Air Pollution – REVIHAAP Project*. Copenhagen: World Health Organization Regional Office for Europe.

WHO (2015). *Countries: China: Country Health Profile*. World Health Organization. Available online at: http://www.who.int/countries/chn/en/

WHO Global Urban Ambient Air Pollution Database (Update 2016) (2016). Available online at: https://www.who.int/phe/health_topics/outdoorair/databases/cities/en/ (accessed April 10, 2021).

Wilson, M. L., Aron, J. L., and Patz, J. A. (2001). *Ecology and Infectious Disease. Ecosystem Change and Public Health: A Global Perspective*.

World Health Organization (WHO) (2005). *Health Impacts From Climate Variability and Change in the Hindu Kush-Himalayan Region. Report of an Inter-Regional Workshop*. Mukteshwar: WHO and Regional Office for South-East, Asia.

World Health Organization and United Nations Children's Fund (WHO and UNICEF) (2000). *Water Sanitation and Health (WSH). Global Water Supply and Sanitation Assessment* 2000 *Report*. Geneva: WHO.

Wu, H., Wang, T., Riemer, N., Chen, P., Li, M., and Li, S. (2017). Urban heat island impacted by fine particles in Nanjing, China. *Sci. Rep.* 7:11422. doi: 10.1038/s41598-017-11705-z

Xing, Y. F., Xu, Y. H., Shi, M. H., and Lian, Y. X. (2016). The impact of PM2.5 on the human respiratory system. *J. Thoracic Dis.* 8:E69. doi: 10.3978/j.issn.2072-1439.2016.01.19

Xu, J., Jiang, H., Zhang, X., Lu, X., and Peng, W. (2014). Study on spatial-temporal variation of aerosol optical depth over the Yangtze Delta and the impact of land-use/cover. *Int. J. Remote Sens.* 35, 1741–1755. doi: 10.1080/01431161.2014.882033

Yadav, S., and Satsangi, P. G. (2013). Characterization of particulate matter and its related metal toxicity in an urban location in South West India. *Environ. Monit. Assess.* 185, 7365–7379. doi: 10.1007/s10661-013-3106-6

Yan, P., Tang, J., Huang, J., Mao, J. T., Zhou, X. J., Liu, Q., et al. (2008). The measurement of aerosol optical properties at a rural site in Northern China. *Atmosp. Chem. Phys.* 8, 2229–2242. doi: 10.5194/acp-8-2229-2008

Yang, B., Zhang, Y., and Qian, Y. (2012). Simulation of urban climate with high-resolution WRF model: a case study in Nanjing, China. *Asia-Pacific J. Atmosp. Sci.* 48, 227–241. doi: 10.1007/s13143-012-0023-5

Yang, C. Y., Chang, C. C., Chuang, H. Y., Tsai, S. S., Wu, T. N., and Ho, C. K. (2004). Relationship between air pollution and daily mortality in a subtropical city: Taipei, Taiwan. *Environ. Int.* 30, 519–523. doi: 10.1016/j.envint.2003.10.006

Yang, K. L., Ting, C. C., Wang, J. L., Wingenter, O. W., and Chan, C. C. (2005). Diurnal and seasonal cycles of ozone precursors observed from continuous measurement at an urban site in Taiwan. *Atmosp. Environ.* 39, 3221–3230. doi: 10.1016/j.atmosenv.2005.02.003

Zhang, S., Wang, M., Ghan, S. J., Ding, A., Wang, H., Zhang, K., et al. (2016). On the characteristics of aerosol indirect effect based on dynamic regimes in global climate models. *Atmosp. Chem. Phys.* 16, 2765–2783. doi: 10.5194/acp-16-2765-2016

Zhang, W., Gu, X., Xu, H., Yu, T., and Zheng, F. (2016). Assessment of OMI near-UV aerosol optical depth over Central and East Asia. *J. Geophysic. Res.* 121, 382–398. doi: 10.1002/2015JD024103

Zhu, T., Weng, F., Liu, H., and Derber, J. (2010). "Improvement of the use of MSG and GOES data in the NCEP GDAS," in *Atmospheric and Environmental Remote Sensing Data Processing and Utilization VI: Readiness for GEOSS IV*. Vol. 7811 (San Diego, CA: International Society for Optics and Photonics), 781103. doi: 10.1117/12.860090

Zou, X., Shen, Z., Yuan, T., Yin, S., Zhang, X., Yin, R., et al. (2007). On an empirical relationship between SO2 concentration and distance from a highway using passive samplers: a case study in Shanghai, China. *Sci. Total Environ.* 377, 434–438. doi: 10.1016/j.scitotenv.2007.01.078

Conflict of Interest: The authors declare that the research was conducted in the absence of any commercial or financial relationships that could be construed as a potential conflict of interest.

Publisher's Note: All claims expressed in this article are solely those of the authors and do not necessarily represent those of their affiliated organizations, or those of the publisher, the editors and the reviewers. Any product that may be evaluated in this article, or claim that may be made by its manufacturer, is not guaranteed or endorsed by the publisher.

frontiers in Sustainable Cities

REVIEW
published: 18 August 2021
doi: 10.3389/frsc.2021.690444

Inhalation Exposure to Atmospheric Nanoparticles and Its Associated Impacts on Human Health: A Review

Saurabh Sonwani[1], Simran Madaan[2], Jagjot Arora[2], Shalini Suryanarayan[3], Deepali Rangra[4], Nancy Mongia[4], Tanvi Vats[5] and Pallavi Saxena[6]*

[1] Department of Environmental Studies, Zakir Husain Delhi College, University of Delhi, New Delhi, India, [2] Department of Zoology, Hindu College, University of Delhi, New Delhi, India, [3] Department of Sociology, Hindu College, University of Delhi, New Delhi, India, [4] Department of Physical Science Chemistry, Hindu College, University of Delhi, New Delhi, India, [5] Gautam Buddha University, Greater Noida, India, [6] Department of Environmental Sciences, Hindu College, University of Delhi, New Delhi, India

OPEN ACCESS

Edited by:
Prashant Rajput,
Banaras Hindu University, India

Reviewed by:
Hamid Omidvarborna,
University of Surrey, United Kingdom
Md Firoz Khan,
University of Malaya, Malaysia

***Correspondence:**
Pallavi Saxena
pallavienvironment@gmail.com;
pallavisaxena@hinducollege.ac.in

Specialty section:
This article was submitted to
Climate Change and Cities,
a section of the journal
Frontiers in Sustainable Cities

Received: 02 April 2021
Accepted: 26 July 2021
Published: 18 August 2021

Citation:
Sonwani S, Madaan S, Arora J, Suryanarayan S, Rangra D, Mongia N, Vats T and Saxena P (2021) Inhalation Exposure to Atmospheric Nanoparticles and Its Associated Impacts on Human Health: A Review. Front. Sustain. Cities 3:690444. doi: 10.3389/frsc.2021.690444

Nanoparticles (NPs) are receiving an increasing attention from many scientific communities due to their strong influence on human health. NPs are an important marker of air pollution caused by a variety of natural and anthropogenic sources. Due to their ultrafine size, they can be suspended in the atmosphere for a long time and can thus travel larger distances and cause several health issues after exposure. A variety of NPs that are found in indoor and outdoor settings cause respiratory and cardiovascular diseases. Exposure to NPs through active and passive smoking and household and occupational subjection is reported with thick septum, shortness of breath, and a high level of interleukin protein and tumour necrosis factor (TNF-α) that cause tumour generation in the exposed population. This comprehensive review summarises NPs' source, exposure, and impact on different organ systems. Respiratory models (experimental and computational) used to determine the particle's deposition, airflow transport, and health impact are also discussed. Further, muco-ciliary escalation and macrophage activity, the body's clearance mechanisms after exposure to NPs, have been mentioned. An in-depth analysis of exposure to NPs through inhalation and their health impact has been provided with detailed insights about oxidative stress, inflammation, genotoxicity, and tumourigenicity. Overall, this review offers scientific evidence and background for researchers working in the field of epidemiology, biochemistry, and toxicological studies with reference to atmospheric nanoparticles.

Keywords: nanoparticles, atmosphere, respiratory system, air quality, human health

INTRODUCTION

Among particles of various sizes present in the atmosphere, NPs are particles with sizes of 1–100 nm in diameter (Kumar et al., 2010; Nemmar et al., 2013). The residence time of particles in the diameter range of 0.1–10 μm is ∼1 week. Coarser particulate matter is removed by settling, while smaller particles can only be removed *via* diffusion and coagulation (Scholl et al., 2012; Slezakova et al., 2013; Bakshi et al., 2015). Moreover, the fine size and higher atmospheric retention time of NPs are the basic reasons behind the difficultly in their removal from the atmosphere, consequently causing human health hazard. Nanoparticles originate from vehicular exhaust, combustion reactions, forest fires, and industrial emission; they are also produced in the bodies of insects, plants, and humans (Jeevanandam et al., 2018). The atmospheric concentration of nanoparticles is high in Asian countries due to the high rate of urbanisation, industrialisation, vehicular emission, extreme events (dust storms, volcanic eruption, forest fire, etc.), and episodic events (such as firework activity and crop residue burning) (Nakajima et al., 2007; Saxena et al., 2020; Sonwani et al., 2021). Most of the anthropogenic nanoparticles are made up of carbon, silicon, metal, or metal oxides (Querol et al., 2004). India's coal-fired plants emit more than 110,000 tonnes of particulate matter, 4.3 million tonnes of SO_2, and 1.2 million tonnes of NOx per year (Oliveira et al., 2014).

According to the 2007 report of the Intergovernmental Panel on Climate Change (IPCC), nanoparticles act as precursors to coarser particles through their aggregation during the atmospheric ageing process thereby influencing the global climate and urban visibility. Due to their distinct chemical composition and reactivity, they also alter the atmospheric chemistry and global climate (Slezakova et al., 2013). Moreover, these particles are responsible for global warming (by absorbing solar radiation) and cooling effects (by scattering solar radiation), further affecting the global radiation budget (Buseck and Adachi, 2008). Another striking phenomenon is the production of atmospheric brown clouds (ABCs). A study found out that 70% of the ABCs over South Asia are made up of soot emitted from biomass burning, responsible for the melting of glaciers, climate change, and reducing sunlight, which further impacts agricultural production (Engling and Gelencsér, 2010).

NPs also play a significant role in plants by entering *via* two pathways, viz. apoplastic and symplastic, and thus interact with the cells and environment mostly using Van Der Waals, electrostatic, and stearic forces (Vera-Reyes et al., 2018). NPs-bound metal oxides are found to be one of the harmful agents for plants (Giorgetti, 2019). NPs are also one of the phytotoxic agents for plant species, besides tropospheric ozone, that affect the global food security system. NPs are believed to have adverse effects on human health as they enter *via* multiple exposure pathways such as dermal, inhalation, and ingestion (Sajid et al., 2015). These exposure pathways are known to have a direct connexion with the incipience of neurodegenerative disorders and defects in apoptosis (Chen et al., 2016). With inhalation exposure being the major pathway, NPs enter the body *via* the nasal passage where it gets deposited on the olfactory mucosa of the nasal chamber more than in any other part of the respiratory system (Seaton et al., 2010). They cause inflammatory responses and oxidative stress in the lungs, impairing the epithelial cells of the system (Rothen-Rutishauser et al., 2008; Nemmar et al., 2013). Bronchial epithelial cells are known to release interleukin 6, a pro-inflammatory cytokine, on exposure to nano-sized diesel exhaust particles (DEP) (Donaldson et al., 2007). The two most prevailing respiratory diseases, asthma and COPD, currently affecting 300 and 210 million people, respectively, across the world are also influenced by exposure to fine particles (Yhee et al., 2016). Moreover, NPs cause acute and chronic problems ranging from asthma and metal fume fever to fibrosis, carcinogenesis, and other chronic lung maladies (Bakand et al., 2012). Herr et al. (2003) also confirms that respiratory tract infections such as bronchitis, wheezing, and general health issues (tiredness, shivering, and nausea) are caused due to the presence of bioaerosols like pollen and fungi moulds in the air. In addition, some studies prove that exposure to NPs cause intestinal fibrosis, ulcers in the gastrointestinal tract, and oxidative DNA damage in caco-2 cells of the colon (Gerloff et al., 2009; Sajid et al., 2015). In low- and middle-income countries, around 4–8% of recorded mortality is solely caused by indoor smoke from solid fuel, urban air pollution, and occupational airborne particulates, after tobacco, leading to chronic respiratory diseases (Moitra et al., 2015). According to a 2009 WHO report, in India, 488,200 people die prematurely every year as a result of indoor air pollution, whereas 119,900 die prematurely every year because of outdoor air pollution. The number of deaths are increasing and alarmingly high due to rapid industrialisation, urbanisation, and change in lifestyle activities. The rapid population expansion in developing nations like India also impose a huge burden on the physical and mental health of people, especially those residing in megacities (Sonwani and Kulshreshtha, 2016; Saxena and Sonwani, 2019; Goel et al., 2021). The incidence of respiratory diseases in Delhi is 12 times the national average, and 30% of the population was found suffering from 166 different respiratory disorders (Gurjar et al., 2016). Many *in vitro* and *in vivo* models of the airway walls of lungs are used to evaluate the extent and outcome of exposure (Nakajima et al., 2007; Slezakova et al., 2013). Several countries are trying to devise measures that can reduce the adverse impacts of atmospheric pollutants (Slezakova et al., 2013; Saxena and Sonwani, 2020); however, there is a lack of studies on the effects of NPs on human health, especially in Asian countries.

Thus, the present review focuses on NPs' source, exposure, and impact on different human body systems, particularly the respiratory system. It also provides a detailed overview of the appearance of toxicological, genotoxic, and tumourigenic effects in the human body due to exposure to NPs. In particular, this is the first review that offers deep insights about the origin of atmospheric NPs, their transportation, deposition, and toxicity, which leads to hazardous diseases in humans.

SOURCES OF NANOPARTICLES

The sources of the nanoparticles in the atmosphere can be natural and anthropogenic. Details on the sources are described in **Figure 1**.

Natural Sources

About 10% of the total aerosols in the atmosphere are generated by human activity, whereas the remaining 90% of atmospheric aerosols are naturally generated (Pipal et al., 2014; Jeevanandam et al., 2018; Sonwani and Saxena, 2021). Nanoparticles are abundant in nature and are released/produced from a variety of sources, mainly from biogenic emission, sea spray, forest fire, volcanic eruption, landslide, and dust storm. Organic compounds form a large proportion of atmospheric nanoparticles because of their ability to react with clouds and air particles (Riipinen et al., 2012). Both natural and anthropogenic

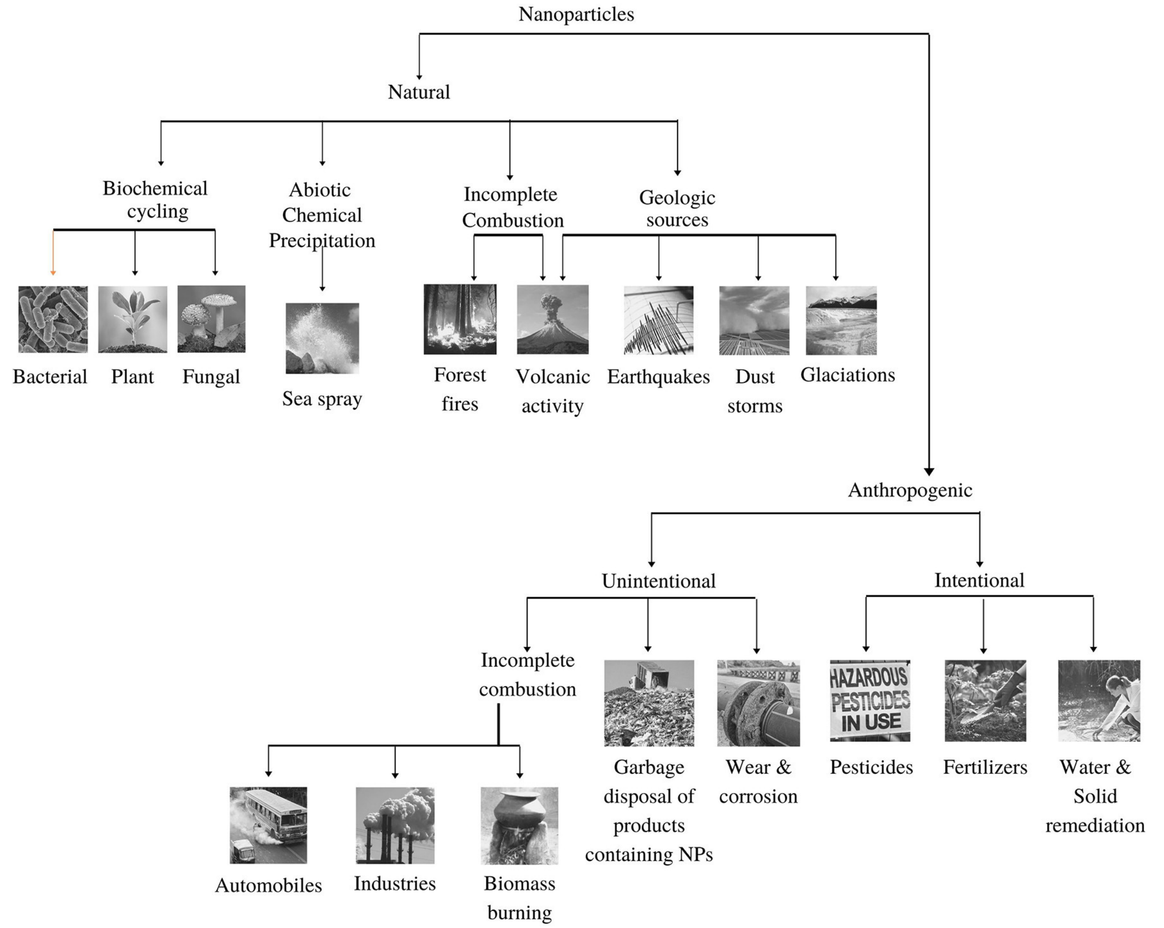

FIGURE 1 | Emission sources (Natural and anthropogenic) of nanoparticles in the environment (adopted from Buzea and Pacheco, 2017).

sources make ambient air rich in VOCs, nitrogen oxides, and primary organic aerosols, which ultimately react to form secondary organic aerosols (SOA) (Tiwari and Saxena, 2021). About 90% of the SOA formation is because of biogenic volatile organic compounds (bVOCs) that constitute about 10–40% of the global organic aerosol mass (Volkamer et al., 2006; Saxena and Kulshrestha, 2016; Sonwani et al., 2016).

The chemical composition of NPs differs significantly from place to place as it depends on the types of local sources and their relative contributions. Very few studies have investigated the contribution of NPs in different ambient atmosphere. A study in Pittsburgh mentioned that NPs are mostly composed of organic carbon (OC) and salts of ammonium and sulphate constituting 45–55% and 35–40% respectively (Kuhn et al., 2005); Another study at two sites in Los Angeles found that the composition of OC ranged from 32 to 69%, EC from 1 to 34%, sulphate from 0 to 24%, and nitrate from 0 to 4% (Sardar et al. (2005). Moreover, a study based in two sites in Helsinki trace elements (Ca, Na, Fe, K, and Zn) in higher fractions as compared with heavy metals (Ni, V, Cu, and Pb) that contribute not more than 1% of the total weight of NPs (Pakkanen et al., 2001). Furthermore, incomplete combustion and geological sources are the other significant sources of nanoparticles production in the atmosphere. Forest fires and volcanic sources are the major combustion-generated sources, whereas volcanic eruption along with earthquakes, glaciation, and dust storms are the significant geological sources (Strambeanu et al., 2015). Volcanic ash plays a crucial role in the global transport of toxic chemical species released with NPs (Ermolin et al., 2018). Ash released during volcanic eruptions has a very complex structure and comprises both solid and liquid particulate matter. With time, its composition changes due to cooling and chemical reactions (Strambeanu et al., 2015). The concentrations of toxic elements (Ni, Zn, Cd, Ag, Sn, Se, Te, Hg, Tl, Pb, and Bi) in volcanic ash NPs are seemingly higher than the total content of these elements in any other samples (Ermolin et al., 2018). The eruption of Krakatoa volcano on 27 August 1883 was a remarkable historic event where the smoke column reached 80 km in height and particles were thrown into the ionosphere. This caused strange optical effects and a decline in the global temperature by 1.5°C for the next 2 years in North America and Europe (Strambeanu et al., 2015). Likewise, the Pinatubo eruption of 1991 (Luzon, Philippines) injected vast quantities of aerosol particles, SO_2, and other sulphate particles into the atmosphere, causing a net effect of global cooling of ∼0.5°C and significant ozone depletion (Buseck and Adachi, 2008).

Anthropogenic Sources

Urban areas are identified as the centre of anthropogenic sources for NPs as compared with natural sources (Slezakova et al., 2013; Jeevanandam et al., 2018). Anthropogenic sources are classified as either intentional or unintentional. Unintentional sources include incomplete combustion (automobiles and industries), biomass burning, and the incineration of non-biodegradable wastes. Intentional sources consist of the use of pesticides and fertilisers producing a lot of NPs. Based on origin, NPs are also classified into primary and secondary sources. Primary sources include ore extraction, industrial emissions, energy production, and transport activities. Primary sources can be both stationary and mobile. Stationary sources comprise emissions from thermal power plants, chemical and metallurgical industries, and mining activities. Thermal power plants are one of the largest sources of NPs, especially in metropolises where the number of power plants are higher than in any other region like semi-urban/rural areas (Sonwani et al., 2021). The mobile sources are mostly motor vehicles, ships, submarines, aeroplanes, engines, and rockets launched into the extra-atmospheric space (Strambeanu et al., 2015).

Vehicular exhaust is a major source of NPs, released after the incomplete combustion of fuel. It is amongst the leading causes for air pollution due to the rapid rise in vehicular fleet (Walsh, 2011; Banerjee and Christian, 2018). The global vehicle population exceeded 1 billion in 2002 and has continued to climb steadily since then (Walsh, 2011). The major constituents of exhaust include carbon monoxide (CO), hydrocarbons (HCs), nitrogen oxides (NO_x), particulate matter (PM), sulphur oxides (SO_x), volatile organic compounds (VOCs), and their secondary by-products (Walsh, 2011; Banerjee and Christian, 2018). Most particles in vehicle exhaust are in the size range of 20–130 nm for diesel engines and 20–60 nm for petrol engines (Buzea et al., 2007). The sulphur content in fuel is an important parameter as it triggers the nucleation mode in PM formation (Chen et al., 2017). These emissions and ultrafine particles pose a serious risk to environmental health as they are known to produce carcinogenic effects (Banerjee and Christian, 2018).

The second major producer of anthropogenic NPs in the atmosphere are the construction and mining sectors. Surface mining and excavation through mine shafts can produce nanoparticles directly, while NPs' indirect production can occur through decantation, sedimentation, and floatation (Strambeanu et al., 2015). Meteorology and demolition methods also affect the concentration of NPs in the atmosphere. Respirable asbestos fibres, lead, glass, wood, and other toxic particles besides dust are found at the sites of demolition, and these particles can rise high up in the air, sometimes even forming dust clouds that can travel several kilometres, affecting nearby regions (Kumar et al., 2013). The inhalation of metal fumes (copper and zinc) and dust (nickel, chromium, and cobalt) causes pulmonary fibrosis and, in severe cases, cancer, which attributes to 15% of occupational hazards (Buzea et al., 2007).

Transboundary Movement of NPs

The transboundary movement of air pollutants also play an important role in increasing the pollution load in a particular area, raising the NPs' level in the atmosphere. Air mass movement from desert and ocean area significantly affects the air quality in remote locations as it carries a variety of minerals and salts along with transported fine particles (Sonwani and Saxena, 2021). For example, African mineral dust is transported to the Caribbean basin, resulting in seasonal disturbance (Buzea and Pacheco, 2017). Likewise, volcanic eruptions in Iceland in 2011 and the forest fires in Indonesia's Sumatra in 1997 caused environmental havoc in Asia, especially in Singapore and Malaysia. The transportation of fine particle emissions from anthropogenic sources have also been reported by several authors across the world, particularly in the South Asian region (Abas et al., 2019; Cheong et al., 2019; Saxena et al., 2020). Crop residue burning (CRB) is also one of the main factors responsible for the air quality degradation in neighbouring states through transboundary movement, where a large fraction of emission from CRB affects the air quality in the Indo-Gangetic Plains (IGP) (Badarinath et al., 2009a; Saxena et al., 2021a). One of the most affected regions in the IGP is Delhi, which is often affected by CRB activities in the neighbouring states of Punjab and Haryana during the kharif season (Sarkar et al., 2018b; Saxena et al., 2021a). Interestingly, Delhi's air quality has also been affected in the Rabi season due to CRB in Haryana, reported in a recent study by Saxena et al. (2021b). At present, three-fourths of the crop residue, amounting to ∼70–80 million tones, is disposed of by burning; therefore, it becomes a major source of NPs in the air and is well-known to aggravate respiratory disorders. The daily newspapers of northern India during October–November published reports on the incidences of thick clouds of smog formed due to crop residue burning by farmers, reducing the visibility that makes the Air Quality Index (AQI) severe (Badarinath et al., 2009b). In Asia, dust storms are more pronounced around the pre-monsoon period (March to early June) due to high temperatures and wind speed as compared with the other seasons. Such episodic events are largely responsible for contributing to NP pollution in downwind locations (Sarkar et al., 2018a). While in winters, low temperature, lower boundary layers, relatively stable atmosphere, and the transportation of air masses from the adjoining areas enhance the concentration of NPs in that particular area. Badarinath et al. (2009a), using multi-satellite data, reported that crop residue burning in the IGP affects the air quality over the south coast and the Arabian Sea coast of India every year with smoke columns as high as 2.5–3.5 kilometres (Pipal et al., 2014; Singh and Kaskaoutis, 2014; Ravindra et al., 2019).

INHALATION EXPOSURE AND THE EFFECT OF NPs ON THE RESPIRATORY SYSTEM

Human exposure to NPs through inhalation produces various respiratory ailments. Ezzati et al. (2004) argued that indoor air

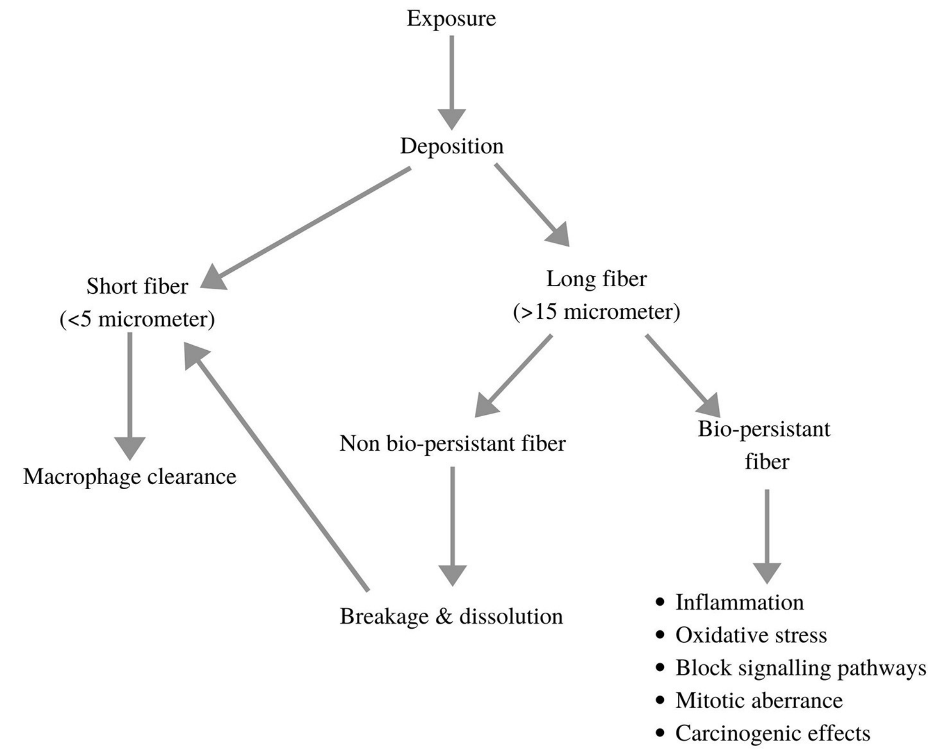

FIGURE 2 | Demonstration of clearance and deposition mechanisms of NP fibres and with their potential impacts on human body (adopted and modified from Donaldson et al., 2011).

pollution due to domestic fuel combustion acts as the eighth-largest risk factor for the global burden of disease. The indoor nanoparticle pollution in households is mainly due to the smoke from inefficient burning stoves and biomass fuels used most commonly in rural areas. Traditional practises, illiteracy, and unawareness are some of the key problems that inhibit the people of rural areas from shifting to modern *chulas* and ecofriendly fuels. The most popular fuel used for domestic cooking in rural regions is the unprocessed biomass solid fuel, known to cause 50 times more pollution than gas stoves (Ravindra et al., 2019). According to a study in rural Senegal, West Africa, out of 1,103 Senegalese women, only 1% used propane gas cylinders (combustion pollution-free) as their primary cooking equipment (Hooper et al., 2015). A 10-year long research carried out in 11 villages of Bangladesh reported 946 cardiopulmonary deaths, out of which 884 people used solid fuels and only 62 deaths were reported in gas-supplied households (Alam et al., 2012). A survey done in 15 homes in Xuanwei and Fuyuan, China, demonstrated experimentally how combustion-derived nanoparticles were generated using all kinds of stoves, while they were significantly reduced with the use of chimneys (Hosgood et al., 2012). An experimental study conducted in Uttar Pradesh, India, reported the average concentration of black carbon (an important fraction of fine particles) emissions was 6–20 $\mu g/m^3$ and 3–1,070 $\mu g/m^3$ for an urban and rural kitchen, respectively (Ravindra et al., 2019). Project Surya, carried out in India, advocated for the use of improved cookstoves widely proposed as a black carbon mitigation measure for Indian households and hence suggested a need for extensive testing and improved machinery for traditional cookstoves (Kar et al., 2012). Such eco-friendly sustainable techniques can reduce the concentration of NPs in the atmosphere.

Cigarette smoking is yet another common reason for exposure to NPs. One cigarette is known to emit almost 8.8×10^9 nanoparticles. Pertaining to the high particle concentrations and the rapid dilution in air, studies on identifying different types of particles present in cigarette smoke are limited. A study in Netherlands experimentally proved how a longer duration of puff and higher concentrations of tar values in one cigarette contribute directly to a large number of NPs (Williams et al., 2013). Adam et al. (2009) demonstrated the increase in NPs in low-ventilation conditions. They also studied how NP concentration was directly proportional to the number of puffs from a cigarette. Studies suggest an increased incidence of cancers, increased body mass index (BMI), and lower lung function in passive smokers than non-smokers (Gordon et al., 2002; Mohammad et al., 2013). Benzene, 1,3-butadiene, and particulate-bound 2,5-dimethylfuran (DMF) are human carcinogens that showed increased levels in non-smokers due to cigarette smoke exposure, thereby proving the adverse effects of passive smoking (Gordon et al., 2002). Occupational health hazards due to exposure to NPs are a common problem rising in developing and under-developed nations. Elevated cases of respiratory and cardiovascular disorders have been recorded in traffic officers due to their excessive exposure to vehicular exhaust. A collaborative study done by India and the

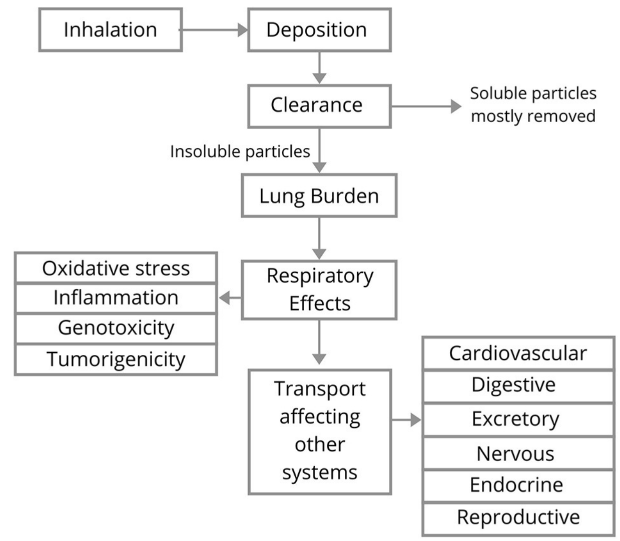

FIGURE 3 | Overview of pathway of nanoparticles from inhalation to disease site.

United Kingdom in 2017, wherein various medical tests of 532 traffic officers (exposed to atmospheric NPs) were compared with 150 office workers (working in indoor environments), reported 50% increased cases of thick sputum, pain in joints, and shortness of breath in traffic officers (Bajaj et al., 2017). A similar study conducted in Kathmandu, Nepal, observed increased levels of inflammatory interleukins and tumour necrosis factor (TNF-α) in traffic officers (Shakya et al., 2019). NPs released from welding, flour dust, and diesel exhaust have long-term inflammatory and carcinogenic effects. Welding fumes contain large quantities of partially oxidised, ionised, and reactive metallic nanoparticles (Nasterlack et al., 2008). Another study suggested that the exposure to NPs can cause the production of reactive oxygen species (ROS), cytotoxicity, genotoxicity, and stimulation of ToxTracker reporter cell lines (Bajaj et al., 2017). Asbestos fibre (in all its commercial forms) is classified as one of the potential carcinogens by the International Agency of Research on Cancer (IARC) (Donaldson et al., 2011). Tungsten carbide-cobalt dust fumes (WC-Co particles) released during mining and drilling showed deposition in keratinocytes (epidermal cells; skin cell), DNA damage, inhibition of DNA repair, and alterations in gene expression and cell function after short-term exposure (Armstead and Li, 2016). Donaldson et al. (2011) determined the bio-persistence of different size fractions of occupational fibres in several human body systems. Longer slender fibres are usually more persistent, thereby causing various health hazards in our body. **Figure 2** illustrates the clearance and deposition mechanisms of these fibres in our body and their potential impacts on humans. The detailed impact of nanoparticles from inhalation to disease site is described in **Figure 3**.

Mechanism of Exposure to NPs

Authors provide detailed insights about the NP's inhalation, deposition, clearance, and impacts on the respiratory system and related human body systems. A summary of the effects of NPs on various organs and organ systems of the human body are mentioned in **Table 1**.

Inhalation

Human lungs have an internal surface area between 75 and 140 m^2 and about 3,00,106 alveoli (Buzea et al., 2007). Lungs have a direct contact with the outside environment and hence acts as the main gateway for the entry of nanoparticles into the body. They are also considered important and the primary target site to study the effects of nanoparticles (Bakand et al., 2012; Pacurari et al., 2016).

Air is inhaled *via* nasal and oral routes that pass through the pharynx, progresses into the tracheobronchial tree, and finally reaches the alveoli. The transport of particles dependent on the structure of the respiratory airway, which can be described using the Weibel bifurcating tubes' model, classified into the conducting zone and respiratory zone, as already described in detail. Owing to their small size and high retention time, NPs can diffuse and accumulate in the alveolar region and some may pass through the alveolar epithelium and capillary endothelial cells to enter the cardiovascular system and other internal organs (Buzea et al., 2007; Qiao et al., 2015). Furthermore, electron microscopy proves that the penetration of nanoparticles can occur in both the outer and inner cellular compartments, deep inside the cytoplasm and karyoplasm of pulmonary epithelial and mesothelial cells of the lungs (Bakand et al., 2012).

Deposition

The site of NP deposition in the respiratory tract depends on the particle's aerodynamic diameter (Ferreira et al., 2013). Many fibres with larger diameters are mostly deposited at the "saddle points" in the branching respiratory airways. Thus, they are unable to penetrate deep into the respiratory tract (Buzea et al., 2007). For smaller particles, deposition is mostly governed by Brownian movements. Energy filtering transmission electron microscopy (EFTEM) provides the evidence that aerosol NPs of 20 nm size, within 24 h of inhalation, bypass most of the clearance mechanisms and get deposited in the alveolar region of the lungs (Geiser, 2010).

According to the classical model developed by the International Commission on Radiological Protection (ICRP), NPs ($\leq$20 nm diameter) have a high probability to reach the alveolar region (Kreyling et al., 2006; Ferreira et al., 2013). Thus, particles larger than 20 nm in diameter are restricted in the previous sections of the respiratory tract through mucociliary escalation and macrophage activity. Such activities help with the clearance of particles in the tract before they enter the pulmonary region.

Clearance

The deposition is chiefly determined by particle size, the ventilatory parameters, and airway characteristics, whereas the clearance of particulate compounds, once deposited, is dependent on the physicochemical characteristics of the compound. During inhalation, larger particles are deposited at the extra-thoracic region (nose and larynx) and intrathoracic

TABLE 1 | Summary of effects of nanoparticles on various organs and organ systems of the human body.

S. No.	Biological system	Target organ	Effect of nanoparticles	References
1.	Respiratory system	Lungs	Inflammation Oxidative-stress Genotoxicity Tumorogenicity	Clift et al., 2011 Sharma et al., 2012 Zhu et al., 2013 Stueckle et al., 2017
		Alveoli	Activation of macrophages causing pro-inflammatory cytokine release	Nho, 2020
2.	Digestive system	Stomach	Increased mucus production and Inflammation	Georgantzopoulou et al., 2015
		Intestine	Accumulation in lamina propria and degenerating goblet cells	Zhang et al., 2014
3.	Cardiovascular system	Heart	Increased blood pressure and decreased heart rate	Yu et al., 2016
			Increased ROS production leading to oxidative stress	Miller et al., 2012
			Heart muscle fibre degeneration and cellular necrosis	Yu et al., 2016
		Endothelial lining	Inhibition of NO pathways and vasoconstriction	Mills and Miller, 2011
4.	Excretory system	Kidneys	Accumulation in Proximal convoluted tubules	Pujalté et al., 2011
			Nephrotoxicity and DNA-Damage	Sramkova et al., 2019
			Shrinkage of kidney cells and nuclear condensation leading to oxidative stress	Wang et al., 2009; Pujalté et al., 2011
			Cytotoxic effects on glomerular and renal cells	Pujalté et al., 2011
		Epithelial lining	Cytotoxcity in HK-2 cell lines of the lining	Pujalté et al., 2011
5.	Neural system	Brain	Accumulation and effecting expressions of genes	Yang et al., 2010
			Apoptosis, cell cycle alterations and oxidative DNA damage	Valdiglesias et al., 2013
			Inflammation and hormone imbalance	Haase et al., 2012; Feng et al., 2015
6.	Reproductive system	Ovary	Decrease in tissue weight and abnormal cell structures	Asadi et al., 2019
		Testes	Inflammation and cytotoxicity	Santonastaso et al., 2019
		Gametes	Loss of integrity of sperm DNA	Santonastaso et al., 2019
			Problems in the process of oogenesis leading to hormone disbalance	Iavicoli et al., 2013
		Epithelial lining	ROS-Overproduction, Oxidative stress and Apoptosis	Iavicoli et al., 2013
7.	Endocrine system	Thyroid	Overproduction of T-3 Thyroid hormone and decrease in thyroid-stimulating hormone	Jiang et al., 2019
		Hormone receptors	Blockage of signal cascades, Overstimulation of hormones	Leso et al., 2018
		EDCs (Endocrine-disrupting chemicals)	Cytotoxicity and imbalance in production	Iavicoli et al., 2013; Lu et al., 2013
		Kidney	Degrading effects on testes and kidney hormones	Li et al., 2009
		Liver	Elevated serum levels of • Alanine aminotransferase • Alkaline phosphatase Lipid peroxidation and pathological lesion	Miller et al., 2012; Sharma et al., 2012

bifurcations due to impaction. These upper respiratory airways are covered with mucus (a complex fluid containing mucins [hydrogel-forming glycoproteins] that protect the body from environmental influences) (Moller et al., 2004; Kirch et al., 2012). This mucus layer traps the large particles, which are transported out by ciliary beating, removing the inhaled NPs, making it the dominant pathway of clearance from the regions of trachea, bronchus, and upper bronchioles (Moller et al., 2004; Geiser, 2010; Kirch et al., 2012). The outer viscoelastic mucus blanket has an underlying periciliary layer that provides conditions for an efficient ciliary beating cycle. The tips of the cilia reach the mucus blanket and accelerate this layer by a coordinated beating (Kirch et al., 2012). Upon entering the pharyngeal region, the mucus along with the NPs are finally swallowed and undergo further processing in the gastrointestinal tract (Henning et al., 2010). Smaller particles penetrate deep inside the lungs where air velocity decreases substantially and are deposited in the bronchioles and alveoli. This is the site where

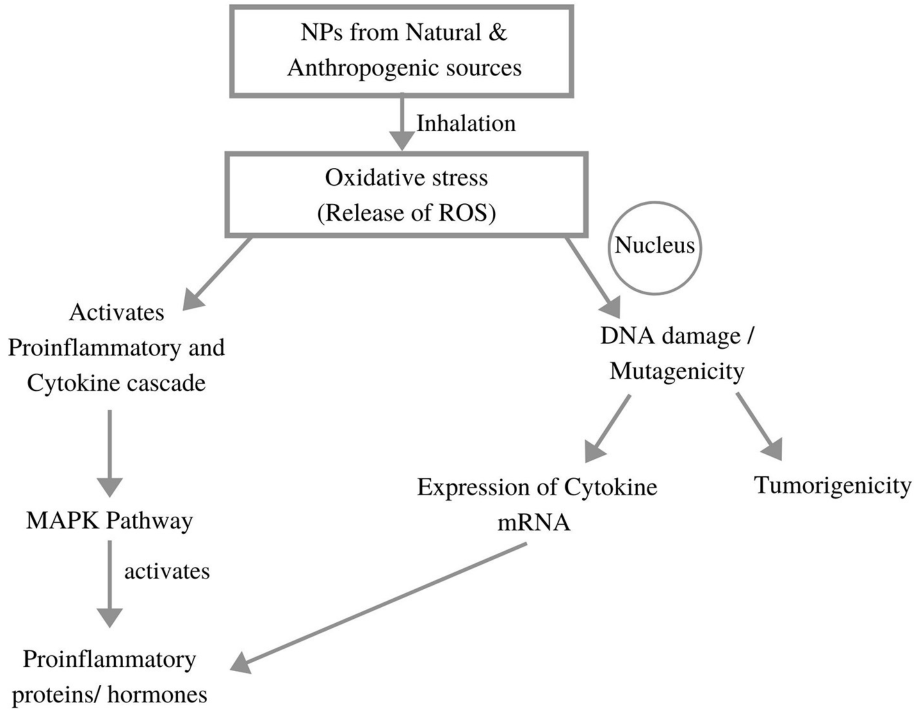

FIGURE 4 | Impacts of nanoparticle generated toxicity to the human body (adopted from Li et al., 2010; Chakraborty et al., 2018).

NPs undergo mucus transport and macrophages participate in the phagocytosis of biogenic NPs like viruses, protozoans, and bacteria (Moller et al., 2004). Macrophage-associated clearance is a much slower process as compared with mucociliary clearance (Henning et al., 2010). Most of these NPs translocate to the connective tissues and involve in the blood circulation, bringing the NPs in contact with the macrophage populations in the non-alveolar region. NPs are mostly cleared by interstitial and intravascular macrophages, as surface macrophages are relatively less effective in NP clearance (Geiser, 2010). After the inhalation and deposition of NPs on the surfactant layer with the underlying epithelial lining fluid, they come in contact with several proteins and biomolecules (including opsonins that enhance phagocytosis by marking an antigen), which makes NPs more susceptible to macrophages. It was observed that there was less phagocytosis in the absence of opsonins; moreover, rapid phagocytosis by alveolar macrophages was reported in the case of opsonin-directed migration towards the NPs (Kreyling et al., 2006).

Lung Burden

A significant difference is observed in the behaviour and clearance of soluble and insoluble NPs in the lungs. Soluble NPs dissolve in the aqueous fluid and further goes into the cardiovascular systems. In contrast, the insoluble NPs (black carbon) are removed through mucociliary escalator or macrophage phagocytosis (Buzea et al., 2007). It has been reported that the insoluble NPs cause more tissue damage, inflammation, and lung tumours (Ferreira et al., 2013). The insoluble NPs accumulate more rapidly, exceeding the macrophage clearing capacity, and hence the defence mechanisms of the lungs fail to operate, resulting in lung injury (Buzea et al., 2007). It was also observed that acute lung inflammation is induced by the production of IL-1β and TGF-β1 for a shorter period in the bronchoalveolar lavage fluid. However, a longer exposure duration leads to collagen production, causing lung burden and potential pulmonary fibrosis (Lin et al., 2014).

Human health hazards due to lung burden is directly associated with the increasing cases of premature mortality, especially in developing nations. The determination of lung burden is dependent on the rate of particle deposition, rate of clearance, and residence time of the NPs (Buzea et al., 2007). Morphological observations and retrospective evidence indicate a slower particle clearance of insoluble NPs in large mammalian species (humans and primates) and a greater tendency for retained lung burden, which can translocate from the original alveolar deposition sites to the interstitial compartment of the respiratory system (Warheit, 2004). A long-term exposure to NPs causes high lung burden that leads to carcinogenesis in the lung tissues (Buzea et al., 2007). However, this level of exposure rarely happens in humans, suggesting lower chances of acquiring the malady (Donaldson and Poland, 2012).

Nano-Toxicity

Figure 4 explains the impact of toxicity generated through NP inhalation on human body. Human lungs constitute pseudostratified epithelium in the lung–blood stream barrier. The airways are composed of thin columnar epithelium, together with the bronchial epithelium (3–5 mm) and bronchiolar epithelium (0.5–1 mm), that all protected with mucous layer (Praphawatvet et al., 2020). The lung tissue consists of more than 40 different cells, so to study the aggregated effect of NPs on lungs, different cell models were made and tested. The exposure to NPs primarily affects the epithelial lining of the respiratory system, where A549 cell lines (derived from the human adenocarcinoma of the lung) are most often used in toxicity testing, and Calu-3, 16HBE14o-, and BEAS-2B cell lines are used as models for the bronchial barrier system (Fröhlich and Salar-Behzadi, 2014).

The size of NPs is inversely proportional to the damage they cause in the respiratory tract, as smaller particles easily reach and get deposited in the distal parts of the respiratory tract (Donaldson et al., 2005).

Four main types of toxicological effects of nanoparticles are discussed as follows:

- Oxidative Stress
- Inflammation
- Genotoxicity
- Tumourigenicity

Oxidative Stress

Oxidative stress is the prime consequence of nano-toxicity that occurs due to the imbalance between free radicals and antioxidants in the body in such a way that the extra free radicals with uneven number of electrons react inadvertently with other molecules to produce an imbalance in the respiratory system (Sharma et al., 2012).

Reactive Oxygen Species (ROS) Generation. The production of ROS is one of the important oxidative steps for creating toxicity in human lungs. The overproduction of ROS is caused by NPs' activity in the mitochondrial electron transport chain of the cell (Donaldson et al., 2010). Metallic NPs trigger Fenton-type reactions causing free-radical-mediated toxicity, and carbon NPs are known to affect mitochondrial reactions (Martin and Sarkar, 2017). The increased potential of hydrogen peroxide (H_2O_2) (due to special oxygen transfer properties of some metals) causes the generation of highly reactive hydroxyl radicals ($OH^{\cdot}$), and this process is called as Fenton's reaction (Li et al., 2008).

$$Fe^{2+} + H_2O_2 ----> Fe^{3+} + OH\cdot + OH^-$$
$$Fe^{3+} + H_2O_2 ----> Fe^{2+} + OOH\cdot + H^+$$

The extent of ROS production (produced by a particular NP) depends on the catalytic activity of surface groups. In a particle of 30 nm in size, about 10% of its molecules are expressed, whereas in the case particles of 10 and 3 nm in size, only around 20 and 50% molecules are expressed respectively (Hao and Chen, 2012).

The deposition of nanoparticles leads to the formation of molecular oxygen-dependent superoxide anion radicals (O_2^{2-}), H_2O_2, and hydroxyl radicals ($OH^{\cdot}$). These chemical species are proven to have cytotoxic responses in BEAS-2B bronchial epithelial cells. It was also reported that inflammatory phagocytes (macrophages and neutrophils) are also released from the respiratory system in response to NPs. Such inflammatory phagocytes induce oxidative outburst as a defence mechanism and ultimately raises the number of ROS in that particular region (Martin and Sarkar, 2017).

The Creation of Oxidative Stress. Oxidative stress is caused in the body either due to the overproduction of ROS or by the weakening of the processes of antioxidant defence. Another factor that determines the presence of oxidative stress in a region is the GSH/GSSG ratio, i.e., the cellular glutathione/glutathione disulphide ratio. Low values of this ratio indicate stress and toxicity in the tested region, where stress is created when lower quantities of glutathione are present and glutathione disulphide accumulates (Nel et al., 2006; Hao and Chen, 2012).

An *in vitro* study by scientists in Korea on BEAS-2B cell lines clearly indicated a rise in oxidative stress due to silica nanoparticle exposure as well as the induction of HO-1 (heme oxygenase-1—an antioxidant enzyme) *via* the Nrf-2–ERK MAP kinase signalling pathway, which suggests how oxidative stress disrupts the ROS balance of the cells (Huang et al., 2010). Meanwhile, in another study done in the United States, oxidative stress caused by ZnO NPs was directly linked to the increased calcium levels in cells, causing cellular dysfunction, impaired signal transduction, and other diseased states (Nho, 2020). Scientists have raised concerns over the inadequate results pertaining to NP exposure gained by *in vitro* models and have therefore adapted a more realistic approach by switching to *in vivo* models to study these xenobiotics (Ursini et al., 2014).

A study conducted in China in 2012 on the different organs of carp (*Cyprinus carpio*), wherein three different concentrations of 0.5, 5, and 50 mg/L of zinc oxide (ZnO) nanoparticles were tested for their effects on the concentrations of antioxidant enzymes (e.g., superoxide dismutase [SOD], catalase [CAT], etc.) before and after administration, indicated an increased mucus production and apoptosis of cells at higher concentrations and exposure time of ZnO NPs (Cho et al., 2012). TiO_2 nanoparticles on a 90-day exposure increased the concentration of ROS as well as the level of lipid peroxidation and therefore decreased the antioxidant capacity of the lungs, leading to the creation of oxidative stress, which is the direct cause of inflammation and genotoxicity (Lu et al., 2014). Oxidative response is directly linked to inflammatory response as it is proven to cause chronic inflammation. The macrophages of the immune system are known to produce free radicals (the cause of oxidative stress) and pro-inflammatory hormones. A mitogen-activated protein kinase (MAPK) pathway activates and produces transcription factors that ultimately produce proteins responsible for inflammation, cell stress, cancer in the cell, etc.

Inflammation

Our immune system is divided into innate and adaptive immune systems. The innate immune system is the first line of defence against any foreign particle encountering on entering the body. If the innate immune system is not able to deactivate the foreign particle (antigen) on its own, it then induces the adaptive immune system, which is much more complex and effective. This activation is carried out by the dendritic cells in the body. Nanoparticles, being foreign particles, also activate dendritic cells, which in turn generate

ROS, cytokines, and chemokines and activate naïve T-cells and various inflammasomes.

Determinants of Inflammation. NPs elicit an inflammatory response in the respiratory system as well as the other systems of the body (Medina et al., 2007; Clift et al., 2011; Padmanabhan and Kyriakides, 2015). A well-known determinant of an NP's ability to cause inflammation is the zeta potential (ξP) of the particle. ξP is the electric potential created when charged groups (present at the surface of a particle) interact with the suspension medium. Since the medium in human body is acidic, if more positively charged groups are present on the surface, more will be the solubility of that particle in the medium and hence there will be more interaction with macrophages, leading to inflammation (Schins, 2013). Magnesium and zinc oxide nanoparticles show high solubility in these solutions. A study reported that non-biodegradable NPs and cationic polymers induce even more inflammation than biodegradable and anionic makeshifts as titanium- and silicon-based NPs induce more inflammation than zinc (Nishi et al., 2020).

The presence of white blood cells (WBCs) in blood is another measure used to determine the presence of inflammation in the body. Inflammation is noticed based on the increase in WBC count above the normal range, which signals a decreasing immunity. When NPs enter *via* inhalation, their deposition in the lungs leads to the release of pro-inflammatory hormones, and they encounter alveolar macrophages (as they constitute the first line of immunity). Thus, the inactive macrophages become activated to stimulate the movement of various types of pro-inflammatory cytokines (IL-1 family, IL-6, IL-8, and i-CAM pro-inflammatory protein expression) to the affected site (Clift et al., 2011; Foldbjerg et al., 2011). An experiment was performed in the United Kingdom using eight different metal oxides in an *in vivo* rat model to investigate the effect of exposure on bronchoalveolar lavage fluid (BALF). This study reported that the cerium and nickel metal oxides are associated with an immediate neutrophilic cytotoxicity pattern, wherein the increased levels of IL-1β, MIP-2, and LDH indicate neutrophilic inflammation, and the same has been observed for copper and zinc by the end of 4 weeks of exposure (Magdolenova et al., 2014). Another study demonstrates that particle size is directly linked to inflammation, and this has been proven by an experiment performed on rats, wherein they were exposed to equal masses of titanium dioxide in two particle size ranges, showing more retention of ultrafine particles in the lung interstitium and the development of an increased inflammatory response (Peters et al., 2007). It was also reported that A549 cells (human alveolar carcinoma cells) were used to detect the change in cytokine secretion after treating the cell lines with TiO_2 NPs and an increased release of the pro-inflammatory hormone interleukin-6 (Medina et al., 2007). Moreover, an *in vivo* experiment with nickel oxide NPs on rats' lungs found that chronic lung inflammations persist for long durations after exposure (Brown et al., 2001). A similar study done by Padmanabhan and Kyriakides (2015) showed that rats exposed to C13 ultrafine particles were deposited more in olfactory bulb on Day 7 than on Day 1, which clearly indicates how these particles get circulated in the body after inhalation.

The Adverse Effects of Inflammation. Inflammation results in the destruction of cilia in the respiratory tract and hence impairs the movement of mucus (mucus basically traps infectious agents and dirt) through cilia. Inflammation also leads to epithelial injury by breaking the epithelial barrier between the lung surface and blood stream, leading to clotting, decreased lung function, the impaired circulation of blood and oxygen in the body. Pneumonitis and the inflammation of lung tissue are the symptoms of lung cancer, pulmonary fibrosis, chronic obstructive pulmonary disease (COPD), asthma, and cystic fibrosis. Various types of pulmonary fibrosis are the main causes of death in patients diagnosed with chronic lung diseases (Chen et al., 2006). This has been proved in a study done on rats, wherein they were exposed to a long multi-walled carbon nanotube for 30 days, which showed the presence of irreversible granuloma, considered as chronic inflammation in lungs (Lu et al., 2014). Inflammation also results in blood clotting, which activates thrombosis cascade at different locations, ultimately leading to problems in the cardiovascular system, upsetting the cardiac rhythm and increasing the chances of cardiac arrest in the body (Donaldson et al., 2005).

Genotoxicity

Genotoxicity can be induced either by the direct interaction of NPs with DNA or indirectly because of oxidative stress or inflammation. Based on different studies and consequent effects, genotoxicity can be divided into primary and secondary genotoxicity. Primary genotoxicity occurs when ultrafine particles enter the nucleus and cause modifications in DNA. Another primary indirect mechanism is related to the DNA repair cascade. Secondary genotoxicity is caused by oxidative stress and inflammation induced by NPs (Zhu et al., 2013; Magdolenova et al., 2014). **Figure 5** shows silica NPs' deposition in the lungs (via p53 signalling) and the related genotoxicity involved in the tumour formation in rats.

Primary Genotoxicity

Direct Primary Genotoxicity

The oxidation of DNA results in mutagenic modifications such as the hydroxylation of adenine and guanine, thereby leading to the formation of DNA adducts (Donaldson et al., 2005; Berube et al., 2007). DNA adducts are a result of the covalent modifications in DNA in the presence of certain carcinogens. Particulate carcinogens such as asbestos, crystalline silica, etc., have the ability to directly enter the cellular membranes and nucleus. They then interact/disrupt the process and functionality of the different components of the mitotic spindle and ergo produces dysfunctionalities (Magdolenova et al., 2014). These foreign NPs can disrupt all cellular processes including mitosis, the replication of DNA, and the transcription of DNA into mRNA. A study reported that aluminium NPs induced structural damage and DNA instability, besides other mechanisms that explained the DNA damage (including single-strand breaks and double-strand breaks), DNA deletions, and genomic instability

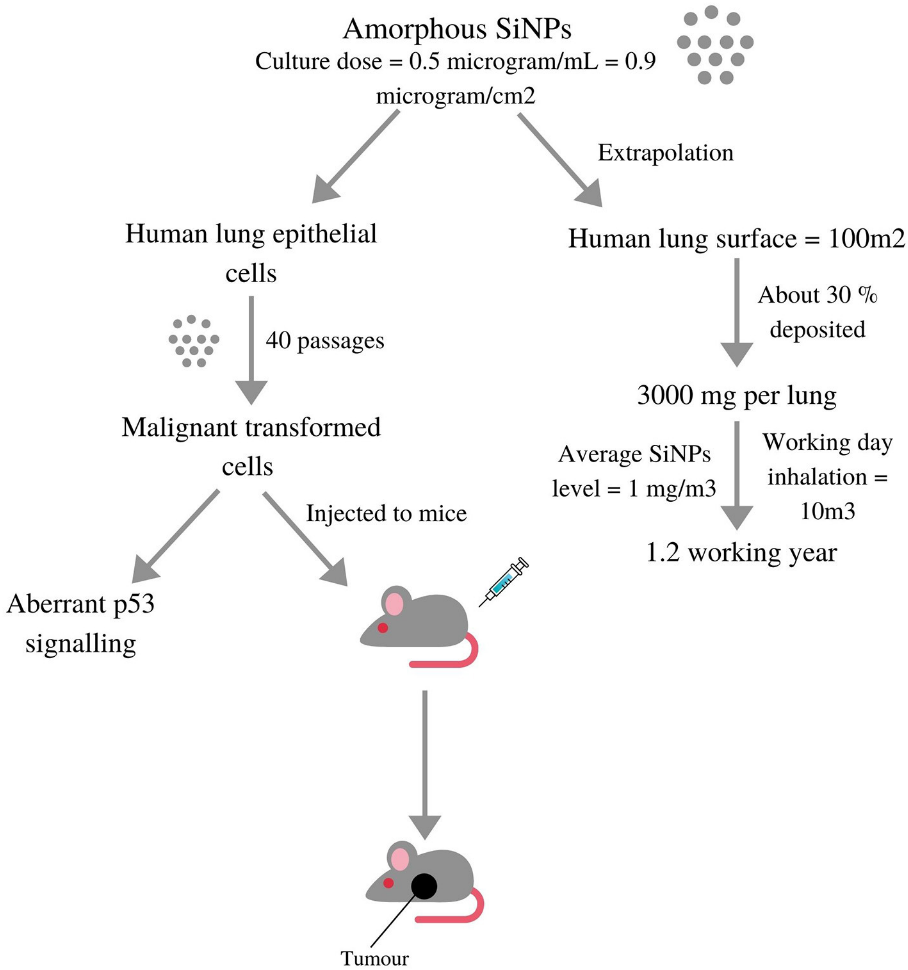

FIGURE 5 | Diagrammatic depiction of a study where Silica nanoparticles were deposited in lungs *via* p53 signalling and then tested *in-vitro* on lung cell models as well *in-vivo* on live rats induced aberrant p53 signalling and malignant tumours, respectively (adopted from Stueckle et al., 2017).

in the form of an increase in 8-hydroxy-20 -deoxyguanosine levels (Donaldson et al., 2013; Chakraborty et al., 2018). Cobalt-chromium nanoparticles significantly increased single- and double-strand breaks and the chromosomal aberrations in mice on exposure, consequently affecting the brain cells in the resulting offspring (Clift et al., 2011).

Indirect Primary Genotoxicity

In the indirect method, NPs attach to the nuclear proteins responsible for DNA repair mechanisms, disrupting their functioning and hence indirectly favouring slip-ups in the nuclear processes. Topoisomerases are the enzymes responsible for carrying out this repair cascade. An experiment showed that Carbon-60 fullerenes can bind to human topoisomerase-II alpha in the ATP-binding domain and therefore disturb its enzymatic activity (Donaldson et al., 2013; Magdolenova et al., 2014).

Secondary Genotoxicity

Secondary genotoxicity refers to the errors created in the structure and function of nuclear components due to the increased ROS production and inflammation, ultimately leading to disrupted DNA sequences. Nanoparticles trigger ROS production in phagocytes (macrophages, neutrophils, etc.), which induces DNA damage and mutagenesis in the neighbouring cells (Donaldson et al., 2013; Magdolenova et al., 2014). It has been reported that in any mechanism, silica triggers the production of ROS leading to the activation of NF-kβ (necrosis factor) and AP-1 (primarily in gene expression), causing an increase in the quantities of growth factors and oncogenes that causes mutations and ultimately cancer (Hong et al., 2017). Exposure to diesel exhaust particles produces inflammation, leading to epigenetic changes that include impairment in gene expression, the formation of adducts, cell proliferation, and interruptions in DNA repair (Shi et al., 1998). In another experiment, researchers demonstrated how the A549 cell line (present in alveoli) is more susceptible to DNA damage than the BEAS-2B cell line (present in bronchi) using FPG comet assay (Medina et al., 2007). A study undertaken in Denmark on the A549 cell lines clearly demonstrates that silver NPs induce oxidative stress correlated to cytotoxicity and genotoxicity (Berube et al., 2007).

Tumourigenicity

The MAPK/ERK pathway (also known as the Ras-Raf-MEK-ERK pathway) is a chain of proteins in the cell that communicates a signal from a receptor on the cell's surface to the DNA in the cell nucleus. The signal starts when a signalling molecule binds to the receptor on the cell surface called epidermal growth factor receptor (EGFR). In normal state, extracellular ligands such as epidermal growth factors bind to this receptor and phosphorylates activates it, signalling a cascade of docking proteins that ultimately result in the making of mRNA, which gets encoded to form various proteins.

In this case, ROS and sometimes direct NPs interact with these receptors, and abnormal proteins could either be formed or not due to the changes in the DNA code. When one of the proteins in the pathway mutates, it can become stuck in the "on" or "off" position, which is a fundamental step in the development of many cancers. The entry of NPs plays a major role in increasing the levels of 8-hydroxy-2′-deoxyguanosine (8-OHdG) in the body. 8-OHdG can give rise to G-to-T transversion mutations in the key genes known to be involved in the development of cancer, hence giving rise to tumours (Guo et al., 2017). Thus, an excessive level of 8-OHdG is directly proportional to the occurrence of carcinogenicity that weakens the immunity. A study observed the levels of 8-OHdG in the urine and white blood cells of 130 workers handling indium tin oxide who were easily exposed to metal oxide NPs (Falcone et al., 2018). Other pathways include p53 inactivation and caveolin-1 overexpression. p53 inactivation occurs when NPs decrease the phosphate levels (required to activate proteins) in cells and therefore increase the chances of tumour formation (Stueckle et al., 2017). Likewise, there are many proteins that are found in high concentrations in the body in the presence of a tumour, and such high levels of proteins are often used to test the presence of neoplasm (the abnormal growth of cells). Caveolin-1 protein's overexpression is associated with carcinogenesis and metastasis. A study reported the inhalation exposure to Titanium oxide NPs on mice, wherein an increased level of squamous cell carcinoma antigen (SCC-Ag) (tumour marker) was observed in high concentrations due to the formation of tumours (Shi et al., 1998).

Tumour suppressor genes in the body are responsible for expressing proteins that prevent the uncontrolled growth of cells forming tumours and hence the decrease chances of genomic mutability. Mutated tumour suppressor genes due to the genotoxicity caused by NPs aren't able to carry out their function, eventually leading to the loss of growth regulation (Luanpitpong et al., 2010). Liou et al. (2017) identified the appearance of cancer stem-like cells on chronic exposure to carbon NPs. Ceria NPs have an ability to generate ROS and cause DNA damage, leading to alveolar papillary neoplasm and carcinoma. Carcinoma also depends on particle size, bio-persistence, and the co-morbidity in an individual. Other recent *in vivo* studies confirm that the iron oxide NPs as an important cause of hyperplasia and fibrosis of the lungs (Manke et al., 2013). Thus, an excessive increase in fibrosis leads to the death of an individual. Chromium, nickel, and iron oxides released with NPs from welding fumes act as major carcinogens for the human body that significantly increase the chances of tumour formation (Chen et al., 2006).

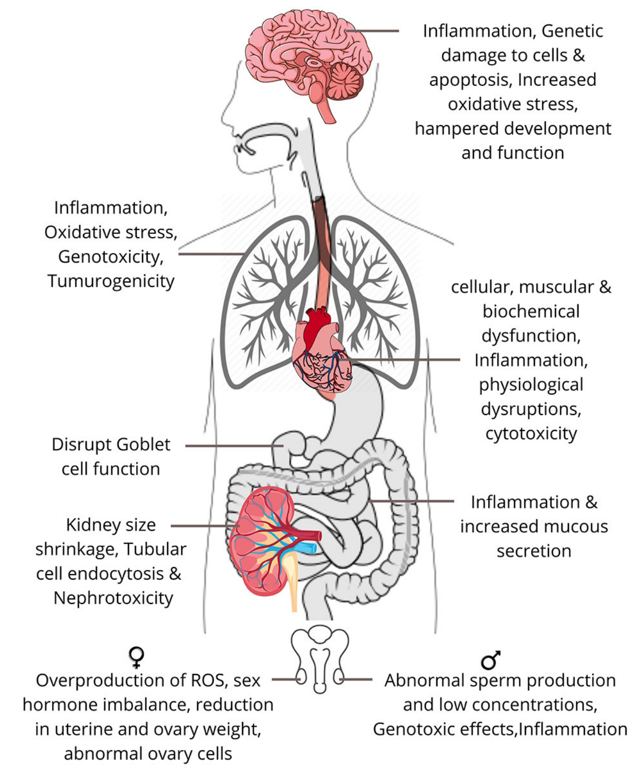

FIGURE 6 | Impact of Nanoparticles on various systems of the human body.

EFFECT OF NANOPARTICLES ON OTHER SYSTEMS

As discussed previously, the respiratory system is one of the most important pathways for the entry of airborne pollutants into the body and the distribution of NPs to the other biological systems of the body. The retained NPs in the lungs come in contact with the alveoli–blood barrier (present between the alveoli of the lungs and the transporting vessels of the circulatory system), which helps in the exchange of gases stored by alveoli to the entire body and vice versa by the process of diffusion of air particles. The retained NPs seep into these vessels through endocytosis in the alveolar epithelial cells and get transported to the other organs *via* blood. Endocytosis is a process by which a cell transports particles in and out of the cell by the formation of vacuoles. The second mechanism involves in the diffusion of these ultrafine particles into the olfactory bulbs of neurons *via* the nasal epithelial barrier for reaching the central nervous system of the body. This system is spread throughout the body and therefore the NPs travel and get deposited in distant places of the different systems of the body (Iversen et al., 2011; Elsaesser and Howard, 2012). **Figure 6** shows the impact of exposure to NPs on the different systems of the human body.

Effect of Nanoparticles on the Digestive System

The digestive system also called as the gastrointestinal tract consists mainly of the oesophagus, stomach, and intestines. NP exposure to the gut mostly occurs either through water or food intake. The presence of silver NPs increases the interleukin-8 levels, directly linked to inflammation and increased mucus production (Georgantzopoulou et al., 2015). Depending on their size, some NPs escape the junctions between the intestinal epithelial cells to enter blood vessels, perturbing the mucus and epithelial cell layers. Furthermore, they finally accumulate in the lamina propria of the intestines where they disrupt the function of goblet cells (Zhang et al., 2014). If there are already underlying conditions such as Crohn's disease or ulcerative colitis in the individual, then the rate of NP accumulation is even higher, leading to inflammation in the intestinal areas (Lomer et al., 2004; Jones et al., 2015). Consequently, the toxicity levels get increased and will lead to colon cancer and other carcinomas.

Effect of Nanoparticles on the Cardiovascular System

NPs can enter our body *via* inhalation (intranasal or intra-tracheal) or by oral exposure to the gastro-intestinal tract, which subsequently reaches the circulatory system. These can cause significant alterations in the normal functioning of the system. The increase in blood pressure, decrease in heart rate, and altered vascular tone and dysfunction are some of the initial effects of NPs on the cardiovascular system (Yu et al., 2016). Depending upon the physical properties, concentration, and retention time of NPs, they can have angiogenic/antiangiogenic, vasodilation/vasoconstriction, pro-oxidant/antioxidant, cytotoxic, apoptotic, and phagocytic effects on our body (Gonzalez et al., 2016). Individuals with pre-existing cardiovascular diseases are more susceptible to these changes. Such persons are more prone to sudden cardiac arrests, heart attacks, and blood clotting due to the assimilation of NPs in the blood stream. Epidemiological studies have revealed evidence of both the acute and chronic effects of NPs (Donaldson et al., 2013). An increased ROS generation because of nanoparticles has been observed as the main cause for these maladies due to the increased oxidative stress (Miller et al., 2012).

Silver NPs that are currently used in pacemakers, drugs, and coupled antibodies have a dual and opposite effect on blood composition, angiogenesis (vessel formation), and the permeability of membranes (Gonzalez et al., 2016). Long-term exposure to TiO_2 NPs can lead to their accumulation in the heart, causing sparse cardiac muscle fibres, inflammation, cellular necrosis, and cardiac biochemical dysfunction. A study on SiO_2 NPs in old rats suggested increased Fbg concentrations and blood viscosity along with myocardial ischemic damage and atrioventricular blockage (Yu et al., 2016). Experiments performed on rodents by Mills and Miller (2011) support the aforementioned results and also provide evidence to endothelial cell dysfunction, the inhibition of NO pathways, and the enhanced responsiveness to vasoconstrictors.

Effect of Nanoparticles on the Excretory System

The kidney contains a network of blood capillaries in each nephron that philtres the toxins from blood; therefore, it is quite susceptible to xenobiotics and the bioaccumulation of toxins (Pujalté et al., 2011). NPs, after glomerular filtration, tend to concentrate in the proximal convoluted tubules (PCT), which can lead to internalisation *via* tubular cells through endocytosis. A study on TH1 cells exposed to inorganic NPs showed not only the acceleration of NP-induced nephrotoxicity but also the DNA damage in these cells (Sramkova et al., 2019). Similar effects were observed by another study when tubular cells in mice were exposed to copper NPs (Pujalté et al., 2011). This will further lead to genetic disorders and chromosomal aberrations in the genetic material.

Wang et al. (2009) observed that the smaller the particle, the greater its toxicity. This study on HEK293 cells (cultured human embryonic kidney cells) demonstrated that kidney cells underwent shrinkage and nuclear condensation, which are signs of apoptosis on exposure to SiO_2 nanoparticles at dosage levels of 20–100 μg/ml. ROS production in HEK293 cells and oxidative stress induction also indicate the nephrotoxic potential by nanoparticles. Impaired nephrotoxic potential causes dysfunction in the elasticity of nephrons and may cause cerebral epilepsy. The cytotoxicity of NPs was also evaluated in the IP15 (glomerular mesangial) and HK-2 (epithelial proximal) cell lines (Pujalté et al., 2011). The study observed that ZnO and CdS nanoparticles exerted cytotoxic effects on glomerular and tubular human renal cells. These effects were correlated with metal composition, particle size, and metal solubility (Pujalté et al., 2011).

Effect of Nanoparticles on the Neural System

Neurons together with neuroglial cells constitute the nervous tissue making up the nervous system. NPs can reach the central nervous system (CNS) *via* different routes, most commonly by inhalation that can reach the brain through the upper respiratory tract to the olfactory bulb to the trigeminal nerve to the trigeminal nucleus and thalamus to the blood-brain barrier and ultimately to different parts of the brain (Haase et al., 2012; Feng et al., 2015). NPs produce toxicity effects on neural cells by accumulating in different regions of the brain and affecting the expression of genes that helps in the development and function of CNS (Yang et al., 2010). The malfunctioning of CNS can show symptoms like depression, lack of concentration, and even mental retardation. ZnO NPs induce significant cytotoxicity, including a decrease in viability, apoptosis, cell cycle alterations, and different kinds of genetic damage such as oxidative DNA damage (Valdiglesias et al., 2013). Studies show induced inflammation in rats' brain due to manganese oxide inhalation. Silver NPs cause oxidative stress and the upregulation of oxidative stress-related genes in the cortex and hippocampus of mice (Haase et al., 2012; Feng et al., 2015).

Effect of Nanoparticles on the Endocrine System

In the past few decades, there has been a substantial rise in disorders of the immune system. One of the reasons associated with it is the exposure of workers and the general population to contaminants that exert adverse effects on endocrine-disrupting chemicals (EDCs) (e.g., CdTe quantum dots), which play a prime role in altering the hormonal and homeostatic systems (Iavicoli et al., 2013; Lu et al., 2013). A study shows how 150 µg/kg of iron oxide NPs administered in male rats increased the T3 thyroid hormone and decreased the thyroid-stimulating hormone, thus creating a net imbalance (Jiang et al., 2019). Commencing with overstimulation, palladium NPs have shown to gradually act on hormone receptors, blocking the signal cascades (Leso et al., 2018). Some studies have observed that diabetic animals are more prone to hormonal disbalance that non-diabetic ones due to NP exposure (Li et al., 2009; Lu et al., 2013).

Effect of Nanoparticles on the Reproductive System

One of the main reasons for the recent spike in infertility cases has been attributed to the accumulation of NPs. An experimental study on high-fat diet rats shows that administering silica NPs (which are common at workplaces) decreased sperm concentration and motility rates and increased the abnormality rates of sperm (Zhang et al., 2020). TiO2 NPs exhibit genotoxic effects as they cross the blood–testis barrier and causes inflammation and cytotoxicity, thus a significant loss of sperm DNA integrity was observed (Santonastaso et al., 2019). NPs affect the reproductive system by inducing cytotoxicity in ovarian cells, thereby disrupting the process of oogenesis and eventually causing the overproduction of ROS, apoptosis, and sex-hormone imbalance in the body (Iavicoli et al., 2013). In a study, an animal administered with MoO3 showed a significant decrease in the right ovary's weight and uterine weight, which ultimately led to an adverse effect on the reproduction process (Asadi et al., 2019). Hence, NPs are significantly responsible for decreasing birth rates and causing abnormalities in offsprings. In urban areas, such cases are commonly found in females who are exposed to air pollutants, particularly particulate matter (especially NPs), due to their daily lifestyle.

RESPIRATORY MODELS

Specific models have been devised to understand the structure and effects of NPs on individual organs. The Weibel bifurcating tubes' model with 23 bifurcation units describes the branching pattern of lungs, i.e., the 23 levels of bifurcations—G0–G23. The first 16 bifurcations (G0–G16) comprise the conducting zone, while the rest (G17–G23) comprise the respiratory zone involved in the exchange of gases. This model helps in understanding the structure of the airway path (Qiao et al., 2015), and models similar to the organ have been prepared to study the effects of NPs on other body systems. To comprehend and quantify the rates and mechanism of particle deposition, clearing, and impact, the models were divided into experimental and computational methods (Qiao et al., 2015). The experimental methods include *in vivo* and *in vitro* experiments on a model organism exposed to different doses of NPs to determine deposition, clearing, and health impacts (Ji and Yu, 2012; Qiao et al., 2015).

A computational method like computational fluid dynamics (CFD) is primarily used an effective tool in predicting the airflow, particle transport, deposition, and the particle number concentration in fine particles. It is also used in the field of NP instrumentation, evolution of NP dynamics in different environment (human respiratory tract, workplaces, aerosol transport/delivery system, energy systems, etc.), and NP synthesis (Qiao et al., 2015).

Experimental Models

Respiratory tract dosimetry is a biologically based, mechanistic method that is a useful experimental technique to estimate the exposure concentrations of an inhaled substance in a model organism (Kuempel et al., 2006) that can be extrapolated to human equivalent exposure levels by adjusting the lung mass and lung surface area (Kuempel et al., 2006; Ji and Yu, 2012). The multiple-path particle dosimetry model (MPPD) developed by the Chemical Industry Institute of Toxicology (CIIT, currently known as the Hamner Institutes for Health Sciences) and the Dutch National Institute for Public Health and the Environment (RIVM) is used in the assessment of deposition and clearance of course to ultrafine particles (Ji and Yu, 2012). MPPD provides a quick, inexpensive, and efficient means to assess the internal estimates of tissue dose. This model is an efficient tool to determine the percentage change in the particulate load of respirable deposits in the human respiratory system. MPPD estimates particle deposition in the tracheobronchial region where most of the respirable particulate deposition occurs as compared with the pulmonary region (Goel et al., 2021). As the respiratory tract is divided into various regions based on anatomical function, sub-models of ventilation and aerosol transport are constructed (Asgharian et al., 2014). Settings like flow characteristics, orientation, inspiratory fraction, and parameters including multiple respiratory volumes can be altered to meet the needs of the experiment (Manigrasso et al., 2019). Another popular *in vitro* model is the air–blood barrier (ABB) models that elucidates the biological mechanisms related to the potential effects of inhaled nanoparticles. In this model, the effect of NPs on the cell lines of respiratory epithelium, endothelium, and monocyte cells are studied (Bengalli et al., 2017).

Computational Models

The CFD method is mostly used to highlight the impact of several factors including upstream flow, inlet profiles, and turbulent enhanced dispersion (Longest and Vinchurkar, 2007). Like MPPD, the airway is divided into subdivisions called tiny meshes that can help quantify the deposition of particles (Longest and Vinchurkar, 2007; Garcia and Kimbell, 2009; Qiao et al., 2015). Two approaches have been used to investigate the deposition study. First is the Eulerian approach that uses a constant laminar flow rate with non-stop fluid process, dilute particle phase (treated as interpenetrating fields), Brownian motion (depending on the concentration gradient), and a diffusion coefficient (depending on particle size). This model is used to calculate the deposition efficiency of various particle sizes. Deposition efficiency (DE) can be calculated using the following equation:

$$DE = 1 - \left(0.819e^{-14.63\Delta} + 0.0976e^{-89.22\Delta} + 0.0325e^{228\Delta} + 0.0509e^{125.9\Delta^{\frac{2}{3}}}\right),$$

where $\Delta = \frac{DL_{pipe}}{4R^2 U_{inlet}}$,
L_{pipe} is the pipe length, U_{inlet} is the inlet velocity, and R is the pipe radius. This approach neglects particle inertia and is effective for studying a large number of particles (Inthavong et al., 2011). The assumption of laminar flow is supported by the low Reynolds number (Re) (Longest and Vinchurkar, 2007; Garcia and Kimbell, 2009). The second approach is called the Lagrangian approach that considers all the above variables along with particle inertia. This is effective in studying individual particle motion. The trajectories of each particle are traced by integrating a force balance equation on the individual particles:

$$\frac{du_i^p}{dt} = F_D + F_g + F_B + F_L + F_T \qquad (1)$$

Here, F_g is the gravity term; F_D is the drag force per unit particle mass; F_B is the amplitude of the Brownian force component; F_L is the lift due to shear; and F_T is the thermophoretic force. In comparison, the Eulerian model is less computationally demanding due to the single convection–diffusion equation that controls the fluid–particle interrelationship (Inthavong et al., 2011).

Apart from the aforementioned models, the World Health Organisation (WHO) recently introduced new models for the assessment of air quality. Air quality models like the AirQ model and the AirQ 2.2 software are currently in use (Conti et al., 2017). Air quality models use mathematical and numerical methods to simulate the physical and chemical processes caused by air pollutants that trigger their dispersion and chemical transformation in the atmosphere. The purpose of these models is to relate the effects of emission sources with the pollutant concentrations and to cheque whether they are crossing the standard limits or not.

CONCLUSION

The health effects of nanoparticles are well-known, and their exposure can cause serious respiratory and cardiovascular diseases. Epidemiological and toxicological studies have mentioned that nanoparticles are much toxic than coarser particles due to their ultrafine size, chemical reactivity, and longer residence time in the atmosphere. It has also be observed that as particles decrease in size, their ability to penetrate deep inside the lungs increases. The source of nanoparticles varies from anthropogenic activities (vehicular emission, industrial emission, welding fume, cigarette smoke, etc.) to natural activities (forest fire, dust storm, volcanic eruption, etc.). The transport of NP in the lungs is explained with the Weibel bifurcating tubes' model, classified into the conducting zone and respiratory zone. Owing to the ultrafine size and high retention time, nanoparticles diffuse and accumulate in the alveolar region, and some pass through the alveolar epithelium and capillary endothelial cells to enter the cardiovascular system and other internal organs. Different types of clearance mechanisms are exhibited by the human body to counter the effect of NP exposure and protect the body before the onset of the disease. Mucociliary escalation clears the upper respiratory tract, while macrophages with certain proteins help ingest the deep deposited material. Regardless, insoluble NPs get bioaccumulated in the respiratory zone over time, causing lung burden. Such NPs are attacked by phagocytes as a part of the immune response. The exposure to NPs cause the generation of ROS, resulting in cytotoxicity that leads to genotoxicity and tumourigenesis. The overproduction of ROS and the weakening of antioxidant defence system cause oxidative stress, known to trigger the release of more pro-inflammatory hormones that lead to inflammation as well as acute and chronic lung diseases. Thus, NPs cause damage in single-stranded and double-stranded DNA or deletions of its parts and induce mutations in the genetic material, generating neoplasms and carcinomas in the lungs. Besides the harm caused in the lungs, NPs also cause damage in the other body systems including the cardiovascular and gastrointestinal system and lead to cardiac arrest and ulcer, respectively. Comorbid individuals are always at a higher risk of several health complications due to NP accumulation.

This is the first comprehensive review about NPs' source, exposure, and impact on different human body systems, focusing on the respiratory system. The review provides detailed insights about the complex mechanism of NP transportation, clearance, and deposition in lungs that cause lung burden after long-term NP exposure. It offers a detailed overview of the influence of NP exposure in causing toxicological, genotoxic, and tumourigenic effects on the human body. It also mentions the experimental and computational respiratory models, which can be important tools to understand NP's transportation, clearance mechanism, and deposition patterns in human body.

AUTHOR CONTRIBUTIONS

SSo wrote the full text of manuscript. SSo and PS involved in conceptualization and design of the work. SM and JA contributed in acquisition, analysis and interpretation of data for the work, and helped in manuscript writing. SSu involved in acquisition and interpretation of data and critically reviewed the manuscript. DR, NM, and TV performed the whole formatting and editing of manuscript. PS coordinated and supervised the entire team. All authors contributed to the article and approved the submitted version.

ACKNOWLEDGMENTS

Authors express their sincere thanks to the reviewers for providing constructive comments and suggestions.

REFERENCES

Abas, N., Saleem, M. S., Kalair, E., and Khan, N. (2019). Cooperative control of regional transboundary air pollutants. *Environ. Syst. Res.* 8, 1–14. doi: 10.1186/s40068-019-0138-0

Adam, T., McAughey, J., McGrath, C., Mocker, C., and Zimmermann, R. (2009). Simultaneous on-line size and chemical analysis of gas phase and particulate phase of cigarette mainstream smoke. *Anal. Bioanal. Chem*. 394, 1193–1203. doi: 10.1007/s00216-009-2784-y

Alam, D. S., Chowdhury, M. A. H., Siddiquee, A. T., Ahmed, S., Hossain, M. D., Pervin, S., et al. (2012). Adult cardiopulmonary mortality and indoor air pollution: a 10-year retrospective cohort study in a low-income rural setting. *Glob. Heart*. 7, 215–221. doi: 10.1016/j.gheart.2012.06.008

Armstead, A. L., and Li, B. (2016). Nanotoxicity: emerging concerns regarding nanomaterial safety and occupational hard metal (WC-Co) nanoparticle exposure. *Int. J. Nanomed*. 11:6421. doi: 10.2147/IJN.S121238

Asadi, F., Sadeghzadeh, M., Jalilvand, A., Nedaei, K., Asadi, Y., and Heidari, A. (2019). Effect of molybdenum trioxide nanoparticles on ovary function in female rats. *J. Adv. Med. Biomed. Res*. 27, 48–53. doi: 10.30699/jambs.27.121.48

Asgharian, B., Price, O. T., Oldham, M., Chen, L. C., Saunders, E. L., Gordon, T., et al. (2014). Computational modeling of nanoscale and microscale particle deposition, retention and dosimetry in the mouse respiratory tract. *Inhal. Toxicol*. 26, 829–842. doi: 10.3109/08958378.2014.935535

Badarinath, K. V. S., Kharol, S. K., and Sharma, A. R. (2009a). Long-range transport of aerosols from agriculture crop residue burning in Indo-Gangetic Plains—a study using LIDAR, ground measurements and satellite data. *J. Atmos. Solar Terrestr. Phys*. 71, 112–120. doi: 10.1016/j.jastp.2008.09.035

Badarinath, K. V. S., Kharol, S. K., Sharma, A. R., and Prasad, V. K. (2009b). Analysis of aerosol and carbon monoxide characteristics over Arabian Sea during crop residue burning period in the Indo-Gangetic Plains using multi-satellite remote sensing datasets. *J. Atmos. Solar Terrestr. Phys*. 71, 1267–1276. doi: 10.1016/j.jastp.2009.04.004

Bajaj, N., Sharma, T., Suneja, D., Jain, S., and Kumar, P. (2017). Determinants of respiratory and cardiovascular health effects in traffic policemen: A perception-based comparative analysis. *J. Transport Health* 4, 30–39. doi: 10.1016/j.jth.2016.12.003

Bakand, S., Hayes, A., and Dechsakulthorn, F. (2012). Nanoparticles: a review of particle toxicology following inhalation exposure. *Inhal. Toxicol*. 24, 125–135. doi: 10.3109/08958378.2010.642021

Bakshi, S., He, Z. L., and Harris, W. G. (2015). Natural nanoparticles: implications for environment and human health. *Crit. Rev. Environ. Sci. Technol*. 45, 861–904. doi: 10.1080/10643389.2014.921975

Banerjee, T., and Christian, R. A. (2018). A review on nanoparticle dispersion from vehicular exhaust: assessment of Indian urban environment. *Atmos. Pollut. Res*. 9, 342–357. doi: 10.1016/j.apr.2017.10.009

Bengalli, R., Gualtieri, M., Capasso, L., Urani, C., and Camatini, M. (2017). Impact of zinc oxide nanoparticles on an *in vitro* model of the human air-blood barrier. *Toxicol. Lett*. 279, 22–32. doi: 10.1016/j.toxlet.2017.07.877

Berube, K. A., Balharry, D., Sexton, K. J., Koshy, L., and Jones, T. P. (2007). Combustion-derived nanoparticles: mechanisms of pulmonary toxicity. *Clin. Exp. Pharmacol. Physiol*. 34, 1044–1050. doi: 10.1111/j.1440-1681.2007.04733.x

Brown, D. M., Wilson, M. R., MacNee, W., Stone, V., and Donaldson, K. (2001). Size-dependent proinflammatory effects of ultrafine polystyrene particles: a role for surface area and oxidative stress in the enhanced activity of ultrafines. *Toxicol. Appl. Pharmacol*. 175, 191–199. doi: 10.1006/taap.2001.9240

Buseck, P. R., and Adachi, K. (2008). Nanoparticles in the atmosphere. *Elements* 4, 389–394. doi: 10.2113/gselements.4.6.389

Buzea, C., and Pacheco, I. (2017). "Nanomaterial and nanoparticle: origin and activity," in *Nanoscience and Plant-Soil Systems. Soil Biology, Vol. 48*, eds M. Ghorbanpour, K. Manika, and A. Varma (Cham: Springer). doi: 10.1007/978-3-319-46835-8_3

Buzea, C., Pacheco, I. I., and Robbie, K. (2007). Nanomaterials and nanoparticles: sources and toxicity. *Biointerphases* 2:MR17-MR71. doi: 10.1116/1.2815690

Chakraborty, A., Ghosh, S., Chakraborty, R., Chatterjee, S. M., and Hopper, W. (2018). Molecular mechanism of nanotoxicity-a critical review. *Int. J. Curr. Biotechnol*. 6, 1–12.

Chen, H. W., Su, S. F., Chien, C. T., Lin, W. H., Yu, S. L., Chou, C. C., et al. (2006). Titanium dioxide nanoparticles induce emphysema-like lung injury in mice. *FASEB J*. 20, 2393–2395. doi: 10.1096/fj.06-6485fje

Chen, L., Liang, Z., Liu, H., Ding, S., and Li, Y. (2017). Sensitivity analysis of fuel types and operational parameters on the particulate matter emissions from an aviation piston engine burning heavy fuels. *Fuel* 202, 520–528. doi: 10.1016/j.fuel.2017.04.052

Chen, R., Hu, B., Liu, Y., Xu, J., Yang, G., Xu, D., et al. (2016). Beyond PM2. 5: the role of ultrafine particles on adverse health effects of air pollution. *Biochim. Biophys. Acta Gen. Subj*. 1860, 2844–2855. doi: 10.1016/j.bbagen.2016.03.019

Cheong, K. H., Ngiam, N. J., Morgan, G. G., Pek, P. P., Tan, B. Y. Q., Lai, J. W., et al. (2019). Acute health impacts of the Southeast Asian transboundary haze problem—a review. *Int. J. Environ. Res. Public Health* 16:3286. doi: 10.3390/ijerph16183286

Cho, W. S., Duffin, R., Thielbeer, F., Bradley, M., Megson, I. L., MacNee, W., et al. (2012). Zeta potential and solubility to toxic ions as mechanisms of lung inflammation caused by metal/metal oxide nanoparticles. *Toxicol. Sci*. 126, 469–477. doi: 10.1093/toxsci/kfs006

Clift, M. J., Gehr, P., and Rothen-Rutishauser, B. (2011). Nanotoxicology: a perspective and discussion of whether or not *in vitro* testing is a valid alternative. *Arch. Toxicol*. 85, 723–731. doi: 10.1007/s00204-010-0560-6

Conti, G. O., Heibati, B., Kloog, I., Fiore, M., and Ferrante, M. (2017). A review of AirQ Models and their applications for forecasting the air pollution health outcomes. *Environ. Sci. Pollut. Res*. 24, 6426–6445. doi: 10.1007/s11356-016-8180-1

Donaldson, K., Duffin, R., Langrish, J. P., Miller, M. R., Mills, N. L., Poland, C. A., et al. (2013). Nanoparticles and the cardiovascular system: a critical review. *Nanomedicine* 8, 403–423. doi: 10.2217/nnm.13.16

Donaldson, K., Murphy, F., Schinwald, A., Duffin, R., and Poland, C. A. (2011). Identifying the pulmonary hazard of high aspect ratio nanoparticles to enable their safety-by-design. *Nanomedicine* 6, 143–156. doi: 10.2217/nnm.10.139

Donaldson, K., Newby, D. E., MacNee, W., Duffin, R., Lucking, A. J., and Mills, N. L. (2007). "Pulmonary and cardiovascular effects of nanoparticles. characterization, dosing and health effects," in *Nanotoxicology: Characterization, Dosing and Health Effects*, eds N. A. Monteiro-Riviere and C. L. Tran (CRC Press), 267–295. doi: 10.3109/9781420045154-18

Donaldson, K., and Poland, C. A. (2012). Inhaled nanoparticles and lung cancer-what we can learn from conventional particle toxicology. *Swiss Med. Wkly*. 142:w13547. doi: 10.4414/smw.2012.13547

Donaldson, K., Poland, C. A., and Schins, R. P. (2010). Possible genotoxic mechanisms of nanoparticles: criteria for improved test strategies. *Nanotoxicology* 4, 414–420. doi: 10.3109/17435390.2010.482751

Donaldson, K., Tran, L., Jimenez, L. A., Duffin, R., Newby, D. E., Mills, N., et al. (2005). Combustion-derived nanoparticles: a review of their toxicology following inhalation exposure. *Part. Fibre Toxicol*. 2, 1–14. doi: 10.1186/1743-8977-2-10

Elsaesser, A., and Howard, C. V. (2012). Toxicology of nanoparticles. *Adv. Drug Deliv. Rev*. 64, 129–137. doi: 10.1016/j.addr.2011.09.001

Engling, G., and Gelencsér, A. (2010). Atmospheric brown clouds: from local air pollution to climate change. *Elements* 6, 223–228. doi: 10.2113/gselements.6.4.223

Ermolin, M. S., Fedotov, P. S., Malik, N. A., and Karandashev, V. K. (2018). Nanoparticles of volcanic ash as a carrier for toxic elements on the global scale. *Chemosphere* 200, 16–22. doi: 10.1016/j.chemosphere.2018.02.089

Ezzati, M., Lopez, A. D., Rodgers, A., and Murray, C. J. (2004). *Comparative Quantification of Health Risks. Global and Regional Burden of Disease Attributable to Selected Major Risk Factors*. Geneva: World Health Organization, 1987–1997.

Falcone, L. M., Erdely, A., Salmen, R., Keane, M., Battelli, L., Kodali, V., et al. (2018). Pulmonary toxicity and lung tumorigenic potential of surrogate metal oxides in gas metal arc welding–stainless steel fume: Iron as a primary mediator versus chromium and nickel. *PLoS ONE* 13:e0209413. doi: 10.1371/journal.pone.0209413

Feng, X., Chen, A., Zhang, Y., Wang, J., Shao, L., and Wei, L. (2015). Central nervous system toxicity of metallic nanoparticles. *Int. J. Nanomed*. 10:4321. doi: 10.2147/IJN.S78308

Ferreira, A. J., Cemlyn-Jones, J., and Cordeiro, C. R. (2013). Nanoparticles, nanotechnology and pulmonary nanotoxicology. *Rev. Portuguesa Pneumol.* 19, 28–37. doi: 10.1016/j.rppnen.2013.01.004

Foldbjerg, R., Dang, D. A., and Autrup, H. (2011). Cytotoxicity and genotoxicity of silver nanoparticles in the human lung cancer cell line, A549. *Arch. Toxicol.* 85, 743–750. doi: 10.1007/s00204-010-0545-5

Fröhlich, E., and Salar-Behzadi, S. (2014). Toxicological assessment of inhaled nanoparticles: role of *in vivo*, *ex vivo*, *in vitro*, and *in silico* studies. *Int. J. Mol. Sci.* 15, 4795–4822. doi: 10.3390/ijms15034795

Garcia, G. J., and Kimbell, J. S. (2009). Deposition of inhaled nanoparticles in the rat nasal passages: dose to the olfactory region. *Inhal. Toxicol.* 21, 1165–1175. doi: 10.3109/08958370902882713

Geiser, M. (2010). Update on macrophage clearance of inhaled micro- and nanoparticles. *J. Aerosol Med. Pulm. Drug Deliv.* 23, 207–217. doi: 10.1089/jamp.2009.0797

Georgantzopoulou, A., Serchi, T., Cambier, S., Leclercq, C. C., Renaut, J., Shao, J., et al. (2015). Effects of silver nanoparticles and ions on a co-culture model for the gastrointestinal epithelium. *Part. Fibre Toxicol.* 13, 1–17. doi: 10.1186/s12989-016-0117-9

Gerloff, K., Albrecht, C., Boots, A. W., Förster, I., and Schins, R. P. (2009). Cytotoxicity and oxidative DNA damage by nanoparticles in human intestinal Caco-2 cells. *Nanotoxicology* 3, 355–364. doi: 10.3109/17435390903276933

Giorgetti, L. (2019). Effects of nanoparticles in plants: phytotoxicity and genotoxicity assessment. *Nanomater. Plants Algae Microorg.* 1, 65–87. doi: 10.1016/B978-0-12-811488-9.00004-4

Goel, A., Saxena, P., Sonwani, S., Rathi, S., Srivastava, A., Bharti, A. K., et al. (2021). Health benefits due to reduction in respirable particulates during COVID-19 lockdown in India. *Aerosol Air Qual. Res.* 21:200460. doi: 10.4209/aaqr.200460

Gonzalez, C., Rosas-Hernandez, H., Ramirez-Lee, M. A., Salazar-García, S., and Ali, S. F. (2016). Role of silver nanoparticles (AgNPs) on the cardiovascular system. *Arch. Toxicol.* 90, 493–511. doi: 10.1007/s00204-014-1447-8

Gordon, S. M., Wallace, L. A., Brinkman, M. C., Callahan, P. J., and Kenny, D. V. (2002). Volatile organic compounds as breath biomarkers for active and passive smoking. *Environ. Health Perspect.* 110, 689–698. doi: 10.1289/ehp.02110689

Guo, C., Wang, J., Yang, M., Li, Y., Cui, S., Zhou, X., et al. (2017). Amorphous silica nanoparticles induce malignant transformation and tumorigenesis of human lung epithelial cells *via* P53 signaling. *Nanotoxicology* 11, 1176–1194. doi: 10.1080/17435390.2017.1403658

Gurjar, B. R., Ravindra, K., and Nagpure, A. S. (2016). Air pollution trends over Indian megacities and their local-to-global implications. *Atmos. Environ.* 142, 475–495. doi: 10.1016/j.atmosenv.2016.06.030

Haase, A., Rott, S., Mantion, A., Graf, P., Plendl, J., Thünemann, A. F., et al. (2012). Effects of silver nanoparticles on primary mixed neural cell cultures: uptake, oxidative stress and acute calcium responses. *Toxicol. Sci.* 126, 457–468. doi: 10.1093/toxsci/kfs003

Hao, L., and Chen, L. (2012). Oxidative stress responses in different organs of carp (*Cyprinus carpio*) with exposure to ZnO nanoparticles. *Ecotoxicol. Environ. Saf.* 80, 103–110. doi: 10.1016/j.ecoenv.2012.02.017

Henning, A., Schneider, M., Nafee, N., Muijs, L., Rytting, E., Wang, X., et al. (2010). Influence of particle size and material properties on mucociliary clearance from the airways. *J. Aerosol Med. Pulm. Drug Deliv.* 23, 233–241. doi: 10.1089/jamp.2009.0806

Herr, C. E. W., Zur Nieden, A., Jankofsky, M., Stilianakis, N. I., Boedeker, R. H., and Eikmann, T. F. (2003). Effects of bioaerosol polluted outdoor air on airways of residents: a cross sectional study. *Occup. Environ. Med.* 60, 336–342. doi: 10.1136/oem.60.5.336

Hong, F., Ji, L., Zhou, Y., and Wang, L. (2017). Retracted: chronic nasal exposure to nanoparticulate TiO2 causes pulmonary tumorigenesis in male mice. *Environ. Toxicol.* 32, 1651–1657. doi: 10.1002/tox.22393

Hooper, L. G., Dieye, Y., Ndiaye, A., Fan, V. S., Diallo, A., and Ortiz, J. R. (2015). B46 health effects of air pollution and nanoparticles: women's exposure to household air pollution in rural senegal. *Am. J. Respir. Crit. Care Med.* 191:1.

Hosgood, H. D., Lan, Q., Vermeulen, R., Wei, H., Reiss, B., Coble, J., et al. (2012). Combustion-derived nanoparticle exposure and household solid fuel use in Xuanwei and Fuyuan, China. *Int. J. Environ. Health Res.* 22, 571–581. doi: 10.1080/09603123.2012.684147

Huang, C. C., Aronstam, R. S., Chen, D. R., and Huang, Y. W. (2010). Oxidative stress, calcium homeostasis, and altered gene expression in human lung epithelial cells exposed to ZnO nanoparticles. *Toxicol. In Vitro* 24, 45–55. doi: 10.1016/j.tiv.2009.09.007

Iavicoli, I., Fontana, L., Leso, V., and Bergamaschi, A. (2013). The effects of nanomaterials as endocrine disruptors. *Int. J. Mol. Sci.* 14, 16732–16801. doi: 10.3390/ijms140816732

Inthavong, K., Zhang, K., and Tu, J. (2011). Numerical modelling of nanoparticle deposition in the nasal cavity and the tracheobronchial airway. *Comput. Methods Biomech. Biomed. Engin.* 14, 633–643. doi: 10.1080/10255842.2010.493510

Iversen, T. G., Skotland, T., and Sandvig, K. (2011). Endocytosis and intracellular transport of nanoparticles: present knowledge and need for future studies. *Nano Today* 6, 176–185. doi: 10.1016/j.nantod.2011.02.003

Jeevanandam, J., Barhoum, A., Chan, Y. S., Dufresne, A., and Danquah, M. K. (2018). Review on nanoparticles and nanostructured materials: history, sources, toxicity and regulations. *Beilstein J. Nanotechnol.* 9, 1050–1074. doi: 10.3762/bjnano.9.98

Ji, J. H., and Yu, I. J. (2012). Estimation of human equivalent exposure from rat inhalation toxicity study of silver nanoparticles using multi-path particle dosimetry model. *Toxicol. Res.* 1, 206–210. doi: 10.1039/c2tx20029e

Jiang, Z., Shan, K., Song, J., Liu, J., Rajendran, S., Pugazhendhi, A., et al. (2019). Toxic effects of magnetic nanoparticles on normal cells and organs. *Life Sci.* 220, 156–161. doi: 10.1016/j.lfs.2019.01.056

Jones, K., Morton, J., Smith, I., Jurkschat, K., Harding, A. H., and Evans, G. (2015). Human *in vivo* and *in vitro* studies on gastrointestinal absorption of titanium dioxide nanoparticles. *Toxicol. Lett.* 233, 95–101. doi: 10.1016/j.toxlet.2014.12.005

Kar, A., Rehman, I. H., Burney, J., Puppala, S. P., Suresh, R., Singh, L., et al. (2012). Real-time assessment of black carbon pollution in Indian households due to traditional and improved biomass cookstoves. *Environ. Sci. Technol.* 46, 2993–3000. doi: 10.1021/es203388g

Kirch, J., Guenther, M., Doshi, N., Schaefer, U. F., Schneider, M., Mitragotri, S., et al. (2012). Mucociliary clearance of micro-and nanoparticles is independent of size, shape and charge—an *ex vivo* and *in silico* approach. *J. Controlled Release* 159, 128–134. doi: 10.1016/j.jconrel.2011.12.015

Kreyling, W. G., Semmler-Behnke, M., and Möller, W. (2006). Ultrafine particle–lung interactions: does size matter?. *Jo. Aerosol Med.* 19, 74–83. doi: 10.1089/jam.2006.19.74

Kuempel, E. D., Tran, C. L., Castranova, V., and Bailer, A. J. (2006). Lung dosimetry and risk assessment of nanoparticles: evaluating and extending current models in rats and humans. *Inhal. Toxicol.* 18, 717–724. doi: 10.1080/08958370600747887

Kuhn, T., Biswas, S., and Sioutas, C. (2005). Diurnal and seasonal characteristics of particle volatility and chemical composition in the vicinity of a light-duty vehicle freeway. *Atmos. Environ.* 39, 7154–7166. doi: 10.1016/j.atmosenv.2005.08.025

Kumar, P., Pirjola, L., Ketzel, M., and Harrison, R. M. (2013). Nanoparticle emissions from 11 non-vehicle exhaust sources–a review. *Atmos. Environ.* 67, 252–277. doi: 10.1016/j.atmosenv.2012.11.011

Kumar, P., Robins, A., Vardoulakis, S., and Britter, R. (2010). A review of the characteristics of nanoparticles in the urban atmosphere and the prospects for developing regulatory controls. *Atmos. Environ.* 44, 5035–5052. doi: 10.1016/j.atmosenv.2010.08.016

Leso, V., Fontana, L., Marinaccio, A., Leopold, K., Fanali, C., Lucchetti, D., et al. (2018). Palladium nanoparticle effects on endocrine reproductive system of female rats. *Hum. Exp. Toxicol.* 37, 1069–1079. doi: 10.1177/0960327118756722

Li, C., Taneda, S., Taya, K., Watanabe, G., Li, X., Fujitani, Y., et al. (2009). Effects of inhaled nanoparticle-rich diesel exhaust on regulation of testicular function in adult male rats. *Inhal. Toxicol.* 21, 803–811. doi: 10.1080/08958370802524381

Li, J. J. E., Muralikrishnan, S., Ng, C. T., Yung, L. Y. L., and Bay, B. H. (2010). Nanoparticle-induced pulmonary toxicity. *Exp. Biol. Med.* 235, 1025–1033. doi: 10.1258/ebm.2010.010021

Li, N., Xia, T., and Nel, A. E. (2008). The role of oxidative stress in ambient particulate matter-induced lung diseases and its implications in the toxicity of engineered nanoparticles. *Free Radic. Biol. Med*. 44, 1689–1699. doi: 10.1016/j.freeradbiomed.2008.01.028

Lin, S., Wang, X., Ji, Z., Chang, C. H., Dong, Y., Meng, H., et al. (2014). Aspect ratio plays a role in the hazard potential of CeO2 nanoparticles in mouse lung and zebrafish gastrointestinal tract. *ACS Nano* 8, 4450–4464. doi: 10.1021/nn5012754

Liou, S. H., Wu, W. T., Liao, H. Y., Chen, C. Y., Tsai, C. Y., Jung, W. T., et al. (2017). Global DNA methylation and oxidative stress biomarkers in workers exposed to metal oxide nanoparticles. *J. Hazard. Mater*. 331, 329–335. doi: 10.1016/j.jhazmat.2017.02.042

Lomer, M. C., Hutchinson, C., Volkert, S., Greenfield, S. M., Catterall, A., Thompson, R. P., et al. (2004). Dietary sources of inorganic microparticles and their intake in healthy subjects and patients with Crohn's disease. *Br. J. Nutr*. 92, 947–955. doi: 10.1079/BJN20041276

Longest, P. W., and Vinchurkar, S. (2007). Validating CFD predictions of respiratory aerosol deposition: effects of upstream transition and turbulence. *J. Biomech*. 40, 305–316. doi: 10.1016/j.jbiomech.2006.01.006

Lu, X., Liu, Y., Kong, X., Lobie, P. E., Chen, C., and Zhu, T. (2013). Nanotoxicity: a growing need for study in the endocrine system. *Small* 9, 1654–1671. doi: 10.1002/smll.201201517

Lu, X., Zhu, T., Chen, C., and Liu, Y. (2014). Right or left: the role of nanoparticles in pulmonary diseases. *Int. J. Mol. Sci*. 15, 17577–17600. doi: 10.3390/ijms151017577

Luanpitpong, S., Talbott, S. J., Rojanasakul, Y., Nimmannit, U., Pongrakhananon, V., Wang, L., et al. (2010). Regulation of lung cancer cell migration and invasion by reactive oxygen species and caveolin-1. *J. Biol. Chem*. 285, 38832–38840. doi: 10.1074/jbc.M110.124958

Magdolenova, Z., Collins, A., Kumar, A., Dhawan, A., Stone, V., and Dusinska, M. (2014). Mechanisms of genotoxicity. A review of *in vitro* and *in vivo* studies with engineered nanoparticles. *Nanotoxicology* 8, 233–278. doi: 10.3109/17435390.2013.773464

Manigrasso, M., Protano, C., Astolfi, M. L., Massimi, L., Avino, P., Vitali, M., et al. (2019). Evidences of copper nanoparticle exposure in indoor environments: Long-term assessment, high-resolution field emission scanning electron microscopy evaluation, *in silico* respiratory dosimetry study and possible health implications. *Sci. Total Environ*. 653, 1192–1203. doi: 10.1016/j.scitotenv.2018.11.044

Manke, A., Wang, L., and Rojanasakul, Y. (2013). Mechanisms of nanoparticle-induced oxidative stress and toxicity. *Biomed Res. Int*. 2013:942916. doi: 10.1155/2013/942916

Martin, A., and Sarkar, A. (2017). Overview on biological implications of metal oxide nanoparticle exposure to human alveolar A549 cell line. *Nanotoxicology* 11, 713–724. doi: 10.1080/17435390.2017.1366574

Medina, C., Santos-Martinez, M. J., Radomski, A., Corrigan, O. I., and Radomski, M. W. (2007). Nanoparticles: pharmacological and toxicological significance. *Br. J. Pharmacol*. 150, 552–558. doi: 10.1038/sj.bjp.0707130

Miller, M. R., Shaw, C. A., and Langrish, J. P. (2012). From particles to patients: oxidative stress and the cardiovascular effects of air pollution. *Fut. Cardiol*. 8, 577–602. doi: 10.2217/fca.12.43

Mills, N. L., and Miller, M. R. (2011). Particles and the vascular endothelium. *Cardiovasc. Effects Inhaled Ultrafine Nanosized Particles* 1, 379–402. doi: 10.1002/9780470910917.ch19

Mohammad, Y., Shaaban, R., Abou Al-Zahab, B., Khaltaev, N., Bousquet, J., and Dubaybo, B. (2013). Impact of active and passive smoking as risk factors for asthma and COPD in women presenting to primary care in Syria: first report by the WHO-GARD survey group. *Int. J. Chron. Obstruct. Pulmon. Dis*. 8:473. doi: 10.2147/COPD.S50551

Moitra, S., Puri, R., Paul, D., and Huang, Y. C. T. (2015). Global perspectives of emerging occupational and environmental lung diseases. *Curr. Opin. Pulm. Med*. 21, 114–120. doi: 10.1097/MCP.0000000000000136

Moller, W., Haussinger, K., Winkler-Heil, R., Stahlhofen, W., Meyer, T., Hofmann, W., et al. (2004). Mucociliary and long-term particle clearance in the airways of healthy nonsmoker subjects. *J. Appl. Physiol*. 97, 2200–2206. doi: 10.1152/japplphysiol.00970.2003

Nakajima, T., Yoon, S. C., Ramanathan, V., Shi, G. Y., Takemura, T., Higurashi, A., et al. (2007). Overview of the atmospheric brown cloud East Asian regional experiment 2005 and a study of the aerosol direct radiative forcing in east Asia. *J. Geophys. Res. Atmos*. 112:1–23. doi: 10.1029/2007JD009009

Nasterlack, M., Zober, A., and Oberlinner, C. (2008). Considerations on occupational medical surveillance in employees handling nanoparticles. *Int. Arch. Occup. Environ. Health*. 81, 721–726. doi: 10.1007/s00420-007-0245-5

Nel, A., Xia, T., Mädler, L., and Li, N. (2006). Toxic potential of materials at the nanolevel. *Science* 311, 622–627. doi: 10.1126/science.1114397

Nemmar, A., Holme, J. A., Rosas, I., Schwarze, P. E., and Alfaro-Moreno, E. (2013). Recent advances in particulate matter and nanoparticle toxicology: a review of the *in vivo* and *in vitro* studies. *Biomed Res. Int*. 2013:279371. doi: 10.1155/2013/279371

Nho, R. (2020). Pathological effects of nano-sized particles on the respiratory system. *Nanomed. Nanotechnol. Biol. Med*. 29:102242. doi: 10.1016/j.nano.2020.102242

Nishi, K. I., Kadoya, C., Ogami, A., Oyabu, T., Morimoto, Y., Ueno, S., et al. (2020). Changes over time in pulmonary inflammatory response in rat lungs after intratracheal instillation of nickel oxide nanoparticles. *J. Occup. Health*. 62:e12162. doi: 10.1002/1348-9585.12162

Oliveira, M. L., Marostega, F., Taffarel, S. R., Saikia, B. K., Waanders, F. B., DaBoit, K., et al. (2014). Nano-mineralogical investigation of coal and fly ashes from coal-based captive power plant (India): an introduction of occupational health hazards. *Sci. Total Environ*. 468, 1128–1137. doi: 10.1016/j.scitotenv.2013.09.040

Pacurari, M., Lowe, K., Tchounwou, P. B., and Kafoury, R. (2016). A review on the respiratory system toxicity of carbon nanoparticles. *Int. J. Environ. Res. Public Health* 13:325. doi: 10.3390/ijerph13030325

Padmanabhan, J., and Kyriakides, T. R. (2015). Nanomaterials, inflammation, and tissue engineering. *Wiley Interdiscip. Rev. Nanomed. Nanobiotechnol*. 7, 355–370. doi: 10.1002/wnan.1320

Pakkanen, T. A., Kerminen, V. M., Korhonen, C. H., Hillamo, R. E., Aarnio, P., Koskentalo, T., et al. (2001). Urban and rural ultrafine (PM0. 1) particles in the Helsinki area. *Atmos. Environ.* 35, 4593–4607. doi: 10.1016/S1352-2310(01)00167-4

Peters, K., Unger, R. E., Gatti, A. M., Sabbioni, E., Tsaryk, R., and Kirkpatrick, C. J. (2007). Metallic nanoparticles exhibit paradoxical effects on oxidative stress and pro-inflammatory response in endothelial cells *in vitro*. *Int. J. Immunopathol. Pharmacol*. 20, 685–695. doi: 10.1177/039463200702000404

Pipal, A. S., Taneja, A., and Jaiswar, G. (2014). "Risk assessment and toxic effects of exposure to nanoparticles associated with natural and anthropogenic sources," in *Chemistry: The Key to our Sustainable Future*, eds M. Gupta Bhowon, S. Jhaumeer-Laulloo, H. Li Kam Wah, and P. Ramasami (Dordrecht: Springer). doi: 10.1007/978-94-007-7389-9_6

Praphawatvet, T., Peters, J. I., and Williams, R. O. III. (2020). Inhaled nanoparticles—an updated review. *Int. J. Pharm*. 587:119671. doi: 10.1016/j.ijpharm.2020.119671

Pujalté, I., Passagne, I., Brouillaud, B., Tréguer, M., Durand, E., Ohayon-Courtès, C., et al. (2011). Cytotoxicity and oxidative stress induced by different metallic nanoparticles on human kidney cells. *Part. Fibre Toxicol*. 8, 1–16. doi: 10.1186/1743-8977-8-10

Qiao, H., Liu, W., Gu, H., Wang, D., and Wang, Y. (2015). The transport and deposition of nanoparticles in respiratory system by inhalation. *J. Nanomater*. 2015:394507. doi: 10.1155/2015/394507

Querol, X., Alastuey, A., Pey, J., Viana, M., Moreno, T., Minguillón, M. C., et al. (2004). Nanoparticles in the atmosphere. *Seminario Sem*. 8, 24–39.

Ravindra, K., Singh, T., Mor, S., Singh, V., Mandal, T. K., Bhatti, M. S., et al. (2019). Real-time monitoring of air pollutants in seven cities of North India during crop residue burning and their relationship with meteorology and transboundary movement of air. *Sci. Total Environ*. 690, 717–729. doi: 10.1016/j.scitotenv.2019.06.216

Riipinen, I., Yli-Juuti, T., Pierce, J. R., Petäjä, T., Worsnop, D. R., Kulmala, M., et al. (2012). The contribution of organics to atmospheric nanoparticle growth. *Nat. Geosci*. 5, 453–458. doi: 10.1038/ngeo1499

Rothen-Rutishauser, B., Müller, L., Blank, F., Brandenberger, C., Mühlfeld, C., and Gehr, P. (2008). A newly developed *in vitro* model of the human epithelial airway barrier to study the toxic potential of nanoparticles.

ALTEX-Altern. Anim. Experiment. 25, 191–196. doi: 10.14573/altex.2008.3.191

Sajid, M., Ilyas, M., Basheer, C., Tariq, M., Daud, M., Baig, N., et al. (2015). Impact of nanoparticles on human and environment: review of toxicity factors, exposures, control strategies, and future prospects. *Environ. Sci. Pollut. Res*. 22, 4122–4143. doi: 10.1007/s11356-014-3994-1

Santonastaso, M., Mottola, F., Colacurci, N., Iovine, C., Pacifico, S., Cammarota, M., et al. (2019). *In vitro* genotoxic effects of titanium dioxide nanoparticles (n-TiO2) in human sperm cells. *Mol. Reprod. Dev*. 86, 1369–1377. doi: 10.1002/mrd.23134

Sardar, S. B., Fine, P. M., Mayo, P. R., and Sioutas, C. (2005). Size-fractionated measurements of ambient ultrafine particle chemical composition in Los Angeles using the NanoMOUDI. *Environ. Sci. Technol.* 39, 932–944. doi: 10.1021/es049478j

Sarkar, S., Singh, R. P., and Chauhan, A. (2018a). Crop residue burning in northern India: increasing threat to Greater India. *J. Geophys. Res. Atmos*. 123, 6920–6934. doi: 10.1029/2018JD028428

Sarkar, S., Singh, R. P., and Chauhan, A. (2018b). Increasing health threat to greater parts of India due to crop residue burning. *Lancet Planetary Health* 2, e327–e328. doi: 10.1016/S2542-5196(18)30166-9

Saxena, P., and Kulshrestha, U. C. (2016). Contribution of carbonaceous species in SOA formation during fog and non-fog period. *J. Chem. Biol. Phys. Sci.* 7, 31–48.

Saxena, P., and Sonwani, S. (2019). *Criteria Air Pollutants and Their Impact on Environmental Health*. Singapore: Springer.

Saxena, P., and Sonwani, S. (2020). Remediation of ozone pollution by ornamental plants in indoor environment. *Global J. Environ. Sci. Manag.* 6, 497–508. doi: 10.22034/GJESM.2020.04.06

Saxena, P., Sonwani, S., Srivastava, A., Jain, M., Srivastava, A., Bharti, A., et al. (2021b). Impact of crop residue burning in Haryana on the air quality of Delhi, India. *Heliyon* 7:e06973. doi: 10.1016/j.heliyon.2021.e06973

Saxena, P., Srivastava, A., Shweta, Rangra, D., Nancy, Bharti, A., Bhardwaj S., et al. (2021a). "Chapter 15 - Investigating the Problem of Crop Residue Burning in an Indo-Gangetic Plain (IGP)-An Emerging Concern to Air Quality," in *Management of Contaminants of Emerging Concern (CEC) in Environment*, eds P. Singh, C. M. Hussain, and S. Rajkhowa (Elsevier), 395–414. doi: 10.1016/B978-0-12-822263-8.00015-4

Saxena, P., Srivastava, A., Verma, S., Shweta, Singh L., and Sonwani, S. (2020). "Analysis of atmospheric pollutants during fireworks festival 'diwali' at a residential site Delhi in India," in *Measurement, Analysis and Remediation of Environmental Pollutants. Energy, Environment, and Sustainability*, eds T. Gupta, S. Singh, P. Rajput, and A. Agarwal (Singapore: Springer). doi: 10.1007/978-981-15-0540-9_4

Schins, R. (2013). Genotoxicity of nanoparticles. *Nanomaterials* 1, 60–64. doi: 10.1002/9783527673919.ch8

Scholl, J. A., Koh, A. L., and Dionne, J. A. (2012). Quantum plasmon resonances of individual metallic nanoparticles. *Nature* 483, 421–427. doi: 10.1038/nature10904

Seaton, A., Tran, L., Aitken, R., and Donaldson, K. (2010). Nanoparticles, human health hazard and regulation. *J. R. Soc. Interface* 7, S119–S129. doi: 10.1098/rsif.2009.0252.focus

Shakya, K. M., Peltier, R. E., Zhang, Y., and Pandey, B. D. (2019). Roadside exposure and inflammation biomarkers among a cohort of traffic police in Kathmandu, Nepal. *Int. J. Environ. Res. Public Health* 16:377. doi: 10.3390/ijerph16030377

Sharma, V., Singh, P., Pandey, A. K., and Dhawan, A. (2012). Induction of oxidative stress, DNA damage and apoptosis in mouse liver after sub-acute oral exposure to zinc oxide nanoparticles. *Mutat. Res. Genet. Toxicol. Environ. Mutagenesis* 745, 84–91. doi: 10.1016/j.mrgentox.2011.12.009

Shi, X., Castranova, V., Halliwell, B., and Vallyathan, V. (1998). Reactive oxygen species and silica-induced carcinogenesis. *J. Toxicol. Environ. Health Part B Crit. Rev*. 1, 181–197. doi: 10.1080/10937409809524551

Singh, R. P., and Kaskaoutis, D. G. (2014). Crop residue burning: a threat to South Asian air quality. *Eos Transac. Am. Geophys. Union* 95, 333–334. doi: 10.1002/2014EO370001

Slezakova, K., Morais, S., and do Carmo Pereira, M. (2013). "Atmospheric nanoparticles and their impacts on public health," in *Current Topics in Public Health,* eds A. J. Rodriguez-Morales (London: IntechOpen), 503–529. doi: 10.5772/54775

Sonwani, S., and Kulshreshtha, U. (2016). "Particulate matter levels and it's associated health risks in East Delhi," in *Proceedings of Indian Aerosol Science and Technology Association Conference on Aerosol and Climate Change: Insight and Challenges. IASTA Bull*, Vol. 22 (Ahmedabad), 269–272.

Sonwani, S., and Saxena, P. (2021). Water-insoluble carbonaceous components in rainwater over an urban background location in Northern India during pre-monsoon and monsoon seasons. *Environ. Sci. Pollut. Res*. 1–16. doi: 10.1007/s11356-021-14132-w

Sonwani, S., Saxena, P., and Kulshrestha, U. (2016). "Role of global warming and plant signaling in BVOC emissions," in *Plant Responses to Air Pollution*, eds U. Kulshrestha and P. Saxena (Singapore: Springer). doi: 10.1007/978-981-10-1201-3_5

Sonwani, S., Saxena, P., and Shukla, A. (2021). Carbonaceous aerosol characterization and their relationship with meteorological parameters during summer monsoon and winter monsoon at an industrial region in Delhi, India. *Earth Space Sci.* 8, 1–16. doi: 10.1029/2020EA001303

Sramkova, M., Kozics, K., Masanova, V., Uhnakova, I., Razga, F., Nemethova, V., et al. (2019). Kidney nanotoxicity studied in human renal proximal tubule epithelial cell line TH1. *Mutat. Res. Genet. Toxicol. Environ. Mutagenesis* 845:403017. doi: 10.1016/j.mrgentox.2019.01.012

Strambeanu, N., Demetrovici, L., and Dragos, D. (2015). "Anthropogenic sources of nanoparticles," in *Nanoparticles' Promises and Risks* (Cham: Springer), 21–54.

Stueckle, T. A., Davidson, D. C., Derk, R., Kornberg, T. G., Schwegler-Berry, D., Pirela, S. V., et al. (2017). Evaluation of tumorigenic potential of CeO2 and Fe2O3 engineered nanoparticles by a human cell *in vitro* screening model. *Nanoimpact* 6, 39–54. doi: 10.1016/j.impact.2016.11.001

Tiwari, S., and Saxena, P. (2021). *Air Pollution and Its Complications From the Regional to the Global Scale.* Cham: Springer.

Ursini, C. L., Cavallo, D., Fresegna, A. M., Ciervo, A., Maiello, R., Tassone, P., et al. (2014). Evaluation of cytotoxic, genotoxic and inflammatory response in human alveolar and bronchial epithelial cells exposed to titanium dioxide nanoparticles. *J. Appl. Toxicol.* 34, 1209–1219. doi: 10.1002/jat.3038

Valdiglesias, V., Costa, C., Kiliç, G., Costa, S., Pásaro, E., Laffon, B., et al. (2013). Neuronal cytotoxicity and genotoxicity induced by zinc oxide nanoparticles. *Environ. Int*. 55, 92–100. doi: 10.1016/j.envint.2013.02.013

Vera-Reyes, I., Vázquez-Núñez, E., Lira-Saldivar, R. H., and Méndez-Argüello, B. (2018). "Effects of nanoparticles on germination, growth, and plant crop development," in *Agricultural Nanobiotechnology* (Cham: Springer), 77–110.

Volkamer, R., Jimenez, J. L., San Martini, F., Dzepina, K., Zhang, Q., Salcedo, D., et al. (2006). Secondary organic aerosol formation from anthropogenic air pollution: Rapid and higher than expected. *Geophys. Res. Lett*. 33:L17811. doi: 10.1029/2006GL026899

Walsh, M. (2011). Global trends in motor vehicle pollution control: a 2011 update. Part 1. *Silniki Spalinowe* 50, 106–117. doi: 10.19206/CE-117109

Wang, F., Gao, F., Lan, M., Yuan, H., Huang, Y., and Liu, J. (2009). Oxidative stress contributes to silica nanoparticle-induced cytotoxicity in human embryonic kidney cells. *Toxicol. In Vitro* 23, 808–815. doi: 10.1016/j.tiv.2009.04.009

Warheit, D. B. (2004). Nanoparticles: health impacts?. *Mater. Today* 7, 32–35. doi: 10.1016/S1369-7021(04)00081-1

Williams, M., Villarreal, A., Bozhilov, K., Lin, S., and Talbot, P. (2013). Metal and silicate particles including nanoparticles are present in electronic cigarette cartomizer fluid and aerosol. *PLoS ONE* 8:e57987. doi: 10.1371/journal.pone.0057987

Yang, Z., Liu, Z. W., Allaker, R. P., Reip, P., Oxford, J., Ahmad, Z., et al. (2010). A review of nanoparticle functionality and toxicity on the central nervous system. *J. Roy. Soc. Interface* 7, S411–S422. doi: 10.1098/rsif.2010.0158.focus

Yhee, J. Y., Im, J., and Nho, R. S. (2016). Advanced therapeutic strategies for chronic lung disease using nanoparticle-based drug delivery. *J. Clin. Med*. 5:82. doi: 10.3390/jcm5090082

Yu, X., Hong, F., and Zhang, Y. Q. (2016). Bio-effect of nanoparticles in the cardiovascular system. *J. Biomed. Mater. Res. Part A* 104, 2881–2897. doi: 10.1002/jbm.a.35804

Zhang, L., Wei, J., Duan, J., Guo, C., Zhang, J., Ren, L., et al. (2020). Silica nanoparticles exacerbates reproductive toxicity development in high-fat diet-treated Wistar rats. *J. Hazard. Mater*. 384:121361. doi: 10.1016/j.jhazmat.2019.121361

Zhang, Y., Bai, Y., Jia, J., Gao, N., Li, Y., Zhang, R., et al. (2014). Perturbation of physiological systems by nanoparticles. *Chem. Soc. Rev*. 43, 3762–3809. doi: 10.1039/C3CS60338E

Zhu, X., Hondroulis, E., Liu, W., and Li, C. Z. (2013). Biosensing approaches for rapid genotoxicity and cytotoxicity assays upon nanomaterial exposure. *Small* 9, 1821–1830. doi: 10.1002/smll.201201593

Conflict of Interest: The authors declare that the research was conducted in the absence of any commercial or financial relationships that could be construed as a potential conflict of interest.

Publisher's Note: All claims expressed in this article are solely those of the authors and do not necessarily represent those of their affiliated organizations, or those of the publisher, the editors and the reviewers. Any product that may be evaluated in this article, or claim that may be made by its manufacturer, is not guaranteed or endorsed by the publisher.

frontiers in Sustainable Cities

ORIGINAL RESEARCH
published: 29 September 2021
doi: 10.3389/frsc.2021.705051

Check for updates

Effect of Lockdown Amid COVID-19 on Ambient Air Quality in 16 Indian Cities

Amit Kumar Mishra[1]*, *Prashant Rajput*[2], *Amit Singh*[3], *Chander Kumar Singh*[3] and *Rajesh Kumar Mall*[2]

[1] School of Environmental Sciences, Jawaharlal Nehru University, New Delhi, India, [2] Department of Science and Technology-Mahamana Centre of Excellence in Climate Change Research, Institute of Environment & Sustainable Development, Banaras Hindu University, Varanasi, India, [3] Department of Energy and Environment, The Energy and Resources Institute School of Advanced Studies, New Delhi, India

The COVID-19 pandemic has affected severely the economic structure and health care system, among others, of India and the rest of the world. The magnitude of its aftermath is exceptionally devastating in India, with the first case reported in January 2020, and the number has risen to ∼31.3 million as of July 23, 2021. India imposed a complete lockdown on March 25, which severely impacted migrant population, industrial sector, tourism industry, and overall economic growth. Herein, the impacts of lockdown and unlock phases on ambient atmospheric air quality variables have been assessed across 16 major cities of India covering the north-to-south stretch of the country. In general, all assessed air pollutants showed a substantial decrease in AQI values during the lockdown compared with the reference period (2017–2019) for almost all the reported cities across India. On an average, about 30–50% reduction in AQI has been observed for $PM_{2.5}$, PM_{10}, and CO, and maximum reduction of 40–60% of NO_2 has been observed herein, while the data was average for northern, western, and southern India. SO_2 and O_3 showed an increase over a few cities as well as a decrease over the other cities. Maximum reduction (49%) in $PM_{2.5}$ was observed over north India during the lockdown period. Furthermore, the changes in pollution levels showed a significant reduction in the first three phases of lockdown and a steady increase during subsequent phase of lockdown and unlock period. Our results show the substantial effect of lockdown on reduction in atmospheric loading of key anthropogenic pollutants due to less-to-no impact from industrial activities and vehicular emissions, and relatively clean transport of air masses from the upwind region. These results indicate that by adopting cleaner fuel technology and avoiding poor combustion activities across the urban agglomerations in India could bring down ambient levels of air pollution at least by 30%.

Keywords: lockdown, COVID-19, air quality, Indian cities, mitigation

OPEN ACCESS

Edited by:
Yuli Shan,
University of Groningen, Netherlands

Reviewed by:
Sarvan Kumar,
Veer Bahadur Singh Purvanchal University, India
Shubham Sharma,
Indian Institutes of Technology (IIT), India

Correspondence:
Amit Kumar Mishra
amit.mishra.jnu@gmail.com;
amitmishra@mail.jnu.ac.in

Specialty section:
This article was submitted to Climate Change and Cities, a section of the journal Frontiers in Sustainable Cities

Received: *04 May 2021*
Accepted: *27 August 2021*
Published: *29 September 2021*

Citation:
Mishra AK, Rajput P, Singh A, Singh CK and Mall RK (2021) Effect of Lockdown Amid COVID-19 on Ambient Air Quality in 16 Indian Cities. Front. Sustain. Cities 3:705051. doi: 10.3389/frsc.2021.705051

INTRODUCTION

A novel infectious disease for the first time was identified in Wuhan, China, in late December 2019 and was named as 2019 novel corona virus and later on renamed as the COVID-19 (Chen et al., 2020) on February 11, 2020 by the International Committee on Taxonomy of Viruses. Later on in January 2020, the World Health Organization (WHO) revealed human transmission of COVID-19 through respiratory droplets (WHO, 2020), which subsequently got spread throughout the China, and the outbreak was turned into an epidemic (Dutheil et al., 2020). On January 30, 2020, the WHO declared the COVID-19 as a global pandemic. Subsequently, the transmission of pandemic COVID-19 *via* airborne pathway was recognized by the WHO. After the severe acute respiratory syndrome coronavirus (SARS-CoV) in 2002, which influenced around 37 countries and the Middle East respiratory syndrome coronavirus (MERS-CoV) in 2012, the COVID-19 is the third major zoonotically spread calamity of the current century.

To slow down the rate of spread of virus, almost all the countries have followed partial-to-complete lockdown practice (Tosepu et al., 2020). Globally, the economic activities were ceased, and stock markets plunged along with the falling carbon emission. The industrial activities were shut down globally due to the imposed lockdown. The informal economic sector suffered a major fall along with the transport sector as most of the countries imposed complete lockdown. Global fossil fuel demand dropped down severely, as industrial and transport sectors came to a halt for a while across the world. As far as the scenario of COVID-19 in India is concerned, the first COVID-19 incidence in India was registered on January 30, 2020, in the state of Kerala, and the travel restrictions to several countries were imposed from March 11, 2020 soon after a steep rise in the number of incidences on March 4, 2020. From March 16 onward, all places of public gathering were shut down across India. The first nationwide lockdown, on a trial mode, was witnessed on March 22, 2020, and subsequently, from March 24, 2020 a nationwide complete lockdown for 21 days was announced by the Central Government of India. The different phases of lockdown and unlock in India are given in **Table 1**.

Significant impacts of lockdown were observed on air quality across the world (Berman and Ebisu, 2020; Nakada et al., 2020; Venter et al., 2020) and in India (Kumar, 2020; Kumar, 2020; Sarfraz et al., 2020; Sharma et al., 2020; Dumka et al., 2021). A positive association between COVID-19 cases and meteorological parameters has also been shown recently (Kumar, 2020). Dumka et al. (2021) has shown that more than 50% reduction in $PM_{2.5}$ and NO_2 concentrations occurred over Delhi—NCR, mainly due to restrictions in traffic-related activities. Nationwide lockdown amid the COVID-19 pandemic had a significant impact on the air quality index. Thus, a quantitative assessment of air quality variables is needed to understand the impact of lockdown on anthropogenic emission source impact and their reframe mitigation policies in India. The major objective of the present study was to assess the changes in ambient air quality during lockdown and in the subsequent unlock phases across India.

Data and Methodology

To assess the impact of nationwide lockdown on ambient air quality in India, we have chosen 16 major cities (Chandigarh, Delhi, Jaipur, Lucknow, Patna, Kolkata, Gandhinagar, Bhopal, Nashik, Mumbai, Nagpur, Hyderabad, Bengaluru, Chennai, Visakhapatnam, and Thiruvananthapuram) across the country (**Figure 1**). The selection of these cities is based on the level of urbanization linked to air pollution, implementation of lockdown policy, coverage of typical major cities in the country, and availability of data set of air pollution and meteorological parameters. The daily average (and median) along with minimum, maximum, and standard deviation of each of the air pollutants and meteorological parameters during January 1 to June 30 for 4 years (2017–2020) were retrieved from the World Air Quality Index (WAQI) Project (https://aqicn.org/data-platform/covid19/) having data source (for Indian region) originally from India's Central Pollution Control Board (cpcb.nic.in/), U.S. Embassy and Consulates' Air Quality Monitor in India (in.usembassy.gov/embassy-consulates/new-delhi/air-quality-data/), Delhi Pollution Control Committee (dpccairdata.com/), and India Meteorological Department (www.imd.gov.in/). The daily average air pollutants and meteorological data set for each of the cities have been deduced from the average of the respective data recorded from monitoring stations located in that city. The key air pollutant species such as particulate matter with aerodynamic diameter $\leq$2.5 and $\leq$10 μm ($PM_{2.5}$ and PM_{10}), nitrogen dioxide (NO_2), sulfur dioxide (SO_2), carbon monoxide (CO), and tropospheric ozone (O_3) along with the meteorological parameters [relative humidity (RH), near surface air temperature (T), and wind speed (WS)] have been assessed herein.

All air pollutants reported in this study were converted with respect to the United States Environmental Protection Agency (US EPA) standard (Mintz, 2018). The first step is to identify the highest concentration of pollutants among all of the monitors within each locations and then truncate it as $PM_{2.5}$ (μg/m^3) to one decimal place, PM_{10} (μg/m^3) to integer, CO (ppm) to one decimal place, SO_2 (ppb) to integer, NO_2 (ppb) to integer, and O_3 (ppm) to three decimal places. Subsequently, with the aid of the two breakpoints, the concentration was summarized (**Supplementary Table 1**). Finally, the index was calculated using the following equation:

$$I_p = \frac{I_{Hi} - I_{Lo}}{BP_{Hi} - BP_{Lo}} \left(C_p - BP_{Lo}\right) + I_{Lo} \tag{1}$$

where, I_p is the index of a pollutant p, C_p is the truncated concentration of that pollutant p, BP_{Hi} is the concentration breakpoint $\geq C_p$, BP_{Lo} is the concentration breakpoint $\leq C_p$, I_{Hi} is the AQI value corresponding to BP_{Hi}, and I_{Lo} is the AQI value corresponding to BP_{Lo}. The details of AQI estimation for different pollutants have been provided elsewhere (Bishoi et al., 2009; Mintz, 2018).

The concentration of the ambient air pollutant not only depends on the intensity of its emission but also on meteorological conditions. Therefore, in order to see the net change due to restrictions on emission sources, we need to normalize the concentration of the pollutant with meteorology. There are various methods existing to account for (or normalize) meteorological effects on the concentration of the ambient air (Dai et al., 2020; Petetin et al., 2020; Falocchi et al., 2021). In this study, we have used the ventilation coefficient (VC) to normalize the meteorological influence (Dai et al., 2020)

TABLE 1 | Different timelines that India adopted for lockdown and unlock phases.

Phases	Timeline	Duration	Activities restricted/permitted
Phase 1	March 25, 2020 to April 14, 2020	21 days	All industries and services suspended except essential services
Phase 2	April 15, 2020 to May 3, 2020	19 days	Conditional relaxation from April 20 for the COVID-contained regions. Classification of regions into red, orange, and green zones. Agribusinesses, public work programs allowed to reopen with social distancing. Cargo transportation vehicles, including trucks, trains, and planes were started. Banks and small retail shops were reopened. Interstate movement of stranded allowed
Phase 3	May 4, 2020 to May 17, 2020	14 days	On May 1, red zones (130 districts), orange zones (284 districts), and green zones (319 districts)
Phase 4	May 18, 2020 to May 31, 2020	14 days	States control the demarcation of green, orange, and red zones. Red zones further divided into containment and buffer zones
Unlock			
Unlock 1.0	June 1, 2020 to June 30, 2020	30 days	First phase of reopening shopping malls, religious places, hotels, and restaurants. Large gatherings were still banned, no restrictions on interstate travel. Night curfews to be in effect
Unlock 2.0	July 1, 2020 to July 31, 2020	31 days	Lockdown measures were imposed in containment zones. In all other areas, most activities were permitted. Night curfews to be in effect. Limited international travel has been permitted as part of the Vande Bharat Mission

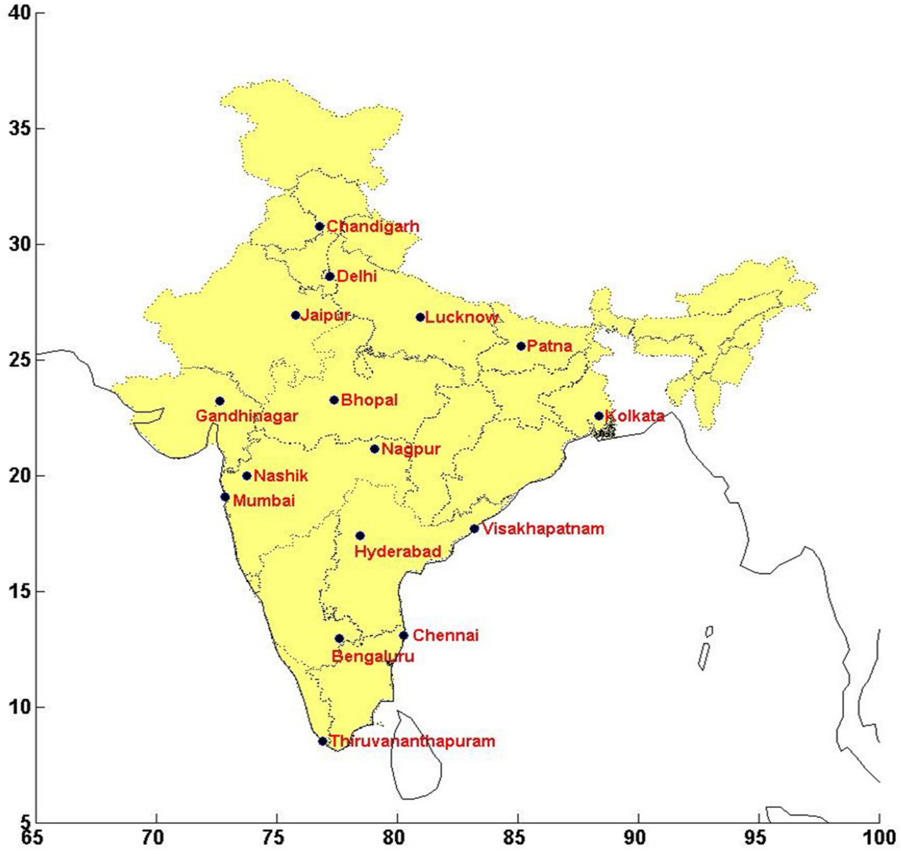

FIGURE 1 | Map of India showing the geographical location of all the 16 cities studied herein.

on ambient AQI. The hourly wind vector at 2 m (above the ground) and mixing-layer height data over all studied 16 cities (during March to June, 2017–2020) have been obtained from ERA5 global reanalysis products (Hersbach et al., 2020). The daily mean VC is estimated by taking the product of the daily mean mixing-layer height and wind speed for each of the cities during the study period. Furthermore, climatological or the long-term mean of VC (VC_{mean}) specific to each city has been estimated by taking the average of daily VCs during the study period (2017–2020). The influence of meteorological dispersion on observed AQI has been removed by normalizing the AQI data of each pollutant with VC_{mean}

for every city using the following equation (2) as given by Dai et al. (2020).

$$AQI_{VC,i} = AQI_i^{*}(VC_i/VC_{mean}) \tag{2}$$

where $AQI_{VC,i}$ is meteorology normalized AQI for the ith day, AQI_i is the AQI measured on the ith day, and VC_i is the ventilation coefficient on the ith day. Furthermore, meteorologically normalized (hereafter represented as "met normalized") AQI data of each pollutant has been used to see the relative changes in AQI during the lockdown period compared with the reference period across the 16 Indian cities.

RESULTS AND DISCUSSION

Effect of Meteorology on Observed Changes in Ambient AQI

The wind speed and direction are important parameters that significantly impact the concentration of the pollutants in ambient air. We have analyzed the wind rose maps for reference and lockdown period for each city. **Supplementary Figure 1** shows the prevailing wind direction and speeds in selected cities in north India for the study period. The suffixes "Ref" and "Cov" refer to reference period (in 2017, 2018, and 2019) and lockdown period due to COVID (in 2020) trends, respectively. The legend colors represent increasing wind speed from top to bottom. The wind rose plots for other cities are provided in the **Supplementary Material** for western Indian cities (**Supplementary Figure 2**) and south Indian cities (**Supplementary Figure 3**) in our study. Briefly, we have not found any significant change in prevailed wind directions during the COVID year with respect to reference period over any city. In other words, we can say that both the periods have a similar kind of wind pattern over the Indian cities. Furthermore, **Table 2** shows the mean values of meteorological parameters (RH, T, and WS) during the reference and lockdown period for the 16 major cities of India. In general, the lockdown period was, on an average, characterized by relatively high humidity and lower mean temperature compared with the reference period. The wind speed appeared to be nearly similar during lockdown as well as the reference period. Nevertheless, the day-to-day variability in meteorological parameters for 1 year to another could be quite significant, and thus, taking into account for meteorological variability, while comparing pollutant concentrations is of utmost importance (Dandotiya et al., 2019; Nandi, 2020).

Table 1 shows the different phases of lockdown and unlock period practiced in India to control the spread of COVID-19. Lockdown period was imposed in four phases: P1 (March 25 to April 14), P2 (April 15 to May 3), P3 (May 4 to May 17), and P4 (May 18 to May 31) (Saha and Chouhan, 2021). P1 and P2 were the periods of complete nationwide lockdown, whereas P3 and P4 were the periods of partial lockdown. In order to assess the maximum reduction in anthropogenic contribution to AQI, we choose the complete lockdown period. The mean USEPA standardized AQI values (with and without normalization to meteorological parameter) of various air pollutants averaged

TABLE 2 | Mean values of meteorological parameters during complete lockdown period (in 2020, as Cov.) and reference period (as Ref.).

	RH (%)		T (°C)		WS (m/s)	
	Ref.	*Cov.*	*Ref.*	*Cov.*	*Ref.*	*Cov.*
Chandigarh	45.3	55.3	28.1	23.4	1.5	1.6
Jaipur	21.4	32.5	31.9	29.2	1.3	1.1
Delhi	34.6	47.6	29.8	27.8	1.6	1.4
Lucknow	39.1	47.3	31.5	29.6	0.5	0.6
Patna	53.3	56.7	31.6	27.6	0.8	0.6
Kolkata	71	68.7	28.3	28.1	1.4	0.7
Gandhinagar	28.4	40.3	33	30.5	1.9	1.1
Nashik	33.4	38.6	27	27.9	2.5	2.2
Nagpur	–	49.2	–	30.7	–	0.4
Mumbai	65.6	76.1	30.3	30	0.9	1.3
Bengaluru	44.5	47.4	26.9	25.7	1.6	1
Hyderabad	43.9	47.2	29.4	30	1.3	1
Chennai	64.3	71.1	30.6	29.7	–	2.6
Bhopal	23.4	31.3	29.7	30.9	0.7	0.8
Thiruvananthapuram	71.9	76.6	29.4	28.3	1.5	1
Visakhapatnam	72.6	71.9	28.4	32.2	2.9	2.2

during March 25 to May 3 for the reference and lockdown period for the 16 major cities of India are shown in **Table 3**. **Figure 2** shows city-specific percent change of key pollutants (with and without normalization to meteorological parameter viz. VC) averaged over complete lockdown period (phase 1 and phase 2: March 25 to May 3, 2020) compared with the reference time-period for the 16 major cities across India. **Table 3** shows that the AQI values of key air pollutants get substantially increased after met normalization during the reference period over almost all Indian cities, whereas minimal effect has been observed during the lockdown period. Moreover, percent changes in key pollutants averaged over the complete lockdown period (**Figure 2**) show higher reduction for met normalized data compared with that of without met normalization. If we take only without met normalized data, on an average, more than 30% decrease has been observed in $PM_{2.5}$ (−35% averaged over all cities), PM_{10} (−37% averaged over all cities), and CO (−32% averaged over all cities) over most of the cities in India. The maximum negative change is found in NO_2 AQI over all the cities with about −42% averaged over India. From **Figure 2** and **Table 3**, it is obvious that the average difference in values for with and without met normalization of air pollutants is 11 ± 3%. Furthermore, in general, with met normalized values were lower than without met normalized values. In the further discussion, we would be utilizing with met normalized values of AQI of air pollutants.

Effect of Lockdown on Citywise Ambient AQI

In general, all the air pollutants (met normalized) showed a substantial decrease in AQI values during COVID period compared with the reference period for almost all the assessed cities across India. On an average (over all cities), more than 24%

TABLE 3 | Mean EPA AQI values of various air pollutants (with and without normalization to meteorological parameter) during complete lockdown period (in 2020, as Cov.) and reference period (as Ref.).

		$PM_{2.5}$		PM_{10}		SO_2		CO		NO_2		O_3	
		Ref.	***COV.***	***Ref.***	***COV.***	***Ref.***	***COV.***	***Ref.***	***COV.***	***Ref.***	***COV.***	***Ref.***	***COV.***
Chandigarh	Without met	112	72	–	46	3.0	5.8	4.5	3.1	9.3	6.5	16.8	12.5
	With met	158	68	–	43	4.0	5.5	6.0	2.8	13.4	6.0	20.2	12.0
Jaipur	Without met	134	77	88	51	4.5	5.5	5.9	4.9	12.8	5.6	20.7	21.7
	With met	184	72	119	49	5.7	5.0	7.5	4.4	16.9	5.2	25.2	18.9
Delhi	Without met	163	106	142	68	7.9	6.0	7.9	6.0	19.0	7.2	13.9	15.2
	With met	240	106	211	69	11.7	6.1	11.3	6.1	27.9	7.3	21.7	15.7
Lucknow	Without met	97	76	68	53	11.2	2.9	12.7	3.4	11.4	2.8	10.3	8.9
	With met	127	89	89	62	14.6	3.5	16.4	4.1	14.8	3.3	13.0	11.0
Patna	Without met	158	98	–	61	7.0	4.7	8.9	6.1	8.0	7.4	13.4	15.9
	With met	181	113	–	73	7.9	5.6	10.0	6.9	9.2	8.5	14.8	16.5
Kolkata	Without met	114	80	62	42	2.9	4.1	4.9	3.3	10.3	5.0	10.8	17.0
	With met	165	83	89	45	4.1	4.3	7.4	3.2	14.9	4.9	14.5	17.5
Bhopal	Without met	133	87	118	53	9.6	5.2	10.3	4.6	15.0	4.6	15.3	10.4
	With met	156	89	143	55	10.9	5.2	11.6	4.7	17.0	4.6	17.5	10.0
Gandhinagar	Without met	165	81	–	57	25.3	3.6	7.2	5.7	28.1	5.5	11.9	6.4
	With met	160	77	–	54	25.7	3.5	6.9	5.5	27.9	5.0	12.3	6.3
Nashik	Without met	121	84	65	45	2.5	1.2	4.6	3.5	10.7	9.5	33.6	25.4
	With met	132	76	72	42	2.7	1.2	4.9	3.3	11.3	8.9	35.8	22.2
Nagpur	Without met	135	71	64	38	6.0	0.8	8.0	3.6	11.7	8.5	26.3	18.4
	With met	208	70	99	37	8.3	0.7	11.7	3.6	17.0	8.2	43.4	19.0
Mumbai	Without met	171	122	–	–	3.8	2.7	9.1	9.1	16.3	6.2	21.8	10.3
	With met	153	119	–	–	3.4	2.6	8.1	8.9	13.9	6.1	19.8	9.8
Bengaluru	Without met	111	75	64	43	2.2	3.3	6.2	6.1	10.9	5.1	17.3	16.5
	With met	115	81	68	47	2.4	3.4	6.2	6.3	11.0	5.1	18.7	17.3
Hyderabad	Without met	125	89	80	50	4.3	2.2	6.0	3.8	13.8	6.4	21.0	11.1
	With met	140	87	90	49	4.6	2.1	6.6	3.6	15.0	6.3	22.6	10.8
Visakhapatnam	Without met	98	57	67	44	4.7	3.3	7.1	4.1	11.4	11.5	5.2	7.7
	With met	122	56	82	44	6.3	3.3	9.0	3.9	13.9	11.3	6.1	7.6
Chennai	Without met	87	49	–	8	2.7	2.2	7.7	5.6	6.3	2.6	9.6	10.3
	With met	96	43	–	7	3.0	2.0	8.5	5.4	7.2	2.2	10.9	10.1
Thiruvananthapuram	Without met	85	67	50	39	2.1	2.6	8.1	4.8	3.6	3.5	17.6	14.0
	With met	92	62	56	36	2.1	2.5	8.1	4.5	3.5	3.5	18.7	13.7

decrease has been observed for all the AQI of the pollutant; $PM_{2.5}$ decreased by 45%, PM_{10} decreased by 48%, and CO decreased by 41%. The maximum decrease has been found for NO_2 AQI over all the cities with an overall decrease of 52% when averaged for all 16 cities. The decrease in PM pollution and gaseous pollutants (CO and NO_2) clearly reflects the impact of ceased industrial and vehicular activities during lockdown. SO_2 and O_3 were also decreased in the lockdown period compared with the reference period, except over a few cities wherein these species showed an increase in their concentration during the lockdown period with respect to the reference period. For example, the SO_2 AQI showed a statistically significant increase in Chandigarh (34.4%, from 4.0 ± 2.0 to 5.5 ± 3.2; two-tailed t-value: 3.5), Bengaluru (45%, from 2.4 ± 1.0 to 3.4 ± 1.5; two-tailed t-value: 4.8), and Thiruvanthapuram (15.4%, from 2.1 ± 0.8 to 2.5 ± 1.0; two-tailed t-value: 2.6) in the COVID period compared with the reference period. Mor et al. (2021) has also reported an increase of 2–20% in SO_2 concentration during different lockdown phases compared with the pre-lockdown period over Chandigarh. The increased concentration was attributed to atmospheric transport of SO_2 emissions from coal-based thermal power plants upwind of the measurement location (Mor et al., 2021).

To investigate further about the increase in SO_2 during COVID lockdown in our study over these three cities, we have analyzed the bivariate polar plots for the reference period and COVID period (**Figure 3**). Polar plots suggest that neither the wind speed nor the wind direction was significantly different at Chandigarh, Bengaluru, and Thiruvanthapuram during the COVID year with respect to the reference period. However, the AQI of SO_2 was substantially higher during the lockdown period amid COVID-19 compared with the reference period (**Figure 3**). Though we could not find anywhere the energy

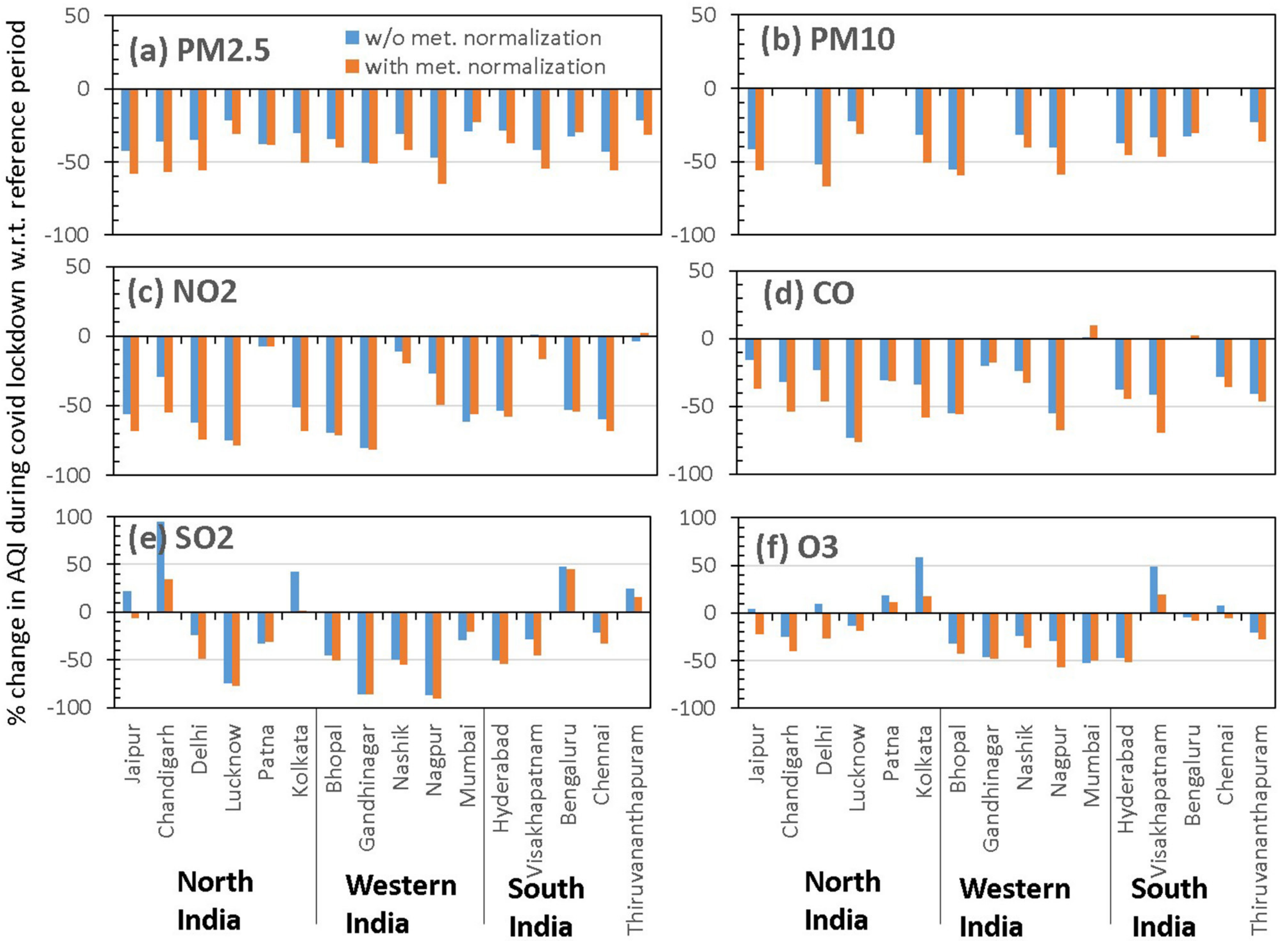

FIGURE 2 | City-specific percent change of key pollutants (with and without meteorology normalization) during complete lockdown with respect to the reference time-period.

demand estimations for these cities during the lockdown period, we have tried to collect the supporting information for the observed increase in SO_2 levels during the lockdown period. In the wake of the COVID-19 pandemic, the Indian government, in collaboration with established textile industries, started domestic manufacturing of personal protective equipment (PPE) in India since March 2020 (Lakshmanan and Nayyar, 2020). Thermal energy consumption in textile manufacturing units is about 70–80% in India (Bhaskar et al., 2013). Moreover, these coal-based thermal power sources in textile industries is the major source of SO_2 in the atmosphere (Rabbi, 2018; Niinimäki et al., 2020).

Since all other industries were shut down during the lockdown period, we therefore are attributing the textile industries, involved in PPE kit manufacturing, as the major energy consumption units in a particular city during the lockdown period. The major hubs identified for PPE kit manufacturing were Ludhiana, Bengaluru, and Ernakulum, among others (Kitex Garments ltd., 2020; The News Minute., 2020; The Tribune., 2021). Thus, it is logical to state here that there would have been higher energy consumption in Ludhiana, Bengaluru, and Ernakulum. The three cities in which we observed increased SO_2 levels during lockdown were Chandigarh, Bengaluru, and Thiruvananthapuram. Ludhiana and Ernakulum are situated in the north-west direction of Chandigarh and Thiruvananthapuram, respectively. Thus, prevailed north-westerly winds would have favored the transport of SO_2 to Chandigarh from power plants feeding the energy to textile industries in Ludhiana (**Figure 3**). Likewise, prevailed north-westerly winds would have favored the transport of SO_2 to Thiruvananthapuram city from power plants feeding the energy to textile industries in Ernakulum. However, Bengaluru itself was one of the major hubs for the manufacturing of PPE kits in south India (The News Minute., 2020). This would have led to higher energy consumption in the city, which would have led to higher emissions of SO_2 from nearby power plants, the effect of which was observed in our results.

We have also witnessed a significant increase in O_3 over Kolkata (∼18%, from 14.5 ± 4.5 to 17.5 ± 11.6; two-tailed t-value: 2.4) and Visakhapatnam (∼20%, from 6.1 ± 2.2 to 7.6 ± 4.2; two-tailed t-value: 2.9) during the lockdown period

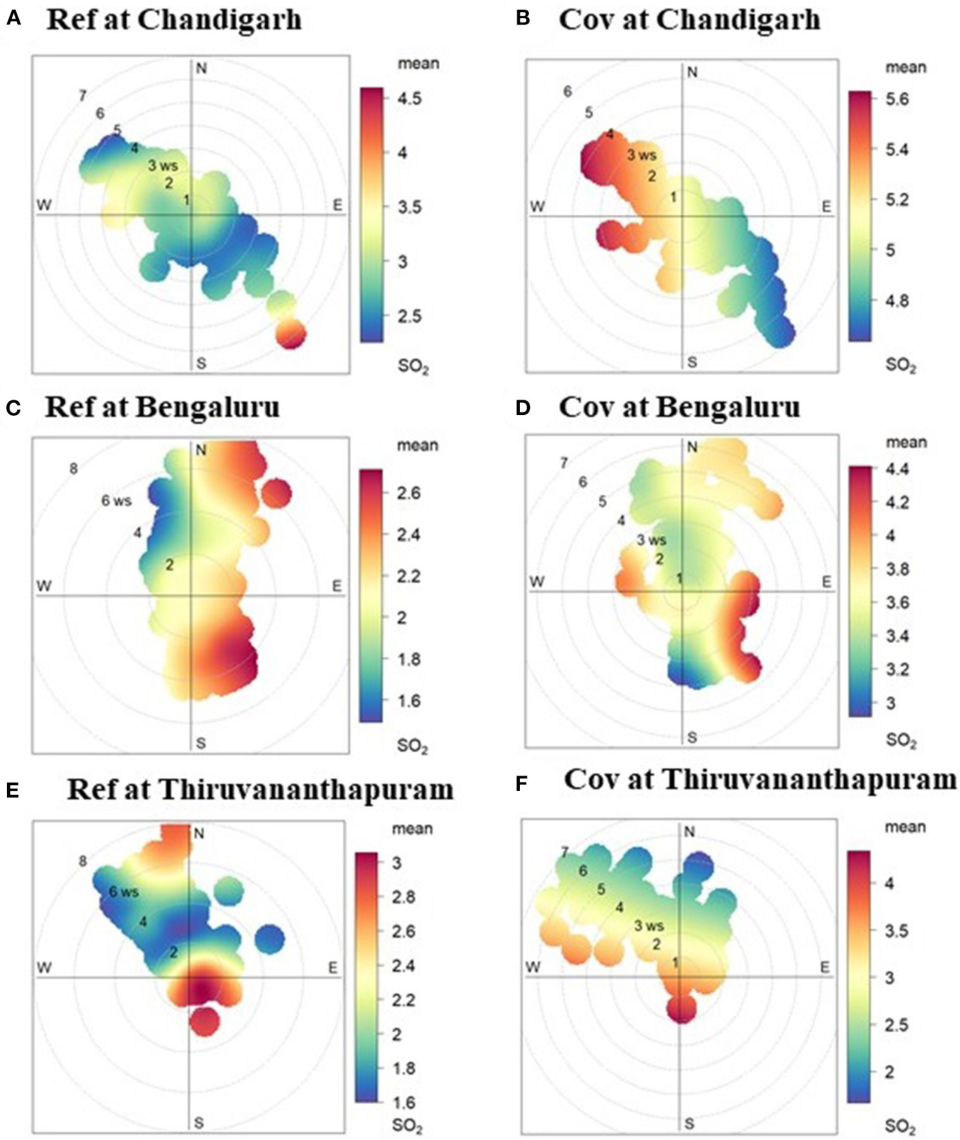

FIGURE 3 | Bivariate polar plots of SO_2 for **(A,B)** Chandigarh, **(C,D)** Bengaluru, and **(E,F)** Thiruvanthapuram during reference and lockdown period due to COVID, respectively. The color bars show SO_2 AQI values for respective plots.

compared with the reference period. Dumka et al. (2021) has shown about 4–8% increase in O_3 concentration over Delhi—NCR, mainly related to NOx chemistry. Pathakoti et al. (2020) has shown a dip of ∼17–18% in mean NO_2 levels (with maximum reduction over Delhi ∼54%) using satellite remote-sensing data over India during the lockdown period. Jain et al. (2021) has also shown a significant reduction (∼50%) in short-lived gaseous air pollutants such as NO_2 and SO_2, whereas minimal reduction (∼10%) in CO and O_3 compared with that of 2019, which has direct as well as indirect impacts of anthropogenic emissions. Venter et al. (2020) has also shown an increase in satellite-based O_3 concentrations over polluted regions of China and India and a decrease in other parts of the world during the lockdown period compared with 2019. These results may be understood as non-linear chemical interactions of volatile organic compounds (VOCs) and oxides of nitrogen (NO_x = $NO + NO_2$) in formation/destruction of tropospheric O_3 under different environmental conditions (Sillman, 1999). Venter et al. (2020) has suggested that the VOC limited region may experience an increase in O_3, whereas the NO_x limited region experiences a decrease in O_3. Thus, our findings on change in air pollution magnitude are consistent with the previous literature.

Effect of Lockdown on Regionwise (North, West, and South India) Ambient AQI

The aforementioned analysis indicates a significant impact of lockdown amid COVID-19 on improvement in ambient air quality in Indian cities, i.e., huge reduction in levels of air

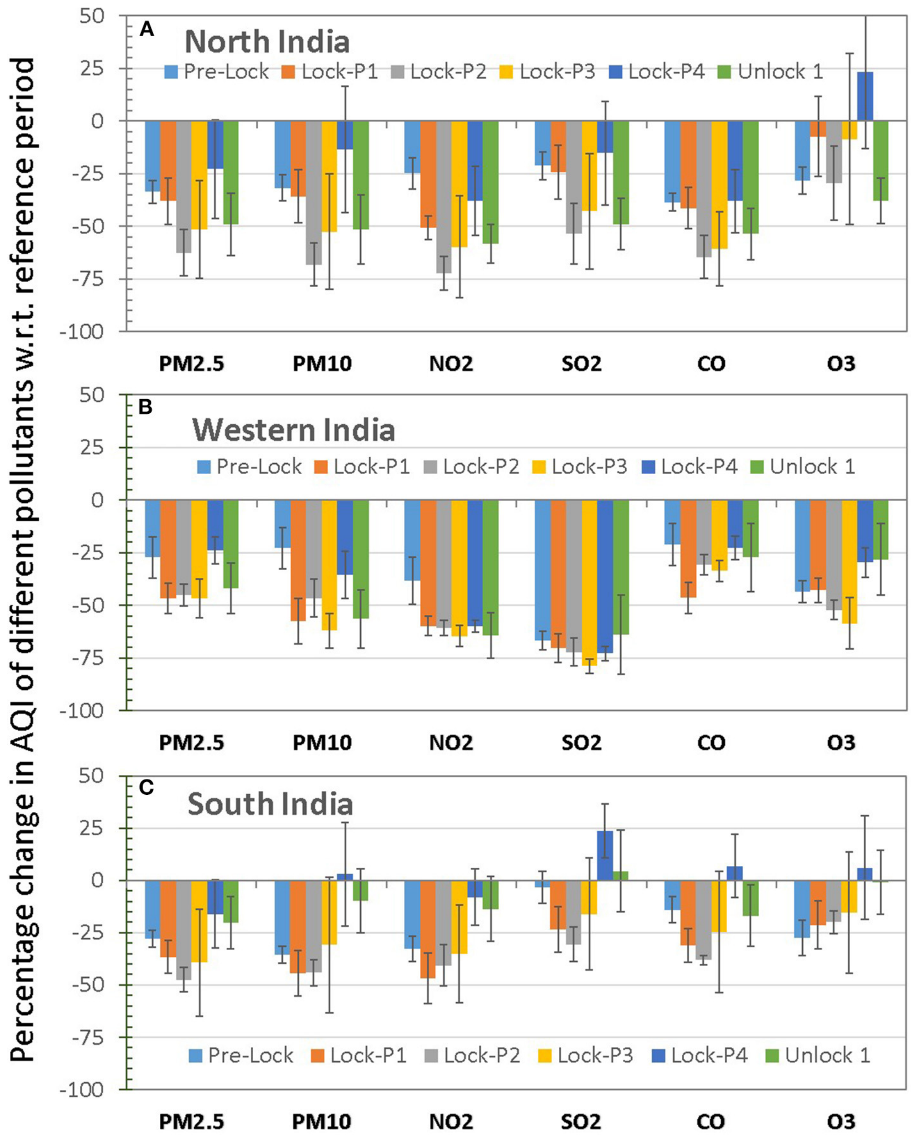

FIGURE 4 | Percent change of different air pollutants averaged on a regional basis: **(A)** north, **(B)** western, and **(C)** south India during different prelockdown, lockdown (P1–P4), and unlock phases. The spread bars show standard deviation.

pollutants. These reductions in AQIs were manifestation of both the weak source intensity, atmospheric chemistry, and favorable meteorological condition. Similar findings for selected air pollutants have been reported for different cities of India and from different geographical locations across the globe (Kumar et al., 2020; Mahato et al., 2020; Otmani et al., 2020; Venter et al., 2020; Dumka et al., 2021).

Since most of the cities are showing near similar trends of change in levels of air pollutants, it would be reasonable to group them regionwise and assess the improvement in air quality due to lockdown amid COVID-19 on a regional basis. We have grouped different cities into three broad regions, viz., north, western, and south India. North India was represented by Chandigarh, Jaipur, Delhi, Lucknow, Patna, and Kolkata, whereas western India was represented herein by Nashik, Gandhinagar, Mumbai, Nagpur, and Bhopal in our study. Hyderabad, Bengaluru, Chennai, Visakhapatnam, and Thiruvananthapuram were grouped as south India. Subsequently, we have averaged the data set of respective cities on a regional basis (north, west, and south) to assess the regionwise change in levels of air pollutants during pre-lockdown (Pre-Lock), lockdown (LockP1, LockP2, LockP3, and LockP4), and post-lockdown (Unlock 1) period over India. **Figure 4** shows the percent change of different air pollutants during different phases [Pre-Lock, Lockdown (P1, P2, P3, and P4) and Unlock 1] over (a) north, (b) west, and (c) south India. It shows that by-and-large, the concentrations of all pollutants were decreased (except for some species during P4) over different regions of India in the lockdown period compared with the reference period. The reduced levels of air pollutants during pre-lockdown in India may be explained on the basis of worldwide lockdown leading to reduced long-range transport or transboundary impact of air pollutants (Venter et al., 2020) as many European and Asian countries had complete to partial lockdown during January–March 2020.

The temporal variability in percentage change of different pollutants shows maximum reduction during lockdown phases over all three regions. However, different interphase (lockdown phases P1, P2, P3, and P4) trends were observed across different regions. In general, maximum reductions (for almost all pollutants) were observed in the first three phases of lockdown (P1, P2, and P3) over west and south India. The increase in residential mobility during lockdown compared with that in pre-lockdown is reported, which steadily decreases from P1 to P4 (∼31 to 18%) over India (Saha and Chouhan, 2021). North India, having the highest air pollution in normal days among regions assessed herein, shows a quite unique pattern where we see large reductions during P2 and P3, and thereafter buildup of pollution in P4 and a drastic decrease during unlock 1 period. This result can be explained on the basis of large temporal variability in the concentration of the pollutant during a short period of P4, as evident by larger error bars in **Figure 4A**. Thus, our analysis shows that the first three phases of lockdown were considerably associated with decreased levels of air pollutants and further relax in lockdown starts building up of pollution over all three Indian cities. In other words, it indicates a quick replenishment of air pollution soon after the lift of lockdown. This is likely due to the increase in economic activities and transportation across the country.

Overall, maximum reduction in SO_2 was observed over west India (∼61%) and in NO_2 (∼59%) over north India, and minimum reduction in almost all pollutants has been observed over south India during the lockdown period. Higher reductions in certain species during the lockdown period amid COVID-19 could be attributed to the shutdown of its major polluting source. For example, the maximum reduction (49%) of $PM_{2.5}$ in this study has been observed over north India. Pathakoti et al. (2020) has also observed maximum reduction in aerosol levels over the IGP region with an average reduction of ∼24% over India. A similar kind of spatiotemporal variability in aerosol optical depth has been reported over India using satellite measurements (Soni, 2021). Nigam et al. (2021) has also found an increase in air pollution over western industrial cities of India, while restrictions were relaxed in P4 and unlock period.

CONCLUSIONS

In this study, we have made an attempt to assess the effect of lockdown amid COVID-19 on the improvement in ambient air quality in the year 2020 over 16 Indian cities. Thus how, this study covers a wide spatial coverage in ambient air quality assessment from north to south in the Indian subcontinent. In general, all the air pollutants assessed herein exhibit a remarkable decline in their abundance during the lockdown period compared with their concentrations during the previous period in the years 2017–2019 (termed as reference period). Averaging over different regions of India, the air quality showed about 30–50% reduction for $PM_{2.5}$, PM_{10}, and CO, and a maximum reduction of 40–60% for the NO_2 with significant spatial variability. The concentrations of SO_2 and O_3 exhibited both the decline as well as rise in their abundance pattern during the lockdown period compared with the reference period plausibly highlighting the role of atmospheric chemistry in regulating these reactive chemical species in the urban airshed under ambient atmospheric condition. Furthermore, we have also assessed the effect of ambient meteorology on observed reduction in air pollution using meteorologically normalized AQI values. Around 10% further reduction during lockdown period compared with the reference period was contributed only due to meteorological condition. The spatiotemporal variability of different air pollutants across India emphasizes the existence of different strengths and/or nature of emission sources in north, west, and south India. Maximum fine particulate matter reduction was observed over north India during the lockdown period. The buildup of air pollution was observed in the later phase of lockdown and unlock due to relaxed restrictions on anthropogenic activities (industrial and transport). This study urges that by adopting cleaner fuel technology and avoiding poor combustion activities (e.g., crude open biomass burning) in the urban agglomerations and rural areas within India, the ambient air pollution could be reduced by around 30–60% compared with business-as-usual levels.

DATA AVAILABILITY STATEMENT

Publicly available datasets were analyzed in this study. This data can be found here: https://aqicn.org/data-platform/covid19/.

AUTHOR CONTRIBUTIONS

AM, AS, and CS collected the required data. Data analysis and interpretation is done by AM and PR. AM and PR drafted the manuscript and final editing is done by all authors. All authors contributed to the article and approved the submitted version.

ACKNOWLEDGMENTS

AM would like to thank DST Purse Grant and DST INSPIRE Faculty Grant (DST/INSPIRE/04/2015/003253) for providing the necessary funds for the analysis cost. PR acknowledges funding support from DST-MCECCR. The authors thank two reviewers for their fruitful comments and suggestions.

SUPPLEMENTARY MATERIAL

The Supplementary Material for this article can be found online at: https://www.frontiersin.org/articles/10.3389/frsc.2021.705051/full#supplementary-material

REFERENCES

Berman, J. D., and Ebisu, K. (2020). Changes in US air pollution during the COVID-19 pandemic. *Sci. Total Environ.* 739:139864. doi: 10.1016/j.scitotenv.2020.139864

Bhaskar, M. S., Verma, P., and Kumar, A. (2013). Indian textile industries towards energy efficiency movement. *Int. J. Envir. Sci. Deve. Mon.* 4, 36–39.

Bishoi, B., Prakash, A., and Jain, V. K. (2009). A comparative study of air quality index based on factor analysis and US-EPA methods for an urban environment. *Aerosol Air Qual. Res.* 9, 1–17. doi: 10.4209/aaqr.2008.02.0007

Chen, H., Guo, J., Wang, C., Luo, F., Yu, X., Zhang, W., et al. (2020). Clinical characteristics and intrauterine vertical transmission potential of COVID-19 infection in nine pregnant women: a retrospective review of medical records. *Lancet* 395, 809–815. doi: 10.1016/S0140-6736(20)30360-3

Dai, Q., Liu, B., Bi, X., Wu, J., Liang, D., Zhang, Y., et al. (2020). Dispersion normalized PMF provides insights into the significant changes in source contributions to PM2. 5 after the COVID-19 outbreak. *Environ. Sci. Technol.* 54, 9917–9927. doi: 10.1021/acs.est.0c02776

Dandotiya, B., Jadon, N., and Sharma, H. K. (2019). Effects of meteorological parameters on gaseous air pollutant concentrations in urban area of Gwalior City, India. *Environ. Claims J.* 31, 32–43. doi: 10.1080/10406026.2018.1507508

Dumka, U. C., Kaskaoutis, D. G., Verma, S., Ningombam, S. S., Kumar, S., and Ghosh, S. (2021). Silver linings in the dark clouds of COVID-19: improvement of air quality over India and Delhi metropolitan area from measurements and WRF-CHIMERE model simulations. *Atmospher. Pollut. Res.* 12, 225–242. doi: 10.1016/j.apr.2020.11.005

Dutheil, F., Baker, S. J., and Navel, V. (2020). COVID-19 as a factor influencing air pollution? *Environ. Pollut.* 263:114466. doi: 10.1016/j.envpol.2020.114466

Falocchi, M., Zardi, D., and Giovannini, L. (2021). Meteorological normalization of NO_2 concentrations in the Province of Bolzano (Italian Alps). *Atmosp. Environ.* 246:118048. doi: 10.1016/j.atmosenv.2020.118048

Hersbach, H., Bell, B., Berrisford, P., Hirahara, S., Horányi, A., Muñoz-Sabater, J., et al. (2020). The ERA5 global reanalysis. *Quart. J. R. Meteorol. Soc.* 146, 1999–2049. doi: 10.1002/qj.3803

Jain, C. D., Madhavan, B. L., Singh, V., Prasad, P., Krishnaveni, A. S., Kiran, V. R., et al. (2021). Phase-wise analysis of the COVID-19 lockdown impact on aerosol, radiation and trace gases and associated chemistry in a tropical rural environment. *Environ. Res.* 194:110665. doi: 10.1016/j.envres.2020.110665

Kitex Garments ltd. (2020). Available online at: http://www.kitexgarments.com/wp-content/uploads/2020/07/KGL_CoVID_19_FY20.pdf (accessed August 20, 2021).

Kumar, P., Hama, S., Omidvarborna, H., Sharma, A., Sahani, J., Abhijith, K. V., et al. (2020). Temporary reduction in fine particulate matter due to 'anthropogenic emissions switch-off'during COVID-19 lockdown in Indian cities. *Sustain. Cities Soc.* 62:102382. doi: 10.1016/j.scs.2020.102382

Kumar, S. (2020). Effect of meteorological parameters on spread of COVID-19 in India and air quality during lockdown. *Sci. Total Environ.* 745:141021. doi: 10.1016/j.scitotenv.2020.141021

Lakshmanan, R., and Nayyar, M. (2020). *Personal Protective Equipment in India: An INR 7,000 Cr industry in the making. Strategic Investment Research Unit, Invest India*. Available online at: https://www.investindia.gov.in/siru/personal-protective-equipment-india-INR-7000-cr-industry-in-the-making (accessed August 20, 2021).

Mahato, S., Pal, S., and Ghosh, K. G. (2020). Effect of lockdown amid COVID-19 pandemic on air quality of the megacity Delhi, India. *Sci. Total Environ.* 730:139086. doi: 10.1016/j.scitotenv.2020.139086

Mintz, D. (2018). *Technical Assistance Document for the Reporting of Daily Air Quality-the Air Quality Index (AQI): US Environmental Protection Agency*. Office of Air Quality Planning and Standards, Research Triangle Park, NC: Air Quality Assessment Division. Publication No. EPA-454/B-18-007.

Mor, S., Kumar, S., Singh, T., Dogra, S., Pandey, V., and Ravindra, K. (2021). Impact of COVID-19 lockdown on air quality in Chandigarh, India: understanding the emission sources during controlled anthropogenic activities. *Chemosphere* 263:127978. doi: 10.1016/j.chemosphere.2020.127978

Nakada, L. Y. K., and Urban, R. C. (2020). COVID-19 pandemic: impacts on the air quality during the partial lockdown in São Paulo state, Brazil. *Sci. Total Environ.* 730:139087. doi: 10.1016/j.scitotenv.2020.139087

Nandi, J. (2020). *Spring Colder Than Usual This Year, Shows IMD Data*. New Delhi: Hindustan Times.

Nigam, R., Pandya, K., Luis, A. J., Sengupta, R., and Kotha, M. (2021). Positive effects of COVID-19 lockdown on air quality of industrial cities (Ankleshwar and Vapi) of Western India. *Sci. Rep.* 11, 1–12. doi: 10.1038/s41598-021-83393-9

Niinimäki, K., Peters, G., Dahlbo, H., Perry, P., Rissanen, T., and Gwilt, A. (2020). The environmental price of fast fashion. *Nat. Rev. Earth Environ.* 1, 189–200. doi: 10.1038/s43017-020-0039-9

Otmani, A., Benchrif, A., Tahri, M., Bounakhla, M., El Bouch, M., and Krombi, M. H. (2020). Impact of Covid-19 lockdown on PM10, SO2 and NO2 concentrations in Salé City (Morocco). *Sci. Total Environ.* 735:139541. doi: 10.1016/j.scitotenv.2020.139541

Pathakoti, M., Muppalla , A., Hazra, S., Venkata , M. D., Lakshmi, K. A., Sagar, V. K., et al. (2020). An assessment of the impact of a nation-wide lockdown on air pollution-a remote sensing perspective over India. *Atmosp. Chem. Phys. Discus.* 21, 1–16. doi: 10.5194/acp-2020-621

Petetin, H., Bowdalo, D., Soret, A., Guevara, M., Jorba, O., Serradell, K., et al. (2020). Meteorology-normalized impact of the COVID-19 lockdown upon NO_2 pollution in Spain. *Atmosph. Chem. Phys.* 20, 11119–11141. doi: 10.5194/acp-20-11119-2020

Rabbi, M. A. (2018). Assessment of nitrogen oxides and sulphur dioxide content in the ambient air near the garments industries of Bangladesh. *J. Environ. Soc. Sci.* 5, 1–4.

Saha, J., and Chouhan, P. (2021). Lockdown and unlock for the COVID-19 pandemic and associated residential mobility in India. *Intern. J. Infect. Dis.* 104, 382–389. doi: 10.1016/j.ijid.2020.11.187

Sarfraz, M., Shehzad, K., and Shah, S. G. M. (2020). The impact of COVID-19 as a necessary evil on air pollution in India during the lockdown. *Environ. Pollut.* 266:115080. doi: 10.1016/j.envpol.2020.115080

Sharma, S., Zhang, M., Gao, J., Zhang, H., and Kota, S. H. (2020). Effect of restricted emissions during COVID-19 on air quality in India. *Sci. Total Environ.* 728:138878. doi: 10.1016/j.scitotenv.2020.138878

Sillman, S. (1999). The relation between ozone, NOx and hydrocarbons in urban and polluted rural environments. *Atmos. Environ.* 33, 1821–1845. doi: 10.1016/S1352-2310(98)00345-8

Soni, P. (2021). Effects of COVID-19 lockdown phases in India: an atmospheric perspective. *Environ. Dev. Sustainab.* 1–12. doi: 10.1007/s10668-020-01156-4

The News Minute. (2020). Available online at: https://www.thenewsminute.com/article/bengaluru-emerges-hub-ppe-manufacturing-50-kits-india-centre-123408 (accessed August 20, 2021).

The Tribune. (2021). Available online at: https://www.tribuneindia.com/news/punjab/punjab-emerges-as-manufacturing-hub-for-covid-protective-kits-82757 (accessed August 20, 2021).

Tosepu, R., Gunawan, J., Effendy, S. D., Ahmad, A. I., Lestari, H., Bahar, H., et al. (2020). Correlation between weather and Covid-19 pandemic in Jakarta, Indonesia. *Sci. Total Environ.* 725:138436. doi: 10.1016/j.scitotenv.2020.138436

Venter, Z. S., Aunan, K., Chowdhury, S., and Lelieveld, J. (2020). COVID-19 lockdowns cause global air pollution declines. *Proc. Natl. Acad. Sci.* 117, 18984–18990. doi: 10.1073/pnas.2006853117

WHO (2020) Novel Coronavirus (2019-nCoV) Situation Report - 10. Available online at: https://www.who.int/emergencies/diseases/novel-coronavirus-2019

Conflict of Interest: The authors declare that the research was conducted in the absence of any commercial or financial relationships that could be construed as a potential conflict of interest.

Publisher's Note: All claims expressed in this article are solely those of the authors and do not necessarily represent those of their affiliated organizations, or those of the publisher, the editors and the reviewers. Any product that may be evaluated in this article, or claim that may be made by its manufacturer, is not guaranteed or endorsed by the publisher.

frontiers in Sustainable Cities

REVIEW
published: 08 October 2021
doi: 10.3389/frsc.2021.705185

Nature-Based Solutions for Co-mitigation of Air Pollution and Urban Heat in Indian Cities

Jyothi S. Menon† and Richa Sharma†*

Center for Environmental Health, Public Health Foundation of India, Gurugram, India

The urban population is subjected to multiple exposures of air pollution and heat stress and bear severe impacts on their health and well-being in terms of premature deaths and morbidity. India tops the list of countries with the highest air pollution exposure and hosts some of the most polluted cities in the world. Similarly, Indian cities are highly vulnerable to extreme heat with the frequency of heatwaves expected to increase several-fold in urban areas in India. It is reported that mitigating air pollution could reduce the rural-urban difference of the incoming radiation thus resulting in mitigation of the urban heat island effect. Since the interaction between urban heat and air pollution is dynamic and complex, both these factors should be considered by the urban authorities in designing mitigation strategies. Given the multi-functional nature and cost-effectiveness of Nature-Based Solutions (NbS), they appear to be the most appropriate remedy for environmental issues of urban areas, particularly in developing countries. In addition to improving public health (through the reduction in air pollution and urban heat), NbS also provides a wide range of co-benefits such as reducing energy cost and health costs as well as conservation of biodiversity. This review is an attempt to understand the potentials of NbS in co-mitigating air pollution and urban heat in Indian cities. A framework for the planning and design of NbS in Indian cities is also proposed based on the review that could help city planners and decision-makers in addressing these two issues in an integrated manner.

Keywords: nature based solution, Urban Heat Island, air pollution mitigation, air pollution tolerance index, co-mitigation

OPEN ACCESS

Edited by:
Prashant Rajput,
Banaras Hindu University, India

Reviewed by:
Sisay E. Debele,
University of Surrey, United Kingdom
Atinderpal Singh,
University of Delhi, India

****Correspondence:***
Jyothi S. Menon
jyothi.menon@phfi.org

†These authors have contributed equally to this work and share first authorship

Specialty section:
This article was submitted to Climate Change and Cities, a section of the journal Frontiers in Sustainable Cities

Received: *04 May 2021*
Accepted: *17 August 2021*
Published: *08 October 2021*

Citation:
Menon JS and Sharma R (2021) Nature-Based Solutions for Co-mitigation of Air Pollution and Urban Heat in Indian Cities. Front. Sustain. Cities 3:705185. doi: 10.3389/frsc.2021.705185

INTRODUCTION

As a rapidly urbanizing nation, India faces the challenge of developing its cities sustainably. Most cities in India have been growing organically lacking prudent planning that often results in degradation of their environment and ultimately resulting in various health implications for the citizens. Urban planners and policymakers hence need to anticipate the various environmental impacts of their plans and policies to ensure sustainable urbanization. The two major issues that cities across the globe facing are: Air Pollution (Manisalidis et al., 2020) and the Urban Heat Island (Ulpiani, 2021). Interestingly, the two phenomena are also intricately linked to each other through positive feedback loops (**Figure 1**). The change in urban microclimate can affect the pollutant dispersion, thus the air quality. The Short-Lived Climate Pollutants (SLCP) such as ozone and black carbon can trap heat thus increasing the temperature. Both air quality and urban microclimate are also affected by other urban characteristics such as urban morphology and

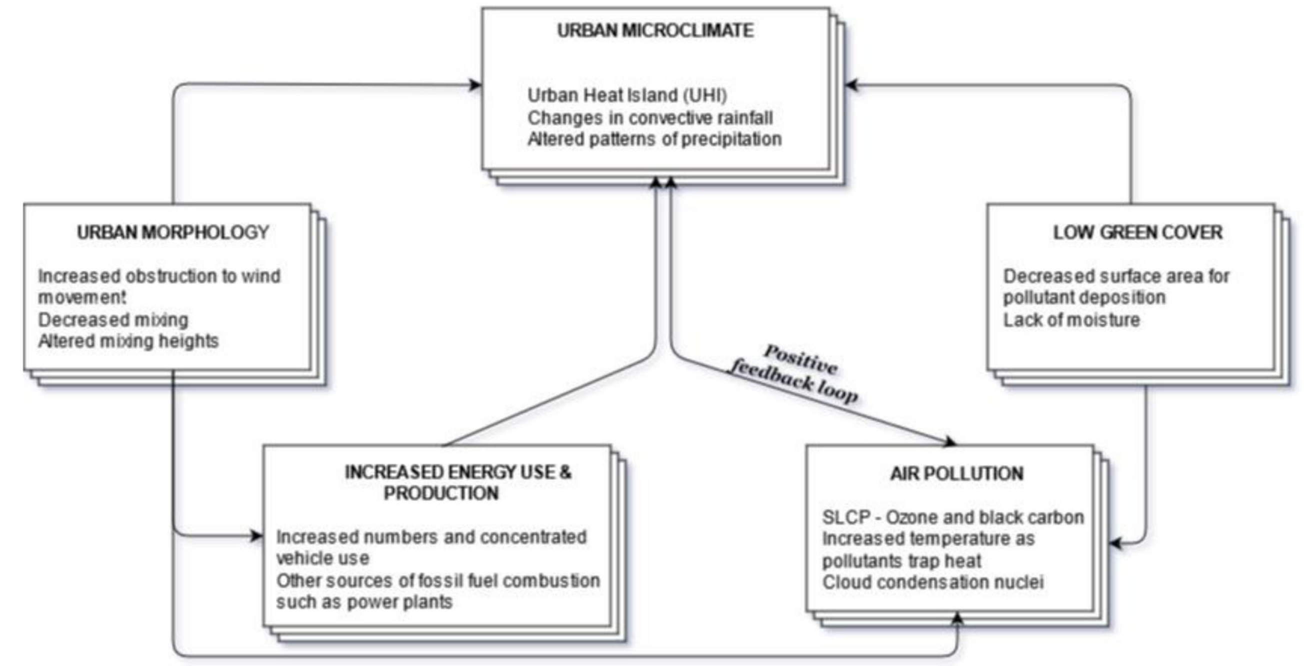

FIGURE 1 | Inter-linkages between changes in urban micro-climate and air pollution.

green cover. Hence, it is important to study the two issues together and understand their integrated exposure.

Rapid urbanization has resulted in significant changes in land use and land cover which is affecting the environment in myriad ways. Specific qualities of urban materials (e.g., low albedo and high volumetric heat capacity of concrete asphalt) (Mohajerani et al., 2017), urban morphology and design (decreased sky view factor due to densely places tall buildings) (Dirksen et al., 2019), along with the heat generated from energy usage and other anthropogenic sources (Singh et al., 2020b) increases the temperature in an urban area in comparison to the surrounding suburban and/or rural areas. The phenomenon is termed as Urban Heat Island or UHI (Oke, 1973). This works as positive feedback for escalating energy consumption through increased demands for cooling. UHI also tends to intensify the effect and impact of extreme heat and heatwave events in cities (Rizvi et al., 2019). Urbanization impacts are not only limited to direct changes in land surface and air properties, but are also characterized by increase in vehicular and industrial activities that cause further deterioration in air quality (Manisalidis et al., 2020). Rapid urbanization and industrialization also result in increased anthropogenic activities which is the main cause for the deterioration of air quality in many cities. Ample studies on changes in Land Use Land Cover (LULC) and urbanization, and its effect on urban temperature and air pollution are available in India. However, there is a significant research gap on understanding the combined exposure and mitigation of urban heat and air pollution in urban areas. This is in spite of the fact that India has a high potential for co-benefits of mitigation of air pollution and climate change.

Considering the degradative nature of the current urbanization and growth and development practices, governments across the world are increasingly investing in ecosystem-based approaches of development. Nature-based Solutions (NbS) for city planning are hence, becoming popular among policy makers and practitioners. NbS has found great applications in water and energy security, disaster management and risk reduction as well as improving social well-being in urban areas. NbS aims to produce more resilient cities through restoring nature which can support conventionally built infrastructure systems (Bush and Doyon, 2019). Given the multi-functional nature and cost-effectiveness of NbS, they appear to be the most appropriate remedy for environmental issues of urban areas, particularly in developing countries like India. However, not enough steps have been taken toward integrating NbS into the city planning process. This review is an attempt to understand the potentials of NbS in co-mitigating air pollution and urban heat in Indian cities. Based on this review, a framework for the successful implementation of NbS in Indian cities is also proposed. Such a framework could facilitate effective and efficient city planning and decision-making while addressing the two issues (discussed) in an integrated manner.

METHODOLOGY

An electronic review was carried out for peer-reviewed research articles using a combination of selected keywords ("nature-based solutions," "nature-based solution + urban," "nature-based solutions + urban heat island," "nature-based solution + air pollution," "nature-based solution + air pollution + urban heat island"). The articles published in the last 10 years (2010–2020) were retrieved from bibliographical databases (Google scholar, Sciencedirect, Pubmed) and from the reference lists of selected articles (**Table 1**). The articles that did not focus on urban areas or cities and non-English articles were excluded. The two authors independently went through the list of abstracts and finalized the articles for review.

TABLE 1 | Search results on the keywords from various databases.

Keywords	Google scholar	Sciencedirect	PubMed
"nature based solutions"	11,100	960	41
"nature based solutions" + "urban"	7,830	727	16
"nature based solutions" + "urban heat island"	1,270	159	3
"nature based solution" + "air pollution"	408	161	0
"nature based solution" + "urban heat island" + "air pollution"	190	76	0

URBAN HEAT ISLAND EXPOSURE IN URBAN AREAS

Urban Heat Island (UHI) is a phenomenon globally experienced by urban areas, wherein the urban built-up areas exhibit higher temperatures as compared to surrounding non-urban or rural landscapes (Oke, 1973). The phenomenon has been extensively documented in various cities across the world including in China (Li et al., 2018), US (Ramamurthy and Sangobanwo, 2016), Canada (Gaur et al., 2018), Australia (Santamouris et al., 2017), countries of Europe (Arnds et al., 2017; De Ridder et al., 2017), Turkey (Dihkan et al., 2018), Iran (Haashemi et al., 2016; Weng et al., 2019), Sri Lanka (Ranagalage et al., 2018), Malaysia (Qaid et al., 2016), Philippines (Estoque and Murayama, 2017), and India (Mathew et al., 2018) to mention a few with varying socio-economic and geo-climatic factors.

UHI is studied as surface UHI (SUHI) and as atmospheric UHI (AUHI). The intensity of SUHI is often measured using remotely sensed Land Surface Temperature (LST) often derived from Landsat thermal bands (Sagris and Sepp, 2017), MODIS LST products (Sidiqui et al., 2016) and ASTER thermal data (dos Santos et al., 2017). For measuring atmospheric UHI, air temperature observations are used, which are either mobile observations recorded with a moving vehicle mounted with data logger (dos Santos et al., 2017) or the meteorological station observations (Arnds et al., 2017). UHI varies both in space and time, as a function of various factors including canyon radiative geometry, thermal properties of materials, anthropogenic heat, urban greenhouse, reduction of evaporating surfaces, reduced turbulent transfer, climate, topography, physical layout of the built environment as well as short-term weather conditions (Golden and Kaloush, 2006; Shahmohamadi et al., 2011; Santamouris et al., 2019). Understanding of these factors is crucial for designing and implementing UHI mitigation solutions.

Understanding the UHI phenomenon for a city becomes crucial as it both directly and indirectly impacts human health (Vargo et al., 2016; Heaviside et al., 2017) through increased heat stress, and inflates the city's energy demands for cooling (Lowe, 2016; Liao et al., 2017). UHI and heat stress increase the building energy consumption by increasing the cooling demand in urban spaces. Literature shows that UHI causes median increase of 19% in cooling energy consumption (Li et al., 2019). However, there are huge inter-city variations ranging from 10–120% increases. Estimating this increase becomes essential given that India is a tropical country. Kumari et al. (2021) observed that UHI formation resulted in an increase of 2,600 GWh (i.e., 11.4%) in annual average electricity consumption in eight districts of Delhi between April 2012 to March 2017.

UHI has also been documented to increase the city's exposure to heatwaves under the global climate change scenario (Founda and Santamouris, 2017).With the changing climate scenario, many countries including India are becoming prone to more intense and frequent heat waves. Cities in particular due to the phenomenon of UHI, exhibit the synergies between urban heat and heatwave, making the urban areas more vulnerable to extreme heat. According to Sharma et al. (2019), frequency of heat waves for urban areas in Delhi is expected to increase from 0.8 times each summer season in current time frame to 2.1 and 5.1 times in short- and long-term projections. In the past few years researchers have focused on understanding the change in land surface temperature (LST) and factors influencing urban areas such as in Delhi (Mohan et al., 2012; Yadav and Sharma, 2018), Ahmedabad (Mathew et al., 2018), Bengaluru (Sussman et al., 2019), Jaipur (Mathew et al., 2018), Chennai (Swamy et al., 2017), Kochi (Thomas et al., 2014), Lucknow (Singh et al., 2017) and Mumbai (Dwivedi and Khire, 2018; Dwivedi et al., 2019).

Various measures for UHI have been explored particularly with contribution from studies by Mat Santamouris (Yang and Santamouris, 2018). These include, balancing the Albedo Effect in urban area and reduction of concrete urban surface (Icaza et al., 2017), planning and development of green belt and increasing of green cover in urban area (Huang et al., 2008), and installing green and white roofs (Detommaso et al., 2020).

AIR POLLUTION EXPOSURE IN URBAN AREAS

The megacities have emerged as engines of economic growth over the years but also as highly polluted urban sheds. The global urban population is expected to grow by 1.5 % per year between 2025 and 2030. Some of the highest levels of outdoor air pollution in the world are recorded in Asian cities belonging to China and India (World Health Organization (WHO), 2016). Globally air pollution is a leading environmental risk factor resulting in an estimated 5 million deaths per year (Balakrishnan et al., 2019). According to WHO, about 80% of the urban population worldwide is exposed to air pollutant concentrations above the prescribed limits. Air pollution and related health impacts are critical in the urban environment due to its high population density and heterogeneity in emission sources resulting in pockets of very high pollutant concentration called as hotspots. The unplanned development in cities has led to the spatial variation in emission intensity which creates these local air quality control regions or hotspots. Globally, it is estimated that around 10% of the urban population lives in such hotspots (Akhtar and Palagiano, 2017). Urban air quality is largely affected by the micro-meteorology that governs the pollutant transport and resulting in hotspots. Due to the high spatial and temporal variability, the determination of air pollution hotspots is always a challenge in urban areas. Researchers have employed monitored data (fixed monitors, mobile monitors and sensors) (Kumar et al., 2015; Menon and Nagendra, 2018), satellite data (Chitranshi et al., 2015; Mahapatra et al., 2019), modeling and combined approaches (Xie et al., 2017; Mandal et al., 2020) to identify air pollution hotpots within the cities.

Other than the air pollutant emission sources, factors like UHI and climate change also affect urban air quality. Since climate change can affect the factors that govern pollutant transport like changes in chemical reaction rates and boundary layer mixing, it can have a significant effect on the regional air quality (Ebi and McGregor, 2008). According to Intergovernmental Panel on Climate Change (IPCC), elevated temperatures can have various other effects and can contribute to air pollution and related health effects (IPCC, 2013). An increase in air pollution exposure has been linked with a reduction in neighborhood greenery in the urban areas and its association with various health impacts such as cardiovascular diseases, premature mortality and children's health has been widely reported recently (Dadvand et al., 2015; Yitshak-Sade et al., 2017; Crouse et al., 2019).

NATURE-BASED SOLUTIONS (NbS)

NbS are gaining popularity in recent years in tackling environmental issues especially climate change and air pollution due to its potential co-benefits. The European Commission has defined NbS as "Solutions that are inspired and supported by nature, which are cost-effective, simultaneously provide environmental, social and economic benefits and help build resilience" (European Commission, n.d.). NbS are sustainable options to mitigate the harmful effects of climate change and pollution, improving the health and well-being of city residents at the same time benefiting biodiversity in the most resource-efficient way. Raymond et al. (2017) has developed a framework to assess the co-benefits of NbS emphasizing the need for a cross-sectoral approach to environmental policy and planning.

NbS for Urban Heat Mitigation and Adaptation

Vegetation cover has a larger effect in controlling temperature especially in urban areas as reported in various studies (Chen et al., 2020). Improving the vegetation cover/greenery is suggested as a way to mitigate UHI and air pollution as well as improving thermal comfort in urban areas. Native plant species tolerant to pollution with higher cooling potential are ideal choices as a common solution for the problem of air pollution and UHI. Thus, planners not only need to focus on the area under green cover, the spatial distribution of green cover but also the plant species that need to be planted when working on the mitigative solutions for air pollution and urban heat.

Green spaces have both local and global adaptation as well as mitigation impacts for climate change. They help in reducing the UHI effect at the city scale as well as reinforce carbon sequestration contributing to the mitigation of global climate change. These are often projected as a "soft engineering" strategy for climate adaptation (Kitha and Lyth, 2011) and also help in climate change adaptation and disaster risk reduction by providing ecosystem services (Munang et al., 2013). Such ecosystem-based approach is often widely reported as a cost-effective tool in climate adaptation.

In addition, green cover and spaces offer numerous environmental advantages. They help improve the hydrology by preventing surface runoff (Zhang et al., 2015), as well as providing ground water recharge (Ramaiah and Avtar, 2019). These could also act as buffer to extreme events such as floods and help in providing climate adaptation by acting as natural storm water drains, thus reducing climate related disaster risks for cities (Bai et al., 2018). In terms of morphology, large green spaces areas with single composition have greater cooling effects (Kong et al., 2014). Various landscape matrices have been explored to understand the significance of morphology of the urban greens. LSI or the Landscape Shape Index is an important defining factor of the morphology of a green area in the city. For small sized green spaces with complex shapes, cooling intensity is usually limited or even negative in some instances (Jaganmohan et al., 2016). Apart from size, the shape of the green areas also influences their capacity to cool. For instance, circular green space has been observed to dissipate more heat than the square one (Yu et al., 2018). In addition, the vegetation configuration is also observed to influence the cooling capacity of the green spaces. Green spaces with trees have stronger cooling effect than grass. Moreover, in London, cooling distance has been found to positively influenced by the canopy height (Monteiro et al., 2016).

NbS for Improving Air Quality

Nature-based approaches could be effectively adopted as a cheaper and sustainable option in reducing exposure to particle and gaseous pollution in urban areas. can be used for monitoring air quality as well as mitigating air pollution. Some of the sensitive species such as lichens, algae, and trees have been used as bio-indicators of air quality. At the same time, some of the plant species have the potential to reduce air pollution through mechanisms such as bioaccumulation and deposition. The tolerance and sensitivity of the plant species vary depending on the type of stress (pollutant) and plant physiology. Air pollution Tolerance Index (APTI) is a measure developed by Singh and Rao to access the plant's tolerance to air pollutants (Singh and Rao, 1983). The plant species with high APTI value can be used to mitigate air pollution and the species with low APTI value can be used as bio-monitors due to their high sensitivity. Other than APTI, several other factors need to be considered depending on the requirement such as canopy structure, type of habitat, economic value etc. The trees with a good canopy and laminar structure can capture more dust and would be useful in removing dust. This is especially important in dusty environments such as roadsides. Tree species such as *Dalbergia Sissoo* and *Polyalthia longifolia* have good canopy structure as well as moderate to high APTI value. Meanwhile, tree species such as *Mangifera indica* and *Azadirachta indica* have economic value as well. Some of the studies have explored the possibility of estimating a new index taking into account all these factors which would help in identifying the ideal species (Pathak et al., 2011; Pandey et al., 2015a). The potential of some of the plant species in accumulating pollutants such as heavy metals has also been studied (Kumar et al., 2021). The metal accumulation species can be used in the green belt development in highly polluted areas such as industrial areas. Hence the careful selection of plant species based on their tolerance, physiological characteristics, and habitat will help in the mitigation of air pollution to a greater extent (Barwise and Kumar, 2020). Some of the commonly studied tree species for their air pollution tolerance and sensitivity in urban and industrial areas are given in **Table 2**.

In recent years, the term Green Infrastructure (GI) has been largely used by researchers referring to the introduction of vegetation into the urban landscape in the form of parks, green roofs, and walls and its effectiveness in reducing air pollution through various processes such as dispersion and deposition and climate change mitigation and adaptation. The World Health Organization(WHO) has recommended a green space per capita of 9 sq.m per person to improve the citizens' quality of life. Several countries such as UK and Malyasia have adopted standard-based approaches in ensuring green space availability. However, India lacks any stringent norms or standard-setting the minimum required green space per capita in urban areas. The urban Greening Guidelines 2014 by the Ministry of Urban Development suggested steps for the protection of trees and integrating green spaces in urban planning and development phases. Rapid urbanization has resulted in a considerable reduction of green cover in major Indian cities over the years. While some of the cities like Delhi have taken significant measures in restoring green spaces, most of the other cities still show a decreasing trend in their green cover. The green spaces in urban areas can be planned either by (a) using/restoring existing green areas or (b) designing new areas to meet the specific purpose in the form of parks, gardens, urban forests, roadside avenues, or vertical greening systems and green roofs.

Vertical Greening Systems (VGS)

VGS are structures where the vegetation is allowed to grow and spread over a wall or building. The potential of VGS in reducing the temperature, improving thermal comfort, energy savings and air pollution mitigation has been studied widely in the recent past (Pérez et al., 2014; Pandey et al., 2015b; Bustami et al., 2018). VGS such as green facades and green walls can reduce the temperature by passive cooling and has been identified as a solution for urban heat islands. VGS will further help in energy savings by providing thermal insulation through its shade effect (reducing solar radiation), cooling effect (evapotranspiration of plants) and insulation effect (due to insulation of different layers) (Price et al., 2015). Based on the type of plants selected, these systems can mitigate air pollution as well. Some of the climber species with high APTI have been identified as ideal plant species for the development of VGS for air pollution mitigation (Pandey et al., 2015b). Thus, if carefully selected and designed, VGS can provide solutions to both climate change and air pollution in urban areas. Vertical gardens or VGS have recently gained much attention with most of the Indian cities installing them in highly polluted areas such as roadsides.

Green Roofing

Green roofing refers to the vegetation grown over the roof of a building. Green roofs can mitigate air pollution, UHI and noise, reduce energy consumption and, manage runoff water (Vijayaraghavan, 2016; Abhijith et al., 2017). Studies have shown that green roofs can substantially sequester carbon in plants through photosynthesis reducing ambient CO_2 concentrations (Rowe, 2011).

Need for an Integrated Approach

Cities have a key role in resolving the sustainability challenges which have to be addressed through all the three pillars of sustainability—(Social) people, planet (Environmental) and profit (Economic). An integrated framework should be in place for assessing exposure, based on the atmospheric environmental quality of the cities and to identify vulnerable areas. This would require an understanding of the spatial and temporal distribution of thermal stress and air pollution in the city. It has been reported that India a has high potential for co-benefits of mitigation of air pollution and climate change. However, the knowledge on the interplay between these variables is still unclear. With intricate linkages between urban climate and air quality, it becomes important to understand their integrated exposure which could be of great interest for researchers in both health and climate studies. From practitioners' perspectives, such data could be of great help for urban planners in planning and designing sustainable cities.

Proposed Framework for Implementing NbS in Urban Areas

Identifying priority areas that require immediate attention is the major and foremost step. Both UHI and air pollution are reported to exhibit spatial as well as temporal (diurnal and seasonal) variations in urban areas. The large temperature variations in urban areas were attributed to various anthropogenic activities such as industries, transportation, air-conditioning and the urban design/geometry leading to changes in land use land cover (Gogoi et al., 2019). Air pollutants show large spatial and temporal variability depending on pollution sources, meteorology, micro-climate and other factors. Hence hotspot mapping of air

TABLE 2 | Air pollution tolerance and sensitivity of commonly studied plant species in Indian cities.

Plant species	APTI value	Use	Location	Reference
		Urban areas		
Mangifera indica	High	AP mitigation, Green belt development	Allahabad, UP	Kuddus et al. (2011)
			Nanded, Maharashtra	Yannawar (2014)
			Varanasi, UP	Pandey et al. (2016)
Azadirachta indica	High to moderate	AP mitigation, High dust deposition due to good foliage	Allahabad, Gujarat Nanded, Maharashtra	Kuddus et al. (2011) Yannawar (2014)
			Ahmedabad, Gujarat	Chaudhary and Rathore (2019)
Eucalyptus	Moderate to sensitive	Can be used as bioindicator	Nanded, Maharashtra	Yannawar (2014)
			Haridwar, Uttarakhand	Swami and Chauhan (2015)
Ficus religiosa	High	Moderate dust removal capacity, Green belt development Excellent performer based on API (anticipated pollution index)	Allahabad, UP Nanded, Maharashtra Gandhinagar, Gujarat Varanasi, UP	Kuddus et al. (2011) Yannawar (2014) Chaudhary and Rathore (2018) Pathak et al. (2011) Pandey et al. (2015a)
			Ahmedabad, Gujarat	Chaudhary and Rathore (2019)
Dalbergia sissoo	Moderate	High dust removal capacity	Gandhinagar, Gujarat	Chaudhary and Rathore (2018)
		Industrial areas		
Mangifera indica	Moderate	Good dust capturing capacity, Phytoextractor of copper	Jamshedpur, Jharkhand	Roy et al. (2020)
Azadirachta indica	Moderate	Tolerant to AP	Jamshedpur, Jharkhand	Roy et al. (2020)
Ficus religiosa	High	Tolerant to AP, Good dust capturing capacity, Phytoextractor of copper	Talkatora Industrial Area, UP Jamshedpur, Jharkhand	Bharti et al. (2018) Roy et al. (2020)
Eucalyptus globus	High	Tolerant to AP	Talkatora Industrial Area, UP	Bharti et al. (2018)
Bougainvillea sp	High	Tolerant to AP	Manali, Chennai	Ranjan et al. (2015)
Shorea robusta	High	Tolerant to AP and good metal accumulation capacity	Bankura, West Bengal	Karmakar and Padhy (2019)

pollution also becomes imperative for understanding its spatial and temporal patterns and to identify Poor Air Quality (PAQ) pockets within the urban area. Spatio-temporal UHI maps (urban and non-urban pockets delineated using Local Climate Zones [LCZ]) and air quality maps (spatial distribution of air pollution) will help in identifying city hotspots for combined exposure to thermal stress and air pollution. In order to design appropriate adaptation strategies, it is essential to further the understanding of the city's vulnerabilities to the risks under consideration. Physiological heat stress affects productivity which could further decrease the adaptive capacity of vulnerable population. Hence, the vulnerable areas also need to be identified based on the socio-economic characteristics of the population. The selection of potential implementation areas and NbS in the identified priority location should go hand in hand and requires detailed planning (Albert et al., 2020). Various stakeholders including researchers, urban planners, ecologists and social scientists should be actively involved in the planning stage as the successful implementation depends on the landscape and land use characteristics, cost-effectiveness, funding, other societal and practical challenges as depicted in **Figure 2**.

The selection of NbS strategy mainly depends on the location characteristics such as major air pollution sources, urban/street morphology, aesthetic use and other benefits such as erosion prevention, noise mitigation, economic value etc. To start with, a database of trees for a particular city has to be developed which could be further classified based on tree physiological characteristics, APTI value and thermal performance. This will help in identifying and designing tree forms to achieve the required reduction in pollution and urban heat.

Air Pollution Characteristics

The plant species for green space development can be selected from the database based on the air pollution characteristics at the location. For example, if industrial pollution is prominent in the location, then pollutant-specific tolerant species can be selected for the development of the green belt. To curb vehicular pollution along the roads, the plants with good dust capturing potential and canopy could be selected along with high pollution tolerance. Vegetation can also be designed as a barrier to protect and separate people from pollution (Abhijith

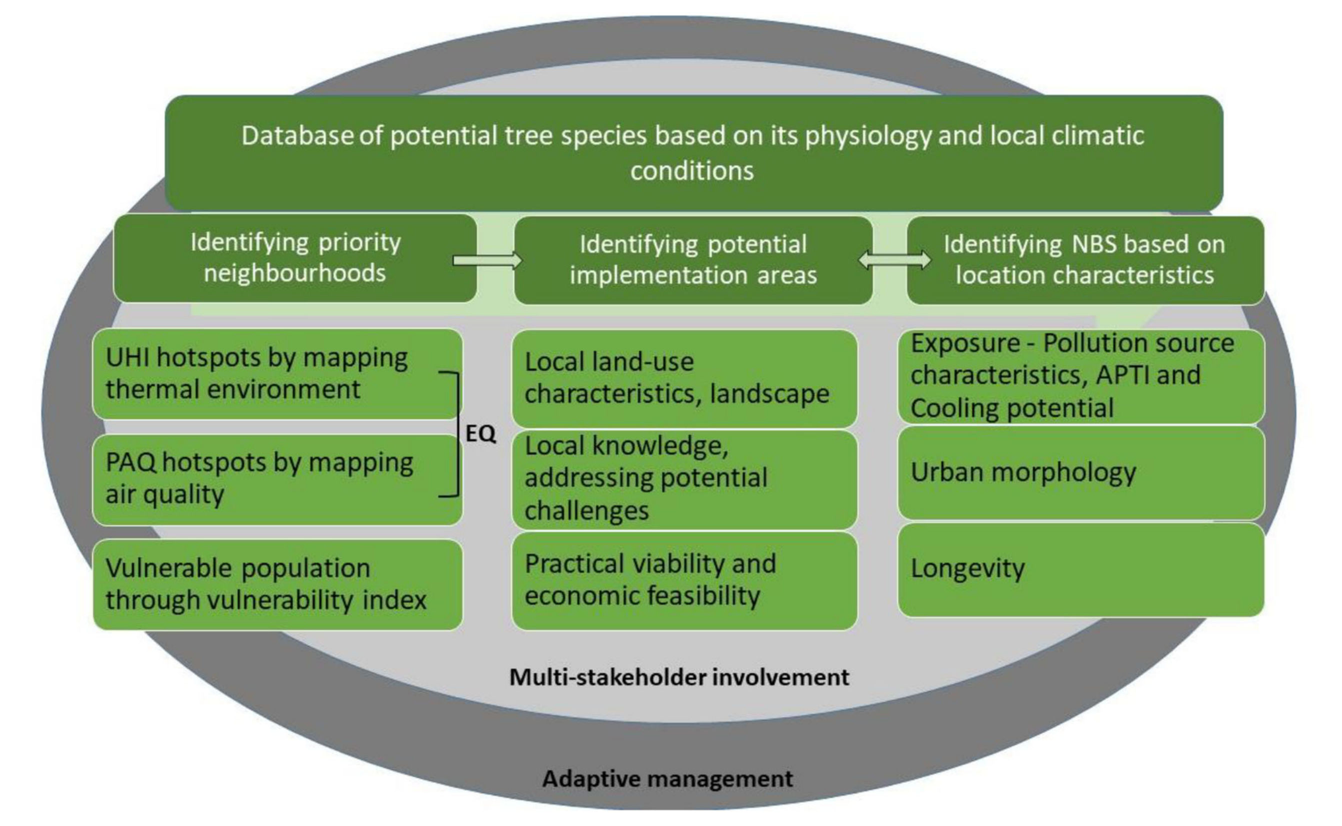

FIGURE 2 | Technical framework for NbS design in urban areas for co-mitigation of air pollution and urban heat (EQ- Environmental Quality).

et al., 2017; Barwise and Kumar, 2020). However, vegetation can sometimes hinder dispersion, thus building up pollutant concentration (Janhäll, 2015). A careful selection of plant species and design parameters as well as meteorological conditions play a major role in the successful mitigation of air pollution in urban areas (Leung et al., 2011).

Thermal Reduction Potential

The thermal performance of the selected plant species should be evaluated to determine the heat reduction potential (HRP) or cooling potential. This could be determined based on various indicators such as air temperature, thermal comfort or surface temperature. A recent study evaluated a methodological framework to select the trees for urban heat mitigation through parametric ENVI-met simulations using thermal comfort as an indicator for assessing the cooling potential of trees (Morakinyo et al., 2020). The study results indicated that a significant reduction in urban heat can be achieved by selecting right tree at the right place.

Urban Morphology

Urban morphology also has a greater role in the successful implementation of NbS strategies. The type of NbS strategy that could be adopted largely depends on the configuration of the urban area i.e., land use, available space, street configuration etc. As mentioned above, tall trees/vegetation is not recommended in street canyons as it can hinder free flow of air thus increasing air pollution and temperature (Janhäll, 2015). At the same time, properly designed green spaces could effectively mitigate UHI by improving natural cooling and, air pollution. In case of space constraints, other strategies such as VGS, green roofing, moss wall (a wall covered with moss) could be implemented. The reclamation of wastelands, landfills and dump yards in the form of parks/gardens are also commonly practiced widely in urban areas. Some of the examples from India include cities such as Delhi, Kolkata, and Bangalore.

Longevity/Sustainability

As vegetation is highly influenced by environmental stress, climate and various other factors such as soil type, water requirement etc, the suitability of plant species to each site determines its longevity (Barwise and Kumar, 2020). The native plant species exhibiting tolerance to environmental stresses experienced by the site as well as other factors as discussed above ensures sustainability and effectiveness of NbS strategies.

Barriers in NbS Implementation

Even though there has been an increased interest in NbS based approaches in recent years with a growing number of studies indicating its co-benefits, it is currently lacking actions at the implementation level. Governance plays a major role in the successful implementation of NbS (Li et al., 2021). Due to its multifunctionality, a participatory process is required with multi-stakeholder involvement and proper financial mechanisms to fund such approaches. In rapidly urbanizing nations like India, inadequate financial resources and space constraints are identified as major factors hindering its implementation (Singh et al., 2020a). The rapid developmental projects put immense pressure on cities in terms of space availability compromising the green spaces in urban areas. A recent report by UNEP estimated that globally, ∼USD 133 billion/year is currently invested into NbS (using 2020 as the base year), which is considerably less than that flows to climate finance (United Nations Environment Programme, 2021). For countries like India, internationally comparable data on NbS financing is not available. The national-level policies in India on air pollution and climate change have individually allocated some funds for greening activities (under NCAP, INR 60.5 million is allocated for greening activities in 28 identified non-attainment cities), but lacks strategic planning. As NbS strategies are largely dependent on the local knowledge as well as socio-political conditions, adaptive governance is required based on the local knowledge and culture. This limits the decision-makers and funders from investing in this approach as they are not confident on its success and scalability. To address this challenge, recently the International Union for Conservation of Nature (IUCN) has established NbS global standard and self-assessment tool that will help to assess the effectiveness of NbS approaches (IUCN, 2020). IUCN has established a governance structure through an International Standard Committee and multistakeholder involvement. This will help in the effective mainstreaming and upscaling of NbS approaches into developmental planning and policies.

CONCLUSION

NbS have great potential in mitigating the harmful impacts of climate change and air pollution. However, to maximize the potential of NbS for combined mitigation of UHI and air pollution, proper planning in the implementation of these strategies is needed. NbS should be adapted to local conditions to be successful and effective. Recently greening strategies have been increasingly promoted through various schemes and programs on air pollution and climate change such as the National Mission for Green India as a part of the National Action Plan on Climate Change (NAPCC) and city clean air action plans and smart city plans, but lack a strategic approach to green space planning and management. Also, there is a need for developing strong evidence base on the effectiveness of NbS, its co-benefits, and successful integration of green infrastructures into the city planning process, especially for a rapidly urbanizing country like India. Equitable access to green spaces has to be ensured for the sustainable and inclusive growth of cities. For example, socially disadvantaged groups are more prone to the negative impacts of air pollution and urban heat and likely to live in less green neighborhoods. Hence, NbS has to be integrated into the urban planning agenda providing a systematic approach including all the relevant stakeholders especially the citizens.

AUTHOR CONTRIBUTIONS

All authors listed have made a substantial, direct and intellectual contribution to the work, and approved it for publication.

REFERENCES

Abhijith, K. V., Kumar, P., Gallagher, J., McNabola, A., Baldauf, R., Pilla, F., et al. (2017). Air pollution abatement performances of green infrastructure in open road and built-up street canyon environments – A review. *Atmos. Environ.* 162, 71–86. doi: 10.1016/j.atmosenv.2017.05.014

Akhtar, R., and Palagiano, C. (2017). *Climate Change and Air Pollution: The Impact on Human Health in Developed and Developing Countries*. New York, NY: Springer. doi: 10.1007/978-3-319-61346-8

Albert, C., Brillinger, M., Guerrero, P., Gottwald, S., Henze, J., Schmidt, S., et al. (2020). Planning nature-based solutions: principles, steps, and insights. *Ambio* 50, 1446–1461. doi: 10.1007/s13280-020-01365-1

Arnds, D., Böhner, J., and Bechtel, B. (2017). Spatio-temporal variance and meteorological drivers of the urban heat island in a European city. *Theor. Appl. Climatol.* 128, 43–61. doi: 10.1007/s00704-015-1687-4

Bai, T., Mayer, A. L., Shuster, W. D., and Tian, G. (2018). The hydrologic role of urban green space in mitigating flooding (Luohe, China). *Sustainability* 10:3584. doi: 10.3390/su10103584

Balakrishnan, K., Dey, S., Gupta, T., Dhaliwal, R. S., Brauer, M., Cohen, A. J., et al. (2019). The impact of air pollution on deaths, disease burden, and life expectancy across the states of India: the Global Burden of Disease Study 2017. *Lancet Planet. Health* 3, e26–e39. doi: 10.1016/S2542-5196(18)30261-4

Barwise, Y., and Kumar, P. (2020). Designing vegetation barriers for urban air pollution abatement: a practical review for appropriate plant species selection. *Npj Climate Atmos. Sci.* 3, 1–19. doi: 10.1038/s41612-020-0115-3

Bharti, S. K., Trivedi, A., and Kumar, N. (2018). Air pollution tolerance index of plants growing near an industrial site. *Urban Climate* 24, 820–829. doi: 10.1016/j.uclim.2017.10.007

Bush, J., and Doyon, A. (2019). Building urban resilience with nature-based solutions: how can urban planning contribute? *Cities* 95:102483. doi: 10.1016/j.cities.2019.102483

Bustami, R. A., Belusko, M., Ward, J., and Beecham, S. (2018). Vertical greenery systems: a systematic review of research trends. *Build. Environ.* 146, 226–237. doi: 10.1016/j.buildenv.2018.09.045

Chaudhary, I. J., and Rathore, D. (2018). Suspended particulate matter deposition and its impact on urban trees. *Atmos. Pollut. Res.* 9, 1072–1082. doi: 10.1016/j.apr.2018.04.006

Chaudhary, I. J., and Rathore, D. (2019). Dust pollution: its removal and effect on foliage physiology of urban trees. *Sustain. Cities Society* 51:101696. doi: 10.1016/j.scs.2019.101696

Chen, M., Zhou, Y., Hu, M., and Zhou, Y. (2020). Influence of urban scale and urban expansion on the urban heat island effect in metropolitan areas: case study of Beijing–Tianjin–Hebei Urban agglomeration. *Remote Sens.* 12:3491. doi: 10.3390/rs12213491

Chitranshi, S., Sharma, S. P., and Dey, S. (2015). Satellite-based estimates of outdoor particulate pollution (PM10) for Agra City in northern India. *Air Qual. Atmos. Health* 8, 55–65. doi: 10.1007/s11869-014-0271-x

Crouse, D. L., Pinault, L., Balram, A., Brauer, M., Burnett, R. T., Martin, R. V., et al. (2019). Complex relationships between greenness, air pollution, and mortality in a population-based Canadian cohort. *Environ. Int.* 128, 292–300. doi: 10.1016/j.envint.2019.04.047

Dadvand, P., Rivas, I., Basagaña, X., Alvarez-pedrerol, M., Su, J., Sunyer, J., et al. (2015). Science of the total environment the association between greenness and traf fi c-related air pollution at schools. *Sci. Total Environ.* 523, 59–63. doi: 10.1016/j.scitotenv.2015.03.103

De Ridder, K., Maiheu, B., Lauwaet, D., Daglis, I. A., Keramitsoglou, I., Kourtidis, K., et al. (2017). Urban heat island intensification during hot spells—The case of Paris during the summer of 2003. *Urban Sci.* 1:3. doi: 10.3390/urbansci10 10003

Detommaso, M., Cascone, S., Gagliano, A., Nocera, F., and Sciuto, G. (2020). "Cool roofs with variable thermal insulation: UHI mitigation and energy savings for several Italian cities," in *Sustainability in Energy and Buildings*, eds J. Littlewood, R. Howlett, A. Capozzoli, and L. Jain (Singapore: Springer), 481–492. doi: 10.1007/978-981-32-9868-2_41

Dihkan, M., Karsli, F., Guneroglu, N., and Guneroglu, A. (2018). Evaluation of urban heat island effect in Turkey. *Arabian J. Geosci.* 11:186. doi: 10.1007/s12517-018-3972-x

Dirksen, M., Ronda, R., Theeuwes, N., and Pagani, G. (2019). Sky view factor calculations and its application in urban heat island studies. *Urban Climate* 30:100498. doi: 10.1016/j.uclim.2019.100498

dos Santos, R. S., Taylor, J., Davies, M., Mavrogianni, A., and Milner, J. (2017). "The variation of air and surface temperatures in London within a 1km grid using vehicle-transect and ASTER data," in *2017 Joint Urban Remote Sensing Event (JURSE)* (Dubai), 1–4. doi: 10.1109/JURSE.2017.7924613

Dwivedi, A., and Khire, M. (2018). Application of split-window algorithm to study Urban heat island effect in Mumbai through land surface temperature approach. *Sustain. Cities Society* 41, 865–877. doi: 10.1016/j.scs.2018.02.030

Dwivedi, A., Khire, M., Mohan, B., and Shah, S. (2019). The role of structure cooling to reduce the effect of urban heat island in Mumbai. *Adv. Build. Energy Res.* 13, 174–192. doi: 10.1080/17512549.2018.1488611

Ebi, K. L., and McGregor, G. (2008). Climate change, tropospheric ozone and particulate matter, and health impacts. *Environ. Health Perspect.* 116, 1449–1455. doi: 10.1289/ehp.11463

Estoque, R. C., and Murayama, Y. (2017). Monitoring surface urban heat island formation in a tropical mountain city using Landsat data (1987–2015). *ISPRS J. Photogramm. Remote Sens.* 133, 18–29. doi: 10.1016/j.isprsjprs.2017.09.008

European Commission (n.d.). *Nature-Based Solutions*. Available online at: https://ec.europa.eu/info/researchand-innovation/researcharea/environment/nature-basedsolutions_en (accessed April 20, 2021).

Founda, D., and Santamouris, M. (2017). Synergies between urban heat island and heat waves in Athens (Greece), during an extremely hot summer (2012). *Sci. Rep.* 7, 1–11. doi: 10.1038/s41598-017-11407-6

Gaur, A., Eichenbaum, M. K., and Simonovic, S. P. (2018). Analysis and modelling of surface Urban Heat Island in 20 Canadian cities under climate and land-cover change. *J. Environ. Manage.* 206, 145–157. doi: 10.1016/j.jenvman.2017.10.002

Gogoi, P. P., Vinoj, V., Swain, D., Roberts, G., Dash, J., and Tripathy, S. (2019). Land use and land cover change effect on surface temperature over Eastern India. *Sci. Rep.* 9, 1–10. doi: 10.1038/s41598-019-45213-z

Golden, J. S., and Kaloush, K. E. (2006). Mesoscale and microscale evaluation of surface pavement impacts on the urban heat island effects. *Int. J. Pavement Eng.* 7, 37–52. doi: 10.1080/10298430500505325

Haashemi, S., Weng, Q., Darvishi, A., and Alavipanah, S. K. (2016). Seasonal variations of the surface urban heat island in a semi-arid city. *Remote Sens.*8:352. doi: 10.3390/rs8040352

Heaviside, C., Macintyre, H., and Vardoulakis, S. (2017). The urban heat island: implications for health in a changing environment. *Curr; Environ. Health Rep.* 4, 296–305. doi: 10.1007/s40572-017-0150-3

Huang, L., Li, J., Zhao, D., and Zhu, J. (2008). A fieldwork study on the diurnal changes of urban microclimate in four types of ground cover and urban heat island of Nanjing, China. *Build. Environ.* 43, 7–17. doi: 10.1016/j.buildenv.2006.11.025

Icaza, L. E., van der Hoeven, F., and van den Dobbelsteen, A. (2017). The urban heat island effect in Dutch city centres. *Archit. Built Environ.* 20, 161–202. doi: 10.7480/abe.2017.20.3472

IPCC (2013). *AR5 - Summary for policymakers. Climate Change 2013 - The physical science basis, contribution of working group I to the fifth assessment report of the intergovernmental panel on climate change.* 78–78.

IUCN (2020). *Global Standard for Nature-based Solutions. A User-Friendly Framework for the Verification, Design and Scaling up of NbS*. Gland, Switzerland: IUCN.

Jaganmohan, M., Knapp, S., Buchmann, C. M., and Schwarz, N. (2016). The bigger, the better? The influence of urban green space design on cooling effects for residential areas. *J. Environ. Qual.* 45, 134–145. doi: 10.2134/jeq2015.01.0062

Janhäll, S. (2015). Review on urban vegetation and particle air pollution - Deposition and dispersion. *Atmos. Environ.* 105, 130–137. doi: 10.1016/j.atmosenv.2015.01.052

Karmakar, D., and Padhy, P. K. (2019). Air pollution tolerance, anticipated performance, and metal accumulation indices of plant species for greenbelt development in urban industrial area. *Chemosphere* 237:124522. doi: 10.1016/j.chemosphere.2019.124522

Kitha, J., and Lyth, A. (2011). Urban wildscapes and green spaces in Mombasa and their potential contribution to climate change adaptation and mitigation. *Environ. Urban.* 23, 251–265. doi: 10.1177/0956247810396054

Kong, F., Yin, H., James, P., Hutyra, L. R., and He, H. S. (2014). Effects of spatial pattern of greenspace on urban cooling in a large metropolitan area of eastern China. *Landsc. Urban Plan.* 128, 35–47. doi: 10.1016/j.landurbplan.2014.04.018

Kuddus, M., Kumari, R., and Ramteke, P. W. (2011). Studies on air pollution tolerance of selected plants in Allahabad city, India. *J. Environ. Res. Manage.* 2, 42–46. Available online at: https://www.e3journals.org/cms/articles/1330779058_Mohammed%20et%20al.pdf

Kumar, A., Kumar, P., Singh, H., and Kumar, N. (2021). Adaptation and mitigation potential of roadside trees with bio-extraction of heavy metals under vehicular emissions and their impact on physiological traits during seasonal regimes. *Urban For. Urban Green.* 58:126900. doi: 10.1016/j.ufug.2020.126900

Kumar, P., Morawska, L., Martani, C., Biskos, G., Neophytou, M., Di Sabatino, S., et al. (2015). The rise of low-cost sensing for managing air pollution in cities. *Environ. Int.* 75, 199–205. doi: 10.1016/j.envint.2014.11.019

Kumari, P., Garg, V., Kumar, R., and Kumar, K. (2021). Impact of urban heat island formation on energy consumption in Delhi. *Urban Climate* 36, 100763. doi: 10.1016/j.uclim.2020.100763

Leung, D. Y. C., Tsui, J. K. Y., Chen, F., Yip, W.-K., Vrijmoed, L. L. P., and Liu, C.-H. (2011). Effects of Urban Vegetation on Urban Air Quality. *Landsc. Res.* 36, 173–188. doi: 10.1080/01426397.2010.547570

Li, G., Zhang, X., Mirzaei, P. A., Zhang, J., and Zhao, Z. (2018). Urban heat island effect of a typical valley city in China: responds to the global warming and rapid urbanization. *Sustain. Cities Society* 38, 736–745. doi: 10.1016/j.scs.2018.01.033

Li, L., Cheshmehzangi, A., Ka, F., Chan, S., and Ives, C. D. (2021). Mapping the Research Landscape of Nature-Based Solutions in Urbanism. *Sustainability* 13:3876. doi: 10.3390/su13073876

Li, X., Zhou, Y., Yu, S., Jia, G., Li, H., and Li, W. (2019). Urban heat island impacts on building energy consumption: a review of approaches and findings. *Energy* 174, 407–419. doi: 10.1016/j.energy.2019.02.183

Liao, W., Liu, X., Wang, D., and Sheng, Y. (2017). The impact of energy consumption on the surface urban heat island in China's 32 major cities. *Remote Sens.* 9:250. doi: 10.3390/rs9030250

Lowe, S. A. (2016). An energy and mortality impact assessment of the urban heat island in the US. *Environ. Impact Assess. Rev.* 56, 139–144. doi: 10.1016/j.eiar.2015.10.004

Mahapatra, P. S., Puppala, S. P., Adhikary, B., Shrestha, K. L., Dawadi, D. P., Paudel, S. P., et al. (2019). Air quality trends of the Kathmandu Valley: a satellite, observation and modeling perspective. *Atmos. Environ.* 201, 334–347. doi: 10.1016/j.atmosenv.2018.12.043

Mandal, S., Madhipatla, K. K., Guttikunda, S., Kloog, I., Prabhakaran, D., and Schwartz, J. D. (2020). Ensemble averaging based assessment of spatiotemporal variations in ambient PM2.5 concentrations over Delhi, India, during 2010–2016. *Atmos. Environ.* 224:117309. doi: 10.1016/j.atmosenv.2020.1 17309

Manisalidis, I., Stavropoulou, E., Stavropoulos, A., and Bezirtzoglou, E. (2020). Environmental and health impacts of air pollution: a review. *Front. Public Health* 8, 14–14. doi: 10.3389/fpubh.2020.00014

Mathew, A., Khandelwal, S., Kaul, N., and Chauhan, S. (2018). Analyzing the diurnal variations of land surface temperatures for surface urban heat island studies: Is time of observation of remote sensing data important? *Sustain. Cities Society* 40, 194–213. doi: 10.1016/j.scs.2018.03.032

Menon, J. S., and Nagendra, S. M. S. (2018). Personal exposure to fine particulate matter concentrations in central business district of a tropical coastal city. *J. Air Waste Manage. Assoc.* 68, 415–429. doi: 10.1080/10962247.2017.1407837

Mohajerani, A., Bakaric, J., and Jeffrey-Bailey, T. (2017). The urban heat island effect, its causes, and mitigation, with reference to the thermal properties of asphalt concrete. *J. Environ. Manage.* 197, 522–538. doi: 10.1016/j.jenvman.2017.03.095

Mohan, M., Kikegawa, Y., Gurjar, B., Bhati, S., Kandya, A., and Ogawa, K. (2012). Urban heat island assessment for a tropical urban airshed in India. *Atmos. Clim. Sci.* 2, 127–138. doi: 10.4236/acs.2012.22014

Monteiro, M. V., Doick, K. J., Handley, P., and Peace, A. (2016). The impact of greenspace size on the extent of local nocturnal air temperature cooling in London. *Urban For. Urban Green.* 16, 160–169. doi: 10.1016/j.ufug.2016.02.008

Morakinyo, T. E., Ouyang, W., Lau, K. K.-L., Ren, C., and Ng, E. (2020). Right tree, right place (urban canyon): Tree species selection approach for optimum urban heat mitigation - development and evaluation. *Sci. Total Environ.* 719:137461. doi: 10.1016/j.scitotenv.2020.137461

Munang, R., Thiaw, I., Alverson, K., Liu, J., and Han, Z. (2013). The role of ecosystem services in climate change adaptation and disaster risk reduction. *Curr. Opin. Environ. Sustain.* 5, 47–52. doi: 10.1016/j.cosust.2013.02.002

Oke, T. R. (1973). City size and the urban heat island. *Atmos. Environ. (1967)* 7, 769–779. doi: 10.1016/0004-6981(73)90140-6

Pandey, A. K., Pandey, M., Mishra, A., Tiwary, S. M., and Tripathi, B. D. (2015a). Air pollution tolerance index and anticipated performance index of some plant species for development of urban forest. *Urban For. Urban Green.* 14, 866–871. doi: 10.1016/j.ufug.2015.08.001

Pandey, A. K., Pandey, M., and Tripathi, B. D. (2015b). Air pollution tolerance index of climber plant species to develop vertical greenery systems in a polluted tropical city. *Landsc. Urban Plan.* 144, 119–127. doi: 10.1016/j.landurbplan.2015.08.014

Pandey, A. K., Pandey, M., and Tripathi, B. D. (2016). Assessment of air pollution tolerance index of some plants to develop vertical gardens near street canyons of a polluted tropical city. *Ecotoxicol. Environ. Saf.* 134, 358–364. doi: 10.1016/j.ecoenv.2015.08.028

Pathak, V., Tripathi, B. D., and Mishra, V. K. (2011). Evaluation of anticipated performance index of some tree species for green belt development to mitigate traffic generated noise. *Urban For. Urban Green.* 10, 61–66. doi: 10.1016/j.ufug.2010.06.008

Pérez, G., Coma, J., Martorell, I., and Cabeza, L. F. (2014). Vertical Greenery Systems (VGS) for energy saving in buildings: a review. *Renew. Sustain. Energy Rev.* 39, 139–165. doi: 10.1016/j.rser.2014.07.055

Price, A., Jones, E. C., and Jefferson, F. (2015). Vertical Greenery Systems as a strategy in urban heat island mitigation. *Water Air Soil Pollut.* 226:247. doi: 10.1007/s11270-015-2464-9

Qaid, A., Lamit, H. B., Ossen, D. R., and Shahminan, R. N. R. (2016). Urban heat island and thermal comfort conditions at micro-climate scale in a tropical planned city. *Energy Build.* 133, 577–595. doi: 10.1016/j.enbuild.2016.10.006

Ramaiah, M., and Avtar, R. (2019). Urban green spaces and their need in cities of rapidly urbanizing India: a review. *Urban Sci.* 3:94. doi: 10.3390/urbansci3030094

Ramamurthy, P., and Sangobanwo, M. (2016). Inter-annual variability in urban heat island intensity over 10 major cities in the United States. *Sustain. Cities Society* 26, 65–75. doi: 10.1016/j.scs.2016.05.012

Ranagalage, M., Dissanayake, D., Murayama, Y., Zhang, X., Estoque, R., Perera, E., et al. (2018). Quantifying surface urban heat island formation in the world heritage tropical mountain city of Sri Lanka. *ISPRS Int. J. Geo-Inf.* 7:341. doi: 10.3390/ijgi7090341

Ranjan, O., Menon, J. S., Nagendra, S. M. S., Ph, D., and Asce, M. (2015). Assessment of air quality impacts on human health and vegetation at an industrial area. *J. Hazard. Toxic Radioact. Waste* 20, 1–10. doi: 10.1061/(ASCE)HZ.2153-5515.0000316

Raymond, C. M., Frantzeskaki, N., Kabisch, N., Berry, P., Breil, M., Nita, M. R., et al. (2017). A framework for assessing and implementing the co-benefits of nature-based solutions in urban areas. *Environ. Sci. Policy* 77, 15–24. doi: 10.1016/j.envsci.2017.07.008

Rizvi, S. H., Alam, K., and Iqbal, M. J. (2019). Spatio-temporal variations in urban heat island and its interaction with heat wave. *J. Atmos. Solar Terrestrial Physics* 185, 50–57. doi: 10.1016/j.jastp.2019.02.001

Rowe, D. B. (2011). Green roofs as a means of pollution abatement. *Environ. Pollut.* 159, 2100–2110. doi: 10.1016/j.envpol.2010.10.029

Roy, A., Bhattacharya, T., and Kumari, M. (2020). Air pollution tolerance, metal accumulation and dust capturing capacity of common tropical trees in commercial and industrial sites. *Sci. Total Environ.* 722:137622. doi: 10.1016/j.scitotenv.2020.137622

Sagris, V., and Sepp, M. (2017). Landsat-8 TIRS data for assessing urban heat island effect and its impact on human health. *IEEE Geosci. Remote Sens. Lett.* 14, 2385–2389. doi: 10.1109/LGRS.2017.2765703

Santamouris, M., Ding, L., and Osmond, P. (2019). "Urban heat island mitigation," in *Decarbonising the Built Environment* (Singapore: Palgrave Macmillan), 337–355. doi: 10.1007/978-981-13-7940-6_18

Santamouris, M., Haddad, S., Fiorito, F., Osmond, P., Ding, L., Prasad, D., et al. (2017). Urban heat island and overheating characteristics in Sydney, Australia. An analysis of multiyear measurements. *Sustainability* 9:712. doi: 10.3390/su9050712

Shahmohamadi, P., Che-Ani, A., Maulud, K., Tawil, N., and Abdullah, N. (2011). The impact of anthropogenic heat on formation of urban heat island and energy consumption balance. *Urban Stud. Res.* 2011:497524. doi: 10.1155/2011/497524

Sharma, R., Hooyberghs, H., Lauwaet, D., and De Ridder, K. (2019). Urban heat island and future climate change—Implications for Delhi's heat. *J. Urban Health* 96, 235–251. doi: 10.1007/s11524-018-0322-y

Sidiqui, P., Huete, A., and Devadas, R. (2016). "Spatio-temporal mapping and monitoring of Urban Heat Island patterns over Sydney, Australia using MODIS and Landsat-8," in *2016 4th International Workshop on Earth Observation and Remote Sensing Applications (EORSA)* (Guangzhou), 217–221. doi: 10.1109/EORSA.2016.7552800

Singh, A., Sarma, A. K., and Hack, J. (2020a). Cost-Effective Optimization of Nature-Based Solutions for Reducing Urban Floods Considering Limited Space Availability. *Environ. Process.* 7, 297–319. doi: 10.1007/s40710-019-00420-8

Singh, P., Kikon, N., and Verma, P. (2017). Impact of land use change and urbanization on urban heat island in Lucknow city, Central India. A remote sensing based estimate. *Sustain. Cities Soc.* 32, 100–114. doi: 10.1016/j.scs.2017.02.018

Singh, S. K., and Rao, D. N. (1983). "Evaluation of plants for their tolerance to air pollution," in *Proceedings of Symposium on Air Pollution Control*, Vol. 1, 218–224.

Singh, V. K., Acero, J. A., and Martilli, A. (2020b). *Evaluation of the impact of anthropogenic heat emissions generated from road transportation and power plants on the UHI intensity of Singapore. Technical Report Cooling Singapore.* Singapore-ETH Centre (SEC).

Sussman, H. S., Raghavendra, A., and Zhou, L. (2019). Impacts of increased urbanization on surface temperature, vegetation, and aerosols over Bengaluru, India. *Remote Sens. Appl. Society Environ.* 16:100261. doi: 10.1016/j.rsase.2019.100261

Swami, A., and Chauhan, D. (2015). Impact of air pollution induced by automobile exhaust pollution on air pollution tolerance index (APTI) on few species of plants. *Int. J. Sci. Res.* 4, 342–343. doi: 10.15373/22778179#sthash.vF0KMdSC.dpuf

Swamy, G., Nagendra, S. S., and Schlink, U. (2017). Urban heat island (UHI) influence on secondary pollutant formation in a tropical humid environment. *J. Air Waste Manage. Assoc.* 67, 1080–1091. doi: 10.1080/10962247.2017.1325417

Thomas, G., Sherin, A., Ansar, S., and Zachariah, E. (2014). Analysis of urban heat island in Kochi, India, using a modified local climate zone classification. *Proc. Environ. Sci.* 21, 3–13. doi: 10.1016/j.proenv.2014.09.002

Ulpiani, G. (2021). On the linkage between urban heat island and urban pollution island: three-decade literature review towards a conceptual framework. *Sci. Total Environ.* 751:141727. doi: 10.1016/j.scitotenv.2020.141727

United Nations Environment Programme (2021). *State of Finance for Nature 2021*. Nairobi: United Nations Environment Programme (UNEP).

Vargo, J., Stone, B., Habeeb, D., Liu, P., and Russell, A. (2016). The social and spatial distribution of temperature-related health impacts from urban heat island reduction policies. *Environ. Sci. Policy* 66, 366–374. doi: 10.1016/j.envsci.2016.08.012

Vijayaraghavan, K. (2016). Green roofs: a critical review on the role of components, benefits, limitations and trends. *Renew. Sustain. Energy Rev.* 57, 740–752. doi: 10.1016/j.rser.2015.12.119

Weng, Q., Firozjaei, M. K., Sedighi, A., Kiavarz, M., and Alavipanah, S. K. (2019). Statistical analysis of surface urban heat island intensity variations: a case study of Babol city, Iran. *GISci. Remote Sens.* 56, 576–604. doi: 10.1080/15481603.2018.1548080

World Health Organization (WHO) (2016). *WHO Global Urban Ambient Air Pollution Database*. Geneva: World Health Organization.

Xie, X., Semanjski, I., Gautama, S., Tsiligianni, E., Deligiannis, N., Rajan, R. T., et al. (2017). A review of urban air pollution monitoring and exposure assessment methods. *ISPRS Int. J. Geo-Inf.* 6, 1–21. doi: 10.3390/ijgi6120389

Yadav, N., and Sharma, C. (2018). Spatial variations of intra-city urban heat island in megacity Delhi. *Sustain. Cities Society* 37, 298–306. doi: 10.1016/j.scs.2017.11.026

Yang, J., and Santamouris, M. (2018). Urban heat island and mitigation technologies in Asian and Australian cities-impact and mitigation. *Urban Sci.* 2:74. doi: 10.3390/urbansci2030074

Yannawar, V. (2014). Air pollution tolerance index of various plant species around Nanded City of Maharashtra, India. *J. Appl. Phytotechnol. Environ. Sanit.* 3, 23–28.

Yitshak-Sade, M., Kloog, I., and Novack, V. (2017). Do air pollution and neighborhood greenness exposures improve the predicted cardiovascular risk? *Environ. Int.* 107, 147–153. doi: 10.1016/j.envint.2017.07.011

Yu, Z., Guo, X., Zeng, Y., Koga, M., and Vejre, H. (2018). Variations in land surface temperature and cooling efficiency of green space in rapid urbanization: the case of Fuzhou city, China. *Urban For. Urban Green.* 29, 113–121. doi: 10.1016/j.ufug.2017.11.008

Zhang, B., Li, N., and Wang, S. (2015). Effect of urban green space changes on the role of rainwater runoff reduction in Beijing, China. *Landsc. Urban Plan.* 140, 8–16. doi: 10.1016/j.landurbplan.2015.03.014

Conflict of Interest: The authors declare that the research was conducted in the absence of any commercial or financial relationships that could be construed as a potential conflict of interest.

Publisher's Note: All claims expressed in this article are solely those of the authors and do not necessarily represent those of their affiliated organizations, or those of the publisher, the editors and the reviewers. Any product that may be evaluated in this article, or claim that may be made by its manufacturer, is not guaranteed or endorsed by the publisher.

frontiers in Sustainable Cities

ORIGINAL RESEARCH
published: 22 March 2022
doi: 10.3389/frsc.2022.792507

Check for updates

Particulate Matter Pollution in Urban Cities of India During Unusually Restricted Anthropogenic Activities

Ravi Yadav[1]*, Pushpendra Vyas[2], Praveen Kumar[1], Lokesh Kumar Sahu[3], Umangkumar Pandya[4], Nidhi Tripathi[3], Mansi Gupta[3], Vikram Singh[5], Pragnesh N. Dave[6], Devendra Singh Rathore[7], Gufran Beig[1,8] and S. N. A. Jaaffrey[9]

[1] Air Pollution and Transport Modeling Division, Indian Institute of Tropical Meteorology, Ministry of Earth Sciences, Government of India, Pune, India, [2] Department of Physics, Janardan Rai Nagar Rajasthan Vidyapeeth (Deemed-to-be University), Udaipur, India, [3] Space and Atmospheric Sciences Division, Physical Research Laboratory, Ahmedabad, India, [4] Department of Physics, Shankersinh Vaghela Bapu Institute of Science, Gandhinagar, India, [5] Department of Physics, Sangam University, Bhilwara, India, [6] Department of Chemistry, Sardar Patel University, Vallabh Vidyanagar, India, [7] Department of Environmental Sciences, Mohanlal Sukhadia University, Udaipur, India, [8] Natural Sciences and Engineering, National Institute of Advanced Studies, Bangalore, India, [9] Department of Physics, Mohanlal Sukhadia University, Udaipur, India

OPEN ACCESS

Edited by:
*Prashant Rajput,
Banaras Hindu University, India*

Reviewed by:
*Pallavi Saxena,
University of Delhi, India
Sergio Ibarra Espinosa,
University of São Paulo, Brazil*

***Correspondence:**
*Ravi Yadav
yadavravi38@gmail.com;
ravi.yadav@tropmet.res.in*

Specialty section:
This article was submitted to Climate Change and Cities, a section of the journal Frontiers in Sustainable Cities

Received: 10 October 2021
Accepted: 13 January 2022
Published: 22 March 2022

Citation:
Yadav R, Vyas P, Kumar P, Sahu LK, Pandya U, Tripathi N, Gupta M, Singh V, Dave PN, Rathore DS, Beig G and Jaaffrey SNA (2022) Particulate Matter Pollution in Urban Cities of India During Unusually Restricted Anthropogenic Activities. Front. Sustain. Cities 4:792507. doi: 10.3389/frsc.2022.792507

The outbreak of COVID-19 is a global public health challenge and has affected many countries, including India. The nationwide lockdown was imposed in India from March 25 to May 31, 2020 to prevent the transmission of COVID-19. The study intends to assess the impact of the absence of major anthropogenic activities during the various phases of the COVID-19 lockdown (LDN) period on the daily mean concentrations of $PM_{2.5}$ and PM_{10} in six populated cities of Jaipur, Jodhpur, Kota, Udaipur, Ajmer, and Alwar in the state of Rajasthan. Investigation has been done for the different periods, including the pre-lockdown—PRELD (January 1–March 4, 2020), partial lockdown—PLDN (March 5–24, 2020), COVID-19 lockdown—LDN (March 25–May 31, 2020), and unlocking—ULC (June 1–August 31, 2020) phases. We have also compared the mean concentrations of $PM_{2.5}$ and PM_{10} with the same period of the year 2019. A significant improvement in air quality during the COVID-19 LDN period was noticed in all cities compared to 2019 and for the same period of the year 2020. However, the levels of $PM_{2.5}$ and PM_{10} were seen to rise during the second, third, and fourth LDN phases compared to the first LDN, indicating that the subsequent lockdowns started with some relaxations and dusty conditions. On the other hand, wind-blown dust is another vital source of PM_{10}, resulting in high concentrations in the summer months (April–May). Significant reductions in $PM_{2.5}$ (∼25–50%) and PM_{10} (20–37%) in all six cities during the LDN period compared with PRELD were estimated. However, with significant variations from city to city, the lowest reductions in $PM_{2.5}$ (∼25%) and PM_{10} (∼20%) were measured in Jodhpur and Ajmer, respectively. It was noticed that the episodes of rainfall and transport of oceanic air masses resulted in a reduction of particles during the ULC period compared to the LDN period. The air quality index was, more or less, in the "good to satisfactory" category during the first 3 LDN periods, whereas it was moderate for Jodhpur, Jaipur, and Ajmer during the last LDN period. The study will be helpful to determine mitigation policies to minimize air pollution, especially in developing regions.

Keywords: particulate matter, COVID-19 lockdown, air quality index, meteorology, India

HIGHLIGHTS

- The investigation shows the impact of the various phases of COVID-19 lockdown on $PM_{2.5}$ and PM_{10} in six cities of Rajasthan.
- There was a reduction during the COVID-19 lockdown, by 16–50% in $PM_{2.5}$ and by 22–47% in PM_{10}.
- Mineral dust pollution is prominent in particle loads over the Rajasthan state.
- Monsoon rains and winds dominate over emissions during the unlocking periods (June–August) in $PM_{2.5}$ and PM_{10} distribution.

INTRODUCTION

The entire world has been facing an acute pandemic and challenging circumstances because of the novel contamination of coronavirus disease (COVID-19) since the beginning of 2020. The first case was identified in Wuhan, China, in December 2019 (Li et al., 2020). In view of the expanding pace of COVID-19 cases worldwide, the transmittable disease has become a global pandemic (WHO, 2020). Therefore, many countries have declared a nationwide strict lockdown with varying rules and regulations to control the spread of COVID-19. In India, the first COVID-19 case was identified on January 30, 2020 in Trisharu, Kerala (India) (WHO, 2020) and in different parts of the country during the first week of March (https://www.mohfw.gov.in/). The multiple cases of infection from India started to come into view in the first week of March 2020. Later, the government of India (Prime Minister) announced "Janata Curfew" for a day on March 22, 2020, with a complete shutdown of daily activities. Later, complete lockdown for 21 days across India was officially announced, from March 25 to April 14, 2020. Later, to deal with the decline of the pandemic in the nation, the lockdown was extended up to May 3, 2020. After looking at the problematic situation, it continued until May 31, 2020 with some relaxation. The details of prohibited and permitted activities during the different lockdown phases, including LDN1 (March 25–April 14, 2020), LDN2 (April 15–May 3, 2020), LDN3 (May 04–17, 2020), LDN4 (May 18–31, 2020), are listed in **Table 1**. Improvements in air quality due to reductions in transport (flights, trains, and vehicles), industrial, academic, economic, and social-related activities are reported in several studies (Dantas et al., 2020; Kumari and Toshniwal, 2020; Nakada and Urban, 2020; Navinya et al., 2020; PPAC, 2020; Sharma et al., 2020; Sicard et al., 2020; Singh et al., 2020; Yadav et al., 2020). About 40–70% reductions were suggested in transport, industrial, and construction activities based on the fuel consumption data during the lockdown period, but ∼12% enhancement was estimated in biofuel consumption for cooking purposes (PPAC, 2020). The combustion-related emissions are considered one of the significant sources of air pollutants in Indian cities. The air quality, in terms of air quality index and health impact, is mainly determined by the levels of hazardous particulate pollutants in a year. In ambient air, the most important anthropogenic sources of fine particulate matter are the incomplete combustion of biofuel and fossil fuels (Sahu et al., 2011). In addition to local emissions, the long-range transport from the regions of biomass burning and dust sources also influence the receptor sites (Yadav et al., 2016, 2017). Exposure to elevated levels

TABLE 1 | Details of the prohibited and permitted activities during the study period.

Study phases and its duration/2020	Total days	Activities
PRELD January 1–March 4	63	Business as usual
PLDN March 5–24	21	Selective restrictions announced by the government, like mass gatherings in institutions, shopping malls, and theaters
LDN1 March 25–April 14	21	All were closed, with the exception of essential services like for health. Security and food delivery and others
LDN2 April 15–May 3, 2020	19	Allowed were agricultural businesses including dairy, banking, telecommunication, power-related services, manufacturing, and transportation units; interstate movement was also allowed for the delivery of essential goods and for law and order
LDN3 May 4–17, 2020	14	Allowed were all activities but with restrictions and social distancing, e.g., travel by air and rail around the metro; running of schools, colleges, and other educational and training/coaching institutions; hospitality services, including hotels and restaurants; places of large public gatherings, such as cinema halls and malls Gymnasiums, sports complexes, etc., were still closed
LDN4 May 18–31, 2020	14	Protection for vulnerable persons, i.e., persons above 65 years of age, persons with co-morbidities, pregnant women, and children below the age of 10 years shall stay at home, except for meeting essential requirements and for health purposes
ULC1 June 1–30, 2020	30	Shopping malls, religious places, hotels, and restaurants were permitted to reopen from June 8. Large gatherings were still banned, but there were no restrictions on interstate travel
ULC2 July 1–31, 2020	31	Shops were permitted to allow more than five persons at a time. Educational institutions, metros, and recreation centers remained close until July 31.
ULC3 August 1–31, 2020	31	Educational institutions would remain close until August 31. All inter- and intrastate travel and transportation modes are permitted. Independence Day celebrations are permitted with social distancing

MHA, 2020.

of $PM_{2.5}$ in ambient air can cause adverse health effects like respiratory and cardiovascular diseases (e.g., Pope et al., 2009). Several studies have reported the association of COVID-19-related mortality and morbidity along with air pollution and meteorological parameters during the lockdown period (Beig et al., 2020; Conticini et al., 2020; Wu et al., 2020; Yao et al., 2020). On the other hand, many studies have reported a significant reduction in air pollution across the world due to the COVID-19 restrictions (Bashir et al., 2020; Jain and Sharma, 2020; Kanniah et al., 2020; Kumar et al., 2020; Kumari and Toshniwal, 2020; Mahato et al., 2020; Nakada and Urban, 2020; Navinya et al., 2020; Singh and Chauhan, 2020; Singh et al., 2020; Tobías et al., 2020; Yadav et al., 2020; Goel et al., 2021; Sokhi et al., 2021). Most of the studies in India have been focused on megacities so far, including Delhi, Mumbai, Ahmedabad, Pune, Chennai, Kolkata, Lucknow, Jaipur, and Bangalore, etc. However, studies during the COVID-19 lockdown period in several cities of Rajasthan are reported for a very limited period (Sharma et al., 2020). Aside from local anthropogenic emissions, the air pollution footprints are unique in Rajasthan, where dust-related sources are also dominant. The geographic characteristics of Rajasthan are the Thar Desert and the Aravalli Range, and the north-western portion of Rajasthan is generally sandy and dry. Hence, due to being the driest region and given the different climatic zones, the study will be very prominent in these locations. The present study highlights the role of long-term COVID-19 lockdown on $PM_{2.5}$ and PM_{10} in six major cities of Rajasthan, including Jaipur, Jodhpur, Kota, Udaipur, Ajmer, and Alwar, and the alteration in air pollution levels during the unlocking periods. We have also discussed the change in the air quality index (AQI) for all cities. Overall, we present a detailed investigation by considering the combined effects of local emissions and meteorology during the lockdown period.

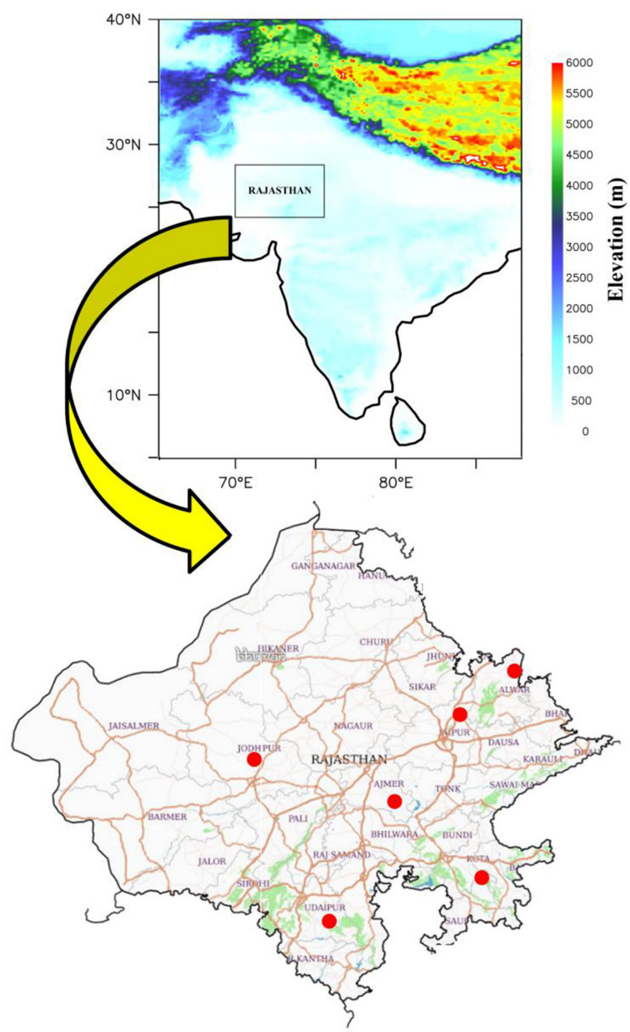

FIGURE 1 | Map of India on surface elevation depicting Rajasthan along with the location of selected cities such as Jaipur, Jodhpur, Kota, Udaipur, Ajmer, Alwar are shown by the red oval. The Rajasthan Map (bottom panel) has been used from ISRO's Earth visualization portal Bhuvan (https://bhuvan.nrsc.gov.in/).

METHODOLOGY

Data Sources, Locations, and Local Meteorology

The concentration data of $PM_{2.5}$ and PM_{10} as measured in six cities, namely, Jaipur, Jodhpur, Kota, Udaipur, Ajmer, and Alwar, in the state of Rajasthan were obtained from the Central Pollution Control Board (CPCB) for the years 2019 and 2020. The $PM_{2.5}$ and PM_{10} data in these cities located in the northwest part of India were analyzed to investigate the pollution levels during the long-term COVID-19 lockdown period. The locations of the study sites in the maps of India and Rajasthan are shown in **Figure 1**.

The data studied include during the pre-lockdown period (PRELD) (January 1 to March 4, 2020), partial lockdown (PLDN) (March 5 to 24, 2020), COVID-19 lockdown (LDN) (March 25 to May 31, 2020), and unlocking (ULC) period (June 1 to August 31, 2020). The average matching periods of the year 2019 were considered as the references to study the change in air quality during the COVID-19 lockdown period. We have used the National Centre for Environmental Prediction reanalysis datasets to derive the wind streamlines and temperature at a spatial resolution of 2.5° × 2.5° during the entire study period for 2019 and 2020, as shown in **Figure 2**. The precipitation rate (mm day^{-1}) data from the CPC Merged Analysis of Precipitation (CMAP), at a spatial resolution of 2.5° × 2.5°, was used. The Moderate Resolution Imaging Spectroradiometer (MODIS) active fire count maps over India during the entire study period for 2019 and 2020 are plotted in **Figure 3**. Rajasthan is the largest state of India, located in the north-western region with a population of ∼6.8 million (http://census2011.co.in). However, being located near most cities, the state has various types of industrial units, including those of marble, steel, cement, handicrafts, textiles, chemicals, IT, and thermal plants (Report 2018). The primary sources of air pollutants are vehicular, industrial, agriculture residual burning, municipal solid waste treatment,

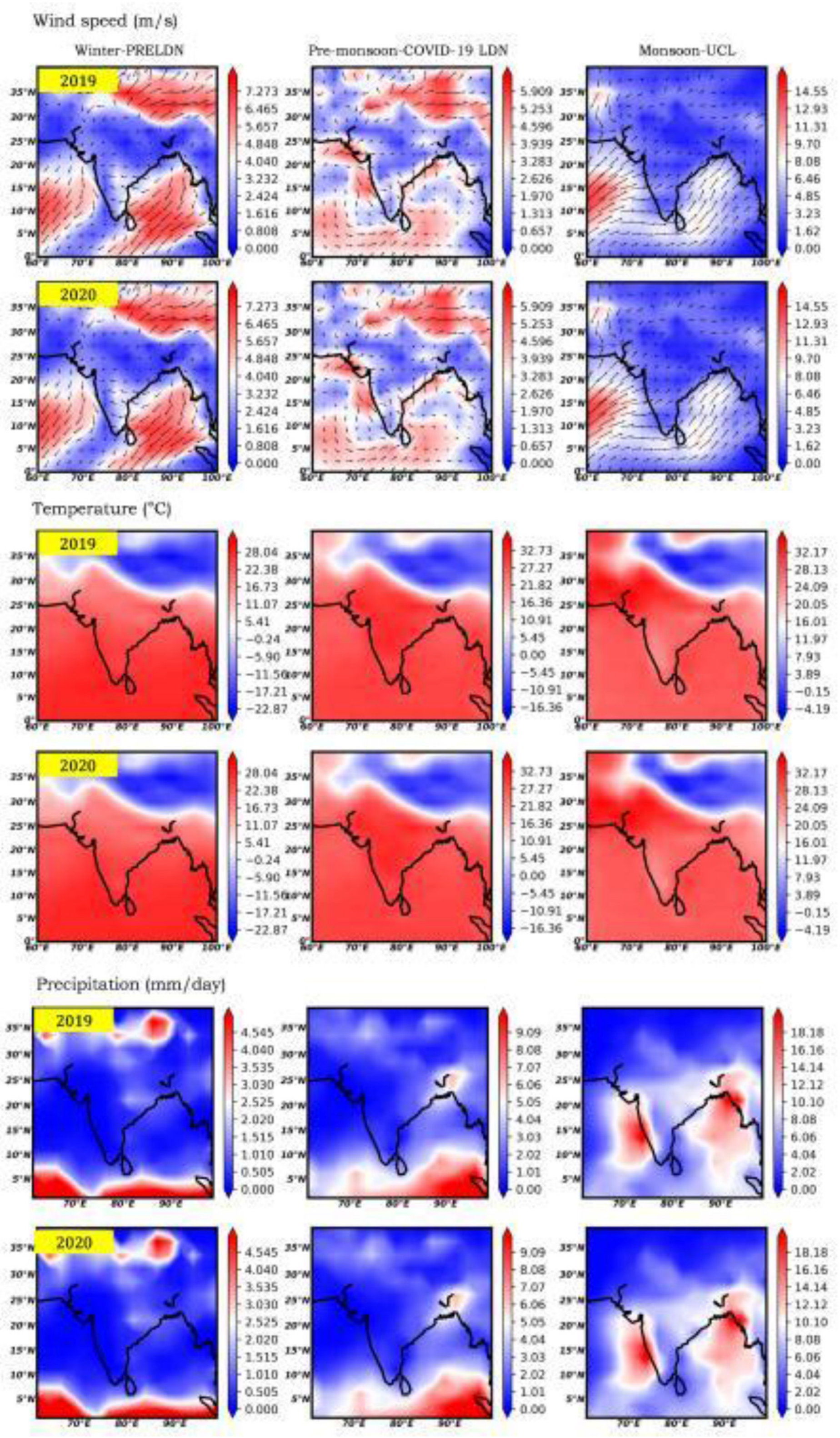

FIGURE 2 | Meteorological parameters during the different phases of the study in the years 2019 and 2020: **(top)** wind speed; **(middle)** temperature; **(bottom)** precipitation.

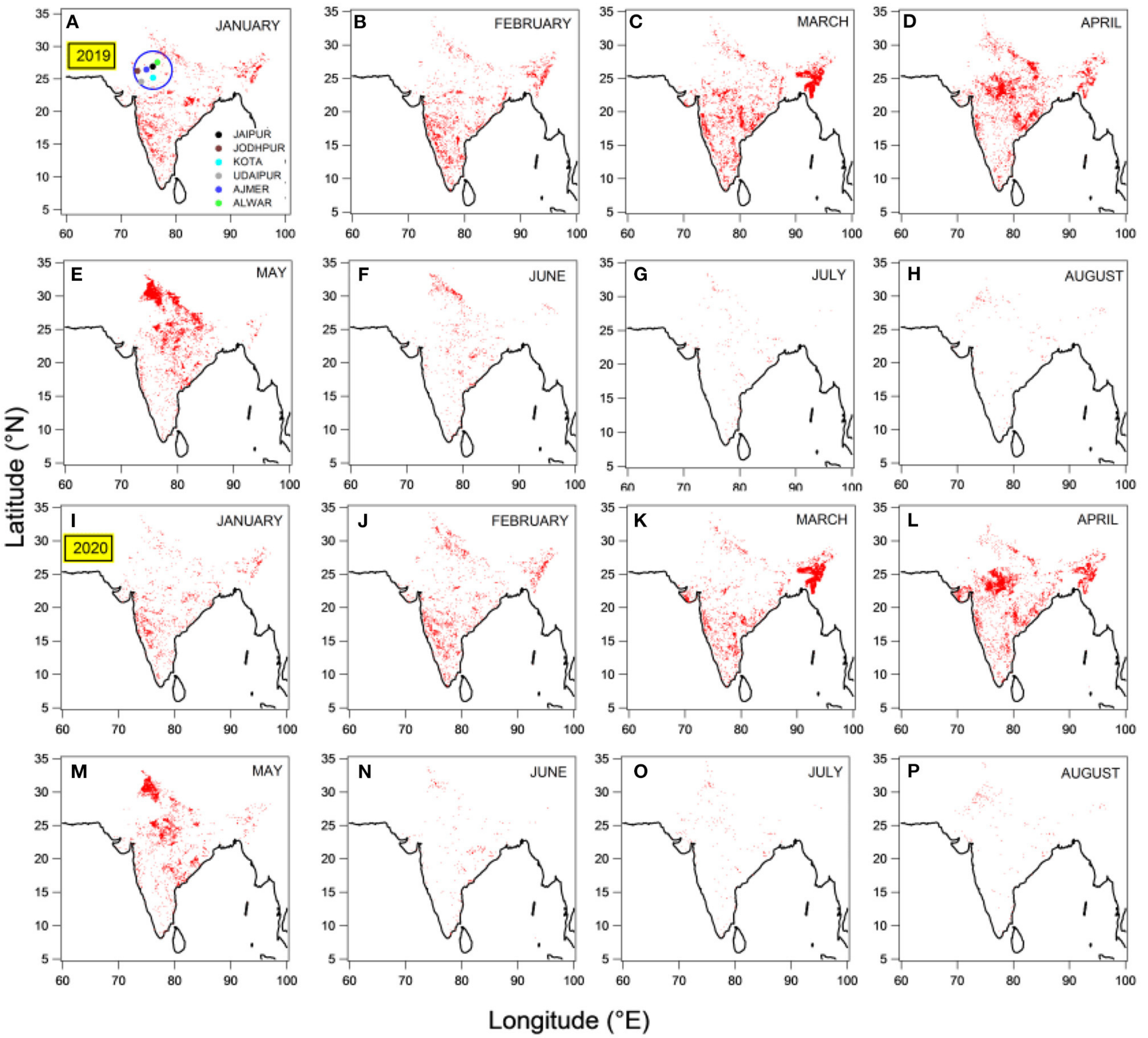

FIGURE 3 | MODIS fire count data maps from January to August for the years 2019 and 2020.

diesel generator, biofuel and LPG (residential cooking), and construction activities. The common sources of $PM_{2.5}$ and PM_{10} include biofuel and fossil fuel combustion, industrial processes, and biomass burning. However, for PM_{10}, wind-blown dust, road dust suspension, building construction, lime kilns, and slab polishing are important non-combustion sources (Yadav et al., 2017). Daily mean temperature ranges of 10–27, 32–45, and 35–40°C are recorded during winter (January–February), pre-monsoon (March–May), and monsoon (June–September) seasons, respectively. The strong hot winds called "Loo" blow from the west during pre-monsoon, while relatively low winds blow from the north and northeast during the winter (Yadav et al., 2014a). Rainfall values as high as 819 mm in the eastern part and as low as 170 mm in the western part of the state were recorded (Maanju and Saha, 2013). In the monsoon season, the inter-tropical convergence zone moves northward across India, and strong southwest (SW) winds prevail over the study region. Therefore, the measurements in this season are influenced by the transport of cleaner air masses from the Arabian Sea (see **Supplementary Figure S1**).

RESULTS AND DISCUSSION

Role of COVID-19 Lockdown in the Variation of $PM_{2.5}$ and PM_{10}

The time series analysis of $PM_{2.5}$ and PM_{10} over a period of 8 months (January 1–August 31, 2020) reveals interesting trends. The daily means of $PM_{2.5}$ and PM_{10} concentrations measured in Jaipur, Jodhpur, Kota, Udaipur, Ajmer, and Alwar are shown in **Figure 4**. The daily mean time series concentrations

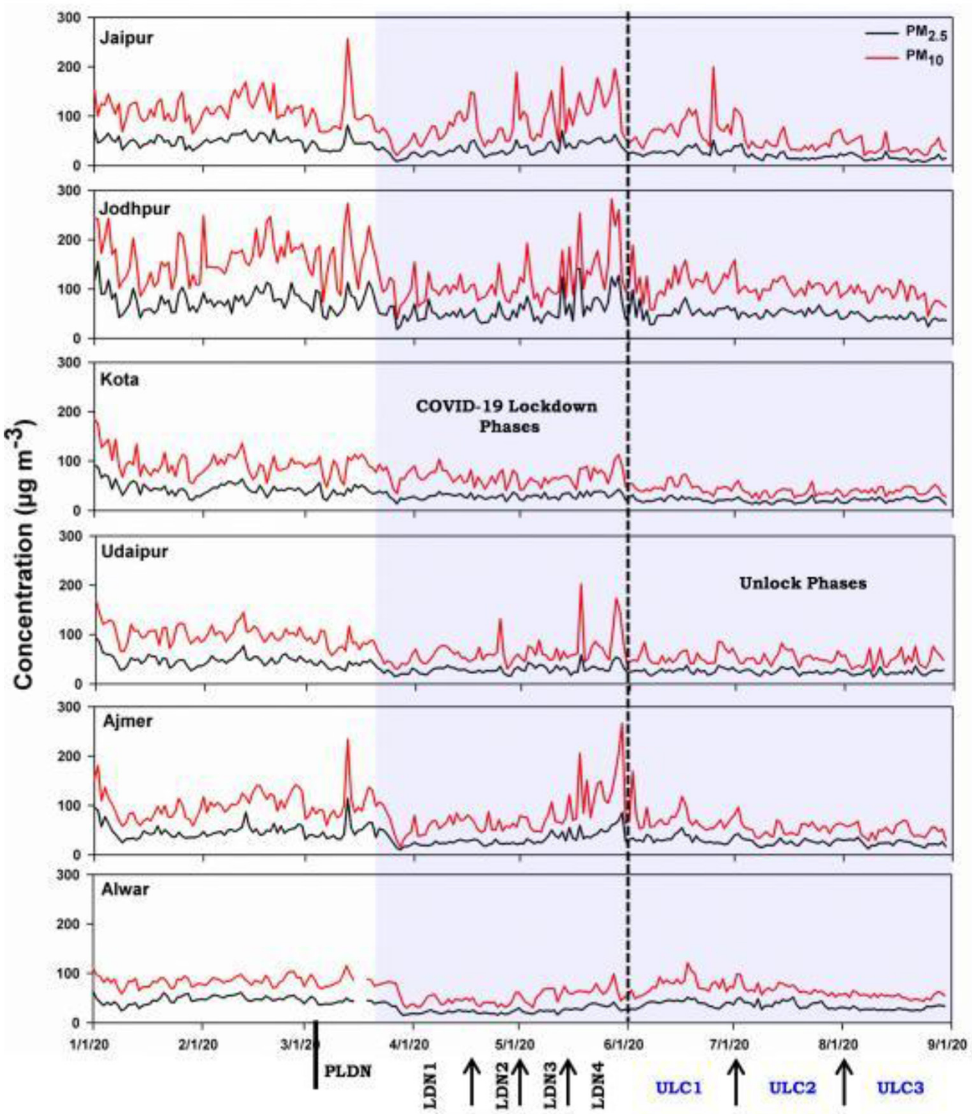

FIGURE 4 | Daily time series variations of $PM_{2.5}$ and PM_{10} in six major cities from January 1 to August 31, 2020.

of $PM_{2.5}$ and PM_{10} for all cities are divided into the four different periods of PRELD (January 1–March 4), PLDN (March 5–24), COVID-19 LDN (March 25–May 31), and ULC (June 1–August 31). During the business-as-usual period, many studies have reported a clear seasonality in the daily mean concentrations of $PM_{2.5}$ and PM_{10}, with the highest in the dry period (winter to pre-monsoon) and the lowest in the monsoon season, in different cities of India (Beig et al., 2007; Yadav et al., 2017; Hama et al., 2020). However, the findings become effectively more crucial in 2020 to researchers and policymakers because of the COVID-19-related consecutive LDN and ULC situations in which anthropogenic activities were restricted. The daily mean concentrations of $PM_{2.5}$ were in the ranges of 7–81, 18–156, 12–91, 14–93, 10–114, and 15–63 µg m^{-3}, while those of PM_{10} varied in the ranges of 20–256, 39–282, 23–185, 26–202, 15–266, and 30–121 µg m^{-3}, respectively, in Jaipur, Jodhpur, Kota, Udaipur, Ajmer, and Alwar during the entire study period. The mean concentrations of $PM_{2.5}$ were 51 ± 10, 78 ± 21, 45 ± 13, 49 ± 12, 47.3 ± 13, and 47.2 ± 8 µg m^{-3} in the PRELD period, which reduced to 34 ± 09, 58 ± 16, 29 ± 3, 29 ± 2, 32 ± 11, and 24 ± 4.4 µg m^{-3} during the LDN period in Jaipur, Jodhpur, Kota, Udaipur, Ajmer, and Alwar, respectively. On the other hand, the mean concentrations of PM_{10} were 115 ± 23, 162 ± 41, 97 ± 25, 104 ± 18, 100 ± 25, and 85 ± 9 µg m^{-3} in the PRELD period, which decreased by 90 ± 27, 116 ± 29, 67 ± 8, 65 ± 14, 80 ± 35, and 53 ± 10 µg m^{-3} during the LDN periods in Jaipur, Jodhpur, Kota, Udaipur, Ajmer, and Alwar, respectively. The

TABLE 2 | The daily average mass concentrations of $PM_{2.5}$ and PM_{10} during different periods, namely, PRELD, PLDN, and LDN phases and unlocking phases in six different cities of Rajasthan in India.

Cities	PRELD	PLDN	LDN1	LDN2	LDN3	LDN4	LDN periods	ULC1	ULC2	ULC3	ULC periods
$PM_{2.5}$											
Jaipur	50.8 ± 10	39.9 ± 12	23.3 ± 8	30.8 ± 11	36.8 ± 12	46.7 ± 8.4	34.4 ± 9.8	28.3 ± 7.1	19.9 ± 8.2	14.9 ± 5.5	21.0 ± 6.7
Jodhpur	78 ± 21	69.6 ± 23	47.8 ± 14	46 ± 11	57.7 ± 23.5	82.3 ± 30	58 ± 16	54.6 ± 14.7	51.7 ± 6.9	42.1 ± 6.5	49.5 ± 6.5
Kota	45.7 ± 13	38 ± 9	27.7 ± 5.3	28 ± 5	28.4 ± 5.3	33 ± 6.5	29 ± 3	22.4 ± 4	18.7 ± 4	21.8 ± 3.9	21 ± 1.9
Udaipur	49 ± 12	36 ± 7	26 ± 6	25 ± 5	31 ± 7	34 ± 11	29.3 ± 2.5	26.8 ± 5	25.1 ± 4.5	23.6 ± 5	25 ± 1.6
Ajmer	47 ± 13	49 ± 18	22 ± 5	24.7 ± 4.2	33.5 ± 10	47.7 ± 16	32.2 ± 11	31.7 ± 7.8	26.4 ± 6.6	23.5 ± 5	27.2 ± 4
Alwar	47 ± 8.2	41.6 ± 3.4	23 ± 5	20.6 ± 3	23.4 ± 3.8	32.5 ± 5	24 ± 4.4	39 ± 7	38 ± 7.2	28.7 ± 3.3	35.3 ± 5.7
PM10											
Jaipur	115 ± 23	96.6 ± 46	60.5 ± 24	81.3 ± 44	94 ± 41	125 ± 38	90.37 ± 27	74 ± 31	50.7 ± 23	36.5 ± 12	54 ± 19
Jodhpur	162 ± 41	154 ± 53	96.2 ± 26	96 ± 19	114 ± 40	159 ± 28	116 ± 29	113 ± 28	103 ± 15.3	89 ± 16	101 ± 12
Kota	96.6 ± 25	88 ± 20	69.8 ± 14.9	63 ± 13.9	59 ± 9	76 ± 19.9	67 ± 8	47.9 ± 10.6	37.5 ± 8.8	39.6±7	42 ± 5
Udaipur	103.6 ± 18.8	76.5 ± 19	54.7 ± 14	59 ± 22.6	60.5 ± 12	87.4 ± 47	65 ± 14	55.4 ± 14	53 ± 10.9	48.9 ± 15	52 ± 3
Ajmer	99.9 ± 25	103 ± 35	55.7 ± 18	60.6 ± 12.6	71.9 ± 20.9	131.6 ± 57	80 ± 25	72 ± 24	54 ± 14	49 ± 12	58 ± 12
Alwar	84.5 ± 9.9	83.4 ± 11	48.7 ± 15	41 ± 7.9	56 ± 13.2	65.3 ± 12	53 ± 10	75.9 ± 16	68.5 ± 10	54 ± 5.5	66 ± 11

PRELD, pre-lockdown; PLDN, partial lockdown; LDN, lockdown; ULC, unlocking.

daily mean concentrations of $PM_{2.5}$ and PM_{10} during PRELD, PLDN, various phases of LDN, and UCL situations are shown in **Table 2**. The National Ambient Air Quality Standards (NAAQS) recommend the daily permissible $PM_{2.5}$ of 60 $\mu g\ m^{-3}$ and PM_{10} of 100 $\mu g\ m^{-3}$ for India (MoEFCC, 2015). About 3, 33, and 6% of $PM_{2.5}$ daily data exceeded the permissible limit of NAAQS during the COVID-19 LDN period in Jaipur, Jodhpur, and Ajmer, while 35, 46, 4, 7, and 19% of PM_{10} exceeded in Jaipur, Jodhpur, Kota, Udaipur, and Ajmer, respectively. It is suggested that the concentrations of $PM_{2.5}$ significantly decreased in all cities that met the NAAQS limits. However, in a few cities, like Jodhpur, Jaipur, and Ajmer, the PM_{10} levels did not fall below the standard limit during most of the COVID-19 LDN period due to non-combustion-related sources like wind-blown dust. The highest reduction by 47% in $PM_{2.5}$ was observed in Alwar, followed by Udaipur (40%), Kota (36%), Jaipur (32%), and Ajmer (32%), while Jodhpur showed the lowest reduction of about 25% during the COVID-19 LDN, respectively. PM_{10} was reduced by 37% in Alwar and 36% in Udaipur. However, the lowest reductions of 19–30% were estimated for Jaipur, Jodhpur, Kota, and Ajmer cities (**Figure 5**). Additionally, we have compared the $PM_{2.5}$ and PM_{10} concentrations measured in 2020 with those during the previous year (2019) for the COVID-19 LDN and ULC periods (see **Figure 6**). The differences are, more or less, the same during PLDN, but significantly lower concentrations of both pollutants were estimated during the COVID-19 LDN and ULC periods. Wilcoxon test has been performed, and P-value < 0.05 was found, which was considered statistically significant in the LDN periods. The reductions in $PM_{2.5}$ and PM_{10} varied in the ranges of 16–50 and 22–47% during the COVID-19 LDN period with respect to the same period of the year 2019 (without meteorological normalization), as shown in **Figure 7**. The reductions of 6–46% in $PM_{2.5}$ and 28–49% in PM_{10} were estimated during the overall ULC period.

Overall, the declining trends of $PM_{2.5}$ and PM_{10} observed in all cities during the COVID-19 LDN period are attributed to the reduction in combustion-related emissions (NASA, 2020; Navinya et al., 2020). Conversely, to some extent, elevated levels of $PM_{2.5}$ and PM_{10} were observed during the LDN3 and LDN4 periods (see **Figure 4**). During all COVID-19 LDN phases, the restrictions were diverse and resulted in variations of $PM_{2.5}$ and PM_{10} in each LDN phase—for example, major anthropogenic and industrial activities were stopped, except for emergency services like the health sector (Yadav et al., 2020). Later, some relaxations with limitations were allowed in the subsequent LDN periods (MHA, 2020). Sahu et al. (2011) have reported that the emissions from transport and industrial sectors have significant contributions to the ambient concentrations of both $PM_{2.5}$ and PM_{10}. In addition to this, wind-blown dust is a more substantial source of coarser particles (PM_{10}) in the northern and western regions of India (Sahu et al., 2011; Yadav et al., 2014b). During the ULC period, only Alwar City exhibited higher values of $PM_{2.5}$ and PM_{10} compared with the overall LDN phases in the same year; this could have happened due to limited local rainfall events. Interestingly, the highest plummet can be attributed to rainfall in the ULC period (monsoon) compared to 2019. In the monsoon period, episodes of rainfall can wash out the dust particles (PM_{10}) much faster than the finer particles ($PM_{2.5}$), unless there is frequent rainfall for many days (Yadav et al., 2014c). **Figure 8** shows the ratios of $PM_{2.5}/PM_{10}$ during the study period in the year 2020 in six cities that were used to investigate aerosol combustion and non-combustion sources. The ratio of $PM_{2.5}/PM_{10}$ was observed to be $<0.50\ \mu g\ \mu g^{-1}$ in all cities due to higher temperatures during the COVID-19 LDN period (pre-monsoon months), leading to dry and dusty conditions (Chan and Yao, 2008). The emissions from wind-blown dust are highly significant, mainly contributing to PM_{10}, and are probably the reason for the high levels of coarser particles. Interestingly, about $0.40\ \mu g\ \mu g^{-1}$ ratio of $PM_{2.5}/PM_{10}$ was observed during all phases

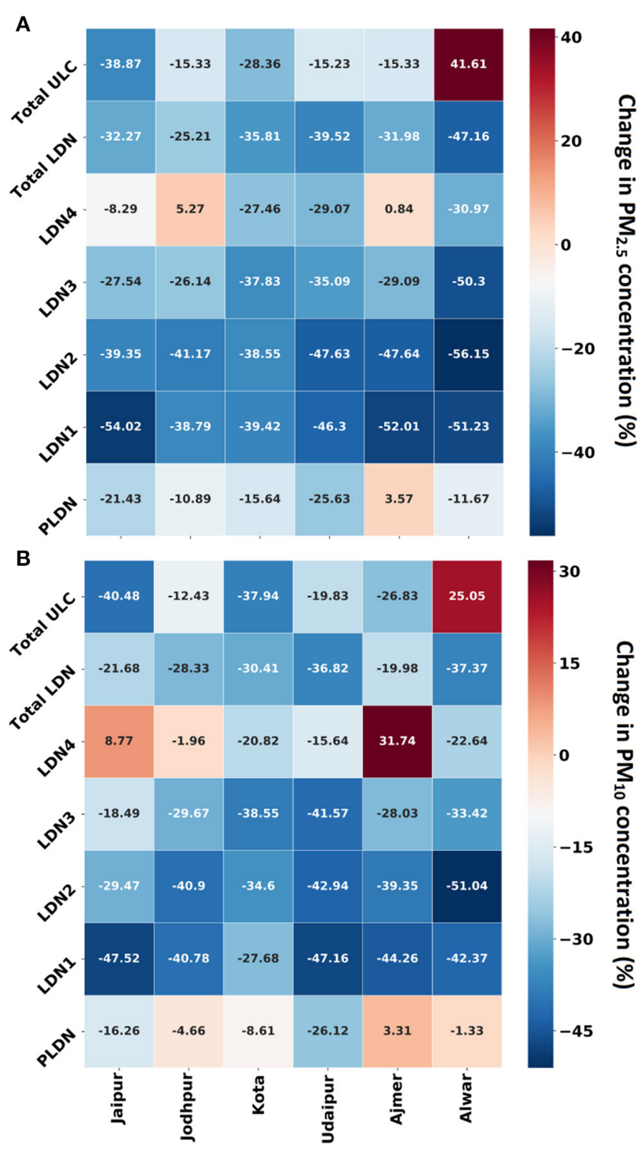

FIGURE 5 | Percentage change in the concentrations of $PM_{2.5}$ and PM_{10} during the COVID-10 lockdown (LDN) phases and unlocking period in six cities. The percentage change in the concentration of $PM_{2.5}$ and PM_{10} was calculated during partial lockdown and LDN phases by comparing the pre-lockdown period and the change in the unlocking period compared to the LDN period.

of COVID-19 LDN in Jaipur City (nearby Delhi) due to the impact of dust storm. In the pre-monsoon season, dust storms originate from Arab countries, and the Thar Desert can influence most regions, like Delhi, Rajasthan, etc., of India (Anand et al., 2019), thus rapidly increasing the PM_{10} levels. Overall, dust pollution is prominent in particle loads over the Rajasthan state. In addition to this, we have incorporated the plots of O_3/NO_2 and SO_2/NO_2 ratios during the study period in **Figure 8**. In the LDN periods (pre-monsoon months), the high O_3/NO_2 ratios were due to the transport of photochemical pollutants from higher altitudes. The efficient vertical mixing with free tropospheric air increases O_3 in the pre-monsoon months. The enhanced SO_2/NO_2 indicates that the predominant source of SO_2 is coal-based thermal power plants. In other words, the site receives reasonably aged SO_2 from distant regions, resulting in high ratios (Mor et al., 2021).

Impact of Meteorology and Biomass Burning on Air Quality

In addition to the local emissions, the variation in ambient air pollutants can also be influenced by the local meteorology, transport, transformation, and scavenging by the precipitation (Sahu et al., 2016a,b, 2020; Yadav et al., 2019a,b). Therefore, the mean wind streamlines along with temperature and precipitation at 925 mb pressure level are used in the study to investigate any unusual changes in meteorological and transport processes during the COVID-19 LDN period. The comparison of meteorological parameters during 2020 and 2019 for the PRELD, COVID-19 LDN, and UCL periods is shown in **Figure 2**. The trends in wind speed, temperature, and precipitation indicate the different features during the entire study period due to the change of seasons from winter to pre-monsoon and then monsoon (Yadav et al., 2014a; Sahu et al., 2017). Hence, the trends of $PM_{2.5}$ and PM_{10} may also include a factor related to the change of meteorological conditions in the same year in comparison with the PRELD period. In the pre-monsoon season (LDN period), high temperatures, high wind speeds, and more profound boundary layer heights may lead to a higher dispersion of pollutants and lower concentrations (Sahu et al., 2020). However, the difference between 2019 and 2020 does not show significant fluctuations in wind speed, temperature, and precipitation in the western region of India during the PRELD to ULC periods. The mean surface temperatures and rainfall were in ranges of 30–32°C and 0–1.5 mm day^{-1} during the COVID-19 LDN period in the years 2019 and 2020 over the study region. The strong westerly wind prevails over the area during both years in the COVID-19 LDN period. In general, all meteorological parameters were, more or less, similar during the study period, especially in the COVID-19 lockdown period in 2019 and 2020. Several studies have reported that the meteorological parameters were identical in the previous years and 2020 during the COVID-19 LDN over the Indian region (Navinya et al., 2020; Sharma et al., 2020; Singh et al., 2020; Yadav et al., 2020). Additionally, in the pre-monsoon season, the local emissions become lesser, but outside contributions become more prominent due to the increased transport of regional air masses. Furthermore, ∼7% open agricultural burning in this season is mainly due to the burning of residues from wheat crops. **Figure 3** shows MODIS-active fire maps over India during the entire study period for the years 2019 and 2020. In addition to this, to some extent, the SW winds also influenced the region after passing through populated areas of central India; they may get polluted during the pre-monsoon-to-monsoon transition period (Sahu et al., 2020; Maji et al., 2021; Yadav et al., 2021). The maps clearly show that the pre-monsoon fire events in 2020 during COVID-19 LDN have

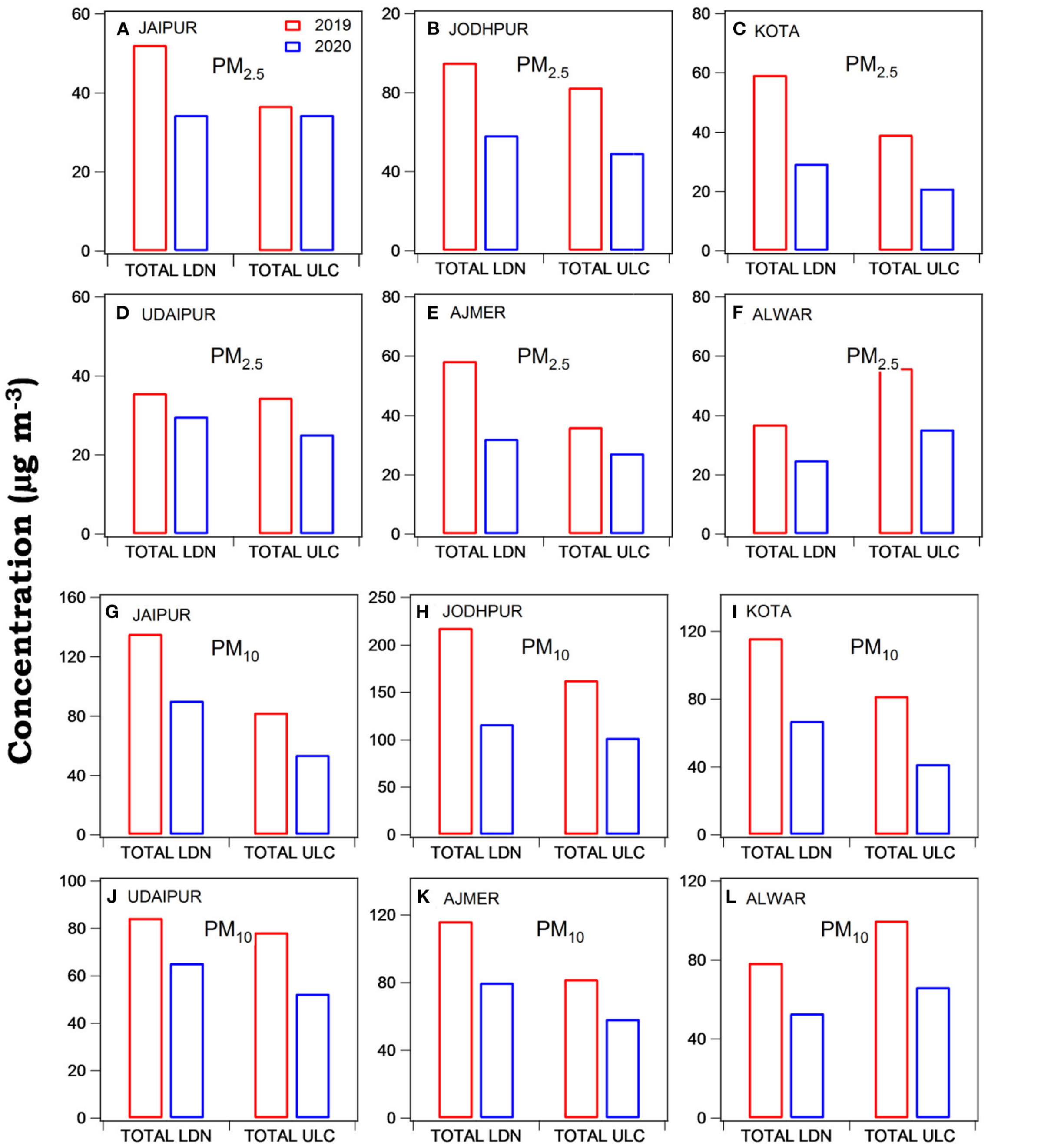

FIGURE 6 | Variations of $PM_{2.5}$ and PM_{10} in Jaipur, Jodhpur, Kota, Udaipur, Ajmer, and Alwar during COVID-19 lockdown and unlocking periods and a comparison to the same period of the previous year (2019).

somewhat decreased to a shallow level compared to those in 2019, especially in western, northern, and central India (Kant et al., bib2020), as biomass burning is a significant aerosol source. Overall, the reductions in fire events along with local emissions have also been deficient. Additionally, we have normalized the mass concentrations of $PM_{2.5}$ and PM_{10} with meteorology to investigate the actual change in emissions due to COVID-19 LDN. In the method, ventilation coefficient, a product of wind speed (WS) and boundary layer height (BLH), is used to see the role of weather dynamics for all cities of Rajasthan. The WS (above 10 m) and BLH datasets used in the study are from Copernicus Emergency Management Service (Climate Data Store) (https://cds.climate.copernicus.eu/cdsapp#!/search?type=dataset). The extensive details of normalizing the meteorological

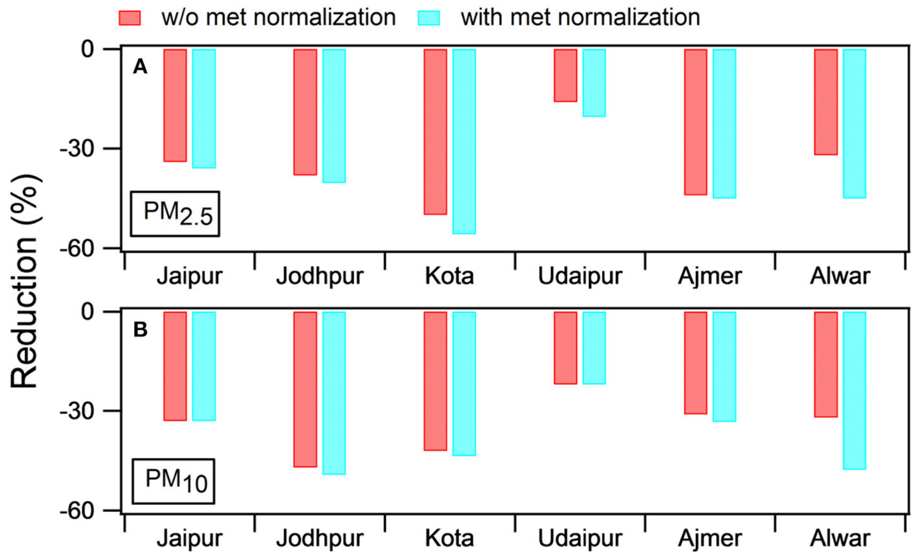

FIGURE 7 | Percentage reduction (without and with meteorology normalization) during the COVID-19 lockdown period in 2020 in all cities of Rajasthan with respect to the mean of the previous years for the same period.

effects on ambient pollutants are reported elsewhere (Dai et al., 2020; Falocchi et al., 2021; Mishra et al., 2021). The reductions in $PM_{2.5}$ and PM_{10} (with meteorology-normalized data) were in the ranges of 20–55 and 22–49% during the COVID-19 LDN period compared to the same period of 2019, as shown in **Figure 7**. Enhancement (differences ~10%) was observed in the reduction of $PM_{2.5}$ and PM_{10} (in meteorology-normalized data) compared to without meteorology-normalized data during the LDN period in all cities.

Air Quality Index in Rajasthan Cities

Air quality index is a tool for people to understand the air quality status in an easy way. This tool transforms the complex data of various pollutants into a single number (index value), classification, and color (Beig et al., 2010). AQI was calculated for all cities to identify the overall improvement in air quality, and the details of AQI are available elsewhere (CPCB, 2014). There are six AQI categories: good + satisfactory (0–100), moderately polluted (101–200), poor (201–200), very poor (301–400), and severe (401–500). We have converted the $PM_{2.5}$, PM_{10}, and SO_2 concentration values into AQI using typical values, as the minimum of three parameters was very much needed for the calculation. Therefore, only SO_2 concentration was used for the AQI analysis. Each category is decided based on the ambient concentration values of air pollutants and their likely health impacts known as health breakpoints. The AQ sub-index and breakpoint concentration of different pollutants are provided elsewhere (CPCB, 2014). **Figure 9** indicates the AQI variation during the entire study period over six cities. Overall, the AQI was satisfactory to moderately polluted categories during the whole study period (PRELD to ULC). The AQI varied in the ranges of 85–161 during PRELD in all cities, with the highest in Jaipur, Jodhpur, and Udaipur cities, during which the traffic was regular. Later, the AQI declined during various LDN periods compared to during PRELD in all cities, except Jaipur, Jodhpur, and Ajmer. More or less, in all cities, increasing values were seen during the subsequent LDN periods but with the highest of 117 in Jaipur, 174 in Jodhpur, and 121 in Ajmer. Overall, in LDN1 to LDN3, all cities were in satisfactory ranges, but Jaipur, Jodhpur, and Ajmer showed moderate air quality conditions in LDN4. Interestingly, Jodhpur City gets good air quality during the third phase of ULC since the LDN periods. It suggests that more contributions to coarser particles (PM_{10}) are wind-blown dust and dust storms and, of course, anthropogenic activities, which have been allowed with limitations in the subsequent LDNs.

CONCLUSIONS

We have investigated the trends of the daily mean concentrations of $PM_{2.5}$ and PM_{10} in six cities, including Jaipur, Jodhpur, Kota, Udaipur, Ajmer, and Alwar of Rajasthan in India. We have obtained the data from CPCB and analyzed it for the years 2019 and 2020 during eight specific months (January to August). The primary aim is to understand the role of unusually low anthropogenic emissions in ambient concentrations of particulate pollutants during the COVID-19 lockdown. The investigation combines the effects of local anthropogenic emissions, meteorology, and the transport of biomass burning in the variations of both pollutants. The $PM_{2.5}$ and PM_{10} concentrations were reduced significantly in all cities and met the national standards during the lockdown. However, in a few cities, like Jodhpur, Jaipur, and Ajmer, the PM_{10} levels have not fallen below the standard

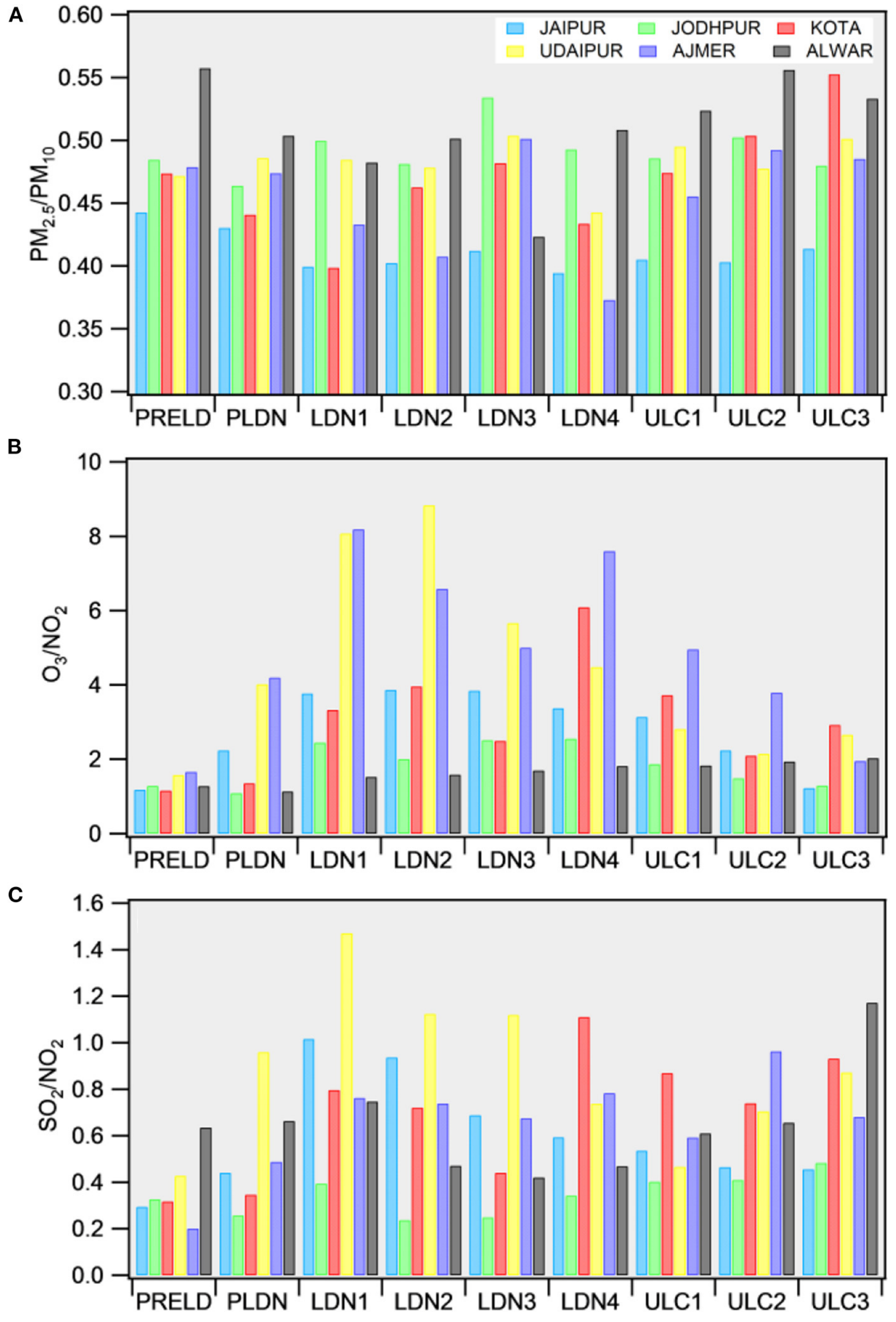

FIGURE 8 | $PM_{2.5}/PM_{10}$, O_2/NO_2 and SO_2/NO_2 ratios in six cities of Rajasthan during the different phases of the study.

limit (100 µg m^{-3}) most of the time during the COVID-19 LDN period due to non-combustion-related sources like wind-blown dust. The highest reduction in $PM_{2.5}$, by 47%, was observed in Alwar, followed by Udaipur (40%), Kota (36%), Jaipur (32%), and Ajmer (32%), while Jodhpur showed the lowest reduction of about 25% during the COVID-19 LDN, respectively. PM_{10} was reduced by 37 and 36% in Alwar and Udaipur. However, the lowest (19–30%) reductions were in Jaipur, Jodhpur, Kota, and Ajmer. More or less, there was 50% of $PM_{2.5}$ and PM_{10} in all cities due to higher temperatures during the COVID-19 LDN period (pre-monsoon months), supporting the uplifting of mineral and dust particles (PM10). In addition to the unusual local emissions, meteorological parameters, such as rainfall and movement of air masses, played a significant role in reducing the particle levels.

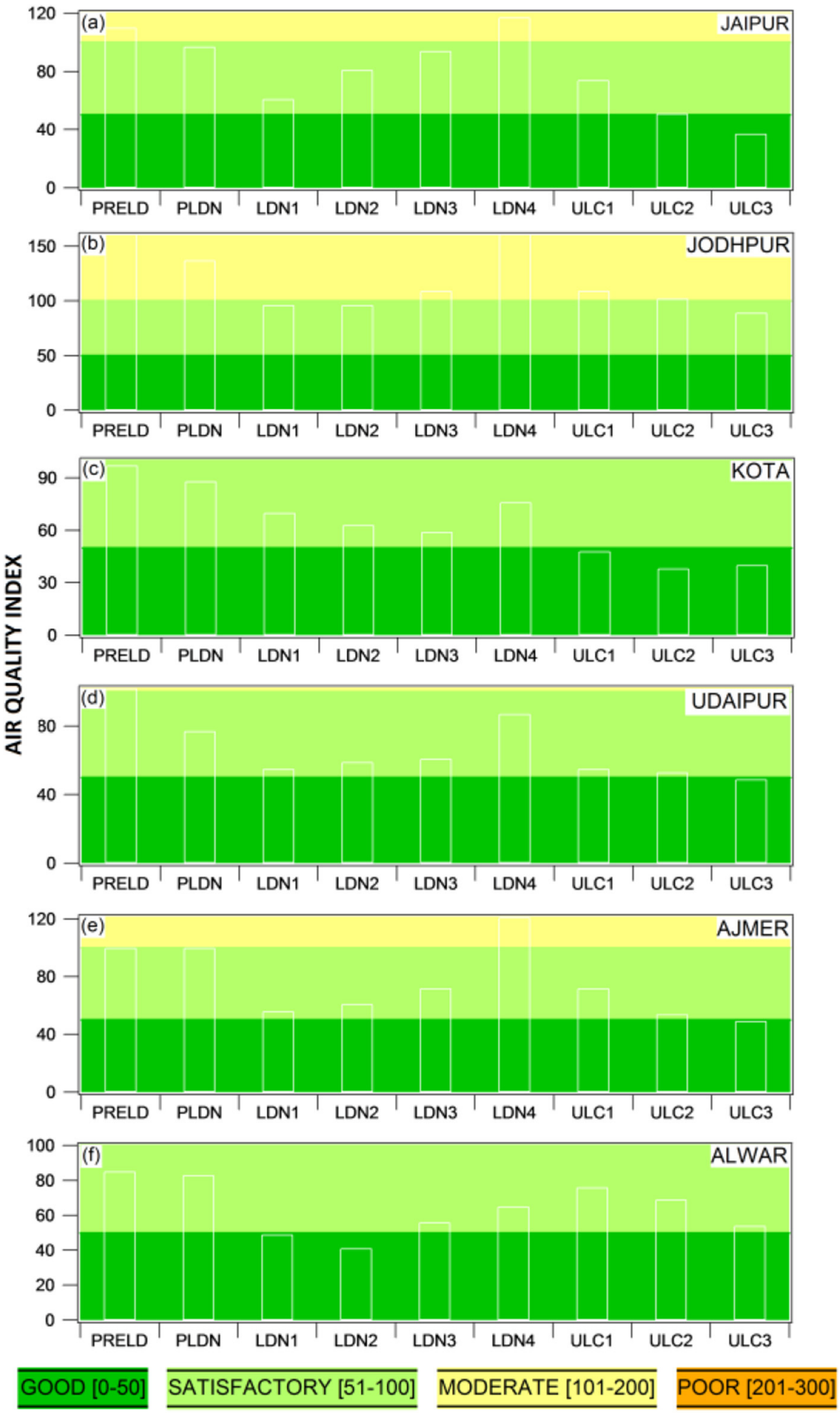

FIGURE 9 | Air quality index for major cities of Rajasthan during the study period in the year 2020.

DATA AVAILABILITY STATEMENT

Publicly available datasets were analyzed in this study. This air quality data can be found form the CPCB (https://cpcb.nic.in/).

AUTHOR CONTRIBUTIONS

RY: conceptualization, software, and writing—original draft. PV: formal data analysis. PK and RY: data analysis. UP, PV, and VS: data collection. MG, PK, RY, and NT: methodology. PD, SJ, LS, GB, and DR: discussion. PD, SJ, LS, GB, DR, RY, PV, PK, UP, VS, MG, and NT: writing—review and editing. GB, RY, and LS: investigation. SJ, LS, and GB: visualization. All authors contributed to the article and approved the submitted version.

ACKNOWLEDGMENTS

We acknowledge and thank the Central Pollution Control Board (India), the Rajasthan State Pollution Control Board, and the Ministry of Environment, Forest, and Climate Change (India) for making the air quality data publicly available. We acknowledge the ISRO-Bhuvan (https://bhuvan.nrsc.gov.in/) for providing the map of Rajasthan state. We acknowledge the Moderate Resolution Imaging Spectroradiometer (MODIS) for providing the active fire count datasets. We are thankful to ECMWF ERA5 (https://climate.copernicus.eu/) for providing the boundary layer height and wind speed datasets used in the study. Authors would like to acknowledge the use of temperature, wind speed and precipitation datasets provided by National Centre for Environmental Prediction (NCEP). We acknowledge the meteorological data explorer (METEX), Centre for Global Environmental Research (CGER) for providing the backward trajectories data. The authors would like to thank the Director, IITM, and Secretary, Ministry of Earth Sciences (Govt. of India), for their encouragement and support. RY and GB also acknowledge the INDO-UK APHH PROMOTE project. PND thanks Indian National Science Academy, New Delhi, for the award of Visiting Scientist-2021.

SUPPLEMENTARY MATERIAL

The Supplementary Material for this article can be found online at: https://www.frontiersin.org/articles/10.3389/frsc.2022.792507/full#supplementary-material

REFERENCES

Anand, V., Korhale, N., Rathod, A., and Beig, G. (2019). On processes controlling fine particulate matters in four Indian megacities. *Environ. Pollut*. 254, 113026. doi: 10.1016/j.envpol.2019.113026

Bashir, M. F., Jiang, B., Komal, B., Bashir, M. A., Farooq, T. H., Iqbal, N., et al. (2020). Correlation between environmental pollution indicators and COVID-19 pandemic: a brief study in Californian context. *Environ. Res*. 187, 109652. doi: 10.1016/j.envres.2020.109652

Beig, G., Bano, S., Sahu, S. K., Anand, V., Korhale, N., Rathod, A., et al. (2020). COVID-19 and environmental -weather markers: unfolding baseline levels and veracity of linkages in tropical India. *Environ. Res.* 191, 110121. doi: 10.1016/j.envres.2020.110121

Beig, G., Ghude, S. D., and Deshpande A. (2010). *Scientific Evaluation of Air Quality Standards and Defining Air Quality Index for India.* Pune: Indian Institute of Tropical Meteorology. Available online at: https://www.tropmet.res.in/~lip/Publication/RR-pdf/RR-127.pdf

Beig, G., Gunthe, S., and Jadhav, D.B. (2007). Simultaneous measurements of Ozone and its precursors on a diurnal scale at a semi-urban site in India. *J Atmos. Chemi.* 57, 239–253. doi: 10.1007/s10874-007-9068-8

Chan, C. K., and Yao, X. (2008). Air pollution in mega cities in China. *Atmos. Environ.* 42, 1–42. doi: 10.1016/j.atmosenv.2007.09.003

Conticini, E., Bruno, F., and Dario, C. (2020). Can atmospheric pollution be considered a co-factor in extremely high level of SARS-CoV-2 lethality in Northern Italy? *Environ. Poll*. 261, 114465. doi: 10.1016/j.envpol.2020.114465

CPCB. (2014). *National Air Quality Index Report*. Central Pollution Control Board, New Delhi (India). Available online at: https://app.cpcbccr.com/ccr_docs/FINAL-REPORT_AQI_.pdf

Dai, Q., Liu, B., Bi, X., Wu, J., Liang, D., Zhang, Y., et al. (2020). Dispersion normalized PMF provides insights into the significant changes in source contributions to PM2. 5 after the COVID-19 outbreak. *Environ. Sci. Technol.* 54, 9917–9927. doi: 10.1021/acs.est.0c02776

Dantas, G., Siciliano, B., França, B. B., da Silva, C. M., and Arbilla, G. (2020). The impact of COVID-19 partial lockdown on the air quality of the city of Rio de Janeiro, Brazil. *Sci. Total Environ.* 729, 139085. doi: 10.1016/j.scitotenv.2020.139085

Falocchi, M., Zardi, D., and Giovannini, L. (2021). Meteorological normalization of NO2 concentrations in the Province of Bolzano (Italian Alps). *Atmos. Environ.* 246, 118048. doi: 10.1016/j.atmosenv.2020.118048

Goel, A., Saxena, P., Sonwani, S., Rathi, S., Srivastava, A., Bharti, A. K., et al. (2021). Health benefits due to reduction in respirable particulates during COVID-19 lockdown in India. *Aerosol Air Qual*. 21, 200460. doi: 10.4209/aaqr.200460

Hama, S. M., Kumar, P., Harrison, R. M., Bloss, W. J., Khare, M., Mishra, S., et al. (2020). Four-year assessment of ambient particulate matter and trace gases in the Delhi-NCR region of India. *Sustain. Cities Soc*. 54, 102003. doi: 10.1016/j.scs.2019.102003

Jain, S., and Sharma, T. (2020). Social and travel lockdown impact considering coronavirus disease (COVID-19) on air quality in megacities of India: present benefits, future challenges and way forward. *Aerosol Air Qual. Res.* 20, 1222–1236. doi: 10.4209/aaqr.2020.04.0171

Kanniah, K. D., Zaman, N. A. F. K., Kaskaoutis, D. G., and Latif, M. T. (2020). COVID-19's impact on the atmospheric environment in the Southeast Asia region. *Sci. Total Environ*. 736, 139658. doi: 10.1016/j.scitotenv.2020.139658

Kant, Y., Mitra, D., and Chauhan, P. (2020). Space-based observations on the impact of COVID-19-induced lockdown on aerosols over India. *Curr. Sci.* 119, 539–544. doi: 10.18520/cs/v119/i3/539-544

Kumar, P., Hama, S., Omidvarborna, H., Sharma, A., Sahani, J., Abhijith, K. V., et al. (2020). Temporary reduction in fine particulate matter due to 'anthropogenic emissions switch-off' during COVID-19 lockdown in Indian cities. *Sustain. Cities Soc*. 62, 102382. doi: 10.1016/j.scs.2020.102382

Kumari, P., and Toshniwal, D. (2020). Impact of lockdown measures during COVID-19 on air quality- A case study of India. *Int. J. Environ. Health Res.* 32, 503–510. doi: 10.1080/09603123.2020.1778646

Li, L., Li, Q., Huang, L., Wang, Q., Zhu, A., Xu, J., et al. (2020). Air quality changes during the COVID-19 lockdown over the Yangtze River Delta Region: an insight into the impact of human activity pattern changes on air pollution variation. *Sci. Total Environ.* 732, 139282. doi: 10.1016/j.scitotenv.2020.139282

Maanju, S. K., and Saha, K. (2013). Impact of mining industry on environmental fabric -a case study of Rajasthan state in India. *J. Environ. Sci. Toxicol. Food Technolo.* 6, 8–13.

Mahato, S., Pal, S., and Ghosh, K. G. (2020). Effect of lockdown amid COVID-19 pandemic on air quality of the megacity Delhi, India. *Sci. Total Environ*. 730, 139086. doi: 10.1016/j.scitotenv.2020.139086

Maji, S., Yadav, R., Beig, G., Gunthe, S. S., and Ojha, N. (2021). On the processes governing the variability of PTR-MS based VOCs and OVOCs in different seasons of a year over hillocky mega city of India. *Atmos. Res.* 261, 105736. doi: 10.1016/j.atmosres.2021.105736

MHA (2020). *No. 40-3/2020-DM-I (A), Government of India, Ministry of Home Affairs*. Available online at: https://www.mha.gov.in/sites/default/files/MHA%20order%20dt%2015.04.2020%2C%20with%20Revised%20Consolidated%20Guidelines_compressed%20%283%29.pdf; http://www.du.ac.in/du/uploads/PR_Consolidated%20Guideline%20of%20MHA_28032020%20(1)_1.PDF

Mishra, A. K., Rajput, P., Singh, A., Singh, C. K., and Mall, R. K. (2021). Effect of lockdown amid COVID-19 on ambient air quality in 16 Indian cities. *Front. Sustain. Cities* 3, 705051. doi: 10.3389/frsc.2021.705051

MoEFCC. (2015). *Environment (Protection) Amendment Rules*. Ministry of Environment, Forest and Climate Change (MoEFCC), Government of India, New Delhi.

Mor, S., Kumar, S., Singh, T., Dogra, S., Pandey, V., and Ravindra, K. (2021). Impact of COVID-19 lockdown on air quality in Chandigarh, India: understanding the emission sources during controlled anthropogenic activities. *Chemosphere* 263, 127978. doi: 10.1016/j.chemosphere.2020.127978

Nakada, L. Y. K., and Urban, R. C. (2020). COVID-19 pandemic: Impacts on the air quality during the partial lockdown in São Paulo state, Brazil. *Sci. Total Environ.* 730, 139087. doi: 10.1016/j.scitotenv.2020.139087

NASA. (2020). Available online at: https://earthobservatory.nasa.gov/images

Navinya, C., Patidar, G., and Phuleria, H. C. (2020). Examining effects of the COVID-19 national lockdown on ambient air quality across urban India. *Aerosol Air Qual. Res.* 20, 1759–1771. doi: 10.4209/aaqr.2020.05.0256

Pope, C. A., Ezzati, M., and Dockery, D. W. (2009). Fine-particulate air pollution and life expectancy in the United States. *N. Engl. J. Med.* 360, 376–386. doi: 10.1056/NEJMsa0805646

PPAC (2020). *Consumption of Petroleum Products, Petroleum Planning & Analysis Cell*. Available online at: https://www.ppac.gov.in/content/147_1_ConsumptionPetroleum.aspx

Sahu, L. K., Pal, D., Yadav, R., and Munkhtur, J. (2016b). Aromatic VOCs at major road junctions of a metropolis in India: measurements using TD-GC-FID and PTR-TOF-MS instruments. *Aerosol Air Qual. Res*. 16, 2405–2420. doi: 10.4209/aaqr.2015.11.0643

Sahu, L. K., Tripathi, N., and Yadav, R. (2017). Contribution of biogenic and photochemical sources to ambient VOCs during winter to summer transition at a semi-arid urban site in India. *Environ. Pollu.* 229, 595–606. doi: 10.1016/j.envpol.2017.06.091

Sahu, L. K., Yadav, R., and Pal, D. (2016a). Source identification of VOCs at an urban site of western India: Effect of marathon events and anthropogenic emissions. *J. Geophys. Res*. 121, 2416–2433. doi: 10.1002/2015JD024454

Sahu, L. K., Yadav, R., and Tripathi, N. (2020). Aromatic compounds in a semi-urban site of western India: Seasonal variability and emission ratios. *Atmos. Res.* 246, 105114. doi: 10.1016/j.atmosres.2020.105114

Sahu, S. K., Beig, G., and Parkhi, N. (2011). Emissions inventory of anthropogenic PM2.5 and PM10 in Delhi during commonwealth games 2010. *Atmos. Environ.* 45, 6180–6190. doi: 10.1016/j.atmosenv.2011.08.014

Sharma, S., Zhang, M., Gao, J., Zhang, H., and Kota, S. H. (2020). Effect of restricted emissions during COVID-19 on air quality in India. *Sci. Total Environ.* 728, 138878. doi: 10.1016/j.scitotenv.2020.138878

Sicard, P., De Marco, A., Agathokleous, E., Feng, Z., Xu, X., Paoletti, E., et al. (2020). Amplified ozone pollution in cities during the COVID-19 lockdown. *Sci. Total Environ.* 735, 139542. doi: 10.1016/j.scitotenv.2020.139542

Singh, R. P., and Chauhan, A. (2020). Impact of lockdown on air quality in India during COVID-19 pandemic. *Air Qual. Atmos. Health* 13, 921–928. doi: 10.1007/s11869-020-00863-1

Singh, V., Singh, S., Biswal, A., Kesarkar, A. P., Mor, S., and Ravindra, K. (2020). Diurnal and temporal changes in air pollution during COVID-19 strict lockdown over different regions of India. *Environ. Pollut.* 266, 115368. doi: 10.1016/j.envpol.2020.115368

Sokhi, R. S., Singh, V., Querol, X., Finardi, S., Targino, A. C., de Fatima Andrade, M., et al. (2021). A global observational analysis to understand changes in air quality during exceptionally low anthropogenic emission conditions. *Environ. Int*. 157, 106818. doi: 10.1016/j.envint.2021.106818

Tobías, A., Carnerero, C., Reche, C., Massagu,é, J., Via, M., Minguillón, M. C., et al. (2020). Changes in air quality during the lockdown in Barcelona (Spain) one month into the SARS-CoV-2 epidemic. *Sci. Total Environ.* 726, 138540. doi: 10.1016/j.scitotenv.2020.138540

WHO (2020). *Rolling Updates on Coronavirus Disease (COVID-19)*. World Health Organization. Available online at: https://www.who.int/emergencies/diseases/novel-coronavirus-2019/events

Wu, A., Peng, Y., Huang, B., Ding, X., Wang, X., Niu, P., et al. (2020). Genome composition and divergence of the novel coronavirus (2019-nCoV) originating in China. *Cell Host Microbe* 27, 325–328. doi: 10.1016/j.chom.2020.02.001

Yadav, R., Beig, G., Anand, V., Kalbande, R., and Maji, S. (2021). Tracer-based characterization of source variations of ambient isoprene mixing ratios in a hillocky megacity, India, influenced by the local meteorology. *Environ. Res.* 205, 112465. doi: 10.1016/j.envres.2021.112465

Yadav, R., Beig, G., and Jaffrey, S. N. A. (2014c). The linkages of anthropogenic emissions and meteorology in the rapid increase of particulate matter at a foothill city in the Arawali range of India. *Atmos. Environ.* 85, 147–151. doi: 10.1016/j.atmosenv.2013.09.007

Yadav, R., Korhale, N., Anand, V., Rathod, A., Bano, S., Shinde, R., et al. (2020). COVID-19 lockdown and air quality of SAFAR-India metro cities. *Urban Clim.* 34, 100729. doi: 10.1016/j.uclim.2020.100729

Yadav, R., Sahu, L. K., Beig, G., and Jaaffrey, S. N. A. (2016). Role of long-range transport and local meteorology in seasonal variation of surface ozone and its precursors at an urban site in India. *Atmos. Res*. 176–177, 96–107. doi: 10.1016/j.atmosres.2016.02.018

Yadav, R., Sahu, L. K., Beig, G., Tripathi, N., and Jaaffrey, S. N. A. (2017). Ambient particulate matter and carbon monoxide at an urban site of India: influence of anthropogenic emissions and dust storms. *Environ. Pollut*. 225, 291–303. doi: 10.1016/j.envpol.2017.01.038

Yadav, R., Sahu, L. K., Beig, G., Tripathi, N., Maji, S., and Jaaffrey, S. N. A. (2019b). The role of local meteorology on ambient particulate and gaseous species at an urban site of western India. *Urban Clim*. 28, 100449. doi: 10.1016/j.uclim.2019.01.003

Yadav, R., Sahu, L. K., Jaaffrey, S. N. A., and Beig, G. (2014a). Temporal variation of particulate matter (PM) and potential sources at an urban site of udaipur in western India. *Aerosol Air Qual. Res*. 14, 1613–1629. doi: 10.4209/aaqr.2013.10.0310

Yadav, R., Sahu, L. K., Jaaffrey, S. N. A., and Beig, G. (2014b). Distributions of ozone and related trace gases at an urban site in western India. *J. Atmos. Chem*. 71, 125–144. doi: 10.1007/s10874-014-9286-9

Yadav, R., Sahu, L. K., Tripathi, N., Pal, D., Beig, G., and Jaaffrey, S. N. A. (2019a). Investigation of emission characteristics of NMVOCs over urban site of Western India. *Environ. Pollut*. 252, 245–255. doi: 10.1016/j.envpol.2019.05.089

Yao, Y., Pan, J., Liu, Z., Meng, X., Wang, W., Kan, H., et al. (2020). No association of COVID-19 transmission with temperature or UV radiation in Chinese cities. *Eur. Respir. J.* 55, 2000517. doi: 10.1183/13993003.00517-2020

Conflict of Interest: The authors declare that the research was conducted in the absence of any commercial or financial relationships that could be construed as a potential conflict of interest.

Publisher's Note: All claims expressed in this article are solely those of the authors and do not necessarily represent those of their affiliated organizations, or those of the publisher, the editors and the reviewers. Any product that may be evaluated in this article, or claim that may be made by its manufacturer, is not guaranteed or endorsed by the publisher.

Advantages of publishing in Frontiers

OPEN ACCESS
Articles are free to read for greatest visibility and readership

FAST PUBLICATION
Around 90 days from submission to decision

HIGH QUALITY PEER-REVIEW
Rigorous, collaborative, and constructive peer-review

TRANSPARENT PEER-REVIEW
Editors and reviewers acknowledged by name on published articles

Frontiers
Avenue du Tribunal-Fédéral 34
1005 Lausanne | Switzerland

Visit us: www.frontiersin.org
Contact us: frontiersin.org/about/contact

REPRODUCIBILITY OF RESEARCH
Support open data and methods to enhance research reproducibility

DIGITAL PUBLISHING
Articles designed for optimal readership across devices

FOLLOW US
@frontiersin

IMPACT METRICS
Advanced article metrics track visibility across digital media

EXTENSIVE PROMOTION
Marketing and promotion of impactful research

LOOP RESEARCH NETWORK
Our network increases your article's readership